

**A.G. BAKHANOVICH
J.E. GUREVICH**

**MECHANICS
OF TRANSMISSIONS OF
POWER BY FLEXIBLE LINK**

Science edition

**New York
2012**

Alexander G. Bakhanovich
Jury E. Gurevich

MECHANICS OF TRANSMISSIONS OF POWER BY FLEXIBLE LINK

Science edition

Copyright © 2012 by Alexander G. Bakhanovich, Jury E. Gurevich

All rights reserved. No part of this book may be translated, reproduced or copied in any form without the permission of the copyright holder.

Published by Big Open World, Inc.
PO BOX 238
Brooklyn, NY.
11238 USA

Library of Congress Control Number: 2012956442

ISBN 978-1-4675-5945-4

Printed in USA
2012

UDC 621.833(075.8)

It is recommended by the scientific and technical council
of the Belarusian National Technical University
(Record №8 from 30.06.2008.)

It is recommended by the scientific and technical council
of the Moscow State Technological University
(Record №7 from 24.10.2008.)

Reviewers:

Academician of the National Academy of Sciences of Belarus,
Laureate of the State Prize of Belarus,
Doctor of Engineering, Prof. V.V. Klubovich;
Doctor of Engineering, Prof. P.N. Uchaev.

Bakhanovich, A.G.

Mechanics of transmissions of power by flexible link: monography/
A.G. Bakhanovich, J.E. Gurevich. – New York: Big Open World, Inc.,
2012. – 306 p. Tab. 21. Fig. 237. Bibl. 182.

ISBN 978-1-4675-5945-4

Library of Congress Control Number: 2012956442

The results of the theoretical and experimental researches of mechanical transmissions of power by flexible link on the improvement of their technical level by the design and technological methods are presented in the monography.

The monography is intended for workers of engineering design institutions, industrial enterprises, students, post-graduate students, **doctoral candidates** and teachers of the machine-building profile.

INTRODUCTION

Belt transmissions belong to the class of transmissions of power by flexible link and are considered to be one of the most spread mechanisms, which define the technical level of machines in general. In view of their functional and economic advantages they are widely used among mechanical transmissions of power.

Nowadays belt transmissions are used practically in all the spheres of machine-building, successfully competing with chain and toothed gears, and in some figures they excel chain and toothed gears greatly (low metal consumption, a low level **of noise**, transmission of power to long distances with high speeds, damping of loading, safety function from overloading of transmission, owing to the existence of elastic sliding, etc.). Alongside with these advantages belt transmissions are characterized by the simplicity of their design and the absence of the lubrication system, which predetermines their low cost.

The evident disadvantages of belt transmissions are the enlarged overall dimensions and the efforts on shafts and supports.

According to the classical definition, a belt transmission is a mechanism for transmission of rotation (power) by means of the interaction of flexible link (belt), which is in tension with rigid cylindrical links – pulleys.

In conformity with functional distinctive features belt transmissions can be divided into two groups: transmissions of friction type and transmissions by gearing. In the first case the transmission of the pull (power) is carried out by means of the friction forces between the working surfaces of a belt and pulleys, made by the belt tension that exceeds the maximum permissible pull. This circumstance predetermines the low loading ability of transmission, large loadings on shafts, but it allows the effective damping of vibrations. The characteristic feature of the belt transmissions of a friction type is the existence of the elastic sliding in gearing, expressed in the lag of a driven pulley of a drive pulley in its rotation speed by **1...2 %**.

Belt transmissions of a friction type come under three functional groups: **flat-belt**, **V-belt** and **poly-V-belt** transmissions.

Alongside with **flat-belt**, **V-belt** and **poly-V-belt** transmissions, which principle of operation is based on the use of the friction forces, **toothed-belt transmissions (TBT)**, **related to** the gearing transmission class, have gained a wide introduction. These transmissions have the advantages of both belt transmissions (multishafting, the transmission of power

for long distances) and chain and toothed transmissions (reduction ratio constancy, high efficiency, etc.).

Besides, **toothed-belt transmissions** possess some advantages, which are not characteristic of other types of transmissions. They are: low specific consumption of materials, smoothness and noiselessness of operation, service simplicity, and the ability of a belt to self-defense from getting of dust and abrasive particles into the zone of gearing as a result of the creation of the air pressure zone around the belt.

Constantly increasing amount of **TBT** introduction instead of toothed, chain, **flat-belt**, **V-belt**, **poly-V-belt** and other kinds of transmissions testifies their significant advantages and high effectiveness of **TBT**. Nowadays the world level of **TBT** production has exceeded 3 billion items a year, **the annual expansion of consumption makes 8...10 %**.

The further spread of **toothed-belt transmissions** is restrained by the necessity of the increase of figures of their working ability. In particular it can be referred to transmissions with the standard geometry, meeting the requirements of compatibility and unification.

The monography is devoted to the solution of an actual scientific, technical and practical problem of the improvement of the technical level of belt transmissions, especially **toothed-belt transmissions**.

The theoretical and practical improvement of technical characteristics of transmissions of power by flexible link should be based on the system and complex approach to the investigation of the principles of their functioning, including the development of modern calculation methods and the choice of rational transmission parameters, designs and the advanced technology of the drive-belt production.

The solution of the problem will increase the load carrying capacity and operational resource of mechanical transmissions of power by flexible link, reduce material and working expenses of the technological process of the drive-belt production, improve the quality and competitive ability of the machine-building production in general.

Chapter 1. COMMON DATA

1.1. Review and analysis of designs of transmissions of power by flexible link

1.1.1. Flat-belt transmissions.

Flat-belt transmissions (Fig. 1.1, 1.2) are widely used in drives with a significant distance from an engine up to an operating device.

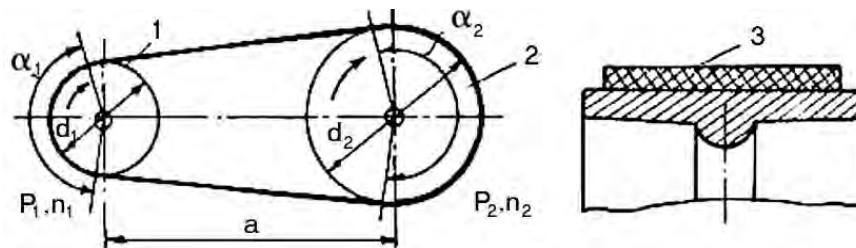


Fig. 1.1. Scheme of a flat-belt transmission: 1, 2 – pulleys, 3 – belt

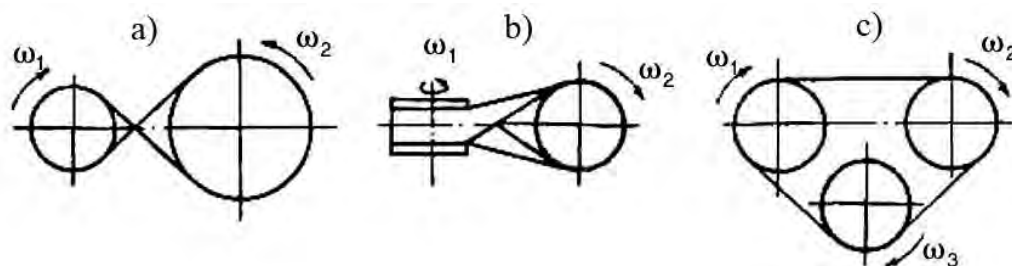


Fig. 1.2. Varieties of flat-belt transmissions: a) cross; b) semicross; c) spatial

Merits: the simplicity of a design, smoothness and noiselessness of operation, low accuracy requirements to the arrangement of the details of transmission, protection from an overload due to the possibility of a belt slipping along a pulley.

Demerits: large dimensions, variability of a reduction ratio in view of the elastic sliding, a large loading on shafts and supports, low durability of a belt.

The transmitted power is up to 50 kW, the reduction ratio is up to 6, the efficiency is 0.93... 0.96, the speed of a belt is up to 100 m/s.

Nowadays the spectrum of the manufactured flat belts varies greatly. The basic types of flat belts, depending on their design, correspond to several standards.

Rubber-fabric belts (Fig. 1.3) are produced in accordance with GOST 23831-79. They consist of one or several layers of a special fabric – belting, linked together by rubber. Such belts are delivered in rolls, having the following standard series of width: 10, 20, 25, 30, 40, 45, 50, 60, 70, 75, 80, 100, 125, 150, 200, 225, 250, 300, 400, 450, 600, 700, 800, 900, 1000, 1100 and 1200 mm (Tab. 1.1).

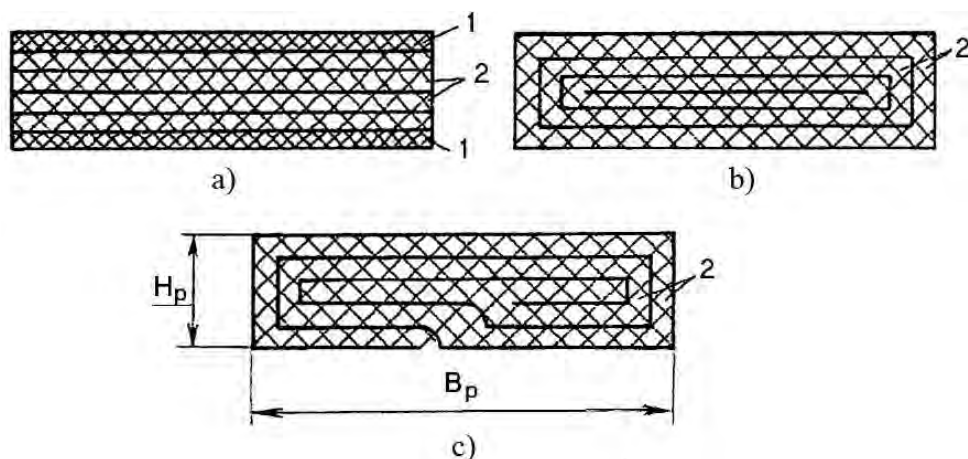


Fig. 1.3. Designs of rubber-fabric belts: a) cut with facings (type A);
 b) wrapped up in layers with facings (without facings) (type B);
 c) spirally wrapped up without facings (type C); 1 – facing; 2 – layer of multicord fabric

Tab. 1.1. Main parameters of rubber-fabric belts

Number of layers i	Belting Б-800 and Б-820				БКНЛ-65 and БКНЛ-65-2			
	with facings		without facings		with facings		without facings	
	H_p , mm	d_{1min} , mm	H_p , mm	d_{1min} , mm	H_p , mm	d_{1min} , mm	H_p , mm	d_{1min} , mm
2	3.0	90	2.5	80	-	-	-	-
3	4.5	140	3.75	112	3.6	112	3.0	90
4	6.0	180	5.0	140	4.8	140	4.0	112
5	7.5	224	6.25	180	6.0	180	5.0	140
6	9.0	280	7.5	224	7.2	200	6.0	180

B_p , mm	20, 25, 30, 40, 50, 63, 71	80, 90, 100, 112	125, 160, 180, 200, ...
i	2 ... 5	3 ... 6	4 ... 6

Single-cord rubber belts (Fig. 1.4) are made in accordance with TU 38105514-77. The bearing layer represents a lavsan single-cord 0.9...1.1 mm in diameter, coiled in the line of a helix. A thin polyamide film may be used to increase the friction force on the working surfaces of a belt (Tab. 1.2).

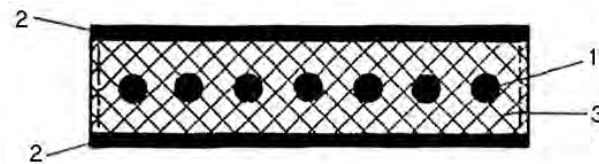


Fig. 1.4. Design of a single-cord belt: 1 – single-cord; 2 – facing; 3 – filler (rubber)

Tab. 1.2. Main parameters of single-cord belts

Width of belt B_p , mm	Maximum deviation of width		Thickness of belt H_p , mm	Maximum deviation of width, mm	Internal length of belt L_p , mm
	%	mm			
30	±1	±0.3	2.2	±0.5	500, 550, 600, 650, 700, 750, 800, 850, 900, 1000, 1050, 1100, 1150, 1200, 1250, 1700, 1800, 2000, 2500, 3000
40	±1	±0.4	2.2	±0.5	
50	±1	±0.5	2.2	±0.5	
60	±1	±0.6	2.8	±0.5	

Kapron belts with polyamide coating (Fig. 1.5) are made in accordance with OST 1769-84 of kapron fabric with a polyamide impregnation. The external surface of belts is covered with a film on the basis of polyamide with nitril rubber, which ensures the improved adhesion of a belt with pulleys (Tab. 1.3).

Tab. 1.3. Main parameters of kapron belts

Width of belt B_p , mm	Maximum deviation of width, mm	Thickness of belt H_p , mm	Internal length of belt L_p , mm
10	±0.25	0.5	250, 260, 280, 300, 320, 340, 350, 380, 400, 420, 450, 480, 500, 530, 560, 600, 630, 670, 710, 750, 800, 850, 900, 950, 1000, 1060, 1120, 1180, 1250, 1320, 1400, 1500, 1600, 1700, 1800, 1900, 2000, 2120, 2240, 2360, 2500, 2650, 2800, 3000, 3150, 3350
15	±0.25	0.5	
20	±0.25	0.5	
25	±0.5	0.5	
30	±0.5	0.7	
40	±0.5	0.7	
50	±0.5	0.7	
60	±0.5	0.7	
80	±0.5	0.7	
100	±0.5	0.7	

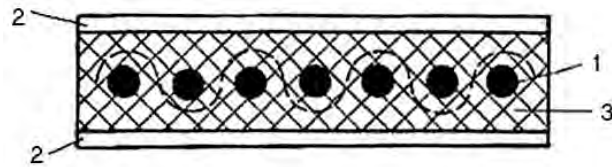


Fig. 1.5. Design of a kapron belt with polyamide coating:

1 – kapron fabric with polyamide impregnation; 2 – film on the basis of polyamide with nitril rubber; 3 – filler (rubber)

Tape-cord polyamide belts, produced by the corporation "Siegling", are of three types: Extremultus-85; 80 and 81 (Fig. 1.6). Such belts are characterized by high acceptable speeds of a belt up to 100 m/s and by specific transmitted powers up to 1...5 kW/mm.

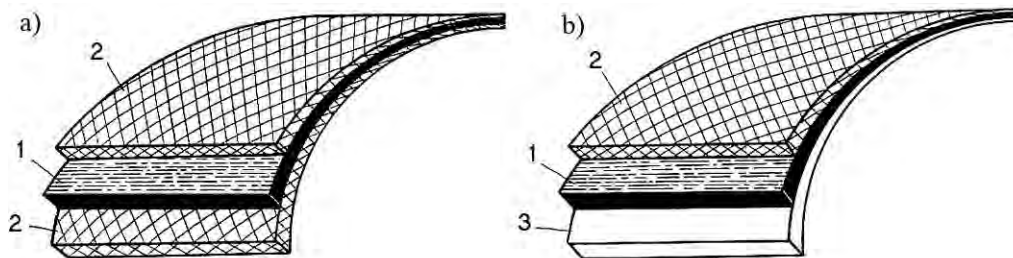


Fig. 1.6. Design of tape-cord polyamide belts:

a) with two-sided transmission of power; b) with one-sided transmission of power;
1 – tape-cord traction layer; 2 – adhesive layer; 3 – polyamide protective coating

1.1.2. V-belt transmissions.

In due time V-belt transmission (Fig. 1.7) was a product of perfecting of a flat-belt transmission. It also carries out transmission of loading (power) due to the friction forces, arising between working surfaces of a belt and pulleys.

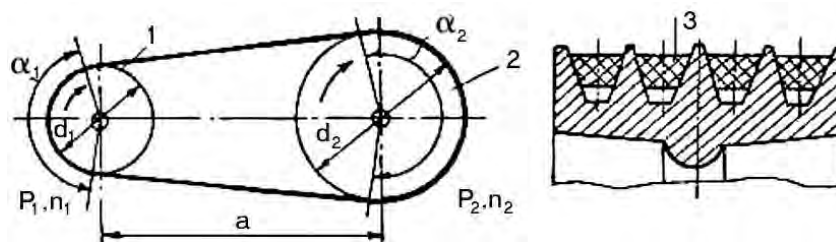


Fig. 1.7. Scheme of V-belt transmissions: 1, 2 – pulleys, 3 – belts

Merits: the simplicity of a design, smoothness and noiselessness of operation, low accuracy requirements to the arrangement of details of transmission, protection from an overload due to the possibility of a belt slipping on a pulley.

Demerits: large dimensions, variability of a reduction ratio in view of elastic sliding, a large loading on shafts and supports, low durability of a belt.

The transmitted power is up to 50 kW, reduction ratio is up to 7 (for transmissions with a tension roller is up to 10), efficiency is 0.94...0.97, **speed of a belt is 25...30 m/s** (with steel cable is up to 60 m/s).

In accordance with GOST 1284.1-89, 1284.2-89 V-belts of a general purpose can have seven various sections: O (Z), A (A), Б (B), В (C), Г (D), Д (E), E. The load element can be presented with a layer of fabric (multicord belts) or cord in the form of polyamide cord or steel cable (single-cord belts) (Fig. 1.8). Rubber is the filler, ensuring elasticity of a belt, and the fabric facing protects a belt from the wear process and increases its durability.

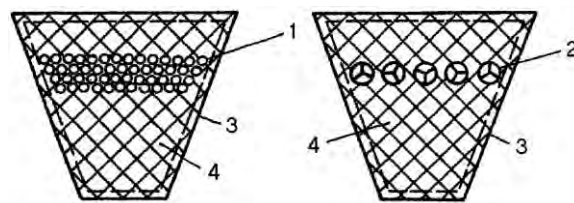


Fig. 1.8. V-belts: 1 – multicord; 2 – single-cord; 3 – facing; 4 – filler (rubber)

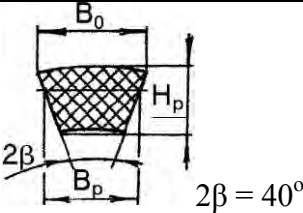
Narrow belts of the following sections **УО** (3У), **УА**, **УБ** (5У), **УВ** (8У) are produced for the agricultural machinery and automotive-tractor industry. They possess higher traction ability due to the better loading distribution of a bearing layer across the width.

The main parameters of V-belts are presented in Tab. 1.4.

1.1.3. Poly-V-belt transmissions.

Poly-V-belt transmissions refer to a class of transmissions of power by flexible link by means of friction forces between a belt and pulleys. Alongside with the demerits of belt transmissions (variability of a reduction ratio as a consequence of elastic sliding of a belt; significant loadings on shafts and supports in view of a cantilever arrangement of pulleys and a preliminary tension of a belt that provides receiving of demanded friction forces on the arcs of contact of pulleys; low durability of belts; lowered efficiency due to elastic

Tab. 1.4. Sizes and parameters of cross-sections of V-belts

							
Section of belt	B_p , mm	Torque T_{1p} , Nm	B_0 , mm	H_p , mm	Area of section A , mm ²	Minimum calculated diameter of pulley d_{1min} , mm	Length of belt L_p , mm
1	2	3	4	5	6	7	8
1	2	3	4	5	6	7	8
O (Z)	8.5	<30	10.0	6.0	47.0	63	400...2500
A (A)	11.0	15...60	13.0	8.0	81.0	90	560...4000
Б (B)	14.0	50...150	17.0	11.0	138.0	125	800...6300
В (C)	19.0	120...600	22.0	14.0	230.0	200	1800...10600
Г (D)	27.0	450...2400	32.0	19 (20)	476.0	315	2800...15000
Д (E)	32.0	1000...5000	38 (40)	24 (25)	692.0	500	4000...18000
E	42.0	>1500	50.0	30.0	1170.0	800	2800...8000
VO (3 V)	8.5	<150	10 (9.5)	8.0	56.0	63	630...4000
YA	11.0	90...400	13.0	10.0	97.0	90	800...4500
YB (5 V)	14.0	300...2000	17.0	13.0	159.0	140	1250...8000
YB (8 V)	19.0	>1500	22 (25.4)	18 (22.2)	278.0	224	1800...8000

sliding and slipping; significant dimensions) poly-V-belt transmissions have a range of positive features:

- poly-V-belts are thinner and less rigid in comparison with V-belts, which allows to diminish the dimensions of transmission, owing to reducing of diameters of pulleys, and to use polyV-belt transmissions at belt speeds up to 40 m/s and the reduction ratio up to 15;

- inaccuracy of fabrication of pulleys and belts has less influence on working ability of transmission;

- section of a belt is used more rationally, which leads to the improvement of its load carrying capacity and durability;

- at the equal transmitted loading the width of poly-V-belts is rather less than the width of a set of V-belts, which allows to diminish the dimensions and mass of transmission in comparison with V-belt transmission, and also to diminish loadings on shafts and supports of transmission due to reducing of the length of a cantilever part of pulleys;

- poly-V-belts ensure more uniform distribution of loading on a working surface, which also promotes the reduction of dimensions of transmission;

- poly-V-belt transmissions are characterized by the improved smoothness of operation, the lowered elastic sliding and they provide more constant reduction ratio.

The more strict requirements to nonparallelism of shafts and the axial displacement of pulleys are considered to be the essential demerit of polyV-belt transmissions.

The belts of three sections are produced: K (J), II (L) and M. The belt of section K (J) is used instead of V-belts O and A at torque $T_1 \leq 40 \text{ Nm}$; the belt of section II (L) – instead of V-belts A, Б and B at $T_1 = 18 \dots 400 \text{ Nm}$; the belt of section M – instead of V-belts B, Г, Д and E at $T_1 > 130 \text{ Nm}$.

The efficiency of transmission is 0.9...0.98 at $v < 25 \text{ m/s}$; it goes down with the increase of a belt speed.

Poly-V-belts are made endless and flat with the edges on the internal surface that get into grooves of pulleys (Fig. 1.9).

The distinctive feature of polyV-belts, providing solidity of the whole design, is a spirally coiled single-cord (Fig. 1.10). The external (non-working) surface of a belt is ground or covered with fabric. Sometimes teeth are formed on the external surface of a belt to raise its flexibility. The accuracy of a belt edge step should be high enough.

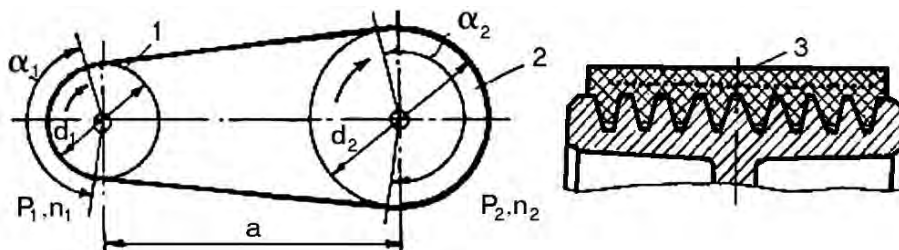


Fig. 1.9. Scheme of poly-V-belt transmissions: 1, 2 – pulleys; 3 – belt

It should be noted that the belts, produced by various corporations, are not interchangeable. Thus, poly-V-belts, produced in the CIS countries, correspond only to the belts of the "Bando" corporation (Japan). The belt edge step of other manufacturers has the following values: 2.34; 4.76 and 9.40 mm ("Hutchinson", France); 2.38; 4.76 and 9.52 mm ("Good Year", USA).

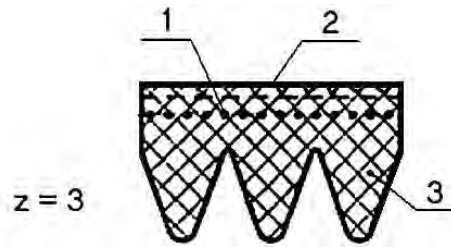


Fig. 1.10. Design of a poly-V-belt:

1 – single-cord (viscose, lavsan, fiber glass); 2 – facing; 3 – filler (rubber)

The parameters of polyV-belt transmissions are specified by TU 38205763-84 (Tab. 1.5).

Tab. 1.5. Sizes and parameters of cross-sections of poly-V-belts

Type of belt	T_1 , Nm	d_{1min} , mm	Number of edges z	Sizes of section, mm							Length of belts L_p , mm
				t_p	H_p	h_p	R_1	R_2	h_0	δ	
K (J)	<40	40	2...36	2.4 ± 0.02	4.0 ± 0.5	2.35 ± 0.1	0.1	0.4	3.3	1.0	400... 2000
II (L)	18...4000	80	4...20	4.8 ± 0.03	9.0 ± 0.7	4.85 ± 0.15	0.2	0.7	6.6	2.4	1250... 4000
M	>130	180	2...20	9.6 ± 0.05	16.5 ± 1.0	10.35 ± 0.2	0.4	1.0	13.05	3.5	2000... 4000

1. The calculated lengths of belts should be accepted from the following numbers: 400, 450, 500, 560, 630, 710, 800, 900, 1000, 1120, 1250, 1400, 1600, 1800, 2000, 2240, 2500, 2800, 3150, 3550, 4000.

2. The angles of a belt profile and pulley grooves for all the sections are $\varphi = 40^\circ$.

1.1.4. Toothed-belt transmissions.

The toothed-belt transmission that combines the merits of transmissions by flexible link and gearing is the most perspective kind of a mechanical transmission of power by flexible link for force and kinematic drives of different machines and mechanisms.

The main advantages of toothed-belt transmissions are:

- availability of high belt speeds (up to 120 m/s);
- sufficiently high durability of details of transmission (shafts, bearings) in view of low values of a preliminary belt tension;
- low specific consumption of materials, combined with a minimum belt mass per unit of transmitted power;
- high values of transmitted power (up to 1000 kW) and a torque (up to 8000 Nm);
- temperature range of belt operation from -55 up to +1000°C;
- efficiency up to 98 %;
- essentially less heating of a belt as a result of its low bending rigidity and absence of sliding on pulleys;
- synchronism of shaft rotation with a reduction ratio up to 400;
- diameter of pulleys from 13 mm, length of belts up to 30 m and more;
- workability of belts in mechanisms of reciprocating precision movement with the **accuracy of positioning $\pm 0,05$ mm;**
- effective operating in a reverse condition;
- compactness, absence of greasing.

The above merits of toothed-belt transmissions have predetermined their broadest introduction in various spheres of modern machinery (Fig.1.11, 1.12):

- avia and rocket production, shipbuilding;
- automobile, road, agricultural and other mobile civil and military equipment;
- machine tools, presses, lifts, compressors, ventilators, pumps, generators, elevators, centrifuges, robotized systems, systems of loading-unloading;
- food, tobacco, shoe, sewing, knitting, textile, fitting, pharmaceutical, wood, paper, building, polygraphic and other industries;
- manufacture of packaging, ceramic tiles, bottles, synthetic filaments, artificial fur, glass, etc.;
- conveyers, automatic doors, escalators, lifts;
- office and home appliances (printers, scanners, copiers, photo and film cameras, multipurpose kitchen processors, electromeat grinders, washing machines, electroinstruments);
- printing of travel cards, trading and slot machines;
- etc.

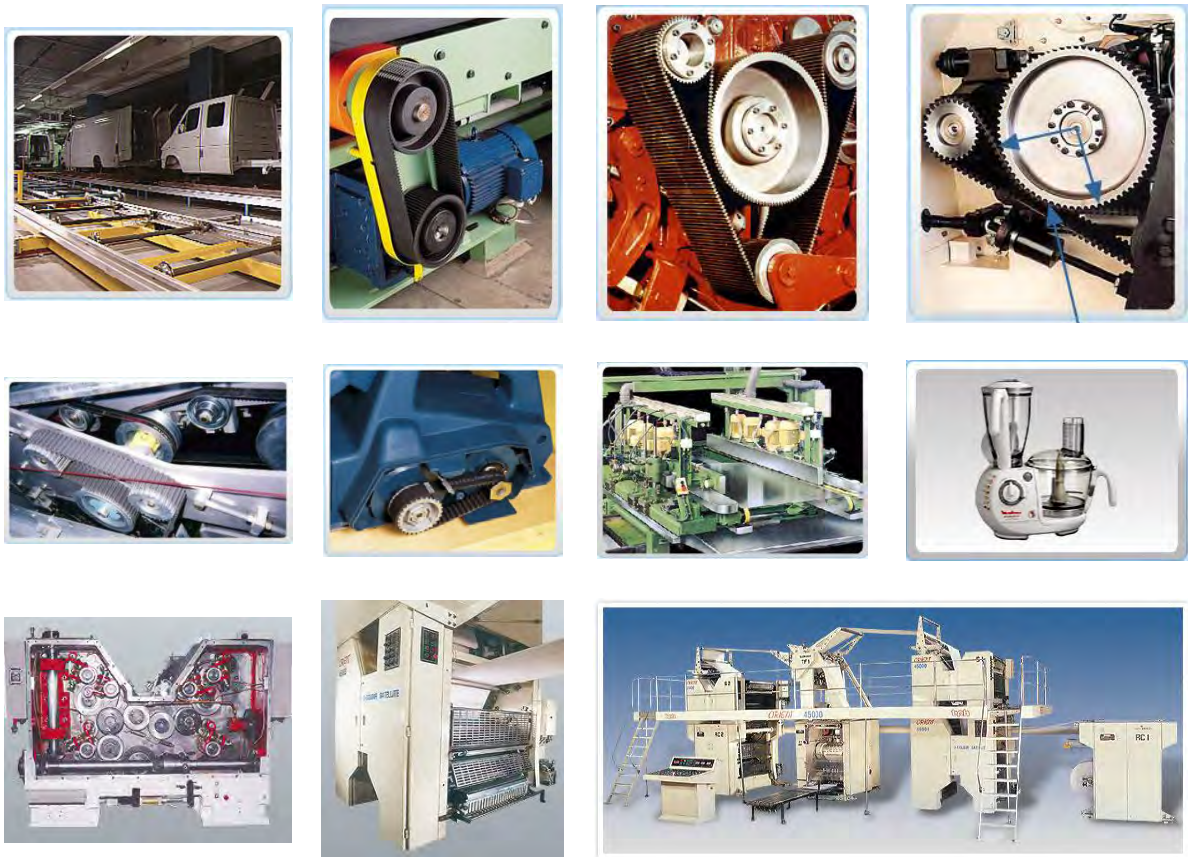


Fig. 1.11. Some areas of application of toothed-belt transmissions



Fig. 1.12. Motorcycle BMW F650 CS with a toothed-belt drive, power of the drive 50 h.p.

Toothed-belt transmissions consist of drive, one or several driven and tension (if necessary) pulleys, a drive-toothed belt, and they relate to the class of transmissions with gearing by flexible link (Fig. 1.13) [1, 2, 3]. Toothed belts are basically made as endless and flat with teeth on the internal surface that input in gearing with teeth of pulleys.

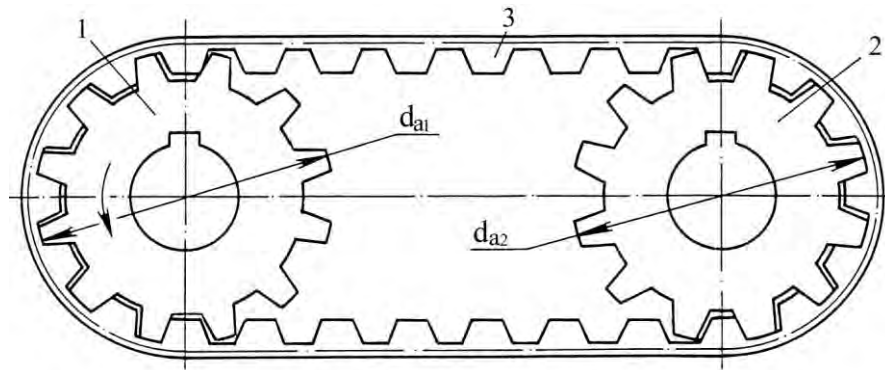


Fig. 1.13. Scheme of a toothed-belt transmission:
 1 – drive pulley, 2 – driven pulley; 3 – toothed belt

The technique of a toothed-belt manufacture is one of the factors, defining its design. Now there are two basic production techniques of belts: moulding in press tools and pressing in a diaphragm autoclave.

The method of moulding is fulfilled in hydraulic presses with flat warmed plattens. The distinctive feature of such belts is the existence of a technological groove in the interdental space and the absence of wear-resistant fabric facing on teeth (Fig. 1.14, a).

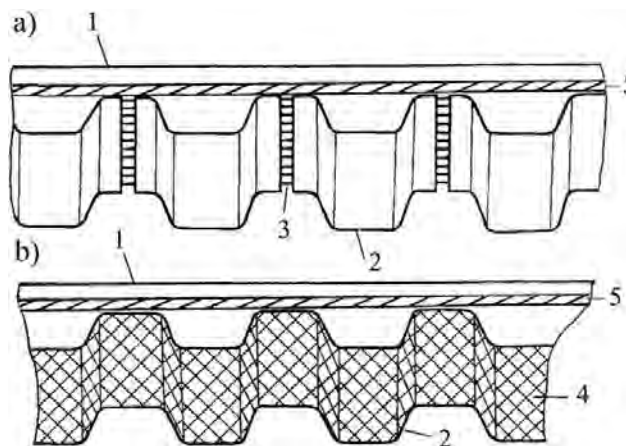


Fig. 1.14. Toothed belts: a) mould; b) assembly; 1 – body of a belt; 2 – teeth;
 3 – technological groove; 4 – wear-resistant fabric facing; 5 – bearing layer

The belts, made by pressing in an autoclave, have a wear resistant coating of working surfaces of teeth (Fig. 1.14, b).

Drive-toothed belts represent the rubber-cord designs, consisting of three basic elements: 1) bearing layer, transmitting a pull; 2) facing material, ensuring antiwear properties of a belt; 3) filler, giving solidity to a belt and linking its elements.

Toothed belts have standard geometrical sizes. The belts with a trapezoidal profile of teeth are mostly used. The parameters of toothed-belt transmissions are specified by TU RB 00149438-073-95. The foreign manufacturers of belts are guided by ISO 5296 and DIN 7721 (Tab. 1.6).

The industrial operation of toothed belts with a trapezoidal profile of teeth has shown that they are not characterized by high operation figures. The teeth of the given belts, which operational resource and load carrying capacity is rather less than of a bearing layer, have the least durability.

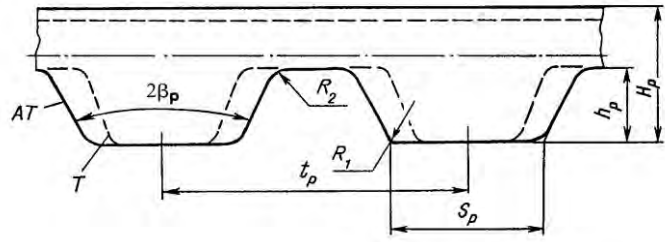
Tab. 1.6. Geometrical parameters of belts with trapezoidal teeth

Defining parameter		Value, designation	Step of teeth t_p , mm	Sizes of section, mm					
				H_p	h_p	S_p	R_1	R_2	$2\beta_p$
OST	Module m	1.0	3.14	1.6	0.8	1.0	0.2	0.2	50
		1.5	4.71	2.2	1.2	1.5	0.3	0.3	50
		2.0	6.28	3.0	1.5	1.8	0.4	0.4	50
		3.0	9.42	4.0	2.0	3.2	0.5	0.5	40
		4.0	12.57	5.0	2.5	4.4	1.0	1.0	40
		5.0	15.71	6.5	3.5	5.0	1.2	1.2	40
		7.0	21.99	11.0	6.0	8.0	1.5	1.2	40
		10.0	31.42	15.0	9.0	12.0	2.0	1.5	40
ISO	Step of teeth t_p	<i>MXL</i>	2.032	1.1	0.51	0.76	0.127	0.127	40
		<i>XL</i>	5.080	2.3	1.27	1.37	0.38	0.38	50
		<i>L</i>	9.525	3.6	1.9	3.25	0.51	0.51	40
		<i>H</i>	12.700	4.3	2.29	4.43	1.02	1.02	40
		<i>XH</i>	22.225	11.2	6.35	7.94	1.57	1.2	40
		<i>XXH</i>	31.750	15.7	9.53	12.2	2.28	1.52	40
DIN	Step of teeth t_p	<i>T2.0</i>	2.0	1.1	0.5	0.7	0.2	0.2	40
		<i>T2.5</i>	2.5	1.3	0.7	1.0	0.2	0.2	40
		<i>T5</i>	5.0	2.2	1.2	1.8	0.4	0.4	40
		<i>T10</i>	10.0	4.5	2.5	3.5	0.6	0.6	40
		<i>T20</i>	20.0	8.0	5.0	6.5	0.8	0.8	40

The failure of standard trapezoidal belts in gas-distributing mechanisms of automobile drives led to engineering of belts of series **AT** (automobile transmitting) (Tab. 1.7) that have larger profile of teeth, which allows augmenting of the transmitted load up to 30 %.

The process of gearing of teeth is accompanied by the interference of teeth of a belt, being more compliant in comparison with teeth of pulleys, and also by their sliding under loading. The combination of these factors leads to the accelerated wear of teeth of a belt.

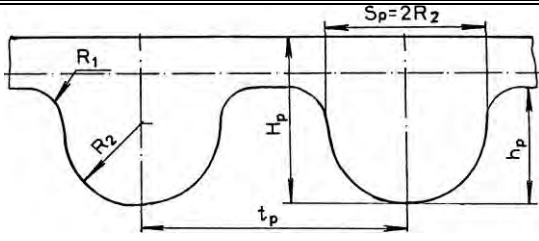
Tab. 1.7. Geometrical parameters of toothed belts of series **AT**



Designation	t_p , mm	S_p , mm	h_p , mm	R_1 , mm	R_2 , mm	H_p , mm	$2\beta_p$
AT5	5.0	2.5	1.2	0.86	0.4	2.7	50
AT10	10.0	5.0	2.5	1.25	0.4	4.5	50
AT20	20.0	10.0	5.0	2.5	1.75	8.0	50

The partial amendment of the above-stated demerits was carried out in the design of a toothed-belt transmission with a semicircular profile of teeth *HTD* (Tab. 1.8).

Tab. 1.8. Geometrical parameters of toothed belts of profile *HTD*



Designation	h_p , mm	R_1 , mm	R_2 , mm	H_p , mm	t_p , mm
1	2	3	4	5	6
1	2	3	4	5	6
<i>m3</i>	4.0	1.0	2.5	6.0	9.42
<i>m4</i>	5.0	1.0	3.5	7.5	12.57
<i>m5</i>	6.0	1.5	4.5	9.0	15.71
3M	1.17	---	0.85	2.41	3.0
5M	2.1	---	1.41	3.6	5.0
8M	3.4	---	2.45	5.6	8.0
14M	6.1	---	4.31	10.0	14.0

The failures, arising in the process of operation of toothed-belt transmissions, are arranged on its elements extremely irregularly. The breakdown of pulleys of transmission is unlikely and characteristic of the constructions made of nonmetallic materials [4]. The wear-out probability of pulleys of reinforced plastics, for example textolite, or made of aluminium alloys is of no account. The resource of pulleys made of steel, crute-iron, ceramic composites is practically unlimited.

Thus, the increase of carrying capacity and an operation resource of toothed-belt transmissions are possible on the basis of improving of figures of working ability of toothed belts. There are three main directions of solution of the problem (Fig. 1.15).

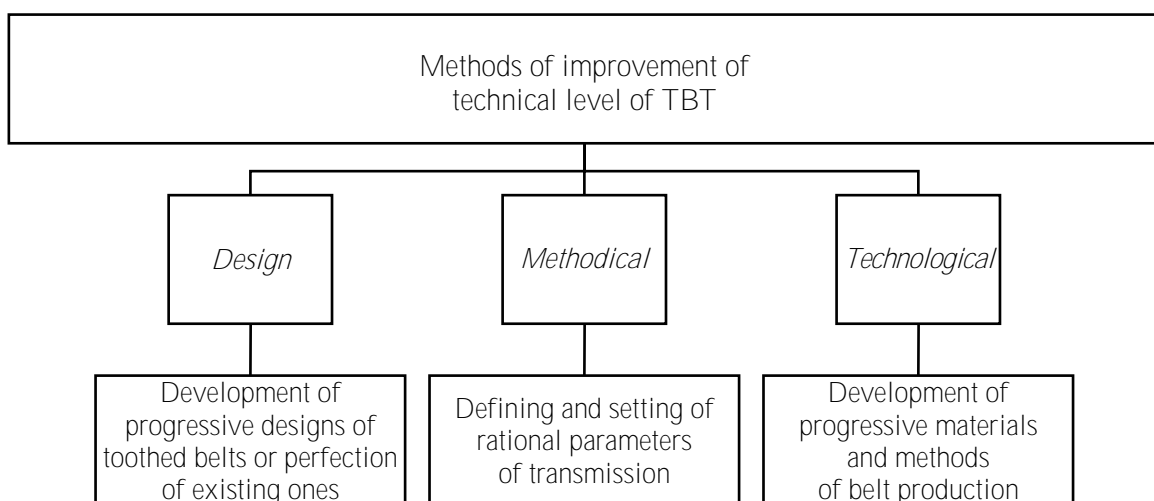


Fig. 1.15. Methods of improvement of a technical level of toothed-belt transmissions

The analysis of the world scientific and technical literature testifies that the greatest number of scientific works is devoted to the development of the design direction which does not need extensive theoretical and experimental studies of physicomechanical qualities of a belt, the conditions of its gearing with pulleys, etc. In this particular case the existence of systematized, statistically adapted results of reasons of belt failures in the operational process is enough. It is necessary to note that the development of toothed-belt designs take place in two ways. On the one hand, standard profiles of belts are being perfected, which enables to maintain the attained level of unification. On the other hand, new types of toothed belts with non-standard working geometry are developed.

One of the main actions in the design of belts, enabling to improve a carrying capacity and durability of standard belts is their reinforcement. There are two types of reinforcement: micro- and macroreinforcement.

Microreinforcement represents a substitution of a part of teeth of a belt, made of rubber or polyurethane by a composite on rubber or other polymeric base. The composite contains the fragments of glass, viscose or metal fibers 0.5...2 mm length, treated by adhesive compositions.

The results of researches have shown, that fatigue strenght of teeth, made of rubber reinforced with pieces of viscose fiber, and impregnated with latex L-19f (Fig. 1.16, a), is augmented by 50 % [5].

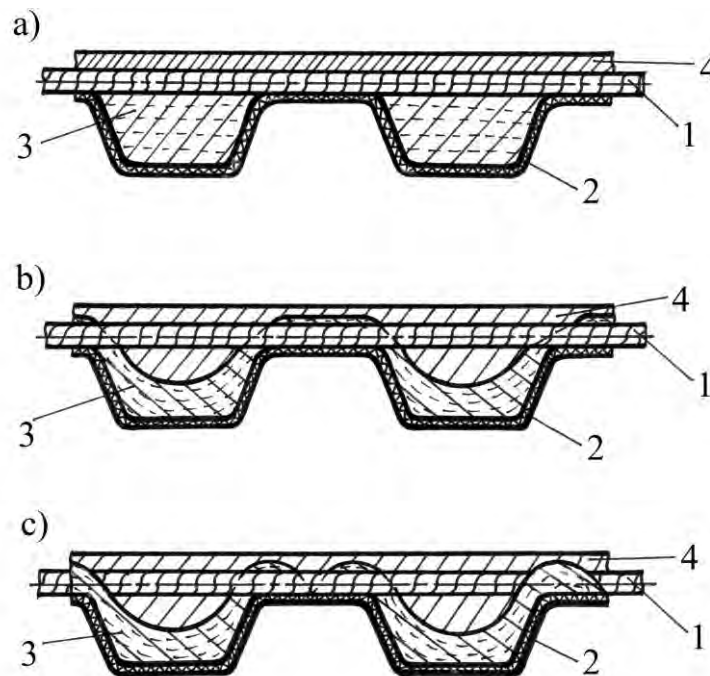


Fig. 1.16. Toothed belts with microreinforcement: a) continuous microreinforcement of teeth; b) rational microreinforcement; c) microreinforced belt with diminished bending rigidity; 1 – bearing layer; 2 – facing fabric; 3, 4 – reinforced and non-reinforced rubber

The analysis of the stress-deformed state of teeth of belts testifies to their substantial irregularity of their loading, therefore it is expedient to reinforce not the whole tooth, but only the most loaded parts of it (Fig. 1.16, b) [6]. The part of reinforced rubber can be made with an arc-wise hollow to increase flexibility of a belt (Fig. 1.16, c) [7].

Raising of efficiency of reinforcement of belts is reached by giving some special direction to fibers that coincides with the direction of operation of shifting forces. Despite of the advantages of the belts reinforced by fibers, they have not received wide introduction because of the absence of effective technique of their production.

Their macroreinforcement, for example, coverage of teeth by an additional layer of facing fabric helps to raise carrying capacity and durability of drive-toothed belts considerably [8]. This action allows augmenting transmitted pull by 35 % at durability of 10^7 cycles, and by 25 % – at durability of 10^8 cycles.

The designs of toothed belts reinforced by loose leaves (from one up to three), placed longitudinal plane of teeth (Fig. 1.17) [9] have been developed.

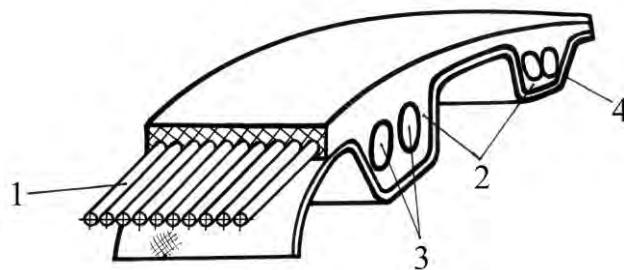


Fig. 1.17. Toothed belt reinforced by loose leaves:
1 – bearing layer; 2 – toothed of a belt; 3 – loose leaves; 4 – facing

It is offered to make loose leaves in a form that corresponds to a profile of teeth of a belt. (Fig. 1.18) [10].

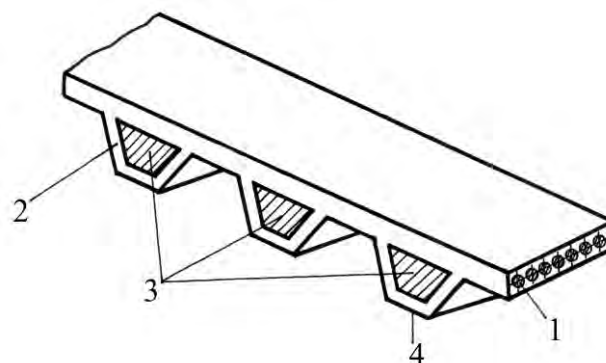


Fig. 1.18. Toothed belt reinforced by profile loose leaves:
1 – bearing layer; 2 – tooth of a belt; 3 – profile loose leaves; 4 – facing

With the same purpose it is recommended to place armature in the zones of density of stresses (Fig. 1.19) [11].

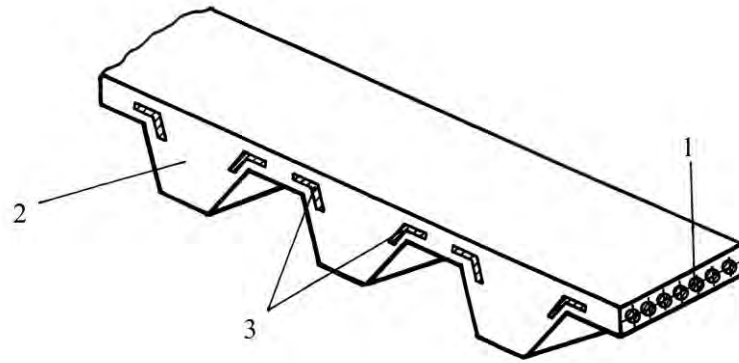


Fig. 1.19. Toothed belt reinforced by loose leaves in zones of density of stresses:
1 – bearing layer; 2 – tooth of a belt; 3 – loose leaves

The main demerits of the above mentioned designs are increased mass and bending rigidity of belts. Alongside with it, shifting stresses in elastomer, located between a bearing layer and reinforcing elements are considerably augmented.

It is offered to use spiral or profile springs for reducing mass and bending rigidity of belts (Fig. 1.20) [12, 13].

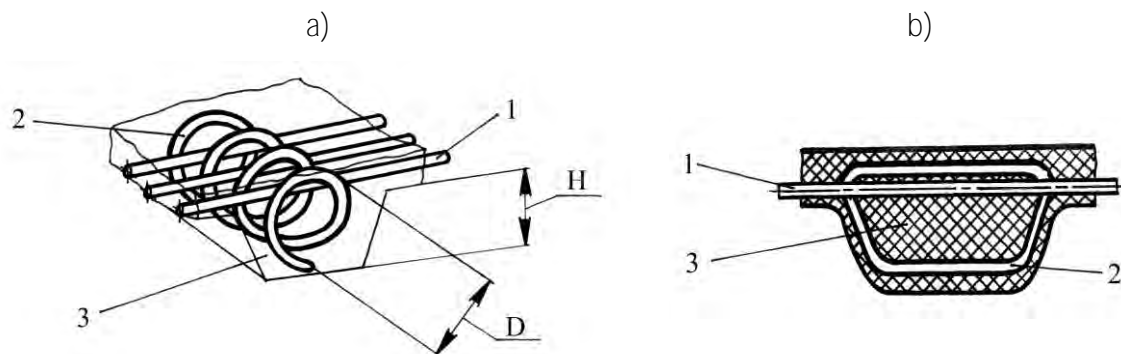


Fig.1.20. Toothed belt reinforced by spiral (a) and profile (b) springs:
1 – bearing layer; 2 – spring; 3 – tooth of a belt

The elimination of shifting stresses in elastomer, located between a bearing layer and reinforcing elements, is reached in the designs of belts with mechanical fixing of armature to a bearing layer. Toothed belts of such a type represent a tape with holes over teeth, and the armature is supplied with thread holes [14]. Belts with screwed teeth or reinforcing elements (Fig. 1.21) [15] are also known.

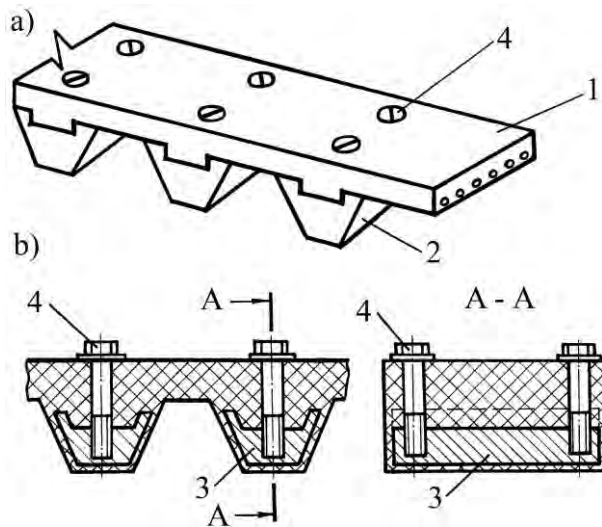


Fig. 1.21. Toothed belts with mechanical fixing of teeth or reinforcing elements:
 a) with mechanical fixing of teeth; b) with mechanical fixing armature;
 1 – framework of a belt; 2 – teeth; 3 – reinforcing elements; 4 – fastening parts

Despite of their advantages (high durability, maintainability) the given belts have not received wide introduction in view of their nonadaptability to manufacture and labor content of service. Besides the holes in a tape are the concentrators of stresses.

The authors of the research works [16, 17] have developed toothed belts with a bearing layer in the form of a metal tape in width 0.08...0.12 mm. The mechanical link of elastomer with a bearing layer is carried out with tabs of the various shape (Fig. 1.22).

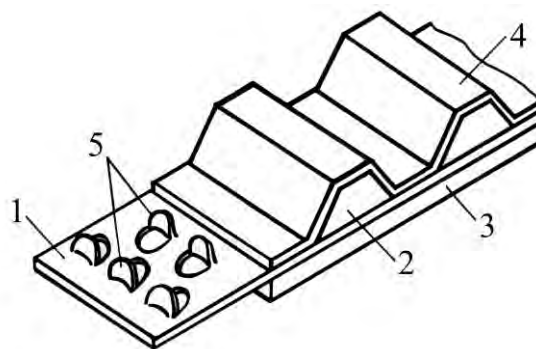


Fig. 1.22. Belt with a framework of a metal tape: 1 – load tape;
 2 – teeth; 3 – elastomer; 4 – facing fabric; 5 – tabs

The given belts possess the high longitudinal rigidity and the highest fatigue durability of teeth, in comparison with the above designs [18]. The main disadvantage is the raised bending rigidity of a belt. The continuous perforation of a tape or the heightened tension of a belt, which leads to lowering of durability of a belt and other details of transmission (shafts, bearings), is necessary for its lowering. The increase in the drive vibration and the decrease of its efficiency is possible.

The construction of a toothed belt with the cross-section reinforcement rods, coiled by loops of the bearing layer (Fig. 1.23) [19], has been developed.

The given belt possesses the high direct and low bending rigidity. Alongside with it, in the given design the mechanical link of armature with the bearing layer is realized, which allows direct transmitting of a pull, escaping intermediate elements. Nevertheless, such belts have not received a wide introduction, because of the nonadaptability to manufacture, caused by the constant change of the armature winding direction.

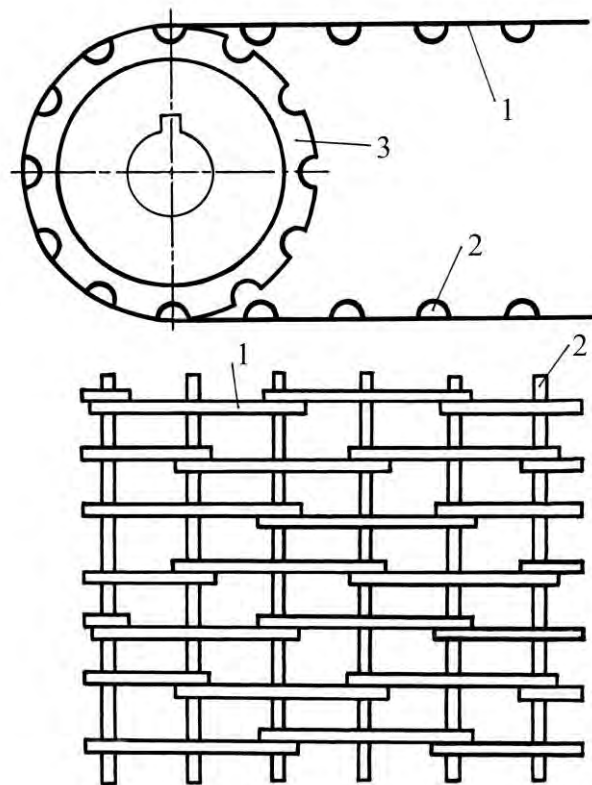


Fig. 1.23. Reinforced toothed belt: 1 – bearing layer; 2 – reinforcing rods; 3 – pulley

Thus, reinforcement does not eliminate the main destructive phenomena, characteristic of toothed-belt gearing, which are defined basically by the geometry of tooth profiles and their kinematic features of their reinterface.

1.2. Geometry and kinematics of toothed-belt gearing

Despite the fact that toothed-belt transmissions with a trapezoidal tooth profile have become widely spread, they have some demerits.

It is underlined in the work [20], that the intersection of the profiles is observed in an input of teeth in gearing. For the elimination of the given phenomenon it is offered to increase **the angle of the profile of teeth up to 25° or the teeth with an involute profile** should be made. The works [21, 22, 23] are devoted to the investigation of the interference of teeth.

The analysis of an input of teeth in gearing (Fig. 1.24) [1] has proved that the interference takes place both at transmitting of a pull, and no-load operation of transmission. Thus, the total interference develops from the profile loading and the interference from the loading [24].

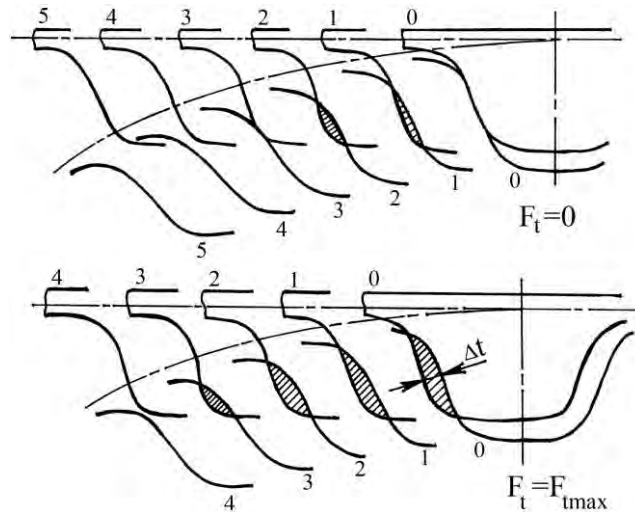


Fig. 1.24. Interference of teeth in a toothed-belt transmission

The interference from loading is practically unrecoverable in view of a high compliance of belt teeth, therefore it is necessary and possible to diminish a profile component of interference.

In the work [22] it is offered to increase the profile angle and radii of rounding of tips of belt teeth and a pulley. In this case, there will be the increase of radial efforts on lateral sides of belt teeth, trying to throw them out from gear. To compensate these efforts heightened pretensioning of a belt is needed.

The belt designs with compliant tips of teeth (Fig. 1.25) [25, 26, 27] have been developed. It is obvious, that the increase in a tangential compliance of belt teeth works towards lowering of the friction force at an input in gearing, but slots, grooves and other hollows are the concentrators of stresses, reducing the load carrying capacity of teeth.

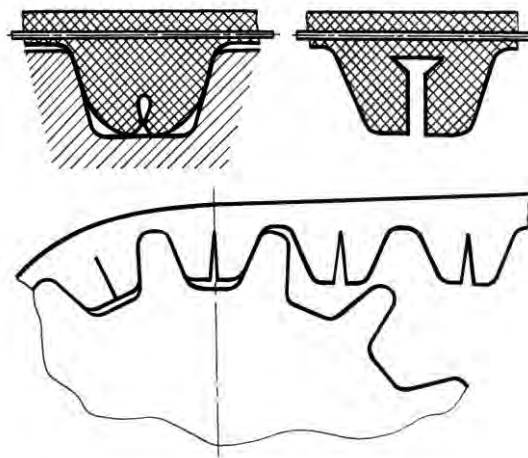


Fig. 1.25. Toothed belts with compliant tips of teeth

The authors [28] have developed the transmission, where the angle of the profile of belt teeth is larger than the angle of the profile of pulley teeth (Fig. 1.26).

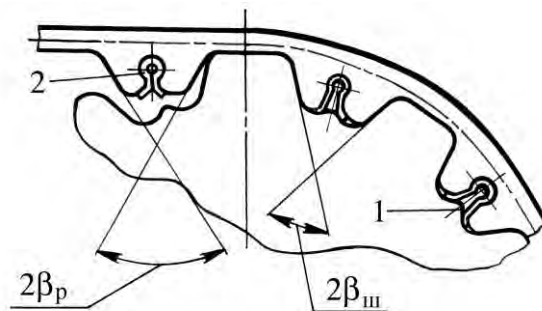


Fig. 1.26. Toothed-belt transmission with the lowered input friction:

1 – protuberance; 2 – loose leaf

The tooth of a belt, inputting in gearing by its tip, interacts with a protuberance on an interdental space of a pulley. The tip of a tooth is pushed apart, providing a firm adherence of profiles. An elastic metal element is inserted in a slit of a tooth for improving its wear resistance.

The above mentioned engineering designs allow lowering of a profile interference of teeth in a different extent. However, the solution of the given problem can be realized on the basis of the analysis of kinematic features of gearing.

Having examined sequential positions of a belt tooth at its input in gearing (Fig. 1.27), it is proved that the movement trajectory is involute with a continuously reducing radius of curvature. At the final stage the tooth moves along an arc of a circle, turning relative to the point P_4 [29, 30]. Thus, lateral surfaces of teeth should be mutually bending around for the elimination of the profile interference.

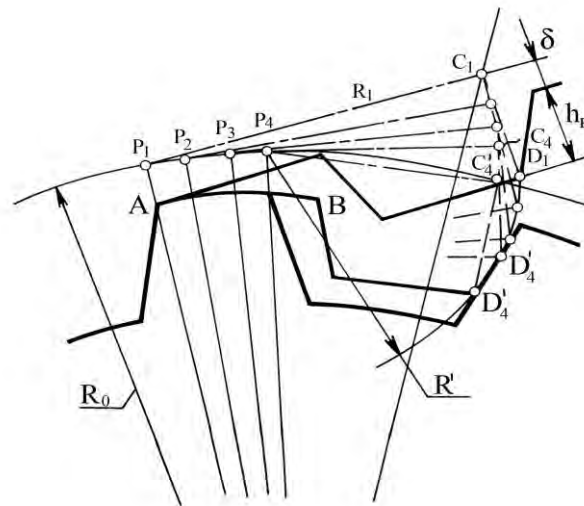


Fig. 1.27. Scheme of formation of the interference of teeth in a toothed-belt transmission

The other main demerit of belts with trapezoidal teeth is a non-uniform distribution of stresses and deformations.

The theoretical and experimental investigations have established that the concentration of stresses is observed in the transition zone of the lateral surface of belt teeth in the interdental space (Fig. 1.28, a) [31, 32, 33, 34], when 2/3 volumes of teeth are practically unloaded. The concentration of shearing stresses takes place on the surface of a bearing layer.

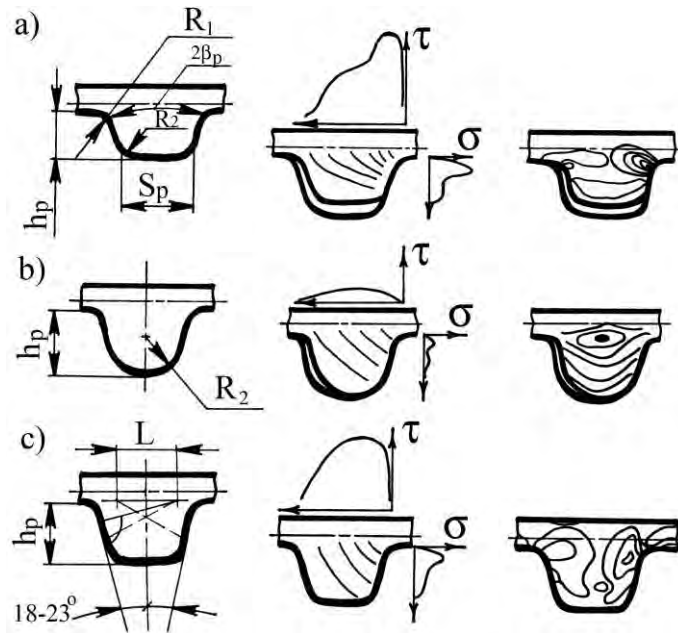


Fig. 1.28. Distribution of normal (σ) and tangent (τ) stresses in teeth of trapezoidal (a), *HTD* (b) and *STS* (c) profiles

In the work [31] it is offered to increase the angle of the profile of a pulley up to 54° , and the radius of rounding of the base of belt teeth – up to $0.2m$ for the elimination of demerits, typical of trapezoidal teeth. It is also offered to increase the radius of rounding of the tips of belt teeth. In the limit it leads to a semicircular profile of teeth *HTD*, similar to **Novikov's tooth transmissions**.

The profile *HTD* was developed by the "Uniroyal" corporation in 1973. [35]. The given profile is characterized by more equal distribution of stresses and deformations (Fig. 1.28, b). The profile interference is lowered 6...8 times, the interference from loading – 1.5 times, which allows to increase a transmitted pull by 20...40 % [36].

The "Pirelli" corporation developed a profile of teeth *STS* (*STPD*) [37] that was received on the basis of the analysis of kinematics of an input of teeth in gearing. The lateral surfaces of teeth are outlined by the arcs of circles with the centers in points (Fig. 1.28, c), corresponding to the center of the turn of belt teeth at the final stage of an input in gearing (see Fig. 1.27). Thus, the profile interference is lowered additionally.

The further development of the profile *STS* is the parabolical profile of teeth *RPP* (Fig. 1.29) [38, 39]. The distinctive feature of the given transmission, alongside with a minimum interference, is the transmission of a part of loading by the tip of the belt tooth, interacting with a protuberance on an interdental space of a pulley. The protuberance rep-

resents an additional tooth of a small length. At its interaction with a groove on the tip of a belt tooth, the tooth is deformed in a vertical direction, filling an interdental space of a pulley, and providing more equal distribution of stresses.

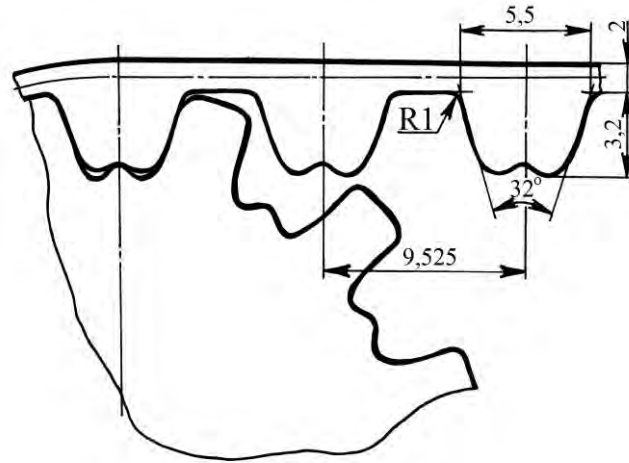


Fig. 1.29. Transmission with teeth of *RPP* profile

The overwhelming majority of the works, devoted to the investigation of kinematics of toothed-belt transmissions, were based on idealized geometry of teeth that were regarded as trapezoids without radii of rounding of tips and spaces. However, the total length of the rounded parts for belts of the various modules comes up to 60 % of the total tooth length.

Basing on the real geometry of trapezoidal teeth, the author of the work [40] offered the so-called "without an interference" profile. The part of a tooth is outlined by an involute with the centers of radii on a neutral axis of a bearing layer. The zone of rounding of a tooth tip is outlined by a circular arc with the center in the point, corresponding to the turn of a tooth at the final stage of its input in gearing (Fig. 1.30).

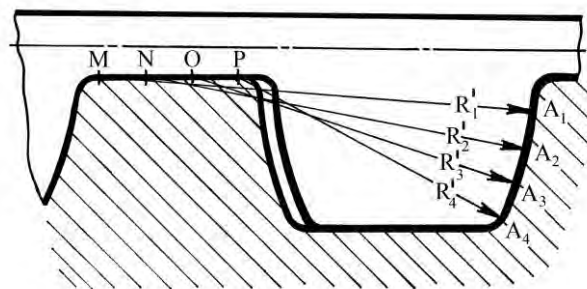


Fig. 1.30. Toothed-belt transmissions with "without an interference" profile of teeth

It should be noted that the development of new designs demands conducting of a complex of operations on their standardization and unification. Therefore, the methodological and technological aspects of the improvement of a technical level of transmission are preferable.

1.3. Load carrying capacity and durability of toothed-belt transmissions

The durability of a toothed-belt transmission is defined by the durability of a toothed belt. The experience of the industrial use and the results of long-run tests testify to the predominance of three main kinds of belt destruction: the fatigue failure and wear of teeth, and also the destruction of a bearing layer (Fig. 1.31).

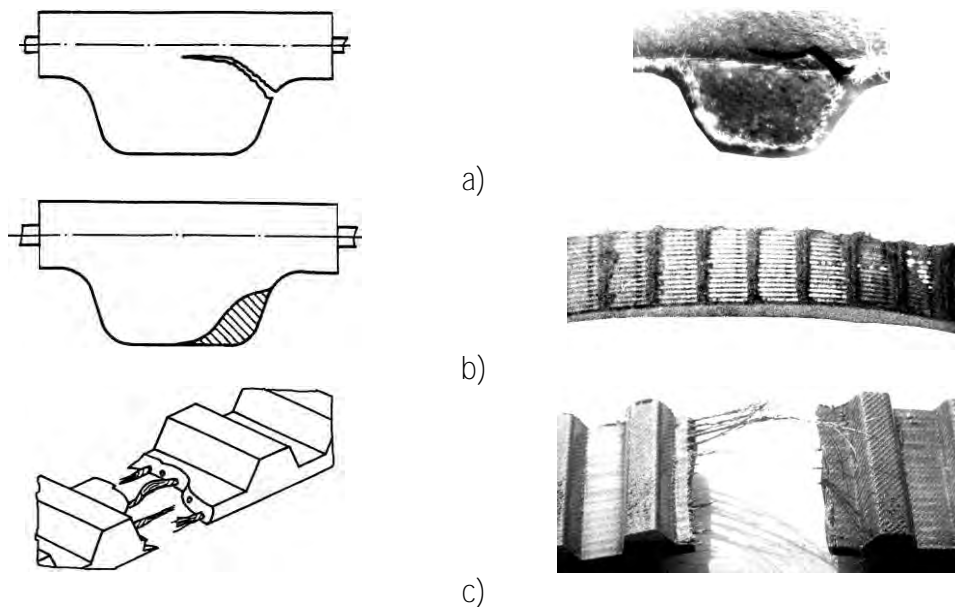


Fig. 1.31. Kinds of the destruction of toothed belts: a) formation of a fatigue crack in the base of a tooth; b) wear of a working profile; c) destruction of a bearing layer

For reducing of transmissions the wear of teeth is mostly observed from the side, interacting with a drive pulley, which results from the kinematic characteristics of reinterface of teeth (Fig. 1.32).

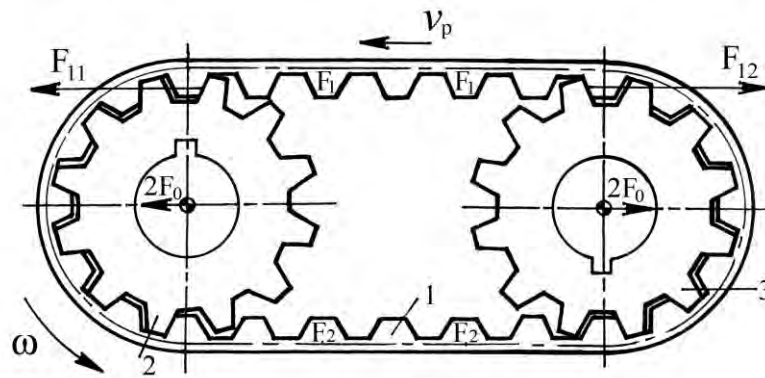


Fig. 1.32. Scheme of tooth loading in a toothed-belt transmission:
 1 – belt; 2, 3 – drive and driven pulleys

The input of teeth in gearing is attended by their mutual sliding. In this case, the increase of loading, which maximum value is observed at the finishing moment of an input in gearing, takes place. The lowering of loading, while the pulley is turning, results from an input in gearing of the subsequent teeth. The combination of sliding and friction forces leads to the wear of belt teeth.

The fatigue failure is observed, as a rule, from the belt teeth, interacting with a driven pulley [23, 41]. It is necessary to note that the existing methods of prediction of the **fatigue durability inadequately reflect the physics of the gearing phenomena, that's why** they should be regarded as estimating phenomena.

The special attention is given to the problem of defining of the intensity of the destructive phenomena. Its solution helps to develop the true methodology of the resource design of toothed-belt transmissions.

The analysis of the results of long-run tests shows that the tooth wear is characteristic of mould belts, and the fatigue failure is characteristic of assembly belts.

In most cases the authors define the resource of belts without differentiating the criteria of their breakdown. So, in the work [42] it is established that at the rotation frequency of a drive pulley $n_1 = 2100 \text{ min}^{-1}$ the durability of assembly belts ($m = 5$ and 7 mm) makes $(2.1...3.1) \times 10^6$ and $(4.2...5.9) \times 10^6$ cycles at the transmitted specific circumferential force $F_t = 32$ and 26.2 N/mm accordingly.

The empirical dependence of the belt durability on its main parameters [41] is also received:

$$L_h = \frac{6,2 \cdot 10^{12}}{(F_t B_p)^{2,5} \omega_1}, \quad (1.1)$$

where L_h – the durability of a belt; F_t – the specific circumferential force; B_p – the width of a belt; ω_1 – the angular velocity of a drive pulley.

However, the expression (1.1) does not allow taking into account the number of teeth of a pulley transmission, mechanical and physical properties of belt elements (the longitudinal rigidity EF and the rigidity of teeth EZ) etc. Besides, it does not reflect the physical phenomena, occurring in gearing at the transmission of power.

The analysis of the phenomena, occurring at the operation of a toothed-belt transmission, shows that there are three varieties of wear of belt teeth: abrasive, frictional and fatigue [24, 43, 44].

The abrasive wear is observed at the existence of the abrasive environment (mineral spots, wear products); the frictional wear is observed **in the case of “dripping”, when the adhesion of a surface layer of elastomer with the basic material is less than with the material of a counterface**; the fatigue wear represents the destruction of a surface layer of elastomer in the result of its frequent deformations.

In mathematical terms the transition from one kind of wear to another is described by means of ratio between the shifting stress τ **in the surface layer of material and its critical value** τ_{cr} , corresponding to the tear of some volume of elastomer. Considering that $\tau = f_{fs} p$, where f_{fs} – the friction factor, p – the pressure in the pair "tooth of a belt – tooth of a pulley", at $\tau / \tau_{cr} > 1$ – **the friction wear and at $\tau / \tau_{cr} < 1$** – the fatigue wear is received.

The fatigue wear is mostly probable at roughness of lateral surfaces of teeth of a pulley $Ra \leq 2.5$ microns.

On the basis of the energetical theory of wear the dependences for the calculation of the belt durability are received. The main equation of the energetical theory [45, 46] takes the form:

$$l = l_0 P_{fr}^x, \quad (1.2)$$

where l – the intensity of wear process; l_0 – the intensity of wear process at the unit power of friction; P_{fr} – the power of friction; χ – the parameter, depending on the type of rubber and on the characteristics of a counterface and loading conditions.

Considering that the power of friction represents the product of the friction force F_{fr} by the speed of tooth sliding v_{st} , divided by the period of one input in gearing, the dependence for the determination of the durability of belt teeth is received in the works [24, 47]:

$$N = \frac{1,6 S_p \lg \left(\frac{1,15 \dots 1,6 \Delta z_1 E Z_d}{F_t \psi} \right) k_f}{h_{t0}} \quad (1.3)$$

where Δ – the tangential shifting movement of the teeth, inputting in gearing; z_1 – the number of teeth of a drive pulley; $E Z_d$ – **the dynamic rigidity of belt teeth**; ψ – the factor of non-uniformity of tooth loading: $\psi = F_{11} z_0 / F_t$; F_{11} – the effort on the first tooth of an arc of contact from the driving side; z_0 – the number of teeth in gearing; k_f – the factor, considering the durability of facing: for assembly belts $k_f = 3.4$; for mould belts $k_f = 1$; h_{t0} – the thickness of a layer on the lateral side of a belt tooth, worn out for one cycle of an input in gearing.

The calculation of the fatigue durability N_f is based on the equation of the fatigue curve:

$$\left(\frac{p_c}{p_b} \right)^{m_n} = \frac{N_b}{N_f} \quad (1.4)$$

where p_c and $[p_b]$ – the calculated and base pressure on lateral sides of teeth; N_b – the base number of load cycles, corresponding to $[p_b]$.

The value $[p_b] = 2.5 \text{ MPa}$ is for rubber belt teeth and $[p_b] = 2 \text{ MPa}$ is for polyurethane belt teeth [33].

The calculated pressure is determined by the expression:

$$p_b = \frac{\psi F_t}{z_0 h_p}$$

The author [24] considers that the dependence (1.4) is characteristic of metal or plastic teeth. In his opinion, for toothed belts the occurrence and distribution of a fatigue crack have adhesive character as it takes place on the dividing line "elastomer – bearing layer". For this case the expression (1.4) should be written in the form:

$$N_f = \left(\frac{\sigma_{ad}}{\sigma_j} \right)^\beta k_f, \quad (1.5)$$

where σ_{ad} – the adhesion strength between a bearing layer and elastomer; σ_j – the stress amplitude, corresponding to the durability N_f ; β – the slope of adherence junction; $k_f = 1.3 \dots 1.7$.

In view of the shape of belt teeth and the features of their deformation, expressed in the predominance of shear deformations, reaching up to 30 % in the total balance, the expression (1.5) is received [24, 47]:

$$N_f = 50 z_2^{-1,8} \left(\frac{\sigma_{ad} h_p E z_2}{0,3 F_t \psi G} \right)^\beta k_f, \quad (1.6)$$

where z_2 – the number of teeth of a driven pulley; G – the module of elastomer shear.

The demerit of the dependence (1.6) is the fact that it describes the destruction of the adherence junction on the boundary "elastomer – bearing layer". However, the fatigue crack originates from the external surface of a belt tooth, where there are no adherence junctions.

It should be noted that the dependences (1.3) – (1.6) are received on the basis of the conjecture that the intensity of both kinds of the destructions of belt teeth is identical, and the occurrence of this or that kind of the destruction depends on the ratio of intensities, in the case of more intensive wear the fatigue crack has no time to develop, since they take place from the opposite sides of a tooth.

Thus, it is necessary to get the dependence of the durability of belt teeth from the main transmission parameters, taking into account the kinematic and power features of the interaction of teeth.

The analysis of the above-stated dependences shows that the methodical way of the increase of the load carrying capacity and durability of belts is not worked out. For example, the expressions (1.3), (1.6) show that at lowering of the factor of non-uniformity of tooth loading the belt durability increases by both criteria. It is proved by the results of the experimental researches [48, 49] (Fig. 1.33).

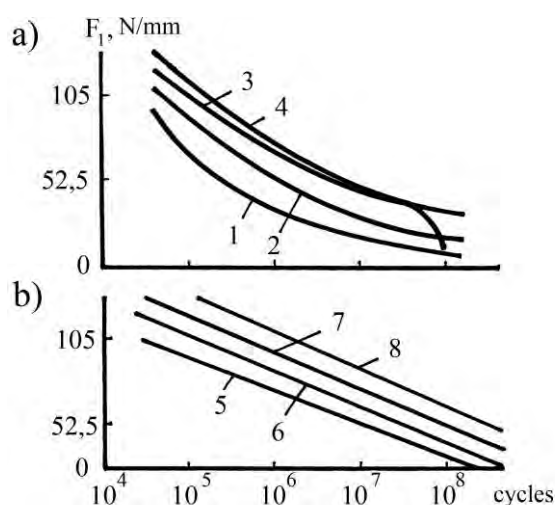


Fig. 1.33. Influence of the effort in the driving side on the durability of mould (a) and assembly (b) belts at the various correction of the step of a pulley tooth $\Delta t_{\text{III}} = t_{\text{p}} - t_{\text{III}}$: +0.017 (1); -0.002 (2); -0.013 (3); -0.022 (4); +0.022 (5); +0.003 (6); -0.018 (7); -0.038 mm (8)

At lowering the correction of the step of a pulley tooth Δt_{III} , compensating elongation of the driving side of a belt, the durability of the belt increases. For assembly belts of the type L with the parameters $t_{\text{p}} = 9.525$ mm; $B_{\text{p}} = 19$ mm; $z_1 = z_2 = 36$, the reduction of Δt_{III} from +0.022 up to -0.038 allows to increase N_{W} by 1...2 orders. The durability of mould belts increases at the reduction of Δt_{III} from +0.017 up to -0.022 to the same extent. At the same time, the choice of the rational value Δt_{III} should be based on the analysis of loading of gearing.

1.4. Force interaction of teeth in gearing

The working ability of toothed belts mostly depends on the distribution of loading in gearing.

The results of the research works [50, 51, 52, 53] testify to the non-uniform distribution of loading in gearing. The most loaded tooth is the one, located at the driving side, i.e. inputting in gearing with a drive pulley. The estimation of its loading is described by the value ψ that should be named as the "factor of an overload of the first tooth" from the methodological point of view. The values of ψ , given in the scientific and technical literature, vary: $\psi = 1.25 \dots 1.7$ [54]; $\psi = 1.5 \dots 2.0$ [53], etc.

Some authors believe that non-uniformity of loading of gearing is caused by the technological errors of a step of teeth [55, 56, 57]. In the works [58, 59] it is established that at the existence of step errors, which do not exceed the maximum permissible values, the vibrations of ψ can reach 100 %.

On the other hand, the essential factors, influencing ψ , are the mechanical properties of a belt (the rigidity of teeth and the longitudinal rigidity) [54].

The account of the mechanical and physical properties of the belt elements leads to receiving the analytical dependences for the calculation of the distribution of loading, which are similar to the calculation of loading of thread turns in a "screw-nut" joint, offered by N.E.Zhukovsky.

On the basis of the calculation of loading of teeth of the arc of contact the values of the correction of the step of pulley teeth, providing the rational ψ , were received (Fig. 1.34) [24].

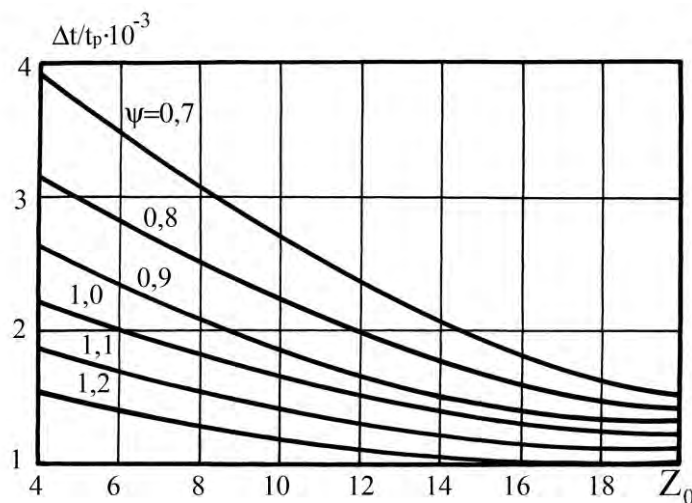


Fig. 1.34. Choice of the value of the correction of the step of pulley teeth on the demanded non-uniformity of loading of teeth

The comparison of the theoretical calculation of loading of gearing with the experimental oscillograms testifies to their essential difference.

The author of the work [60] considers that for the specification of the calculated dependences it is necessary to consider the transmission of a part of the circumferential force by means of the friction forces, arising between the interdental hollows of the belt and the tips of the pulley teeth. However, as the theoretical and experimental researches [61, 62] show, the influence of the friction forces is insignificant. They transmit no more than 5 % of the circumferential force. It is explained by the far less tension of toothed belts in comparison with the tension of belts of a frictional type.

For the specification of the calculated dependences it is also offered to consider the so-called "edge effect", i.e. inability of face threads of a bearing layer to transmit the loading. Besides, the given parts of a belt are more compliant in comparison with the middle parts [63].

In the works [24, 64, 65, 66] it is established that the longitudinal rigidity of belts depends on the stretching loading non-linearly. It is especially typical for the belts with $m = (1; 2; 3)$ mm, and at $F_t \leq 10$ N/mm for the belts with the module $m \geq 4$ mm.

In this connection, the authors of the work [67] offered a non-linear model of a power interaction of teeth in gearing, allowing to define the influence of mechanical and physical properties of the elements of a toothed belt on non-uniformity of loading, and to develop the specified technique of the calculation of the correction of a step of pulley teeth.

The analysis of oscillograms of loading distribution in gearing [52, 62] shows that the damping harmonic component is put over the middle line, coinciding with the calculated one. The given component, in particular, is not observed on the oscillograms of loading distribution on an arc of contact of a flat-belt transmission [68]. Thus, the existence of harmonics is connected with the features of the operation of a toothed-belt transmission.

The authors of the works [47, 66] consider that the occurrence of harmonics is caused by the dynamic mechanical and physical properties of belt elements, demonstrated in the conditions of unsteady loading.

The theoretical research works, describing the occurrence of damping vibrations, owing to a shock input of teeth in gearing, are also known. However, the frequency of such vibrations should be much more than the frequency of an observable harmonic component. In our opinion, the occurrence of harmonics is caused by the reinterface of teeth and the periodic change of loading, because of an input of the subsequent teeth in gearing.

The demerits of the examined theoretical theses essentially influence a choice of the rational value of the correction of a step of pulley teeth. This value ensures the pre-set non-uniformity of loading of gearing and durability of a belt, therefore it requires some specification.

1.5. Perspectives of the development of scientific principles of increasing of the engineering level of power transmissions by flexible link

Many scientists devoted their theoretical and experimental researches to the development of scientific bases of improvement of technical-operational features of mechanical transmissions of power by flexible link.

As a result of the conducted researches it is established, that the most effective improvement of engineering and operating features of the given transmissions can be realized by the increase in indexes of working ability of flexible links. Three basic interdependent aspects of the problem are defined:

- 1) constructional, based on the development of progressive designs of flexible links or perfecting of the existing ones;
- 2) methodological, based on the defining and setting up of optimum parameters of transmission;
- 3) technological, consisting in the use of more perfect materials and the development of progressive methods of producing of flexible links.

It should be mentioned that for the substantial increase of a technical level of transmissions of power by flexible link the complex and system development of the above methods is necessary.

Such an approach is based on the development of the criteria of the destruction of flexible links. The practice testifies that there are three basic aspects of breaking of flexible link:

- fatigue failure of teeth;
- fatigue failure of a bearing layer;
- wear of a working profile of teeth.

It is obvious that all the aspects of the destructions of flexible link are the consequence of its interaction with pulleys of transmission under the certain kinematic and dynamic conditions. Thus, the scientific-proved methodology of the design calculation and the prediction of durability of transmissions of power by flexible link are based on the data about its loading and the stress-strained state.

The calculation of loading of flexible link, that is polymeric anisotropic visco-elastic system of the elements, interconnected by means of adhesive forces, should be done on the basis of its dynamic mechanical and physical properties.

It is necessary to note that the calculation of loading of flexible link on the basis of **Ponsele's principle does not reflect the real observable physical phenomena. Thus, the development of the problem of static indefinability of transmission, in view of the bending rigidity of flexible link and its dynamic loading, is necessary.** The solution of this problem creates the bases for the development of the well-founded calculation technique of the main operation index of transmission – the preliminary tension of flexible link.

The analysis of a patent-informational search and the world scientific and technical literature shows that engineering of flexible links is made practically without the analysis of the criteria of their destruction. The first direction is based on the introduction of improvements, which do not contradict to the developed level of standardization and unification.

The alternative direction means the change of the shape of a working profile of flexible links, allowing the minimization of a profile interference of teeth and raising of their wear resistance. However, the efficiency of the given work is low, since there are no deep theoretical researches of kinematics of reinterface of teeth of flexible link and pulleys.

Alongside with the high requirements to the load carrying capacity and durability of mechanical drives, nowadays the ecological aspect of their operation, consisting in the minimization of the effect of harmful factors and, first of all, of noise and vibrations on a man and the environment, is rather vital.

In our opinion, the solution of the problem is possible on the basis of the creation of theoretically justified methods of lowering of the acoustic emission, consisting in the creation of the designs of transmissions with the lowered aerodynamic acoustics and the increased smoothness of operation, and also by the calculation and the choice of rational parameters of transmission.

The most important method of the improvement of the technological level of flexible links is the development of progressive techniques of their manufacture, ensuring high strength of adhesive links between the components of flexible link, and also the equipment of its working surfaces by a wear-resistant coating. It allows considerable improvement of the load carrying capacity and the operational resource of transmissions of power by flexible link.

Now there are two basic technological processes of manufacturing of drive toothed belts in the world.

The first method is the method of molding in mould tools on hydraulic presses with warmed plates, allowing producing of toothed belts of a small length (up to 1000 mm)

without a wear-resistant coating of teeth. Mould belts are notable for the exact sizes and the excellence of surfaces, owing to the high pressure of moulding (**20...25 MPa**). However, the absence of a wear-resistant coating of working surfaces of teeth predetermines their low durability. The improvement of the technical characteristics of mould belts is reached by the use of wear-resistant polyurethane materials in their manufacturing. However, the cost of such materials several times exceeds the cost of synthetic rubbers, basically used in the manufacture of flexible links.

The second method is the vulcanization in an autoclave. The belts, made in such a way, have the length up to 4000 mm, are equipped with the wear-resistant coating of teeth, and their durability **5...7 times exceeds** the durability of the similar mould belts.

At the same time the technique of the vulcanization in an autoclave has the essential deficiencies, not allowing the realization of all engineering opportunities of produced belts. First of all, it is the low pressure of moulding (up to 1.5 **MPa**), which does not allow to ensure high strength of adhesion of the components of flexible link, determining its load carrying capacity and durability. It also causes some cavities and porosity in the finished articles. Besides, pressing in an autoclave is carried out by means of flexible rubber-cord diaphragm, which does not allow ensuring of the demanded thickness of belts. It can be made by grinding of the back surface of a belt.

The additional deficiencies of the given technological process are:

- raised energy and labour cost;
- elongation of a technological circuit;
- increase in the amount of the industrial equipment;
- low ecological purity, because of the existence of rubber dust and industrial wastes at grinding.

Therefore, the development of the new progressive technique of producing of drive toothed belts, ensuring the high strength of adhesion of its components and the existence of a wear-resistant coating of working surfaces of teeth, is necessary.

In conclusion it is necessary to note, that the further development of scientific bases of the improvement of the engineering level of mechanical transmissions of power by flexible link should be based on the complex and system approach to their research by the development of the progressive methods of the calculation of transmissions, the designs and production techniques of flexible links.

From the practical point of view the solution of the given problem allows to improve the quality and competitive ability of the modern machine-building considerably.

Chapter 2. GEOMETRY AND KINEMATICS
OF TRANSMISSIONS OF POWER BY FLEXIBLE LINK

2.1. Characteristics of geometry and kinematics of belt transmissions

In existing techniques of the calculation the arc of contact of a pulley is identified from the elementary geometrical ratios (Fig. 2.1) [69, 70].

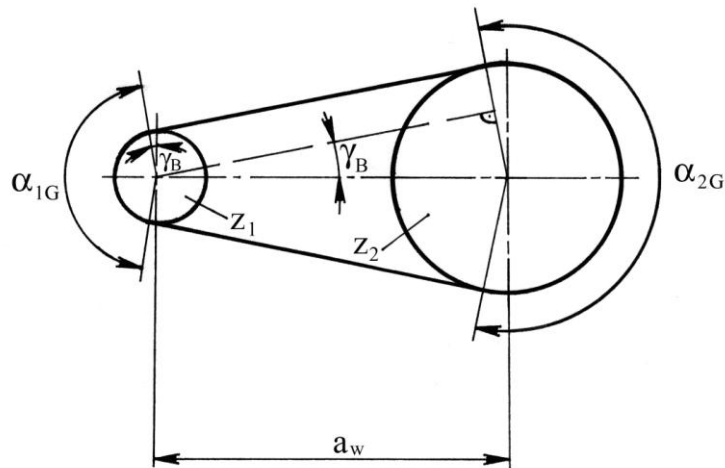


Fig. 2.1. Bending of pulleys by a flexible inextensible belt

Considering a belt as a mathematical fillet, the values of the geometrical angles of contact were received in the form:

$$\alpha_{1G} = 180^\circ - 2\gamma_B; \quad \alpha_{2G} = 180^\circ + 2\gamma_B, \quad (2.1)$$

where $\gamma_B = \arcsin \frac{mz_2 - mz_1}{2a_w}$; a_w – spacing on centers of transmission.

The number of teeth in gearing is defined by rounding to the less integral values, received from the following dependences:

$$z_{01} = \frac{\alpha_{1G}}{f_{p_1}^\circ}; \quad z_{02} = \frac{\alpha_{2G}}{f_{p_2}^\circ}, \quad (2.2)$$

where $f_{p_{1(2)}}^\circ = 360^\circ / z_{1(2)}$ – a tooth spacing angle of a pulley.

In our opinion, the expressions (2.1), (2.2) may be used for the calculation of the angles of contact in flat-belt transmissions. In V-belt transmissions by reason of bending rigidity of a belt the real arc of contact, where an actual contact of a belt with a pulley takes place, is less than the geometrical arc of contact [71]. The inverse phenomenon is characteristic of toothed-belt transmissions where the tooth contact is observed out of a geometrical arc of contact (Fig. 2.2).

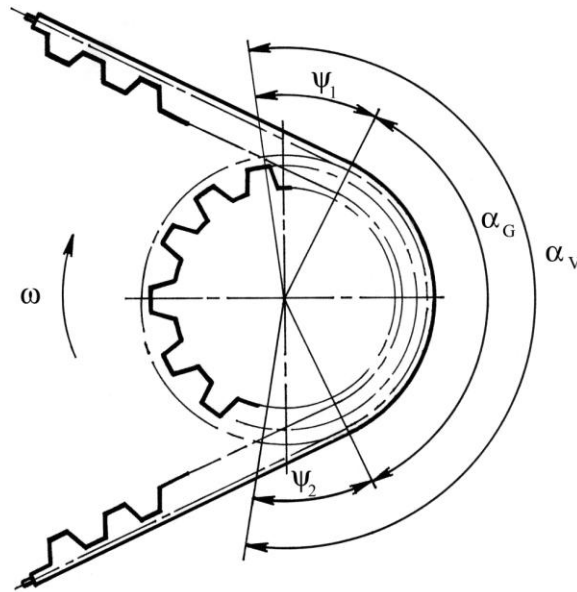


Fig. 2.2. Scheme of the interaction of a toothed belt with a pulley

Thus, for the toothed-belt transmission we have:

$$\alpha_v = \alpha_G + \psi_1 + \psi_2,$$

where ψ_1, ψ_2 – the angles of an input of teeth in gearing and an output from it accordingly (the zones of an incomplete profile gearing of teeth).

At the turn of a pulley by the angle $\psi_{1(2)}$ the mutual sliding of teeth, defining the intensity of their wear, takes place.

Thus, it is necessary to define the values ψ_1 and ψ_2 for the creation of a progressive technique of the resource designing of a toothed-belt transmission. Let's consider the main existing techniques of their definition.

In the work [72] the values $\psi_1 = \psi_2 = 0.5 \varphi_p$ for transmissions with a semicircular profile of teeth are recommended.

The authors of the work [73] received the following ratio on the basis of the idealized geometry of **trapezoidal** teeth (Fig. 2.3):

$$\psi_1 = \psi_2 = \arccos \left[\frac{\frac{mz}{2} - \delta - h_p}{\frac{mz}{2} - \delta} \right], \quad (2.3)$$

where δ – the distance from a neutral axis of a bearing layer to an interdental space of a belt.

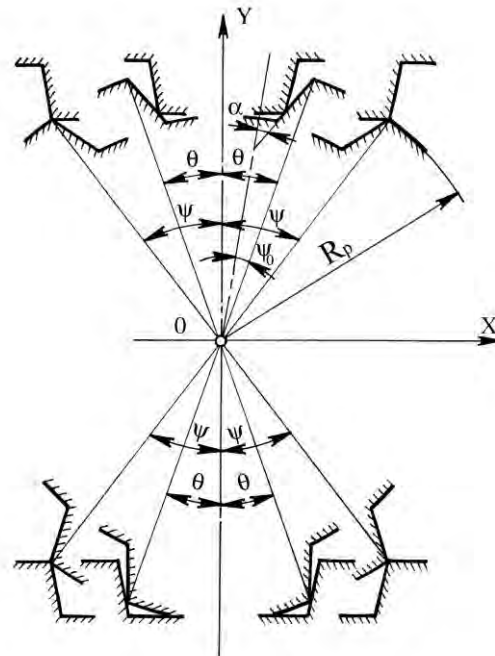


Fig. 2.3. Contact of teeth of a belt and a pulley in transmission with an idealized geometry

The value δ is equal to the sum of a half of diameter of a bearing layer d_c and the thickness of facing of belt teeth h_{ff} . $\delta = d_c / 2 + h_{ff}$.

It is offered to find the sliding velocity of teeth at their input in gearing by the formula:

$$v_{sl} = \frac{dx}{d\Theta} \frac{d\Theta}{dt} = \left(\frac{mz}{2} - \delta \right) \omega_1 \frac{\sin \alpha - \psi_0 - \sin \Theta + \beta_p - \psi_0 \cos \psi_1}{\cos^2 \Theta + \beta_p - \psi_0},$$

where x – displacement ; Θ – the angle of contact of teeth; t – time;

$$\psi_0 = \arcsin \left[\frac{S_{\text{III}} + 2h_{\text{III}} \text{tg}\beta_{\text{III}}}{2 \left(\frac{mZ}{2} - \delta \right)} \right];$$

where S_{III} ; h_{III} ; β_{III} – geometrical parameters of a space of a pulley.

It is offered to define the sliding velocity of teeth at an output from gearing by the formula:

$$v_{s2} = \left(\frac{mZ}{2} - \delta \right) \omega_1 \frac{\sin\Theta}{\cos\beta_p}.$$

The calculations show that at $\omega_1 = 1\text{c}^{-1}$ the sliding velocity at an input in gearing decreases non-linearly from 16 up to 3 mm/s (Fig. 2.4):

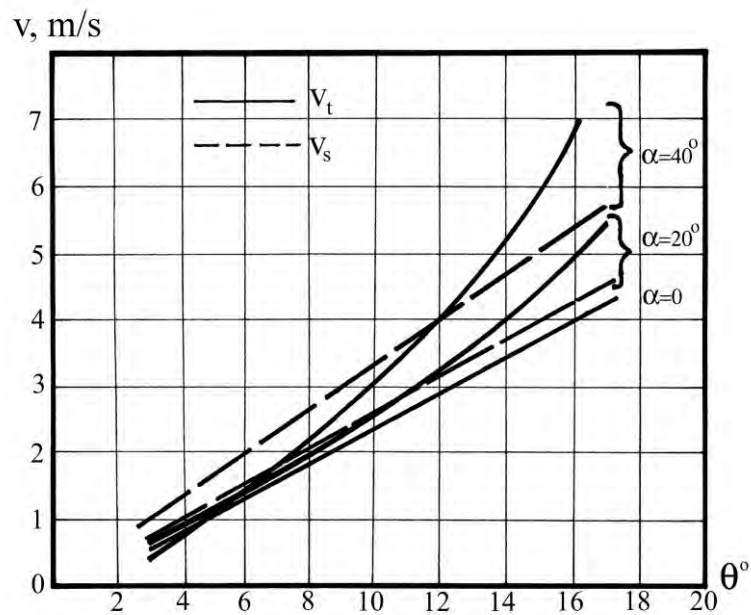


Fig. 2.4. Influence of a phase of gearing on the sliding velocity in the contact of teeth

In the work [41] the equation for the calculation of the value ψ_1 was obtained:

$$C \sin \psi_1 + \lambda_p - \left[\left(\frac{mZ}{2} - \delta \right) \psi_1 + \lambda_p - B \right] \cos \psi_1 + \lambda_p - A = 0, \quad (2.4)$$

where $A = \left[mz/2 - \delta - 0,5h_{\text{III}} \right] \sin \beta_{\text{III}} - 180^\circ / 2z$;

$$B = \Delta - h_p \operatorname{tg} \beta - mz/2 - \delta \lambda_p; C = mz/2 - \delta - h_p; \lambda_p = \arcsin A$$

Having solved (2.4) at $z_1 = (20; 27; 34; 41)$, we received $\psi_1 = (21.2; 16.6; 13.8; 11.5^\circ)$ accordingly.

It is necessary to note, that the expressions (2.3), (2.4) were received geometrically without taking into account the real trajectory of belt teeth at the input in gearing. The point of the initial contact of teeth was not defined. Therefore the results of the calculation of ψ_1 and ψ_2 are approximate.

The author of the work [24] developed a technique, according to which:

$$\psi_1 = \psi_{1I} + \psi_{1C},$$

where ψ_{1I} , ψ_{1C} – the arcs of traverse of a pulley, corresponding to the movement of a belt along the involute and the arc of circle accordingly (Tab. 2.1).

Tab. 2.1.

Parameter	Number of teeth of pulley, z							
	10	15	20	25	30	40	50	60
ψ_{1I}	5.90	5.35	5.20	4.75	4.65	4.50	4.40	4.30
ψ_{1C}	10.6	7.3	5.4	4.5	3.7	3.1	2.8	2.5
ψ_1	16.5	12.6	10.6	9.25	8.35	7.6	7.2	6.8
t_p°	36	24	18	14.4	12	9	7.2	6
ψ_1 / t_p°	0.45	0.52	0.58	0.64	0.69	0.84	1.0	1.13

The analysis of Tab. 2.1 shows that the values, presented in it, are 2 times less than the values, got by the formula (2.4).

It is offered to define the sliding velocity of teeth by the following dependence:

$$v_{sl} = \omega_1 \rho = m \omega_1 \left(\frac{N}{\Phi_2} \right)^{\frac{1}{n}}, \quad (2.5)$$

where ρ – the current value of the turning radius of a tooth of a pulley; φ_2 – the current value of the arc of traverse of a pulley ($0 \dots \psi_1$).

The parameters N and n depend on the number of teeth of a pulley (Tab. 2.2).

Tab. 2.2. Parameters N and n

z_1	15	20	25	30	40
N	348.0	73.0	41.0	21.0	14.5
n	12.4	10.3	8.8	8.2	7.5

For example, at $z_1 = 20$, $m = 7$ mm and $\omega_1 = 1$ s⁻¹, according to (2.5) $v_{sl,max} = 17.84$ mm/s; $v_{sl,min} = 12.53$ mm/s.

The demerit of the above-stated dependences is the use of idealized geometry of teeth that are considered in the form of trapezes, without the radii of rounding of tips and spaces. Meanwhile, the total height of rounding of teeth can come up to 60 % of its height.

Thus, the research of kinematic features of a toothed-belt gearing should be based on the real geometry of teeth and the main principles of their interaction.

2.2. Zones of an incomplete profile gearing of teeth of toothed-belt transmissions

Let's examine a toothed-belt gearing (Fig. 2.5). We introduce some additional geometrical parameters, used in the further calculations. For $t_p = t_{III}$ we have:

$$S'_1 = t_{III} - S_{III} - 2(h_{III} + \delta) \operatorname{tg} \beta_{III}.$$

There are three periods of rolling of an interdental space of a belt along the tip of a tooth of a pulley.

The first period begins at the moment of contact of the interdental space of the belt and the part of the pulley rounding R_{3K} . The second period represents the rolling of the interdental space of the belt along the diameter of the circle of pulley tips. The third period represents the bending of the opposite part of rounding of the pulley tooth R_{3K} by the interdental space of the belt.

By analogy with the analysis of kinematics of tooth transmissions [74] we place a toothed-belt transmission in Cartesian systems of coordinates of the right direction [75] (see Fig. 2.5).

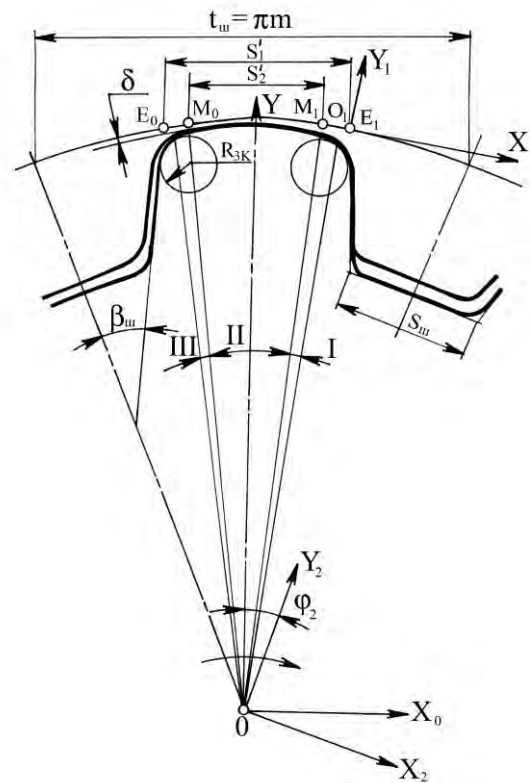


Fig. 2.5. Geometry of gearing of standard **trapezoidal** teeth

The system $S(X; O; Y)$ is fixed and it is placed in the drawing plane. The system $S_1(X_1; O_1; Y_1)$ is moving and it is connected with a belt. The system $S_2(X_2; O_2; Y_2)$ is also moving and it is connected with a pulley. We set the equations of profiles of teeth and unit normal vectors in moving systems of coordinates in the parametric form [74]:

$$\bar{\rho}_i = \bar{\rho}_i U_i \quad ; \quad \bar{\varepsilon}_i = \bar{\varepsilon}_i U_i \quad ,$$

In the fixed system of coordinates the profiles of teeth are described by the equations:

$$\bar{\rho}_i^{(l)} = \bar{\rho}_i^{(l)} U_i; \varphi_i \quad ; \quad \bar{\varepsilon}_i^{(l)} = \bar{\varepsilon}_i^{(l)} U_i; \varphi_i \quad ,$$

where φ_i – the turning angle of the moving system of coordinates.

We set the transition from the moving system of coordinates to the fixed system in a general form by means of the matrix equality:

$$\rho^{(i)} = M_{0i}\rho_i,$$

where $\rho^{(i)}$ и ρ_i – matrix-columns of radius-vectors; M_{0i} – transition matrix.

The matrix of transition has its own form for each period, and the equations of tooth profiles remain constant. Thus, it is necessary to make up two transition matrixes M_{01} and M_{02} for each period.

Let's consider the first period (Fig. 2.6).

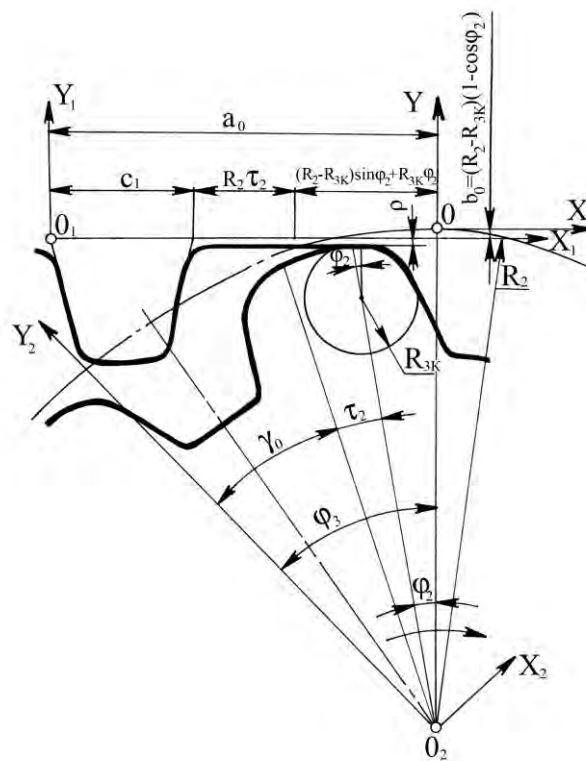


Fig. 2.6. Rolling of an interdental space of a belt along the radius of rounding of the tip of a pulley tooth

Using the rules of analytical geometry [76] and the principles of writing of matrixes, we get:

$$M_{01} = \begin{vmatrix} 1 & 0 & -a_0 \\ 0 & 1 & -b_0 \\ 0 & 0 & 1 \end{vmatrix}, \quad (2.6)$$

where $a_0 = C_1 + R_2\tau_2 + (R_2 - R_{3\kappa}) \sin\varphi_2 + R_{3\kappa}\varphi_2$; $b_0 = (R_2 - R_{3\kappa})(1 - \cos\varphi_2)$.

We show the transition from S_2 to S in the form:

$$M_{02} = \begin{vmatrix} \cos \varphi_3 & -\sin \varphi_3 & 0 \\ \sin \varphi_3 & \cos \varphi_3 & -R_2 \\ 0 & 0 & 1 \end{vmatrix}, \quad (2.7)$$

where $\varphi_3 = \gamma_0 + \tau_2 + \varphi_2$ – the turning angle S_2 relating to S ; $R_2 = mZ_2$.

For the second period (Fig. 2.7) the matrixes of transition have the form:

$$M_{01} = \begin{vmatrix} 1 & 0 & -a_0 \\ 0 & 1 & 0 \\ 0 & 0 & 1 \end{vmatrix}; \quad M_{02} = \begin{vmatrix} \cos \varphi_4 & -\sin \varphi_4 & 0 \\ \sin \varphi_4 & \cos \varphi_4 & -R_2 \\ 0 & 0 & 1 \end{vmatrix}, \quad (2.8)$$

where $a_0 = C_1 + R_2\varphi_2$; $\varphi_4 = \gamma_0 + \varphi_2$ – the turning angle S_2 relating to S .

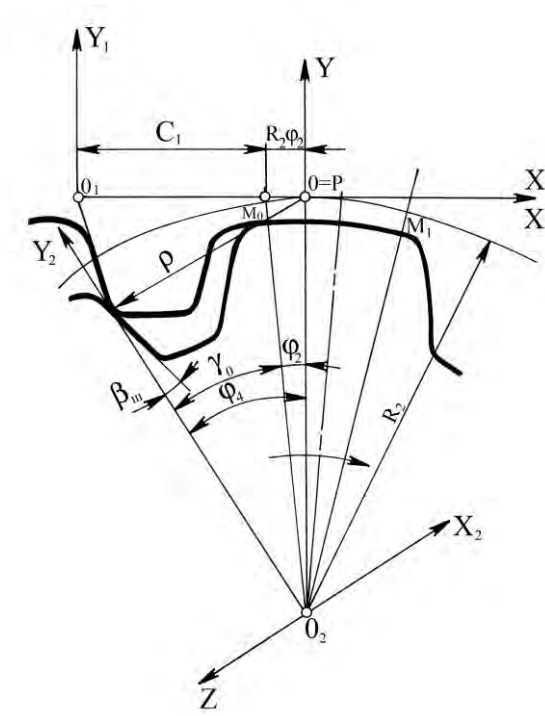


Fig. 2.7. Rolling of an interdental space of a belt along the tip of a tooth of a pulley

By analogy for the third period we get (Fig. 2.8):

$$M_{01} = \begin{vmatrix} 1 & 0 & -a_0 \\ 0 & 1 & -b_0 \\ 0 & 0 & 1 \end{vmatrix}; \quad M_{02} = \begin{vmatrix} \cos \varphi_5 & -\sin \varphi_5 & 0 \\ \sin \varphi_5 & \cos \varphi_5 & -R_2 \\ 0 & 0 & 1 \end{vmatrix}, \quad (2.9)$$

where $a_0 = C_1 - R_{3K}\varphi_2 - (R_2 - R_{3K})\sin\varphi_2$, $b_0 = (R_2 - R_{3K})(1 - \cos\varphi_2)$; φ_5 – the turning angle S_2 relating to S .

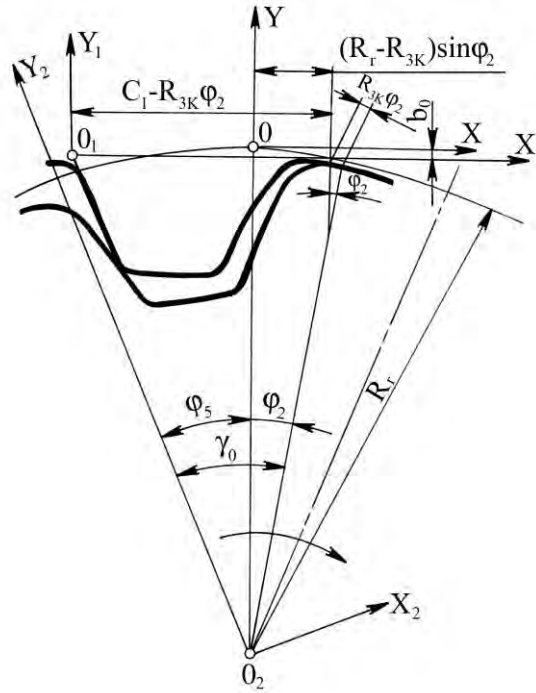


Fig. 2.8. The final stage of a mutual rolling-off of teeth

Thus, the transition matrixes from moving systems of coordinates to the fixed ones, which allow defining of the coordinates of any point of tooth profiles of a pulley and a belt at an arbitrarily chosen instant of time, were received. The position of a pulley is defined by the turning angle relating to the fixed coordinate system φ_2 and corresponds univocally to the position of a belt in the same system.

Hence, setting the profile equations, it is possible to define the angles ψ_1 and ψ_2 . We take ψ_1 as a central angle in the system XOY , corresponding to the turn of the pulley from the beginning of the contact (crossing) of tooth profiles of the belt and the pulley to the turn of the pulley in the position, corresponding to the coincidence of a symmetry axis of an interdental space of a pulley and the axis OY (Fig. 2.9). If they coincide the lateral

sides of teeth of the belt and the pulley become parallel to each other and the sliding of teeth stops.

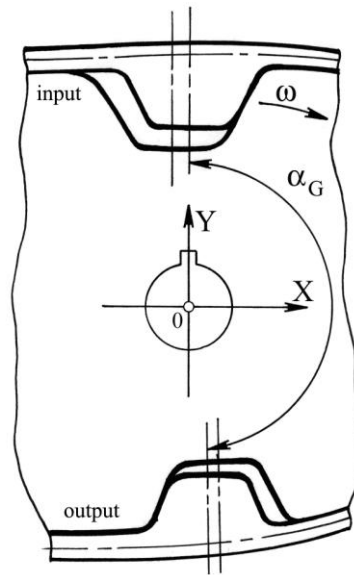


Fig. 2.9. Scheme of the definition of the angles of an input in gearing and output from it

Due to the existence of the lateral backlash between teeth and $S_{\text{in}} > S_{\text{p}}$ the symmetry axis of an interdental space of a pulley reaches the axis OY a little bit earlier than the symmetry axis of a belt tooth.

The value ψ_2 corresponds to the turn of a pulley by the angle with the beginning in the moment of an output of a symmetry axis of a pulley tooth from the limits of a geometrical arc of contact, i.e. the moment of crossing of the axis OY (see Fig. 2.9), and the end is the final moment of a contact (crossing) of profiles of teeth.

It is possible to consider that ψ_1 and ψ_2 correspond to the central angles, pulled together by a tooth gearing line in the zones of an incomplete profile gearing. We find the length of this line for trapezoidal and semicircular teeth.

Let's define ψ_1 , knowing the law of movement and the equation of tooth profiles at $t_{\text{p}} = t_{\text{in}}$. It is obvious that the radius-vectors and unit vectors of normals should be equal in the point of an initial contact of profiles. It can be admitted that the unit vectors of normals $\bar{\epsilon}^{(1)}$ and $\bar{\epsilon}^{(2)}$ have an equal direction [74]:

$$\bar{\rho}^{(1)} U_1; \varphi_1 = \bar{\rho}^{(2)} U_2; \varphi_2 \quad ; \quad \bar{\epsilon}^{(1)} U_1; \varphi_1 = \bar{\epsilon}^{(2)} U_2; \varphi_2 \quad . \quad (2.10)$$

Proceeding to the projections in the fixed system of coordinates and considering that the vectors $\vec{\rho}^{(i)}$ and $\vec{\varepsilon}^{(i)}$ are in the plane, perpendicular to the axis of rotation of a pulley, we get 3 independent scalar equations. Solving them relating to φ_2 , we get the transcendental equation:

$$\varphi_2 = f(U_1; U_2; \varphi_1). \quad (2.11)$$

The expression (2.11) for finding of the arc of traverse of a pulley, corresponding to the initial contact of profiles, can be calculated for the single values of an angle φ_2 by the method of iteration. We use the iterative formula of Newton [77] for it:

$$X^{k+1} = X^k - \frac{f X^k}{f' X^k}, \quad (2.12)$$

where X – an unknown quantity; k – a number of iteration.

At the initial moment of contact of profiles the rounded part of a tip of a belt tooth interacts with a tooth of a pulley. The equations of the rounded part AB (Fig. 2.10) are the following:

$$X_1 = X_{u1} - R_{32} \cos U_1; \quad Y_1 = -Y_{u1} - R_{32} \sin U_1. \quad (2.13)$$

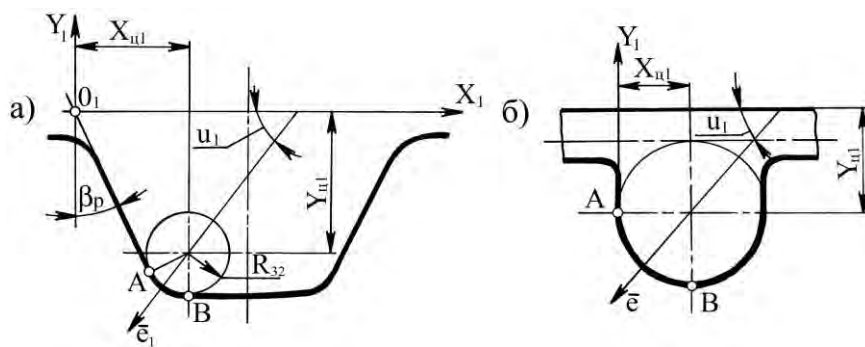


Fig. 2.10. The main geometrical parameters of trapezoidal (a) and semicircular (b) teeth

The unit vector of a normal is determined by the expressions:

$$e_{X1} = -\cos U_1; \quad e_{Y1} = -\sin U_1. \quad (2.14)$$

In the system S_2 the profile of a pulley tooth and a unit vector of a normal are described with the equations (Fig. 2.11):

$$X_2 = U_2 \sin \beta_{\text{III}}; \quad Y_2 = R_2 - U_2 \cos \beta_{\text{III}}. \quad (2.15)$$

$$e_{X2} = -\cos \beta_{\text{III}}; \quad e_{Y2} = -\sin \beta_{\text{III}}. \quad (2.16)$$

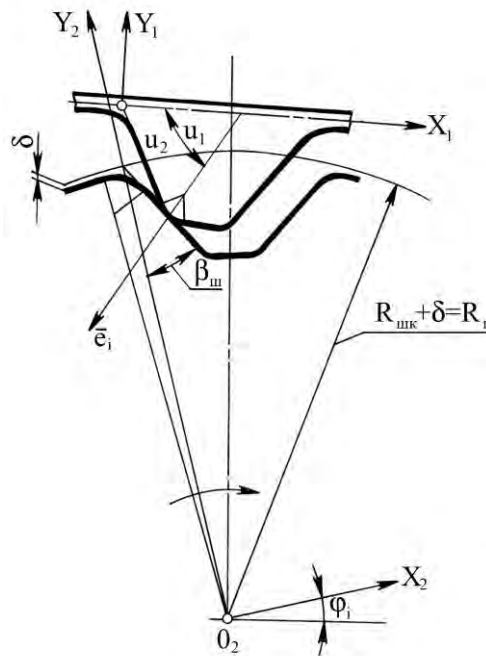


Fig. 2.11. Initial contact of teeth of a belt and pulley

Basing on the formulas of transition (2.6) – (2.9), we change the equations (2.13) – (2.16) from the systems S_1 and S_2 to the system S . For the first period of bending of a belt by a pulley we get:

$$X^{(1)} = X_{\text{II}1} - R_{32} \cos U_1 - [C_1 - (R_2 - R_{3K}) \sin \varphi_2 + R_{3K} \varphi_2 + R_2 \tau_2];$$

$$Y^{(1)} = Y_{\text{II}1} - R_{32} \sin U_1 + (R_2 - R_{3K})(\cos \varphi_2 - 1);$$

$$\chi^{(2)} = U_2 \sin \beta_{\text{III}} \cos \varphi_3 - (R_2 - U_2 \cos \beta_{\text{III}}) \sin \varphi_3; \quad (2.17)$$

$$\gamma^{(2)} = U_2 \sin \beta_{\text{III}} \sin \varphi_3 + (R_2 - U_2 \cos \beta_{\text{III}}) \cos \varphi_3 - R_2;$$

$$e_X^{(1)} = -\cos U_1; \quad e_Y^{(1)} = -\sin U_1;$$

$$e_X^{(2)} = -\cos(\varphi_3 + \beta_{\text{III}}); \quad e_Y^{(2)} = -\sin(\varphi_3 + \beta_{\text{III}}).$$

We obtain the dependences for the second period in a similar way:

$$\chi^{(1)} = X_{\text{II}1} - R_{32} \cos U_1 - C_1 - R_2 \varphi_2;$$

$$\gamma^{(1)} = -Y_{\text{II}1} - R_{32} \sin U_1;$$

$$\chi^{(2)} = U_2 \sin \beta_{\text{III}} \cos \varphi_4 - (R_2 - U_2 \cos \beta_{\text{III}}) \sin \varphi_4; \quad (2.18)$$

$$\gamma^{(2)} = U_2 \sin \beta_{\text{III}} \sin \varphi_4 + (R_2 - U_2 \cos \beta_{\text{III}}) \cos \varphi_4 - R_2;$$

$$e_X^{(1)} = -\cos U_1; \quad e_Y^{(1)} = -\sin U_1;$$

$$e_X^{(2)} = -\cos(\varphi_4 + U_2); \quad e_Y^{(2)} = -\sin(\varphi_4 + U_2).$$

The third period is characterized by the following equations:

$$\chi^{(1)} = X_{\text{II}1} - R_{32} \cos U_1 - [C_1 + (R_2 - R_{3\text{K}}) \sin \varphi_2 + R_{3\text{K}} \varphi_2];$$

$$\gamma^{(1)} = -Y_{\text{II}1} - R_{32} \sin U_1 - (R_2 - R_{3\text{K}})(1 - \cos \varphi_2);$$

$$\chi^{(2)} = U_2 \sin \beta_{\text{III}} \cos \varphi_5 - (R_2 - U_2 \cos \beta_{\text{III}}) \sin \varphi_5;$$

(2.19)

$$\gamma^{(2)} = U_2 \sin \beta_{\text{III}} \sin \varphi_5 + (R_2 - U_2 \cos \beta_{\text{III}}) \cos \varphi_5 - R_2;$$

$$e_X^{(1)} = -\cos U_1; \quad e_Y^{(1)} = -\sin U_1;$$

$$e_X^{(2)} = -\cos(\varphi_5 + \beta_{III}); \quad e_Y^{(2)} = -\sin(\varphi_5 + \beta_{III}).$$

The equations (2.17) – (2.19) make the connection between geometrical parameters of belt teeth, the pulley and the angle φ_2 in the point of the initial contact. As it is not known a priori in what period the contact of profiles takes place, it is necessary to analyze all the periods, using the conditions, arising in the point of contact:

$$X^1 = X^2; \quad Y^1 = Y^2; \quad e_X^1 = e_X^2;$$

$$X^1 = X^2; \quad Y^1 = Y^2; \quad e_Y^1 = e_Y^2.$$

Using the iterative formula (2.12), we find **its constituent elements** (2.12). Let's re-write the expression in the form:

$$\varphi_2^{k+1} = \varphi_2^k - \frac{f \varphi_2^k}{f' \varphi_2^k},$$

$$f' \varphi_2^k \neq 0. \quad (2.20)$$

Omitting the transformations, for the first period through the simultaneous solution of these equations (2.17), we get:

$$U_1 = \gamma_0 + \tau_2 + \varphi_2 + \beta_{III};$$

$$U_2 = \frac{X_{III} - R_{32} \cos U_1 - [C_1 + R_2 - R_{3K} \sin \varphi_2 + R_{3K} \varphi_2 + R_2 \tau_2] + R_2 \sin \varphi_2 + \gamma_0 + \tau_2}{\sin U_1};$$

$$f \varphi_2^k = \gamma^2 - \gamma^1 = -\text{ctg} U_1 [X_{\text{II1}} - R_{32} \cos U_1 - C_1 - R_2 - R_{3\text{K}} \sin \varphi_2 - R_{3\text{K}} \varphi_2 - R_2 \tau_2 + R_2 \sin \varphi_2 + \gamma_0 + \tau_2] + R_2 [\cos -\varphi_2 + \gamma_0 + \tau_2 - 1] + Y_{\text{II1}} - R_2 - R_{3\text{K}} \cos \varphi_2 - 1 + R_{32} \sin U_1; \quad (2.21)$$

$$f' \varphi_2^k = \frac{X_{\text{II1}} - R_{32} \cos U_1 - [C_1 - R_2 - R_{3\text{K}} \sin \varphi_2 - R_{3\text{K}} \varphi_2 - R_2 \tau_2]}{\sin^2 U_1} + \frac{R_2 \sin \varphi_2 + \gamma_0 + \tau_2}{\sin^2 U_1} - \text{ctg} U_1 [R_{32} \sin U_1 - R_2 - R_{3\text{K}} \cos \varphi_2 - R_{3\text{K}} - R_2 \cos \varphi_2 + \gamma_0 + \tau_2] - R_2 \sin \varphi_2 + \gamma_0 + \tau_2 + R_2 - R_{3\text{K}} \sin \varphi_2 + R_{32} \cos U_1.$$

By means of similar transformations for the second period we get:

$$U_1 = \gamma_0 + \varphi_2 + \beta_{\text{III}};$$

$$U_2 = \frac{X_{\text{II1}} - R_{32} \cos U_1 - R_2 [\varphi_2 - \sin \gamma_0 + \varphi_2]}{\sin U_1};$$

$$f \varphi_2^k = \gamma^2 - \gamma^1 = \text{ctg} U_1 [X_{\text{II1}} - R_{32} \cos U_1 - C_1 - R_2 (\varphi_2 - \sin \varphi_2 + \gamma_0)] - Y_{\text{II1}} - R_{32} \sin U_1 - R_2 (\cos \varphi_2 + \gamma_0 - 1); \quad (2.22)$$

$$f' \varphi_2^k = \frac{X_{\text{II1}} - R_{32} \cos U_1 - [C_1 - R_2 (\varphi_2 - \sin \varphi_2 + \gamma_0)]}{\sin^2 U_1} + \text{ctg} U_1 [R_{32} \sin U_1 - R_2 (1 - \cos \varphi_2 + \gamma_0)] + R_2 \sin \varphi_2 + \gamma_0 - R_{32} \cos U_1.$$

Assuming that the contact of teeth takes place during the third period, we get:

$$U_1 = \gamma_0 - \varphi_2 + \beta_{\text{III}};$$

$$U_2 = \frac{X_{\text{II1}} - R_{32} \cos U_1 - [C_1 + R_2 - R_{3\text{K}} \sin \varphi_2 + R_{3\text{K}} \varphi_2] + R_2 \sin -\varphi_2 + \gamma_0}{\sin U_1};$$

$$f \varphi_2^k = Y^2 - Y^1 = R_2[\cos(-\varphi_2 + \gamma_0) - 1] - \operatorname{ctg} U_1 [X_{II1} - R_{32} \cos U_1 - C_1 + R_2 - R_{3K} \sin \varphi_2 + R_{3K} \varphi_2 + R_2 \sin(-\varphi_2 + \gamma_0)] + Y_{II1} + R_2 - R_{3K} [1 - \cos \varphi_2 + R_{32} \sin U_1]; \quad (2.23)$$

$$f' \varphi_2^k = R_2 \sin(-\varphi_2 + \gamma_0) - \operatorname{cosec}^2 U_1 [X_{II1} - R_{32} \cos U_1 - C_1 + R_2 - R_{3K} \sin \varphi_2 + R_{3K} \varphi_2 + R_2 \sin(-\varphi_2 + \gamma_0)] - \operatorname{ctg} U_1 [-R_{32} \sin U_1 + R_2 - R_{3K} \cos \varphi_2 + R_{3K} - R_2 \sin(-\varphi_2 + \gamma_0)] + R_2 - R_{3K} \sin \varphi_2 - R_{32} \cos U_1.$$

On the basis of the equations (2.21) – (2.23) the value of the arc of traverse of a pulley φ_2 , **corresponding to the initial contact of teeth, i.e. the value ψ_1** , is defined.

The formulas are universal, they can be used for the research of kinematics of transmissions with semicircular teeth, where $\beta_p = \beta_{III}$, and the values R_{3K} are a little bit increased (see Fig. 2.10, b).

After the solution of the equations (2.21) – (2.23), it was established that at $t_p = t_{III}$ the contact of teeth takes place at rolling of an interdental space of a belt along a cylindrical part of the tip of a tooth of a pulley, i.e. at the second stage of an input in gearing. The **initial contact during the first period of an input in gearing is observed $\Delta > 0.2m$; $z_{III} > 100$** .

Thus, at the research of kinematics of the majority of designs of toothed-belt transmissions it is possible to limit the analyses to the 2nd and 3^d stages of an input of teeth in gearing.

It is also established that the value ψ_1 depends on the number of teeth of a pulley z_{III} , the angular displacement of **belt teeth under loading Δ and the size of the module of a belt m** . It can be expected that it is connected with the absence of geometrical similarity of tooth profiles of different modules. With a fractional error (no more than 3 %), the values **of ψ_1** can be found by the following dependence [79]:

$$\psi_1^o = k_{m1} z_{III}^{-1} [1 + 0,31\Delta], \quad (2.24)$$

where k_{m1} – the factor of an angle of an input of teeth (Tab. 2.3).

Tab. 2.3. Factor of the input angle of teeth in gearing

Type of teeth	Module m , mm	1.0	1.5	2.0	3.0	4.0	5.0	7.0	10
trapezoidal	k_{m1}	188	212	205	272	217	250	304	313
semi-circular	k_{m1}	---	---	---	346	290	271	---	---

The calculations show that at $\Delta = 0$, $m = 4$ mm, $z = (15; 20; 40)$; $\psi_1 = (14.5; 10.85; 5.42)$ accordingly, which is 1.6...2 times less than the values, got by the dependence (2.4).

We use the above-stated algorithm to define the angle of output from gearing ψ_2 . Let's write the matrixes of transition from the moving systems of coordinates to the fixed one. According to Fig. 2.12 for the first period of an output from gearing we have:

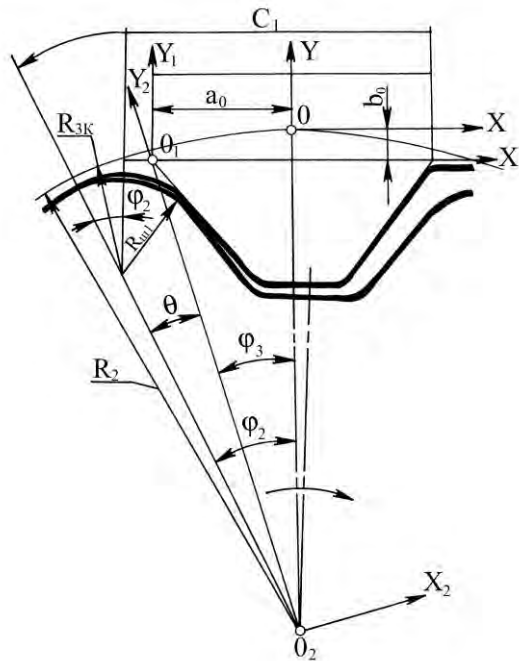


Fig. 2.12. The beginning of disconnection of teeth at an output from gearing:

$$M_{01} = \begin{vmatrix} 1 & 0 & -a_0 \\ 0 & 1 & -b_0 \\ 0 & 0 & 1 \end{vmatrix}, \quad M_{02} = \begin{vmatrix} \cos \varphi_3 & -\sin \varphi_3 & 0 \\ \sin \varphi_3 & \cos \varphi_3 & -R_2 \\ 0 & 0 & 1 \end{vmatrix},$$

where $a_0 = S_p + 2(h_p + \delta)\text{tg}\beta_p - C_1 + (R_2 - R_{3K})\sin\varphi_2 + R_{3K}\varphi_2$; $b_0 = (R_2 - R_{3K})(1 - \cos\varphi_2)$;

$\varphi_3 = \varphi_2 - \Theta$.

For the second period (Fig. 2.13):

$$M_{01} = \begin{vmatrix} 1 & 0 & -a_0 \\ 0 & 1 & 0 \\ 0 & 0 & 1 \end{vmatrix}; \quad M_{02} = \begin{vmatrix} \cos \varphi_4 & \sin \varphi_4 & 0 \\ -\sin \varphi_4 & \cos \varphi_4 & -R_2 \\ 0 & 0 & 1 \end{vmatrix},$$

where $a_0 = S_p + 2(h_p + \delta)\text{tg}\beta_p - C_1 - R_2\varphi_2$; $\varphi_4 = \varphi_2 + \Theta$.

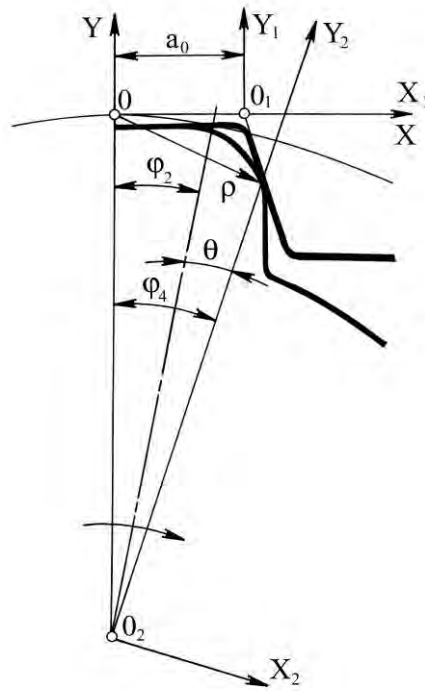


Fig. 2.13. Rolling of an interdenal space of a belt along the tip of a tooth of a pulley

For the third period (Fig. 2.14):

$$M_{01} = \begin{vmatrix} 1 & 0 & -a_0 \\ 0 & 1 & -b_0 \\ 0 & 0 & 1 \end{vmatrix}; \quad M_{02} = \begin{vmatrix} \cos \varphi_5 & \sin \varphi_5 & 0 \\ -\sin \varphi_5 & \cos \varphi_5 & -R_2 \\ 0 & 0 & 1 \end{vmatrix},$$

where $a_0 = -[C_1 + R_{3k}\varphi_2 + (R_2 - R_{3k})\sin\varphi_2 + R_2\tau_2 - [S_p + 2(h_p + \delta)\text{tg}\beta_p]]$,

$b_0 = (R_2 - R_{3k})(1 - \cos\varphi_2)$; $\varphi_5 = \varphi_2 + \Theta + \tau_2$.

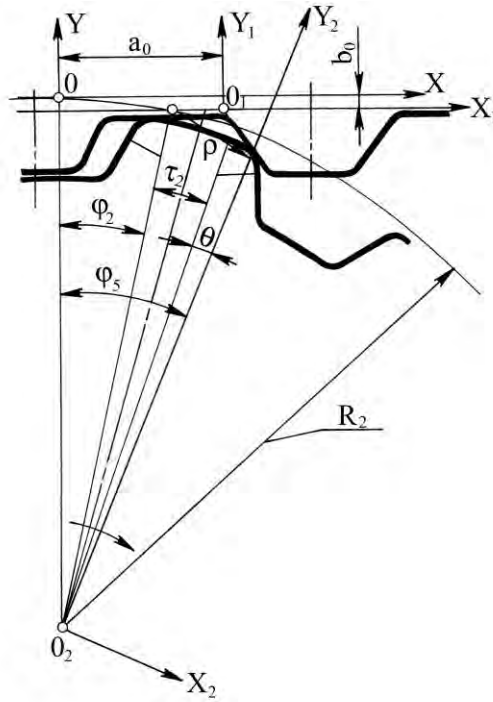


Fig. 2.14. Final phase of an output from gearing

As in the previous case, the full disconnection of profiles can take place in any period. But the condition of equality of radius-vectors in the point of the contact loss is constant.

Let's find the equations for **the determination of ψ_2** . For this purpose we write down the equations of the parts of interacting profiles in their own systems of coordinates.

The first period is characterized by the equations:

$$X_1 = U_1 \sin \beta_p; \quad e_{X1} = \cos \beta_p;$$

$$Y_1 = -U_1 \cos \beta_p; \quad e_{Y1} = \sin \beta_p;$$

$$X_2 = X_{u22} + R_{m1} \cos U_2; \quad Y_2 = Y_{u22} + R_{m1} \sin U_2;$$

$$X_{u22} = -R_2 - R_{m1} - \delta \sin \Theta; \quad Y_{u22} = R_2 - R_{m1} - \delta \cos \Theta;$$

$$e_{X2} = \cos U_2; \quad e_{Y2} = \sin U_2.$$

Proceeding to the fixed system of coordinates, we get:

$$\begin{aligned}
 X^1 &= U_1 \sin \beta_p - a_0; & e_X^1 &= \cos \beta_p; \\
 Y^1 &= -U_1 \cos \beta_p - b_0; & e_Y^1 &= \sin \beta_p; \\
 X^2 &= (X_{u22} + R_{w1} \cos U_2) \cos \varphi_3 - (Y_{u22} + R_{w1} \sin U_2) \sin \varphi_3; \\
 Y^2 &= (X_{u22} + R_{w1} \cos U_2) \sin \varphi_3 + (Y_{u22} + R_{w1} \sin U_2) \cos \varphi_3 - R_2; & (2.25) \\
 e_X^2 &= \cos(U_2 + \varphi_3); & e_Y^2 &= \sin(U_2 + \varphi_3).
 \end{aligned}$$

After some transformations we get:

$$\begin{aligned}
 U_1 &= \frac{X_{u22} \cos \varphi_2 - \Theta - Y_{u22} \sin \varphi_2 - \Theta + R_{w1} \cos \beta_p + a_0}{\sin \beta_p}; \\
 U_2 &= \beta_p - \varphi_2 + \Theta.
 \end{aligned} \tag{2.26}$$

Using the iterative formula (2.20) for the first period, we have:

$$\begin{aligned}
 f \varphi_2^k &= Y^2 - Y^1 = X_{u22} \sin \varphi_2 - \Theta + Y_{u22} \cos \varphi_2 - \Theta - R_2 + R_{w1} \sin \beta_p + \\
 &+ \operatorname{ctg} \beta_p [X_{u22} \cos \varphi_2 - \Theta - Y_{u22} \sin \varphi_2 - \Theta + R_{w1} \cos \beta_p + R_{3k} \varphi_2 + \\
 &+ (R_2 - R_{3k}) \sin \varphi_2 - C_1 + 2 h_p + \delta \operatorname{tg} \beta_p + S_p] + (R_2 - R_{3k})(1 - \cos \varphi_2); \\
 f' \varphi_2^k &= X_{u22} \cos \varphi_2 - \Theta - Y_{u22} \sin \varphi_2 - \Theta + \operatorname{ctg} \beta_p [-X_{u22} \sin \varphi_2 - \Theta - \\
 &- Y_{u22} \cos \varphi_2 - \Theta + R_{3k} + (R_2 - R_{3k}) \cos \varphi_2] + (R_2 - R_{3k}) \sin \varphi_2.
 \end{aligned} \tag{2.27}$$

For the second period:

$$\begin{aligned}
 X_1 &= U_1 \sin \beta_p; & e_{X1} &= \cos \beta_p; \\
 Y_1 &= -U_1 \cos \beta_p; & e_{Y1} &= \sin \beta_p; \\
 X_2 &= X_{u22} + R_{u1} \cos U_2; & Y_2 &= Y_{u22} + R_{u1} \sin U_2; \\
 e_{X2} &= \cos U_2; & e_{Y2} &= \sin U_2.
 \end{aligned}$$

In the fixed system of coordinates the expressions (2.25) become:

$$\begin{aligned}
 X^1 &= U_1 \sin \beta_p + a_0; & e_X^1 &= \cos \beta_p; \\
 Y^1 &= -U_1 \cos \beta_p; & e_Y^1 &= \sin \beta_p; \\
 X^2 &= R_{u1} \cos(U_2 - \varphi_2 - \Theta) + X_{u2} \cos(\varphi_2 + \Theta) + Y_{u2} \sin(\varphi_2 + \Theta); \\
 Y^2 &= R_{u1} \sin(U_2 - \varphi_2 - \Theta) - X_{u2} \sin(\varphi_2 + \Theta) + Y_{u2} \cos(\varphi_2 + \Theta) - R_2; & (2.28) \\
 e_X^2 &= \cos(U_2 - \varphi_2 - \Theta); & e_Y^2 &= \sin(U_2 - \varphi_2 - \Theta).
 \end{aligned}$$

After the transformations we get:

$$\begin{aligned}
 U_1 &= \frac{R_2 + X_{u2} \sin \varphi_2 + \Theta - Y_{u2} \cos \varphi_2 + \Theta - R_{u1} \sin \beta_p}{\cos \beta_p}; \\
 U_2 &= \beta_p + \varphi_2 + \Theta.
 \end{aligned} \tag{2.29}$$

Applying the iterative formula (2.20) to (2.29), we get:

$$f' \varphi_2^k = X^2 - X^1 = \operatorname{tg} \beta_p [X_{u2} \sin \varphi_2 + \Theta - Y_{u2} \cos \varphi_2 + \Theta + R_2 - R_{w1} \sin \beta_p] - [R_2 \varphi_2 + C_1 + 2 h_p + \delta \operatorname{tg} \beta_p - S_p] - R_{w1} \cos \beta_p - X_{u2} \cos \varphi_2 + \Theta - Y_{u2} \sin \varphi_2 + \Theta ; \quad (2.30)$$

$$f' \varphi_2^k = \operatorname{tg} \beta_p [X_{u2} \cos \varphi_2 + \Theta + Y_{u2} \sin \varphi_2 + \Theta] - R_2 + X_{u2} \sin \varphi_2 + \Theta - Y_{u2} \cos \varphi_2 + \Theta .$$

For the third period the equations of the parts of profiles in their own systems of coordinates are the following:

$$X_1 = U_1 \sin \beta_p; \quad e_{X1} = \cos \beta_p;$$

$$Y_1 = -U_1 \cos \beta_p; \quad e_{Y1} = \sin \beta_p;$$

$$X_2 = X_{u2} + R_{w1} \cos U_2; \quad Y_2 = Y_{u2} + R_{w1} \sin U_2;$$

$$e_{X2} = \cos U_2; \quad e_{Y2} = \sin U_2.$$

Coming to the fixed system of coordinates, we get:

$$X^1 = U_1 \sin \beta_p + a_0; \quad e_X^1 = \cos \beta_p;$$

$$Y^1 = -U_1 \cos \beta_p - b_0; \quad e_Y^1 = \sin \beta_p;$$

$$X^2 = R_{w1} \cos(U_2 - \varphi_2 - \Theta - \tau_2) + X_{u2} \cos(\varphi_2 + \Theta + \tau_2) + Y_{u2} \sin(\varphi_2 + \Theta + \tau_2); \quad (2.31)$$

$$Y^2 = R_{w1} \sin(U_2 - \varphi_2 - \Theta - \tau_2) - X_{u2} \sin(\varphi_2 + \Theta + \tau_2) + Y_{u2} \cos(\varphi_2 + \Theta + \tau_2) - R_2;$$

$$e_X^2 = \cos(U_2 - \varphi_2 - \Theta - \tau_2); \quad e_Y^2 = \sin(U_2 - \varphi_2 - \Theta - \tau_2).$$

Solving together (2.31), we receive:

$$U_1 = \frac{R_2 + X_{\text{II}2} \cos \varphi_2 + \Theta + \tau_2 + Y_{\text{II}2} \sin \varphi_2 + \Theta + \tau_2 + R_{\text{III}1} \cos \beta_p}{\sin \beta_p} +$$

$$+ \frac{R_{3\text{K}} \varphi_2 - (R_2 - R_{3\text{K}}) \sin \varphi_2 + C_1 + 2 h_p + \delta \operatorname{tg} \beta_p - S_p + R_2 \tau_2}{\sin \beta_p};$$

$$U_2 = \beta_p + \varphi_2 + \Theta + \tau_2.$$
(2.32)

The equations for the calculation of φ_2 (ψ_2) during the third period, obtained from (2.32), are the following:

$$f \varphi_2^k = Y^2 - Y^1 = -X_{\text{II}2} \sin \varphi_2 + \Theta + \tau_2 + Y_{\text{II}2} \cos \varphi_2 + \Theta + \tau_2 - R_2 + R_{\text{III}1} \sin \beta_p +$$

$$+ \operatorname{ctg} \beta_p [X_{\text{II}2} \cos \varphi_2 + \Theta + \tau_2 + Y_{\text{II}2} \sin \varphi_2 + \Theta + \tau_2 + R_{\text{III}1} \cos \beta_p + R_{3\text{K}} \varphi_2 -$$
(2.33)

$$- (R_2 - R_{3\text{K}}) \sin \varphi_2 + C_1 + 2 h_p + \delta \operatorname{tg} \beta_p - S_p + R_2 \tau_2] + (R_2 - R_{3\text{K}})(1 - \cos \varphi_2);$$

$$f' \varphi_2^k = -X_{\text{II}2} \cos \varphi_2 + \Theta + \tau_2 - Y_{\text{II}2} \sin \varphi_2 + \Theta + \tau_2 + \operatorname{ctg} \beta_p [-X_{\text{II}2} \times$$

$$\times \sin(\varphi_2 + \Theta + \tau_2) + Y_{\text{II}2} \cos \varphi_2 + \Theta + \tau_2 + R_{3\text{K}} - (R_2 - R_{3\text{K}}) \cos \varphi_2] + (R_2 - R_{3\text{K}}) \sin \varphi_2.$$

The results of the calculation of the equations (2.27), (2.30) and (2.33) testify that the mutual sliding of teeth of a belt and a pulley is observed, basically, at the first and second stages of an output from gearing. The loss of contact at the third stage of an output from gearing is possible at $t_p > t_{\text{III}}$ and $z_{\text{III}} > 120$. For engineering calculations the dependence for the **determination of ψ_2** is the following:

$$\psi_2^\circ = k_{m2} z_{\text{III}}^{-1,01} 1 + 0,28 \Delta ,$$

where k_{m2} – the factor of the outlet angle (Tab. 2.4).

Tab. 2.4. Factor of the outlet angle of teeth in gearing

Type of teeth	Module m , mm	1.0	1.5	2.0	3.0	4.0	5.0	7.0	10
trapezoidal	k_{m2}	214	206	235	308	252	286	342	352
semi-circular	k_{m2}	---	---	---	346	290	271	---	---

The developed methodological approach to the research of kinematics of a toothed-belt gearing also allows the determination of the speed of mutual sliding of teeth.

2.3. Sliding of teeth in the zones of the incomplete profile gearing of toothed-belt transmissions

The velocity of the relative sliding of teeth in the zones of the incomplete profile gearing v_{sl} is defined by the angular velocity of a pulley ω and the radius of rolling of a belt along a pulley ρ . Let's define v_{sl} , considering the rotation of a belt around the pitch point P (Fig. 2.7) with the angular velocity $\omega_p = -\omega k$, where k – a unit vector of coordinate axis Z of the system $XOYZ$.

In this case

$$v_{sl} = \omega \rho.$$

We find the length of the vector ρ from the evident relation:

$$\rho = \sqrt{X'^2 + Y'^2},$$

where $X^{(i)}$ и $Y^{(i)}$ – the coordinates of the point of contact of profiles in the fixed system of coordinates, known from (2.17), (2.18) etc.

The calculations show (Fig. 2.15) that the maximum sliding velocities are observed in the points of the beginning of contact of teeth at the input in gearing and their disconnections at the output from it.

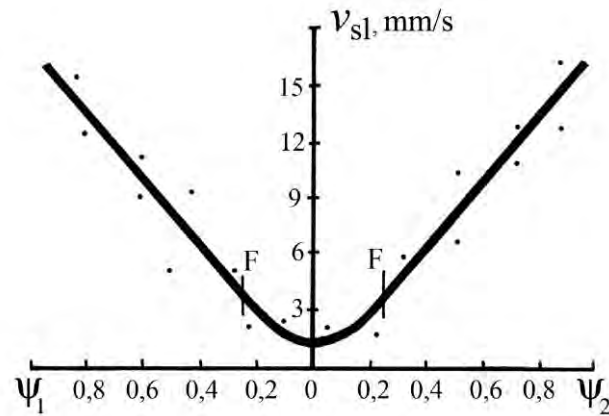


Fig. 2.15. Influence of a phase of gearing on the sliding velocity of profiles:
F – point of transition from rolling along an involute to rolling along a circle
 (• - experimental data)

In such a case, the sliding velocity at an input in gearing is 1.1 times more than at an output from it. It is obvious that it is caused by less values ρ at the output from gearing.

Thus, it might be proved, that at the output from gearing (especially with a driven pulley) the less intensive wear of belt teeth (than at the input) is observed. It happens because the lowered efforts on outputting teeth from gearing (due to the difference of diameters of pulleys) in the combination with the reduced sliding velocity lead to the essential decrease of the friction power.

For the engineering calculations the following dependence for the definition of the sliding velocity is offered [80]:

$$v_{sl} = \begin{cases} k_v \omega K_1 \varphi_x^c + K_2, & \text{mm/s} & 0 \leq \varphi_x \leq F_x \\ k_v \omega K_3, & \text{mm/s} & F_x \leq \varphi_x \leq 1, \end{cases} \quad (2.34)$$

where $\varphi_x = \varphi_2 / \psi_2$ or $\varphi_x = \varphi_2 / \psi_1$ – the relative arc of traverse of a pulley in the limits of entrance and outlet angles; $k_v = 1$ for the angle ψ_1 and $k_v = 0.56$ for the angle ψ_2 .

The other parameters, included into the formula (2.34) for the belts of various modules with **trapezoidal** and semicircular teeth, are given in Tab. 2.5.

Tab. 2.5. Parameters for the definition of sliding velocity of teeth in gearing

Type of teeth	Module m , mm	K_1	K_2	K_3	F_x	c
trapezoidal	3.0	16.72	1.08	8.50	0.23	2.01
	4.0	18.85	1.08	9.51	0.26	1.99
	5.0	13.74	1.47	11.12	0.28	1.67
semi-circular	1.0	3.03	0	2.22	0.375	1.753
	1.5	4.52	0	3.10	0.360	1.80
	2.0	6.05	0	4.01	0.342	1.805
	3.0	6.7	0.637	6.52	0.280	2.445
	4.0	5.62	1.020	7.0	0.265	1.433
	5.0	13.55	1.274	10.15	0.260	1.704
	7.0	17.88	1.528	17.46	0.230	1.342
	10.0	27.25	1.974	25.71	0.190	1.347

The value F_x shows the **part of the angle** $\psi_{1(2)}$, where the sliding of teeth occurs along the involute. In this part v_{sl} decreases linearly at an input in gearing. After passing the involute part, corresponding to the second period of an input in gearing, the center of rotation of an inputting tooth is displaced to the zone of the radius of rounding of a tip of a pulley tooth. The modulated reduction of v_{sl} up to its stabilization begins. In particular, for $m = 7$ mm; $z = 20$ and $\omega = 1 \text{ s}^{-1}$: $v_{sl,max} = 17.46$ mm/s and $v_{sl,min} = 1.73$ mm/s, i.e. in the final phase of the input in gearing the sliding velocity goes down practically up to 0, which corresponds to the really observable phenomena. For the belts with semicircular teeth $m = (3; 4; 5)$ mm, $v_{sl,max} = (8.50; 9.50; 11.12)$ mm/s and $v_{sl,min} = (1.13; 1.14; 1.60)$ mm/s accordingly.

2.4. Sliding of flexible link in the belt transmissions of a frictional type

The accounting of the influence of eccentricity of the tangential effort application (friction forces) to the flexible elastic link, leading to the occurrence of shearing deformations, allowed to explain the mechanism of work (in particular of a belt transmission) more reasonably.

In the case of neglecting of the final thickness of a belt the maximum permissible errors are mostly observed in the belt transmissions, in which high-strength fibers, film, metal cord with rubber covering, are used as traction elements making the bearing layer. In this case, the bearing layer serves for the transmission of a pull, and the layer of a belt be-

tween a pulley and traction elements provides the necessary frictional properties and transmission of loading from the surface of the pulley to the bearing layer.

In the case of the little compliance of a bearing layer, providing practically a non-extensibility of a belt at work, it is impossible to make the proved analysis of the mechanism of work of a belt transmission, taking into account only the deformation of the belt tension.

The account of the final thickness of a belt is given in the works [81, 82, 83, 84]. It was established that the part of an arc of contact, where there is no elastic sliding, is the working section, and within its limits the transmission of a part of a pull, due to the action of shear deformations, is realized.

In the work [81] the preliminary displacement of flexible bodies at their transmission of a tangential force is investigated both theoretically and experimentally.

In the work [82] the determination of the tangential forces is made through shear deformations. The change of these deformations is connected with the relative loss of the belt speed at climbing on pulleys. The given work contains the solution of a problem of sliding in a belt transmission in view of a belt operation within the limits of an arc of mesh, in which the shear deformations are determined by the difference of speeds accepting some additional conditions.

In the work [83] the research of transmission of a pull by an elastic thread at the absence of slippage within the limits of the whole arc of contact is given. In such a case the lining of a pulley has shear deformations, and the model of the interaction of the pulley layer with a thread is taken as a big number of radially directed rods. However, in the given solution at the definition of elastic parameters it is implied that the factor of proportionality of a tangential component of an effort to the deformation is characterized only by the module of the shear. The influence of the lining thickness, which value defines its shear compliance, is not accounted.

In the work [84] the assumption about a non-extensibility of traction elements of a belt is accepted, therefore the shear deformations on an arc of mesh increase linearly. As a consequence of such an assumption a relatively simple solution was worked out. However, the error of this solution increases with the augment of the compliance of a bearing layer.

The account of the final thickness of the belt leads to the following scheme of the interaction of a belt with a pulley. The elastic layer of the belt, providing the transmission of loading from the surface of the pulley to the traction elements, is in the state of the shear deformation at the transmission of the pull by the belt. The shear deformations cause the

occurrence of the tangential forces between the belt and the pulley surface. These deformations, starting in the point of climbing of the belt on the pulley, increase in view of the changes of a belt tension until the adhesion forces between the belt and the pulley p_{cp} are enough for the neutralization of shearing tangential forces p_{sh} (Fig. 2.16).

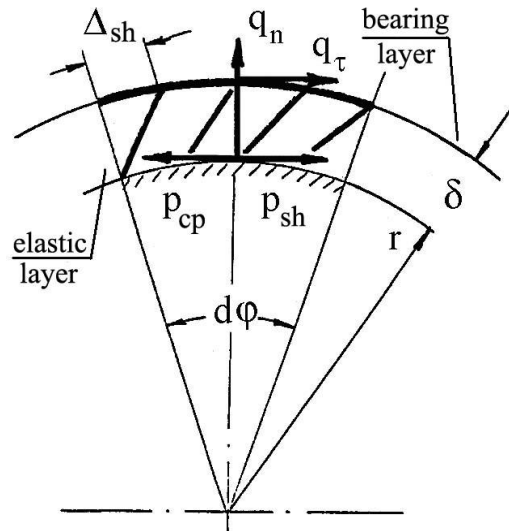


Fig. 2.16. Loading of the element of flexible link on the arc of mesh

In the point, where this condition is not satisfied, the disengagement takes place and the arc of the elastic **slippage develops**. Within the limits of this arc the remained part of the pull is transmitted due to the sliding friction between a belt and a pulley. Thus, the limiting condition of the absence of the belt slippage, relating to the pulley, is the following:

$$P_{sh} = P_{cp} \cdot \quad (2.35)$$

According to the given scheme of the interaction of the belt and the pulley within the limits of the arc of mesh the belt with the pulley represents the bodies, connected **with the help of excentric**-loaded continuous contact layer. The calculation of the elastic contact in the part of the determination of efforts in the zone of contact and kinematic displacement of bodies reduces to the solution of the equations, taken from the condition of the compatibility of displacements for the contacting interfaces of the points of bodies, accounting the balance equations and boundary conditions [85].

The pulley rigidity should be considered as infinitely high in comparison with the belt rigidity. In such a case the equations of balance and boundary conditions should be calculated in accordance with the above scheme of the interaction of the belt with the pulley. According to such a setting of a problem, hereafter, the tangential forces are defined directly from this solution without any connection with kinematic conditions, which allows reducing of the number of assumptions.

Let's study the general case of transference of a pull in a belt transmission, supposing that it is partially realized within the limits of the arcs of the relative rest.

As a supposition we accept that the factor of a frictional rest μ_s has some limiting value; the factor of a sliding friction f_s is constant; the inertial forces are not large; the angle of shear throughout the height of a belt is constant; the factors of compliance of bearing and elastic layers of a belt have the final and constant values.

The factors of compliance of bearing and elastic layers of the element of a belt on an arc of contact of a pulley of the radius r are determined by the expressions:

$$i = \frac{rd\varphi}{E\delta b}; \quad c = \frac{\delta}{Grbd\varphi},$$

where E , G – the modules of elasticity at tension and shear accordingly; δ – the thickness of a belt between a bearing layer and a surface of a pulley; b – the width of a belt; r – the radius of a pulley, mm; $d\varphi$ – the angle of an elementary arc.

The factors of the specific compliance of bearing and elastic layers for the belt of the unit size ($rd\varphi = 1$; $b = 1$) are:

$$i^1 = \frac{1}{E\delta}; \quad c^1 = \frac{\delta}{G}. \quad (2.36)$$

The pull, implemented due to the belt adhesion with a pulley, induces shear deformations in each section of the arc of the relative rest:

$$\Delta_{sh} = q_{\tau} c r d\varphi = \frac{q_{\tau} c^1}{b}, \quad (2.37)$$

where q_t – the pull intensity in the zone of the arc of adhesion, operating along the bearing layer.

In such a case the specific tangential force in the zone of contact of the belt with the pulley is determined by the expression:

$$\rho_{sh} = \frac{\Delta_{sh} b G}{\delta},$$

from which, accounting the expressions (2.36) and (2.37), we get:

$$\rho_{sh} = q_t. \quad (2.38)$$

The adhesion effort of the belt with the pulley depends on the factor of the frictional rest μ_s and the radial specific pressure on the pulley q_n , which is defined from the expression:

$$q_n = \frac{F}{r},$$

where F – the tension of a belt of an arc of adhesion.

Thus,

$$\rho_{cp} = \frac{\mu_s F}{r}. \quad (2.39)$$

The effort q_t and the tension F are the variable values in the expressions (2.38) and (2.39). The connection between these parameters is determined by the differential equation of the stationary motion of flexible link of the first order:

$$q_t = \frac{d}{d\varphi} \left(\frac{F}{r} \right). \quad (2.40)$$

For the determination of the law of the change of intensity of a pull at the absence of the elastic sliding we accept the following model of contact of a belt with a pulley, assuming that the belt adhesion with the pulley surface takes place in a point. The elastic lay-

er of a belt between traction elements and the pulley surface can be reported in the form of the infinitely large number of cross-mounted radial rods, working only for shear.

The similar models are often used at the description of the elastic contact. Such a model is accepted in the work [83], where the angle of declination of rods, replacing the elastic layer **of lining** of a pulley, is proportional to the tangential component of an effort from a thread. Having accepted the discrete model of contact of the belt with the pulley, the intensity of loading change between the rods can be found in the form of a continuous analytical function.

The realization of a pull within the limits of an arc of contact by means of the shear deformations leads to the irregularity of the initial position of rod-connections. Accepting the above scheme of the distribution of shear deformations in the belt, the angle of declination of rods from the radial direction on the both pulleys increases from the point of climbing, in addition, the angle is equal to zero for the rods in the point of climbing of a belt on pulleys (Fig. 2.17).

For the work of a scheme of the deformation of rods, the distance between them over the bearing layer should be less than the distance over the surface of the drive pulley. For the driven pulley this ratio is inverted. In this case the condition of the deformation compatibility is the following:

$$f_n - f_{n+1} = \Delta_{n, n+1} - \Delta, \quad (2.41)$$

where f_n, f_{n+1} – the deformations of n -th and $(n+1)$ -th rods; $\Delta_{n, n+1}$ – the deformation of a bearing layer between rods; Δ – **the** difference of rod steps over the bearing layer and the pulley surface, providing the given scheme of the deformation of rods.

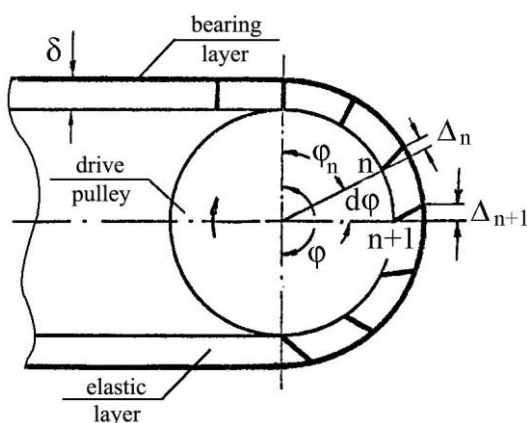


Fig. 2.17. Change of shear deformations in flexible link

Expressing the deformation in terms of the power and elastic parameters of a belt with the length $r d\varphi$ and width b , we get:

$$\frac{c^1}{br d\varphi} (F_n - F_{n+1}) = \frac{i^1 r d\varphi}{b} (F_{tcp} - R_n) - \frac{i^1 r d\varphi}{b} \Delta F, \quad (2.42)$$

where F_{tcp} – the pull, transmitted by the belt (within the limits of the arc of mesh); F_n – the effort to n -th rod; $R_n = F_1 + F_2 + \dots + F_n$; ΔF – the effort, corresponding to the difference of the steps Δ .

In the equations (2.41) and (2.42) the parameters Δ and ΔF are the constant values, independent of n and determined from the boundary conditions.

The distribution of efforts between the rods can be found by analogy with the solution of the problem of the loading distribution between teeth in a toothed-belt transmission [86], as the interaction of a toothed belt with a pulley at the infinitely small thickness of teeth is the analogue of the accepted above model of contact of a belt with a pulley. According to the solution, given in [87], we denote:

$$F_n = R_n - R_{n-1} = \Delta R_n;$$

$$F_{n+1} = R_{n+1} - R_n = \Delta R_{n+1}.$$

Thus,

$$F_n - F_{n+1} = \Delta R_n - \Delta R_{n+1} = \Delta^2 R_n.$$

where ΔR – the first divided difference; $\Delta^2 R_n$ – the second divided difference.

As the second divided difference is close to the value of the second derivative, the equation (2.42) can be written in the form of the differential equation of the second order with a constant right part:

$$\frac{d^2 R_n}{d\varphi^2} + \alpha R_n = \alpha (F_{tcp} - \Delta F),$$

where $\alpha = (i^1 / c^1) r^2$.

The complete solution of this equation is the following:

$$R_n = F_{tcp} - \Delta F + C_1 e^{\sqrt{\alpha}\varphi_n} + C_2 e^{-\sqrt{\alpha}\varphi_n}. \quad (2.43)$$

where C_1, C_2 – constants.

Taking into account the value R_n , the tensions of a belt within the limits of the arcs of mesh on drive and driven pulleys are determined by the expressions:

$$F_{dr} = F_1 - R_n; \quad F_{dv} = F_2 + R_n, \quad (2.44)$$

where $F_{1(2)}$ – the tension of the driving (following) sides of a belt.

The intensity of the change of a pull (tension) along the arc of mesh can be defined by using the differential equation of stationary motion of flexible link of the 1-st order relating to the tension in the form of the expression (2.40), from which, accounting the expressions (2.43) and (2.44), we get:

$$q_\tau = \frac{\sqrt{\alpha}}{r} C_1 e^{\sqrt{\alpha}\varphi_n} + C_2 e^{-\sqrt{\alpha}\varphi_n}. \quad (2.45)$$

For the determination of C_1, C_2 and ΔF we use the following boundary conditions: at $\varphi_n = 0 \rightarrow R_n = 0; q_\tau = 0$; at $\varphi_n = \varphi_{cp} \rightarrow R_n = F_{tcp}$.

As a result, we get:

$$C_1 = C_2 = \frac{F_{tcp}}{2(\operatorname{ch}\sqrt{\alpha}\varphi_{cp} - 1)}; \quad (2.46)$$

$$\Delta F = F_{tcp} \frac{\operatorname{ch}\sqrt{\alpha}\varphi_{cp}}{\operatorname{ch}\sqrt{\alpha}\varphi_{cp} - 1}. \quad (2.47)$$

Accounting the expressions (2.45) and (2.46), the dependence (2.38) becomes:

$$\rho_{sh} = q_{\tau} = \frac{F_{tcp}}{r} \sqrt{\alpha} \frac{\text{sh}\sqrt{\alpha}\varphi_n}{\text{ch}\sqrt{\alpha}\varphi_{cp} - 1}, \quad (2.48)$$

and from the expression (2.39), accounting (2.43), (2.46) and (2.47) for drive and driven pulleys accordingly, we have:

$$\rho_{cp} = \frac{\mu_s}{r} \left(F_{1(2)} \mp F_{tcp} \frac{\text{ch}\sqrt{\alpha}\varphi_n - 1}{\text{ch}\sqrt{\alpha}\varphi_{cp} - 1} \right). \quad (2.49)$$

Finally, accounting the expressions (2.48) and (2.49), the condition (2.35) for the point of the action of the maximum shearing effort, when $\varphi_n = \varphi_{cp}$, becomes:

$$F_{tcp} \cdot A = \mu_s \left(F_{1(2)} \mp F_{tcp} \right), \quad (2.50)$$

where A – the factor, characterizing elastic and geometrical parameters of flexible link

$$A = \frac{\sqrt{\alpha} \text{sh}\sqrt{\alpha}\varphi_{cp}}{\text{ch}\sqrt{\alpha}\varphi_{cp} - 1}. \quad (2.51)$$

Within the limits of the arc of mesh φ_{cp} from the point of climbing of a belt on pulleys to the point with the limiting value of shearing tangential efforts a part of the pull F_{tcp} is transmitted due to the realization of adhesion forces between the belt and the pulley. On the other part of the arc of contact – φ_{sl} , from the point of disengagement to the point of running-out of a belt from pulleys the remained part of the pull F_{tsl} is transmitted. Hence, in the point, corresponding to the border of the arcs of mesh and sliding (Fig. 2.18), the tension of the belt is:

on the drive pulley

$$F_{bn} = F_1 - F_{tcp} = F_2 + F_{tsl};$$

on the driven pulley

$$F_{bn} = F_1 - F_{tsl} = F_2 + F_{cp}.$$

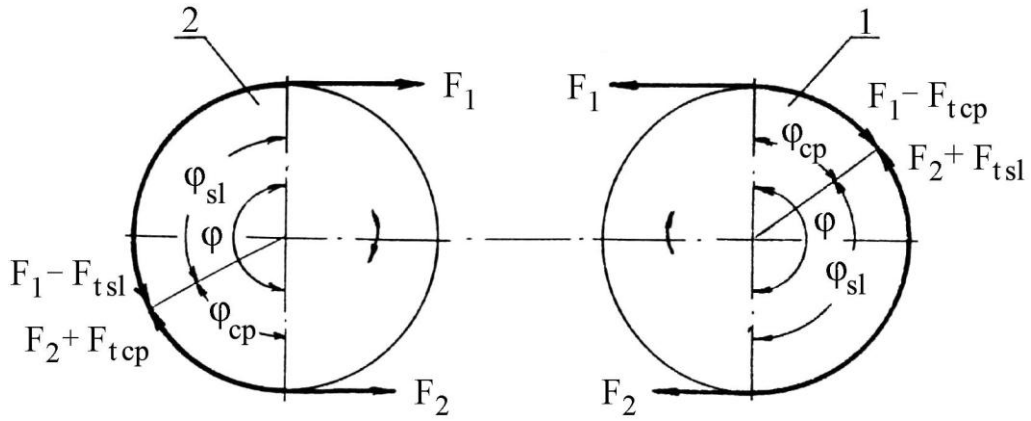


Fig. 2.18. Forces on the belt within the limits of the arcs of contact:
1 – drive pulley; 2 – driven pulley

Using the expression (2.50) for the arcs of mesh and Euler's equation for the arcs of sliding, we can write the following system of equations for the drive and driven pulleys:

$$\frac{F_{tcp}}{F_1} = \frac{1}{\frac{A}{\mu_s} + 1}; \quad \frac{F_2 + F_{tsl}}{F_2} = e^{f\varphi_{sl}}; \quad (2.52)$$

$$\frac{F_{tcp}}{F_2} = \frac{1}{\frac{A}{\mu_s} - 1}; \quad \frac{F_1}{F_1 - F_{tsl}} = e^{f\varphi_{sl}}. \quad (2.53)$$

Solving them with the account of $F_t = F_1 - F_2 = F_{tcp} + F_{tsl}$, we get the dependences for the determination of the traction factor $\chi = \frac{F_1 - F_2}{F_1 + F_2}$:
for the drive pulley

$$\chi = \frac{e^{f\varphi_{sl}} \left(1 + \frac{\mu_s}{A} \right) - 1}{e^{f\varphi_{sl}} \left(1 + \frac{\mu_s}{A} \right) + 1}; \quad (2.54)$$

for the driven pulley

$$\chi = \frac{e^{f\varphi_{sl}} - \left(1 - \frac{\mu_s}{A}\right)}{e^{f\varphi_{sl}} + \left(1 - \frac{\mu_s}{A}\right)}. \quad (2.55)$$

Let's consider some special cases. At the pull transmission and the occurrence of the belt slippage within the limits of the whole arc of contact ($\varphi_{cp} = 0$; $\varphi_{sl} = \varphi$), i.e. at the limit of the origination of slipping, the factor A has the uncertainty $0/0$. Using L'Hospital rule for the expression (2.51), we get:

$$\lim_{\varphi_{cp} \rightarrow 0} A = \sqrt{\alpha} \frac{\operatorname{ch} \sqrt{\alpha} \varphi_{cp}}{\operatorname{sh} \sqrt{\alpha} \varphi_{cp}}$$

where at $\varphi_{cp} = 0 \rightarrow A = \infty$.

Thus, the dependences (2.54) and (2.55) change to Euler's equation:

$$\chi = \frac{e^{f\varphi_{sl}} - 1}{e^{f\varphi_{sl}} + 1}. \quad (2.56)$$

At the pull transmission by means of the shear deformations without a belt slippage relating to the pulley ($\varphi_{sl} = 0$; $\varphi_{cp} = \varphi$) the dependences (2.54) and (2.55) become:

$$\chi = \frac{1}{\frac{2A}{\mu_s} \pm 1}, \quad (2.57)$$

where "+" – for a drive pulley; "-" – for a driven pulley.

From the dependence (2.57) it follows that the danger of the occurrence of slippage arises on the drive pulley at the less value of transmitted pull than on the driven pulley. According to this, the maximum pull, transmitted by the belt at the absence of the elastic sliding, is determined by the expression:

$$F_{tcpmax} = \frac{F_1 + F_2}{\frac{2A}{\mu_s} + 1} \cong \frac{2F_0}{\frac{2A}{\mu_s} + 1}.$$

where F_0 – the preliminary tension of a belt.

In the case of using of flexible links with a bearing layer of the increased rigidity, we accept the assumption about its non-extensibility ($\alpha \rightarrow 0$; $i \rightarrow 0$). In such a case, inserting the small parameter ($i=0$), from the expression (2.48) we get:

$$\rho_{sh} = \frac{F_{tcp}}{r} \frac{\varphi_n}{\varphi_{cp}^2},$$

i.e. at the infinite rigidity of the bearing layer of flexible link the shear deformations, beginning from 0 at the point of its climbing on pulleys, increase linearly along the arc of mesh.

With the introduction of a small parameter from the expression (2.51) we get $A = 2 / \varphi_{cp}$ and, in this case, the dependence (2.57) becomes:

$$\chi = \frac{1}{\frac{4}{\varphi \mu_s} \pm 1}.$$

The analogous dependence is derived at the same initial supposition in the work [84]. Hence, in the assumption of a non-extensibility of a bearing layer of a belt the traction factor does not depend on the radius of a pulley. For the extensible bearing layer with the increase of the pulley radius the traction factor decreases.

The analysis of the received results at the following numerical parameters is given below: $\mu_s = f_{fs} = 0.35$; $G = 1.0$ MPa; $\delta = 2.5$ mm; the compliance of the elastic belt layer $c^1 = \delta / G = 2.5$ mm³/N; the compliance of a bearing layer i^1 changes from 0 to 0.02 mm/N; $r = 50 \dots 100$ mm.

Assuming the absence of the belt **slippage** relating to the pulley within the limits of the whole arc of contact ($\varphi_{cp} = \varphi = 180^\circ$), using the expression (2.57) in Fig. 2.19, the de-

dependences χ of the compliance of a bearing layer of a belt for drive and driven pulleys are shown.

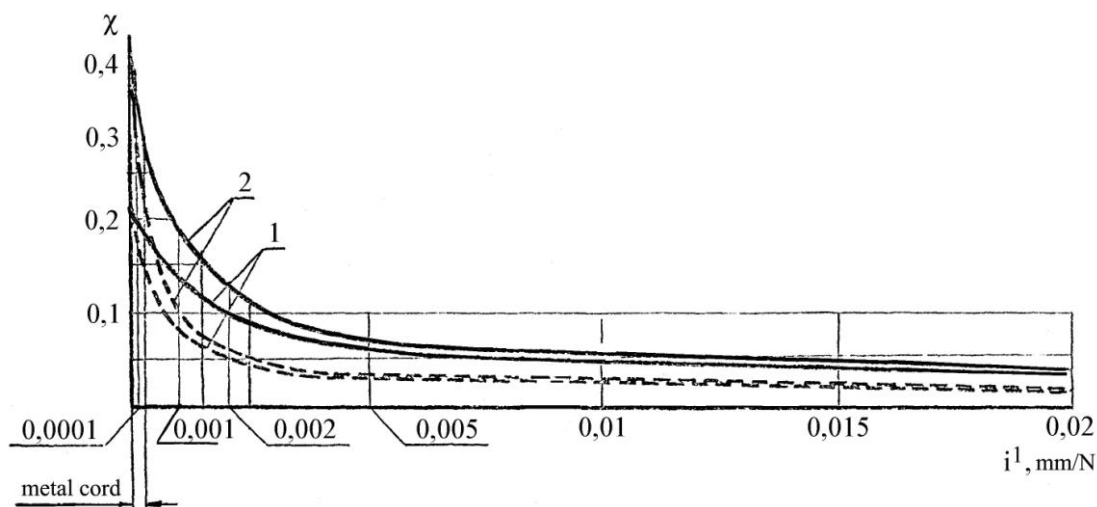


Fig. 2.19. Dependence of traction ability of a belt of the compliance of a bearing layer:
1 – drive pulley; 2 – driven pulley; — — — $r = 50$ mm; - - - - $r = 100$ mm

The received graphs show that for the belts with the metal cord bearing layer (mm/N) $i^1 = 0.0001$ the values χ are: for a drive pulley ≈ 0.19 ; for a driven pulley ≈ 0.31 , and in the interval of possible values of the compliance factor of a bearing layer along with the change of the pulley radius the values change slightly. For common belts (at the compliance factor of a bearing layer $i^1 \geq 0.01$ of mm/N) χ becomes less than 0.5 and changes proportionally to the pulley radius change.

While the arc of mesh decreases, χ increases up to the limiting value at $\varphi_{cp} = 0$.

In Fig. 2.20 the dependences χ of the value of the arc of sliding φ_{sl} , made with the help of the expressions (2.54) and (2.55) at $r = 75$ mm and (2.56), are shown.

According to Euler's formula, at $\varphi_{sl} = \pi$ the limiting value of the traction factor is:

$$\chi_{lim} = \frac{e^{\pi \cdot 0.35} - 1}{e^{\pi \cdot 0.35} + 1} = 0.5.$$

Thus, the calculations, made on the basis of the given technique, show that at the accepted initial parameters for the belts with the metal cord bearing layer at the power making up to 38...40 % from the nominal power, the loading transmission is completely

ensured by means of shear deformations. For common belts this value is less than 10 %. At the transmission of higher power the zone of the elastic sliding (firstly on the drive pulley and then on the driven pulley) takes place.

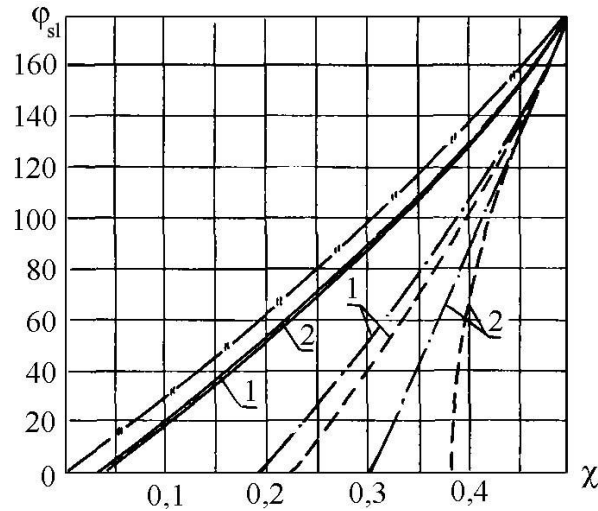


Fig. 2.20. Dependence of traction ability of a belt of the value of the angle of sliding:
 1 – drive pulley; 2 – driven pulley; - - - - $j^1 = 0$; - · - · - $j^1 = 0.0001$ mm/N;
 — — — $j^1 = 0.01$ mm/N – formulas (2.54) and (2.55); — " — — — formula (2.56).

The received results show that the account of shear deformations at the estimation of traction properties of a belt transmission in a much greater measure is important for the belts with a bearing layer, made of slightly-extensible traction elements in the form of metal cords, polyamide cords or cords from fiber glasses ($j^1 \leq 0.002$ mm/N), for which the above model of the interaction of a belt with a pulley.

The compliance of the belt elastic layer also influences the traction ability of transmission. In this case, the more compliant the belt elastic layer is, in comparison with the compliance of its bearing layer, the larger part of the traction effort is transmitted in the zone of the relative rest.

Thus, the predetermined combination of the compliance of bearing and elastic layers of a belt can probably provide its corresponding bearing ability.

At the account of the final thickness of a belt the relative speed loss, which is caused by the different tension of driving and following belt sides, makes only a part of total speed losses in transmission, as the difference of speeds of a pulley and a belt bearing layer is partially provided with the shear deformations of the belt. Hence, the total speed

loss in transmission is developed from the relative speed losses ξ_{sh1} and ξ_{sh2} on the drive and driven pulleys, connected with the process of the increase of shear deformations after climbing of the belt on pulleys, and the relative speed loss ξ_p due to the different tension of sides, i.e.

$$\xi = \xi_{sh1} + \xi_{sh2} + \xi_p.$$

The sliding, determined by the difference of relative elongation of the belt sides, is defined by the known dependence:

$$\xi_p = 2\chi \frac{\sigma_0}{E}, \quad (2.58)$$

where σ_0 – the pretension pressure in a belt.

The sliding, connected with the occurrence of the shear deformation, is determined by the relation of the value of the shear deformation $\Delta_{sh\max}$ to the length of the arc of mesh $r\varphi_{c\kappa}$. Accounting the expressions (2.37), (2.48) and (2.51), the maximum shear deformation on the line of disengagement is:

$$\Delta_{sh\max} = \frac{q_{\tau}}{e} c^1 = \frac{F_{tcp} c^1}{e \cdot r} A.$$

The finally required sliding is determined by the expression:

$$\xi_{sh} = \frac{\Delta_{sh}}{r\varphi_{cp}} = \frac{F_{tcp} A c^1}{br^2 \varphi_{cp}}. \quad (2.59)$$

At a small compliance of a bearing layer, when it can be accepted practically non-extensible ($i=0$), accounting that $A=2/\varphi_{cp}$, the last expression becomes [84]

$$\xi_{sh} = \frac{2F_{tcp} c^1}{br^2 \varphi_{cp}^2}. \quad (2.60)$$

The expressions (2.59) and (2.60) show the dependence of sliding on the radius of a pulley and the values of the arc of mesh, with the reduction of which the relative speed loss increases. This circumstance, confirmed experimentally, is not represented in the formula (2.58). Besides, the linearity of the relative sliding, resulted from the formula (2.58), is fulfilled, according to the expression (2.59), only till the moment when the arc of mesh extends on the whole arc of contact, i.e. at $\varphi_{cp} = \varphi$. In this case,

$$\xi_{sh} = \frac{F_{tcp1}}{e \cdot r^2 \varphi} \sqrt{\alpha} \frac{\text{sh}\sqrt{\alpha}\varphi}{\text{ch}\sqrt{\alpha}\varphi - 1}.$$

At the further increase of a pull, while the arc of mesh is reducing, the linearity of the relative sliding, according to the dependence (2.59), is broken, and in the limit when $\varphi_{cp} = 0$, the slippage extends on the whole arc of contact, in this case, the relative speed loss is equal to the infinity, i.e. it leads to slipping.

The sequence of the determination of the relative speed loss, owing to the shear deformations on the drive and driven pulleys, is the following.

Supposing the validity of the ratio $F_1 + F_2 = 2F_0$ with the use of the dependences (2.54) and (2.55), the pulls on drive and driven pulleys are defined at different values of the angle φ_{sl} :

$$F_{t1} = 2F_0 \frac{e^{f\varphi_{sl}} \left(1 + \frac{\mu_s}{A}\right) - 1}{e^{f\varphi_{sl}} \left(1 + \frac{\mu_s}{A}\right) + 1}; \quad F_{t2} = 2F_0 \frac{e^{f\varphi_{sl}} - \left(1 - \frac{\mu_s}{A}\right)}{e^{f\varphi_{sl}} + \left(1 - \frac{\mu_s}{A}\right)}.$$

Hereafter, according to the expressions (2.52) and (2.53), the values of pull quantities, transferred by means of adhesion forces, are defined:

$$F_{tcp1} = \frac{F_0 + 0.5F_{t1}}{\frac{A}{\mu_s} + 1}; \quad F_{tcp2} = \frac{F_0 - 0.5F_{t2}}{\frac{A}{\mu_s} - 1}.$$

Finally, from the formula (2.59) the sliding, caused by the shear deformations on the drive and driven pulleys, can be defined.

In Fig. 2.21 the curves of the relative sliding, received in the result of the calculations on the developed dependences, are presented. In this case, it is accepted: $c^1 = 2.5 \text{ mm}^3/\text{N}$; $i^1 = 0.0001 \text{ mm}/\text{N}$ (the bearing layer in the form of metal cord); $r = 75 \text{ mm}$; $\mu_s = f_{fs} = 0.35$; $\varphi = \pi$; $F_0 = 70 \text{ N}/\text{mm}$; $u = 1$.

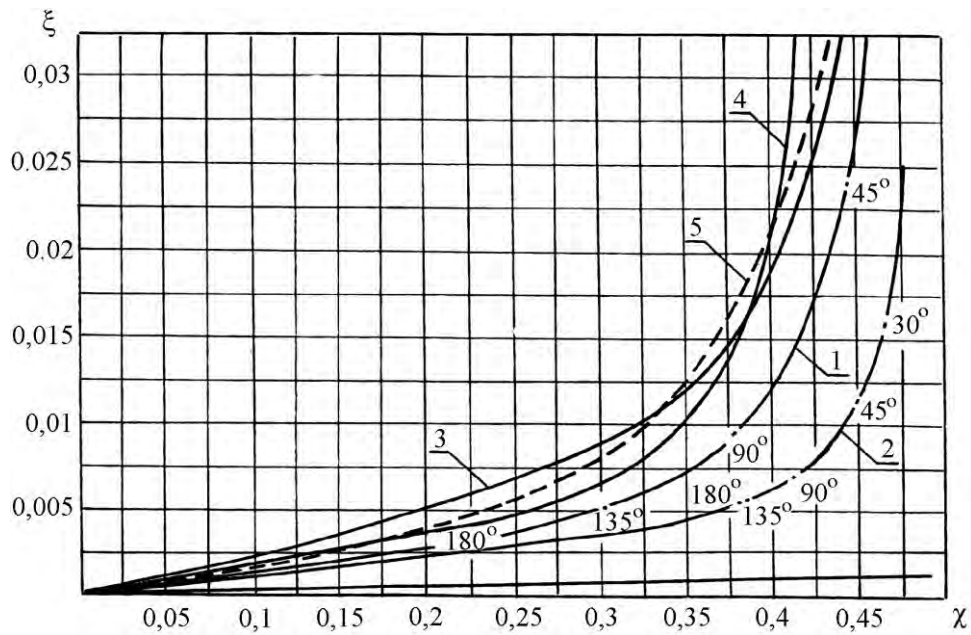


Fig. 2.21. Curves of sliding: 1 – calculated curve for a drive pulley; 2 – calculated curve for a driven pulley; 3 – total calculated curve; 4 – theoretical [84]; 5 – experimental [84]

The values of the angles of mesh are given on the calculated curves of sliding for drive and driven pulleys accordingly. In the same place the experimental curve of relative sliding for a belt with a bearing layer of a steel wire and also the theoretical one (in the assumption of non-extensibility of a bearing layer, according to the data resulted in the work [84]), are given.

The error of the calculated curve of sliding from the linear dependence begins at $\chi = 0.22$, when the angle of mesh becomes less than 180° on a drive pulley, i.e. with the occurrence of the arc of sliding. At $\chi = 0.38$, when the arc of sliding does not occur on the driven pulley yet, and it extends to the half of the arc of contact on the drive pulley, the total curve of sliding has already a considerable declination from the graph of the linear dependence. In the section, where the calculated curve of sliding asymptotically approaches the ordinate, corresponding to χ_{\max} , the angles of mesh on the pulleys make from 30° up to

45° ($\chi_{\max} \approx 0.45$). It follows that not only within the limits of a rectilinear section of the sliding curve, but also within the limits of a curvilinear section, the work of transmission remains stable and it is far from the occurrence of slipping at a sufficiently guaranteed value of the angle of mesh.

In this connection the right method of the approach to the choice of loading corresponds to the calculation of transmission by the reserve of mesh. Thus, having the optimum reserve on the values of the angle of mesh on a drive pulley, it is possible to operate the belt transmission by the loading ability more rationally. This angle makes $\approx 70^\circ$ for the calculated sliding curve.

The analysis of the received results testifies that the relative sliding at a small influence of tension of the bearing layer arises, basically, due to the shear deformations in the belt, and the developed theoretical dependences for the calculation of the relative sliding are adequate to the experimental data.

2.5. Factor of a face overlap of teeth in toothed-belt transmissions

Let's examine the technique of the calculation of the number of teeth in gearing z_0 in view of the fact that the part of a pull is transferred by the teeth, which are in the zones of the incomplete profile gearing, i.e. within the limits of the angles ψ_1 and ψ_2 . In this case, z_0 is equal to the factor of the face overlap of transmission, because toothed-belt transmissions are carried out basically with spur teeth.

Let's consider the case of gearing of the belt with the pulley with the ratio $\alpha_G / t_p^0 = 3.92$ (Fig. 2.22). We mark out the angles ψ_1 and ψ_2 within the limits of one angular step t_p^0 and also $\tau_1 = t_p - \psi_1$ and $\tau_2 = t_p - \psi_2$. We consider the gearing in the reversed motion, the rotation of the arc α_r in an opposite direction is adequate to the clockwise rotation of a pulley.

Let's assume that at the initial moment, corresponding to the position 1-1 of the arc α_G , the initial contact of a pair of teeth, inputting in gearing 00, took place. During the turn of a pulley by the angle ψ_1 and moving of the arc α_G to the positions 2-2; 3-3 the pair of teeth 00 inputs in gearing. When the arc α_G takes the position 4-4, the input in gearing of the pair 00 finishes. The further turn of the pulley (position 6-6) during the angle τ_1 takes place with the tooth 0, which has completely input in gearing, while the next pair of teeth –

11 – does not start its input in gearing. The moment of contact of teeth of the given pair corresponds to the position 7-7 of the arc of contact, and all the actions will repeat later on.

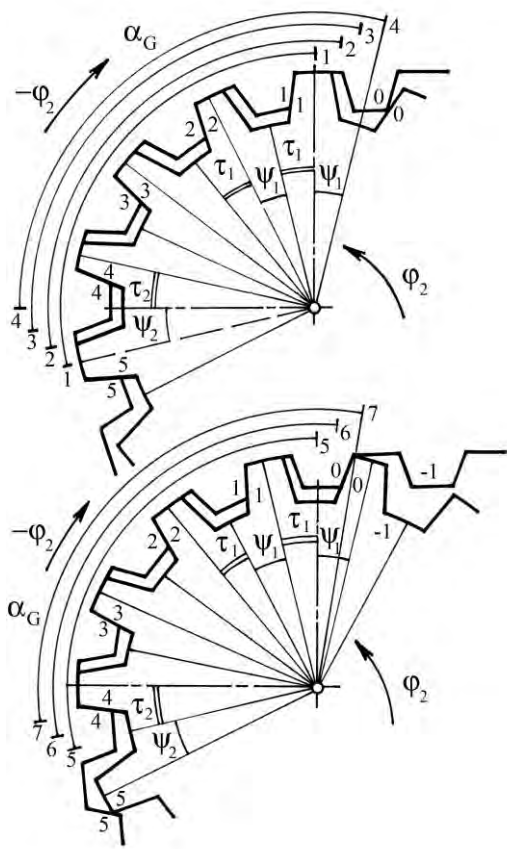


Fig. 2.22. Phases of gearing of a toothed belt with a pulley ($a_G / t_p^0 = 3.92$)

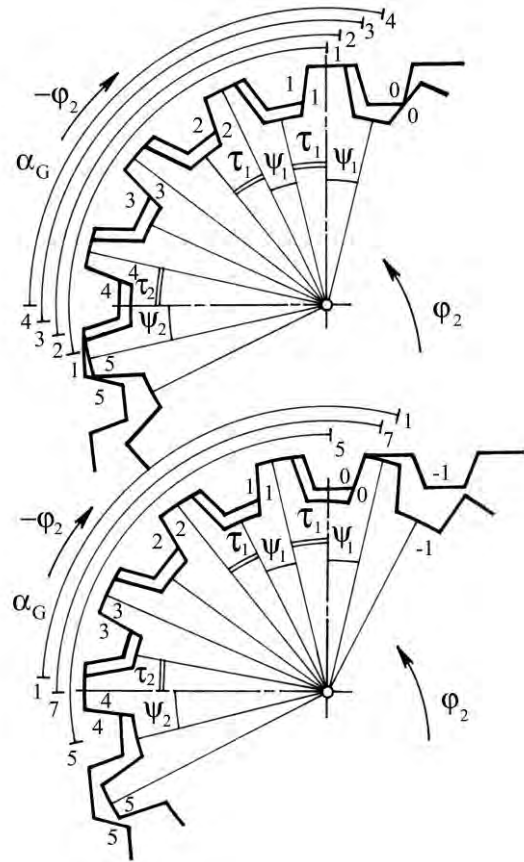


Fig. 2.23. Phases of gearing of a toothed belt with a pulley ($a_G / t_p^0 = 3.85$)

The described input in gearing is similar to the other ratios α_G and t_p^0 . In this case, the quantity of engaging pairs of teeth depends on the situation at an output of teeth from gearing. Thus, the position 1-1 corresponds to the beginning of the contact of teeth 00 at the input and to the beginning of the output from gearing of the pair 55 at the output. Considering all the engaging pairs of teeth at $a_G / t_p^0 = 3.92$, for the position 1-1 we get $\epsilon_\alpha = 4 + 2 = 6$, at that, two pairs of teeth (00 and 55) are in the zone of the incomplete profile gearing. The value $\epsilon_\alpha = 6$ is kept till the position 5-5, when after the turn by the angle ψ_2 the pair 55 outputs from gearing. As the following pair 11 at the input has not input in gearing yet, then $\epsilon_\alpha = 4 + 1 = 5$. At the moment, corresponding to the position 7-7, there is a contact of teeth in the pair 11 and the output from gearing of the pair 44 begins i.e. $\epsilon_\alpha = 4 + 2 = 6$ (as well as in the case 1-1).

The similar processes occur at $a_G / f_p^0 = 3.85$ (Fig. 2.23). The turn during the phases 1-1; 2-2; 3-3; 4-4 corresponds to $\epsilon_\alpha = 4 + 2 = 6$. At the moment, corresponding to 5-5, the disengagement of the pair 55 takes place, and the further turn till the position 7-7 takes place at $\epsilon_\alpha = 4 + 1 = 5$.

At $a_G / f_p^0 = 3.46$ (Fig. 2.24) during the turn 1-1; 2-2: $\epsilon_\alpha = 4 + 2 = 6$. The disengagement of the pair 55 corresponds to the finish of the phase 2-2, and further $\epsilon_\alpha = 4 + 1 = 5$.

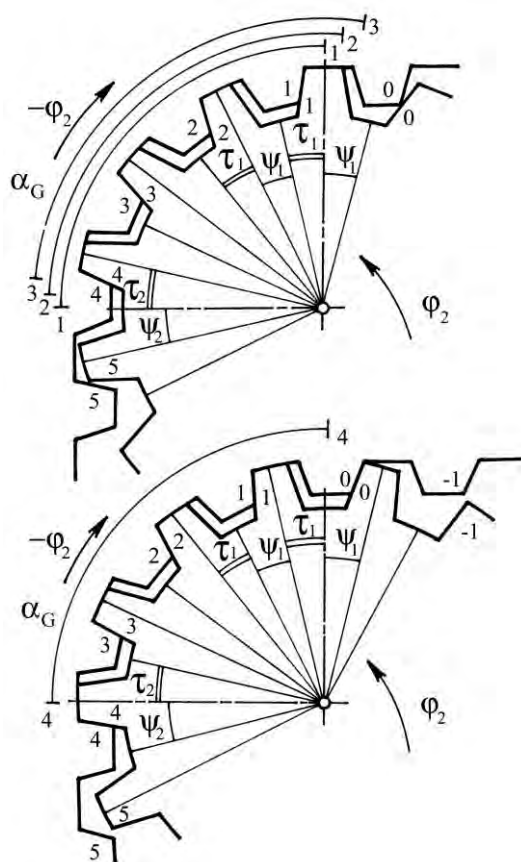


Fig. 2.24. Phases of gearing of a toothed belt with a pulley ($a_G / f_p^0 = 3.46$)

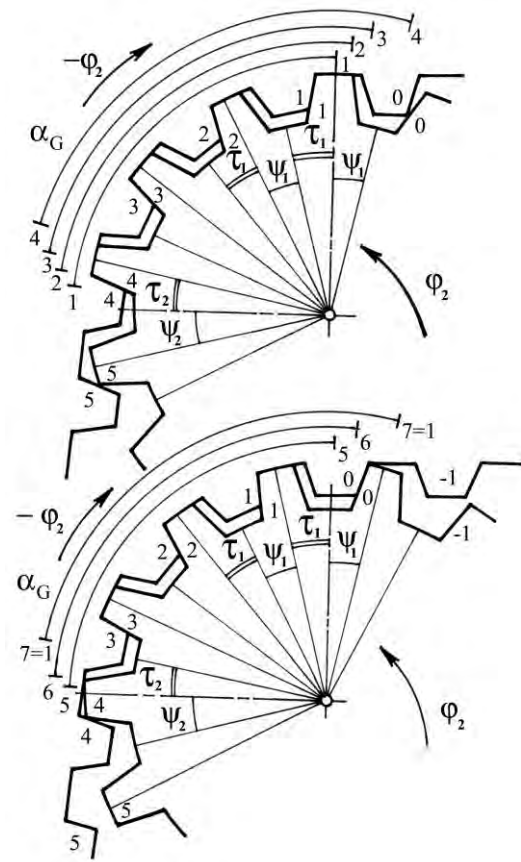


Fig. 2.25. Phases of gearing of a toothed belt with a pulley ($a_G / f_p^0 = 3.24$)

At $a_G / f_p^0 = 3.24$ (Fig. 2.25) the value $\epsilon_\alpha = 6$, corresponding to the beginning of the contact of the pair 00 and to the last moment of the contact of the pair 55, is observed only in the case 1-1.

At $a_G / t_p^0 = 3.08$ (Fig. 2.26) in the case 1-1 the factor of overlap $\epsilon_\alpha = 4 + 1 = 5$ as the pair 55 at the moment of the contact of the pair 00 has already output from gearing. This value ϵ_α is kept for all the positions of the angle α_G .

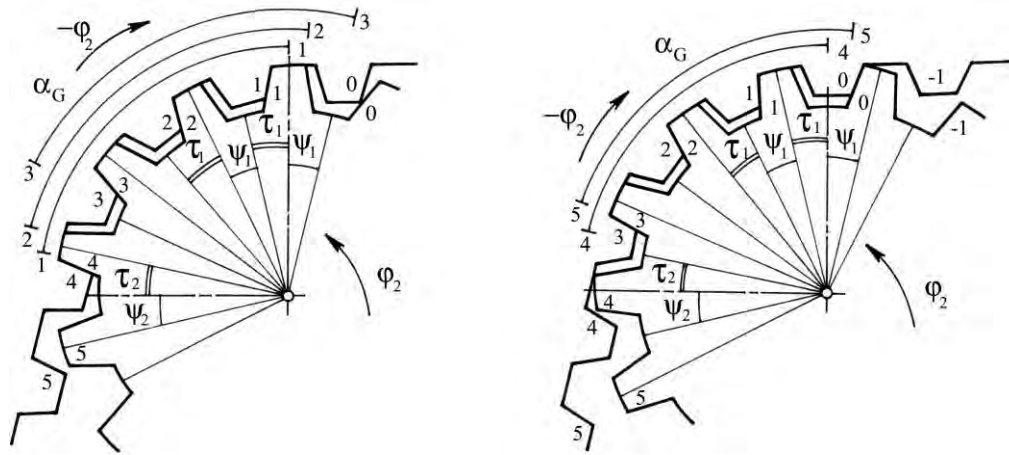


Fig. 2.26. Phases of gearing of a toothed belt with a pulley ($a_G / t_p^0 = 3.08$)

Thus, if the angle α_G braces the arc on the pulley from the beginning of the angle ψ_1 up to the section of the angle τ_2 in the zone of the output from gearing, the quantity of the interfacing (mating) pairs of teeth $z_0 = n+1$, and it does not depend on the arc of traverse of the pulley ϕ_2 . In this case $\epsilon_\alpha = z_0$.

In the last formula n designates the integral part of fraction $[(\alpha_G + \psi_1) / t_p^0] - 0.5$. The value 0.5 shows that the beginnings of **the angles** ψ_1 and ψ_2 are shifted approximately by $0.5 t_p^0$, since the finish of an input in gearing is observed at the input in the zone of the arc of contact α_G of the axis of symmetry of an interdental space of the pulley, and the beginning of the output from gearing corresponds to the moment of the output of the axis of symmetry of a pulley tooth from the zone of the angle α_G .

If α_G braces the arc from the beginning of ψ_1 up to the part of **the angle** ψ_2 , then at the rotation of the pulley ϵ_α changes from z_0 up to $(z_0 + 1)$ with the period t_p^0 , which can be presented by the following periodic function (Fig. 2.27) [79]:

$$\varepsilon_{\alpha} \varphi_2 = \begin{cases} z_0 + 2; & 0 \leq \varphi_2 \leq t_p^0 - z_0 + 0.5 - \psi_2 - \alpha_T, \\ z_0 + 1; & t_p^0 - z_0 + 0.5 - \psi_2 - \alpha_T \leq \varphi_2 \leq t_p^0. \end{cases} \quad (2.61)$$

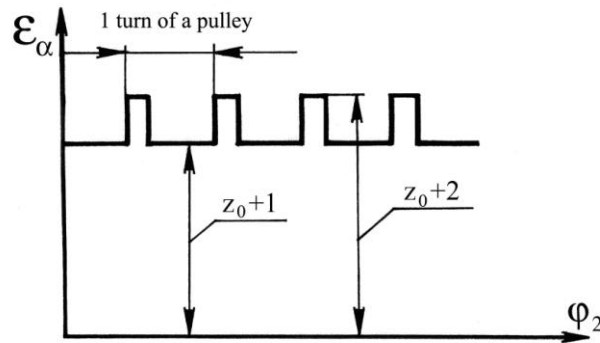


Fig. 2.27. Function of the change of the factor of overlap at the rotation of a pulley

In the expression (2.61) z_0 corresponds to the value of fraction a_G / t_p^0 , rounded up to the nearest larger whole number. Thus, for the attainment of the stable and maximum values ε_{α} the value α_G should be more than the whole quantity t_p^0 by the angle τ_2 .

2.6. Experimental research of the sliding velocity of teeth

The main aim of the given research is to receive the experimental values v_{sl} in order to check the developed theoretical propositions.

Toothed belts with the module $m = 7$ mm; $z_p = 71$; $B_p = 32$ and 50 mm, made by the method of diaphragm vulcanization and having a wear resistant fabric covering of teeth, are the main objects of the researches. The special stand (Fig. 2.28), working on the principle of the open power contour, was developed and made for carrying out of the researches [80].

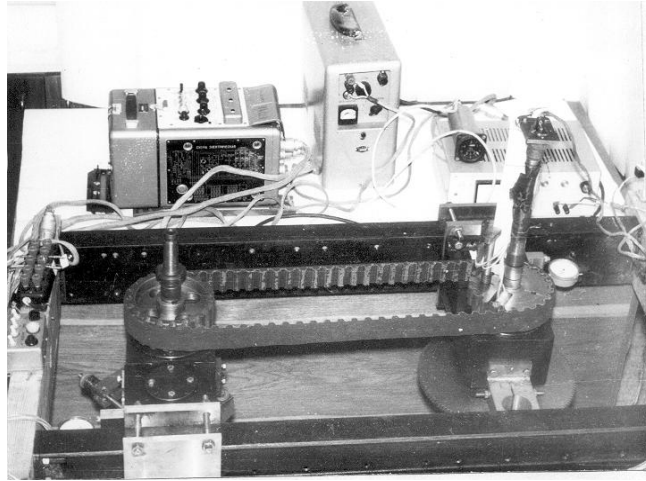


Fig. 2.28. Stand for the measurement of the sliding velocity of teeth and loading of gearing

The strain-gauge beam with a measuring ledge is extended in cantilever on a strain-gauge pulley (Fig. 2.29) with the help of an arm. The ledge moves in a slot parallel to the lateral side of a tooth of a pulley.

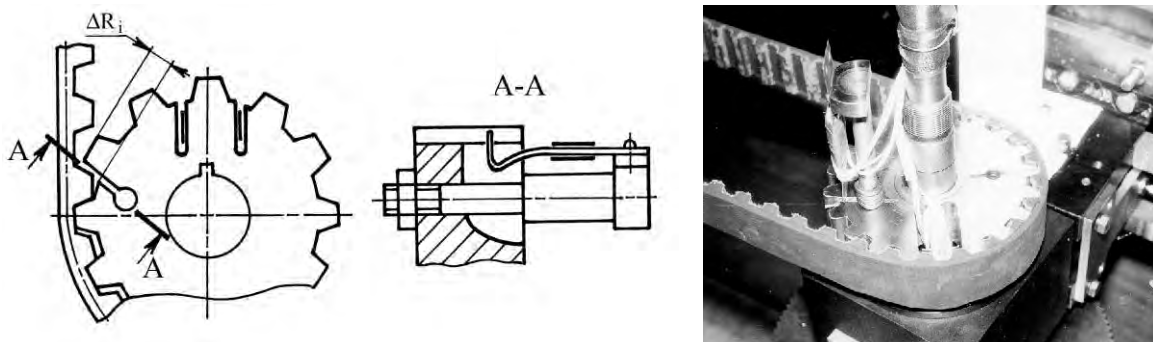


Fig. 2.29. Strain-gauge pulley for the measurement of the sliding velocity of teeth and loading of gearing

At the input in gearing the tooth of the belt interacts with the ledge of the beam, reducing the gap width ΔR_i , which is registered by strain-gauge sensors. At the output of the belt tooth from gearing the elastic beam unsets.

The investigations are made on a toothed-belt transmission with a number of teeth of pulleys $z_1 = z_2 = 20$. The received oscillograms (Fig. 2.30) are treated by the method of ordinates. The replication of the experiment is 4 at reliability 0.95.

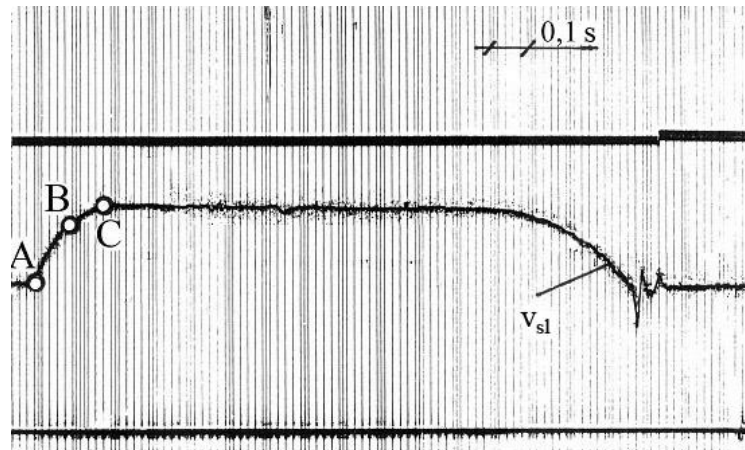


Fig. 2.30. Oscillogram of the sliding velocity of teeth in gearing

The analysis of the received dependences testifies to the existence of two parts **within the limits of ψ_1** . The maximum sliding velocity corresponds to the first part, beginning at the moment of contact of teeth. In this case, $v_{sl,max} = 15.65 \text{ mm/s}$ at $\omega = 0.78 \text{ s}^{-1}$. According to the dependence (2.34) $v_{sl,max} = 17.5 \text{ mm/s}$.

2.7. Phases of gearing and the rigidity of belt teeth

The rigidity of belt teeth is one of the parameters, defining the distribution of loading in a toothed-belt gearing, and, hence, defining the load carrying capacity and the operational resource of transmission.

As a result of the theoretical research of the complex stress condition of the elements of a toothed-belt transmission it is established that the deformation of belt teeth is defined by the stresses of a bearing strain, shear and bending. Solving the problem of the theoretical definition of the deformation of a belt tooth at the known combination of force factors and mechanical properties of a belt, the ratio of the deformations, making a total tangential deformation, is determined. It is established that in the condition of full gearing at $\beta_p = \beta_{III}$ the shear deformations make up the main quantity.

The theoretical research of the stress-strained state of a belt tooth, carried out by the author [23], is also devoted to the analysis of the tooth, which has completely input in gearing of a belt. Considering the problem, the author notes that finding of the analytical solution is extremely complicated, since the problem refers to the type of the non-classical mixed contact problems of the theory of elasticity.

The researches of the stress-strained state with the application of the method of finite elements [33, 56, 87, 88] are also known. However, the results of these researches are presented in the form of the diagrams of stress in the material of a belt tooth, received on the basis of numerous approximations. It is not possible to find the value of the total tangential deformation of a tooth with their help, especially when a tooth is in the state of the incomplete profile gearing. Thus, we can come to the conclusion, made in the work [24], that it is expedient to define the value of the rigidity of teeth experimentally.

At the experimental determination of EZ the following dependence is used (Fig. 2.31):

$$EZ = \frac{F}{\Delta s},$$

where F – the effort on a belt tooth; Δs – the tangential deformation of a tooth.

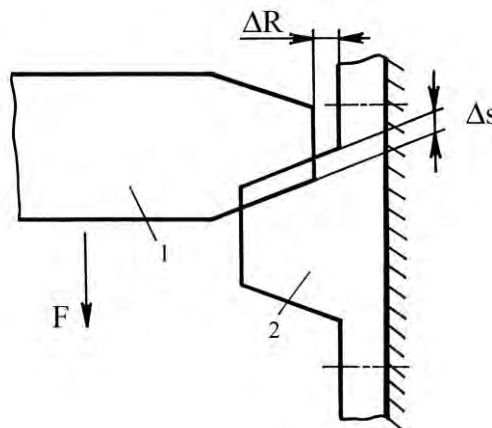


Fig. 2.31. Loading of a belt tooth: 1 – penetrator; 2 – belt tooth

It is established that the value EZ is better to be expressed in relation to the module of shear of rubber of the tooth G , defined by the hardness. In this case:

$$EZ = \frac{G}{a_z},$$

where a_z – the empirical factor: $a_z = 0.230...0.239$ – for the belts with the module $m = 1...10$ mm; $a_z = 0.251...0.264$ – for the belts *MXL-XXH* [1].

The values EZ , received in such a way, cannot be used for the description of the deformation of teeth in the conditions of the incomplete gearing that is characteristic of the angles ψ_1 and ψ_2 . It is possible to assume that in such conditions the value EZ is less than its value at full gearing, since the centroid of the effort F is displaced to the tip of a belt tooth.

This conjecture is proved implicitly by the researches of EZ in the conditions of the incomplete profile gearing, characterized by the existence of the radial **clearance** ΔR [90]. The behavior of EZ within the limits of the angle ψ_1 is described in the work [34], however, the influence of the phase of gearing within the limits of **the angle** ψ_2 on EZ is not established. Due to the opposite direction of loading, applied to the tooth in the zones ψ_1 and ψ_2 , different dependences of the change of EZ (within the limits of the given angles) appear. The experimental researches were conducted to prove the given hypothesis.

The toothed belts with the following parameters: 1) $m = 7$ mm; $z_p = 71$; $B_p = 32$ both 50 mm and 2) $m = 3$ mm; $z_p = 48$; $B_p = 16$ mm with hardness of teeth $HS = (58.6; 64.2; 74.3; 85.2)$ relative units are the objects of the researches. The belts are made by the method of diaphragm vulcanizations and of pressing by rigid elements, made of rubber mixture 1453 with the use of kapron fabric facing of the art.56320, gum-dipped (**№420**).

The values of the angles ψ_1 and ψ_2 vary within the limits, corresponding to $z_{III} = 8...30$. The effort on the examined tooth changes within the limits $0...F_{max}$, where $F_{max} = 2[F_f] / z_{III}$. $[F_f]$ according to [70] for $m = 3$ and 7 mm are taken as 10 and 45 N/mm. The replication of carrying out of the experiments is 7 at their reliability 0.95 [91].

The developed special stand (Fig. 2.32) is used for the experimental researches. It consists of the frame 1 with the guides 2, in which the movable carriage 3 is established. The fragment of the examined belt 4 is fixed on the carriage 3. In the top part of the frame 1 the axis 5 with the lever of the variable length 6 with the penetrator 7 on the end, is placed. The profile of the penetrator corresponds to the profile of the pulley tooth. The lever 8 is positively connected with the lever 6. The lever 8 is equipped with a set of loads 9 and the displacement indicator 10 in the form of the indicator of a clock type with the division value 0.01 mm.

At **the given value** $\psi_{1(2)}$, defined from the value z_{III} , the tooth of the belt (by moving of the carriage 3) is fixed at the distance X from the axis of symmetry of the pulley, corresponding to the demanded arc of traverse of the pulley φ_2 **within the limits of** $0... \psi_{1(2)}$. The length of the lever 6 is adjusted up to the value $R = mz_{III} / 2$. After that the penetrator 7 is engaged with the tooth of the examined belt. Consequently increasing the effort on the

tooth of the belt from 0 to F_{\max} by means of the loads 9, the angular displacement $\Delta\varphi_2$ of the lever 6 is registered.

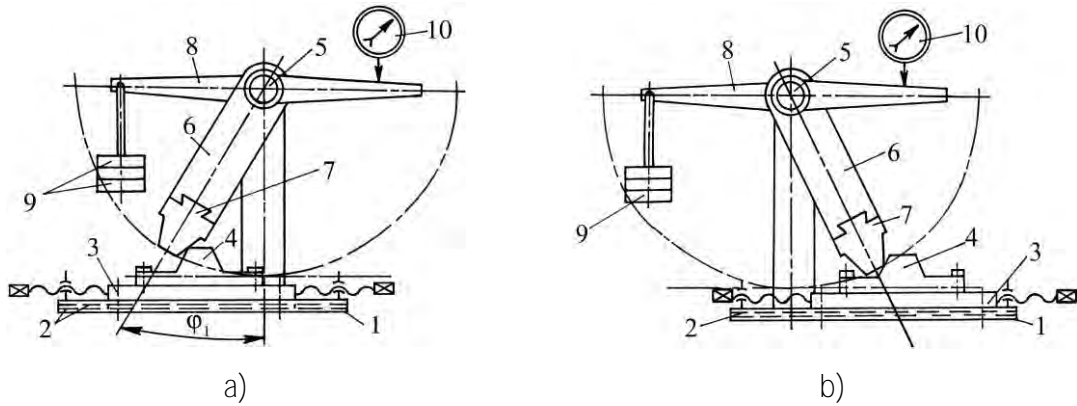


Fig. 2.32. Stand for the research of rigidity of belt teeth:
a) input in gearing; b) output from gearing

The value of the tooth rigidity for each effort F_i , acting on it, is determined by the formula:

$$EZ_i = \frac{F_i}{R \operatorname{tg} \Delta\varphi_2}.$$

Discretely changing the distance X that corresponds to getting of different phases of gearing within the limits of the angles $\psi_{1(2)}$, we make loading of a belt tooth. As a result of the researches the dependences EZ of the phase of gearing, the module of a belt and hardness of its teeth are received (Fig. 2.33).

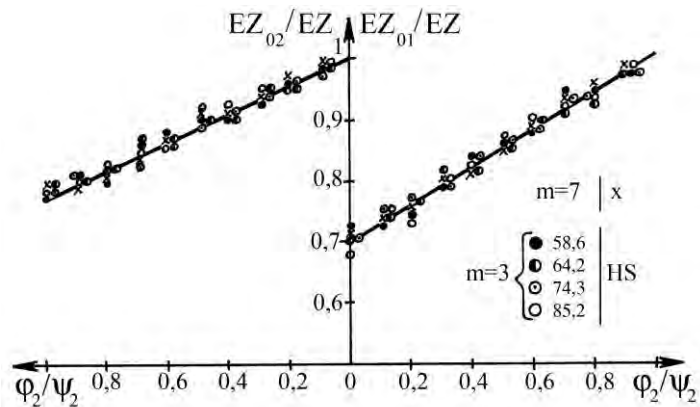


Fig. 2.33. Rigidity of belt teeth at different phases of an input in gearing and an output from it

The dependences EZ of the phase of a pulley turn within the limits of the angles of the input in gearing and the output from it can be expressed as the empirical equations:

$$EZ_{01} = EZ \left(0.7 + 0.3 \frac{\varphi_2}{\psi_1} \right), \quad (2.62)$$

$$EZ_{02} = EZ \left(1 - 0.23 \frac{\varphi_2}{\psi_2} \right). \quad (2.63)$$

The analysis of the dependences (2.62), (2.63) shows the unequal influence of the angles ψ_1 and ψ_2 on the rigidity of teeth. At the equal change of ψ_1 and ψ_2 the increase of EZ_{01} is 1.3 times more intensive than the reduction of EZ_{02} . At the same time the limiting values of EZ_{01} at $\varphi_2 / \psi_1 = 0$ are 10 % less than EZ_{02} at $\varphi_2 / \psi_2 = 1$. It is explained by the fact that the initial contact of teeth at their input in gearing takes place in the zone of the tip of the belt teeth. The disconnection of teeth at the output, as a rule, occurs in the middle part of a belt tooth.

Thus, the empirical dependences, allowing to define the rigidity of the belt teeth in the zones of the incomplete profile gearing, are received.

2.8. Conclusions

1. The real arc of contact of the toothed-belt transmission, within the limits of which there is the contact of teeth and transmission of power, represents the sum of the geometrical arc of contact and the angles of the input of teeth in gearing and the output from it. The mutual sliding of the profiles of teeth, which velocity defines the intensity of their wear, takes place within the limits of the given angles.

2. The kinematics of a toothed-belt gearing on the basis of the matrix transformation of the coordinates, accounting the existence of the zones of the incomplete profile gearing, making to 20 % from the real arc of contact of the pulley, has been investigated.

3. The empirical dependences for the determination of the angles of the input of teeth in gearing and the output from it have been got. It has been found that their value depends on the type of the operating profile and the angular displacement of teeth at the transmission of power, the module and the number of teeth of the pulley. The received dependences have allowed to detail the values of the angles of the input-output 1.6...2 times.

4. The empirical dependences for the determination of the velocity of mutual sliding of teeth within the limits of the angles of the input-output have been received. It has been found that the sliding velocity depends on the phase of turn and the angular speed of the pulley, the profile and the module of teeth. The maximum sliding velocity is observed in the points of the initial contact of teeth at the input in gearing and their disconnection at the output from it. At the input in gearing the maximum speed is 10 % higher than the same at the output, which defines the intensity of the wear of teeth.

5. At the calculation of the loading of teeth of the arc of contact it is necessary to consider the existence of the zones of the incomplete profile gearing and the change of the factor of overlap of teeth, which is described by the periodic function of the dependence of the phase of the pulley turn.

6. The experimental check of the received theoretical dependences for the determination of the sliding velocity of teeth on the developed and made special stand has been carried out.

7. The empirical dependences for the determination of the rigidity of the belt teeth from their module and hardness within the limits of the zones of the incomplete profile gearing have been received.

8. The model of the interaction of the belt with the pulley, allowing to consider the action of shear deformations at the transmission of power, has been developed. The influence of shear deformations of flexible link on the value of its relative sliding has been defined. This influence is extremely characteristic of flexible links with a slightly-extensible bearing layer. The received theoretical results are equal to the experimental results. It allows to recommend the developed technique for the estimation of sliding in the belt transmission, depending on its traction ability.

Chapter 3. DYNAMICS AND LOADING
OF TRANSMISSIONS OF POWER BY FLEXIBLE LINK

3.1. Bases of the calculation of loading of a toothed-belt gearing

Owing to the compliance of a bearing layer and belt teeth at the power transmission, the distribution of a pull in gearing is irregular. It is established that at the equality of steps of teeth of a belt and a pulley, the most loaded are the teeth of the arc of contact, placed at the driving side. Using the analogy with the screw-nut connection, and turning from gearing of a belt with a pulley (**Fig. 3.1**) to the model-development (**Fig. 3.2**), in the work [51] the technique of the calculation of loading of teeth, based on the equation of compatibility of deformations, is offered:

$$t_p + f_{n-1} = t_p + f_n + \Delta_{n,n-1}, \quad (3.1)$$

where f_n, f_{n-1} – the deformations n and $n-1$ of belt teeth on the arc of contact; $\Delta_{n,n-1}$ – lengthening of a bearing layer between n and $n-1$ teeth.

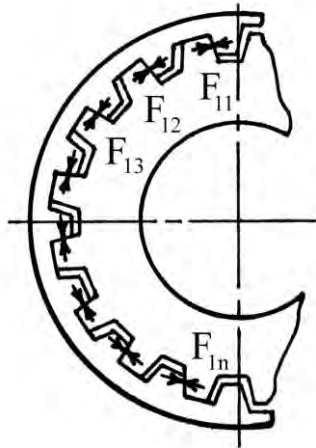


Fig. 3.1. Scheme of gearing of a toothed belt with a drive pulley

Simplifying the equation (3.1) to $f_n = f_{n-1} - \Delta_{n,n-1}$, and considering all the teeth in gearing, we get:

$$\begin{aligned}
 f_2 &= f_1 - \Delta_{1:2}, \\
 f_3 &= f_2 - \Delta_{2:3}, \\
 f_4 &= f_3 - \Delta_{3:4}, \\
 &\text{-----} \\
 f_n &= f_{n-1} - \Delta_{n:n-1}.
 \end{aligned}$$

The absolute deformation of teeth is defined by the efforts, influencing them and the rigidity of teeth: $f_n = F_{1n} / EZ_n$; the lengthening of a bearing layer: $\Delta_{n:n-1} = t_p \cdot F_1 - \sum F_{11:n} / EF_n$.

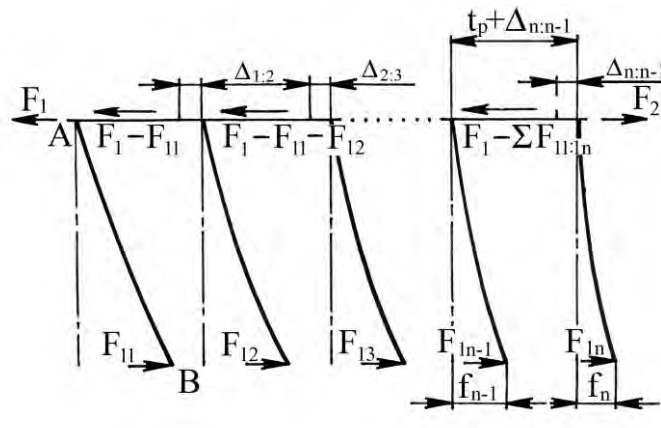


Fig. 3.2. Scheme of the calculation of loading of a toothed-belt gearing

Assuming that the rigidity of all the teeth and the parts of a bearing layer is equal and does not depend on the applied effort, we get:

$$\begin{aligned}
 \frac{F_{12}}{EZ} &= \frac{F_{11}}{EZ} - t_p \frac{F_1 - F_{11}}{EF}; \\
 &\text{-----} \\
 \frac{F_{1n}}{EZ} &= \frac{F_{1n-1}}{EZ} - t_p \frac{F_1 - F_{11} - \dots - F_{1n-1}}{EF};
 \end{aligned} \tag{3.2}$$

$$\sum F_{1n} = F_1 - F_2 = F_t.$$

where F_1 and F_2 – the efforts in driving and following sides of transmission.

As a result of the solution of the system (3.2) by the method of Gauss it is established that the largest effort is the effort F_{11} on the first tooth of the arc of contact. The measure of its overload is the factor of irregularity of loading of teeth ψ [54]:

$$\psi = 1 + z_0^{1/3} \frac{EZ}{EF}. \quad (3.3)$$

The analysis of the expression (3.3) shows that it is necessary to use the belts with the increased longitudinal rigidity for the decrease of irregularity of loading of teeth. At the same time the expression (3.3) does not allow getting the values of the loadings, influencing the other teeth in gearing, which is necessary for the prediction of the operational resource of transmission.

In the work [92] the dependence, allowing to define loading of teeth from their quantity in gearing, is offered:

$$F_{1n} = F_t \left(\frac{1}{z_0} + \left[\frac{z_0 - 1}{6z_0} \frac{2z_0 - 1}{z_0} + \frac{z_0 - 1}{2z_0} - z_0 - 1 \right] \frac{EZ}{EF} \right). \quad (3.4)$$

It is necessary to note that the expressions (3.3), (3.4) are obtained on the basis of the equality of steps of teeth of a belt and a pulley. However, as it was mentioned before, in view of the compliance of teeth and bending of a belt on a pulley, this condition is not observed. Therefore, in the opinion of the authors of the work [2], the calculation of loading on teeth should be carried out by the dependence of such a kind:

$$F_{1n} = b_k F_1 - a_k F_2 + \Delta p - m \cdot 10^{-3} EF a_k - b_k,$$

where $b_k = \frac{\text{sh} \rho}{\text{sh} \rho k}$; $a_k = 1 - \frac{\text{sh} \rho k - 1}{\text{sh} \rho k}$; $\rho = \sqrt{\frac{EZ}{EF}}$; $\Delta p = \frac{\pi \Delta D}{z_{\text{III}}}$;

ΔD – the increment in the diameter, at which $t_p = t_{\text{III}}$.

On the basis of the equations (3.2) the dependences of the engineering kind, allowing to define the loading on the teeth of the arc of contact [60], are also offered:

$$F_{1n} = k_1 x_1^{-1} x_1^{1n-1} + k_2 x_2^{-1} x_2^{1n-1}, \quad (3.5)$$

where

$$k_1 = \frac{F_1 - F_p - F_2 - F_p x_2^{z_0}}{x_1^{z_0} - x_2^{z_0}}; \quad k_2 = \frac{F_1 - F_p - F_2 - F_p x_1^{z_0}}{x_1^{z_0} - x_2^{z_0}};$$

$$x_{1,2} = \left(1 + \frac{EF}{EZ}\right) \pm \sqrt{\frac{EF}{EZ} + \frac{EF^2}{4EZ^2}}; \quad F_p = \frac{\Delta t_{\text{III}}}{EF}.$$

The expression (3.5) allows defining the efforts $F_{11} \dots F_{1n}$ at different ratios of steps of teeth of a belt and a pulley, which is necessary for the choice of the correction of a step of pulley teeth Δt , providing the even load distribution in gearing.

For this purpose the parameter Δt is added to the expression (3.2):

$$\frac{F_{12}}{EZ} = \frac{F_{11}}{EZ} - t_p \frac{F_1 - F_{11}}{EF} + \Delta t;$$

$$\frac{F_{1n}}{EZ} = \frac{F_{1n-1}}{EZ} - t_p \frac{F_1 - F_{11} - \dots - F_{1n-1}}{EF} + \Delta t;$$

$$\sum F_{1n} = F_1 - F_2 = F_t.$$

Predetermining the value ψ , the system of the equations is solved relating to $F_{12} \dots F_{1n}$ and Δt . However, the expression, connecting these parameters, is not received.

The dependence of the form [61] is also known:

$$\frac{F_{1n}}{F_1} = C_1 e^{\frac{A^k}{z_0}} + C_2 e^{-\frac{B^k}{z_0}} + \frac{F_x}{F_1},$$

where C_1, C_2 – the integration constants; $A = \frac{2\sqrt{\frac{EZ}{EF}} + \frac{EZ}{EF}}{2}$; $B = \frac{2\sqrt{\frac{EZ}{EF}} - \frac{EZ}{EF}}{2}$;

$F_x = t_{\text{III}} - t_p$ EF – the force, which is necessary for the elimination of the difference of steps of teeth.

The loadings $F_{12}...F_{1n}$ can be also defined on the basis of the semi-graphical method [93]. However, the poor accuracy of the given method does not allow recommending it for application.

The further improvement of the theoretical bases of the interaction of teeth in gearing followed the line of the refusal of some assumptions. In particular, it is offered to take into account systematic errors of a step of teeth, having the technological origin [94] or random nature [57, 95]. The received results allow to explain the error tolerances of a step of belt teeth t_p .

The essential fault of the examined theoretical models of a toothed-belt gearing is the use of the principle of Ponselle in them:

$$F_1 + F_2 = F_0; \quad F_1 - F_2 = F_t. \quad (3.6)$$

The use of the recommendations [53, 70] and the other authors' recommendations, according to which $2F_0 < F_t$, leads to $F_2 < 0$, which is, obviously, impossible, even in case $2F_0 = F_t \Rightarrow F_1 = F_0 + F_t/2; F_2 = F_0 - F_t/2$. In the absence of the effort in the driving side it should be in a free state and have not a rectilinear, but a curvilinear form with some radius of curvature. The value of this radius at $F_2 = 0$ should be equal to the initial radius, i.e. to the radius of the press mould for manufacturing of the belt $R_0 = mz_p / 2$.

The experimental researches of the efforts in the sides of a moving belt [62] show that $F_2 > 0$. The theoretical aspect of this phenomenon consists in the account of mechanical and physical properties of the elements of a belt. Considering that a belt is not a mathematical fillet, but a physical one, with the longitudinal and bending rigidity EJ , and, using the differential equations of the theory of thin rods of Kirhgoff for the description of bending of a belt on pulleys, in the work [96] it is established that for the locked belts, made in circular forms at any different from zero, the values $2F_0$ and F_t , the value $F_2 > 0$. Taking this into account, the expressions (3.6) are offered to be written in the form [47, 90, 97]: $F_1 + F_2 = 2(F_0 + \Delta F); F_1 - F_2 = F_t$.

Whence

$$F_1 = F_0 + \Delta F + \frac{F_t}{2}; \quad F_2 = F_0 + \Delta F - \frac{F_t}{2},$$

where ΔF – the additional tension ("self-tension") of belt sides.

At $2F_0 < F_t \rightarrow F_0 = \Delta F$. The values of ΔF , received on the basis of the numerical experiment, are determined by the dependence [90]:

$$\Delta F = \frac{F_t}{2} - F_0 + 5,6 \cdot 10^{-3} \frac{EF \cdot EJ \cdot L_p^{0,065}}{R_1 R_2} \left(\frac{2F_0}{F_t} \right)^3, \quad (3.7)$$

where $L_p = \pi m z_p$ – the length of a belt; $R_1 = m z_1 / 2$ and $R_2 = m z_2 / 2$.

The calculations in (3.7) show that the value ΔF is low and it reaches a maximum in the range space of $F_0 \ll F_t / 2$, where it does not exceed $0.45 F_t$. At these efforts the bearing layer of a belt shows non-linear properties [24, 47, 65, 66]. Thus, loading of teeth of the arc of contact is defined by non-linear lengthening of a bearing layer. In this connection, in the work [67] the non-linear model of power interaction of a belt with a pulley is offered:

$$F_{11} = F_{12} + \frac{t_p EZ}{a} F_1 - F_{11}^{1-b};$$

$$F_{1n-1} = F_{1n} + \frac{t_p EZ}{a} F_1 - F_{11} - \dots - F_{1n-1}^{1-b};$$

$$F_{1n} = F_t - \sum_{i=1}^{z_0-1} F_{1n_i},$$

where a and b – the parameters of the equation, defining the longitudinal rigidity of a belt $EF = a F_{sp}^b$; $F_{sp} = F / B_p$, at $m \leq 4$ mm: $a = 550 \dots 620$; $b = 0.60 \dots 0.62$; at $m > 4$ mm: $a = 1350$; $b = 0.65$ [24, 47].

The insufficient effort in the following side of a belt defines the character of its interaction with a driven pulley (Fig. 3.3).

This phenomenon is less expressed on a drive pulley because of a spontaneous straightening of a side of a belt under the action of internal forces at its running-off from the pulley. At the same time the following side should be bent additionally at climbing on a driven pulley. The insufficient effort F_2 is unable to compensate the bending rigidity of a side of a belt, which leads to the occurrence of the angle of rigidity ε on a geometrical arc

of contact of a driven pulley. Thus, the expressions (2.2) for the calculation of z_0 become unacceptable. In the work [90] the real arc of contact is offered to be defined as:

$$\alpha_V = \alpha_F + \alpha_I = \alpha_G - \alpha_A,$$

where α_F , α_I , α_A – the angles, within the limits of which, the teeth of a belt are in full, incomplete gearing, and the absence of gearing is also observed.

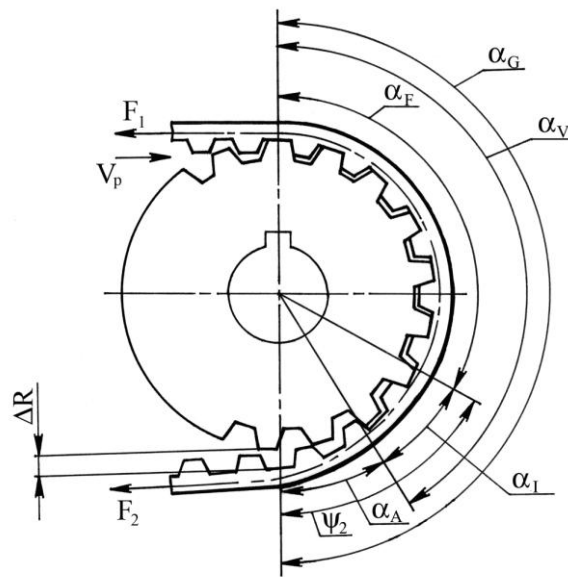


Fig. 3.3. Gearing of the following side of a belt with a driven pulley

The existence of the given angles depends on the ratio of a radial clearance between the tips of the teeth of the pulley and the interdentals spaces of the belt ΔR and the depth of the teeth h_p . At $\Delta R = 0$ the full profile gearing of teeth is observed; at $0 < \Delta R < h_p$ – the teeth of a belt are in the incomplete profile gearing with a pulley; at $\Delta R > h_p$ – the gearing of teeth is not observed.

It is obvious that in the zone of the angle α_I the teeth of a belt cannot transfer the same loading, as the teeth in the full profile gearing, since their rigidity decreases proportionally to the clearance ΔR . Using this fact, the author of the work [90] received the theoretical description of the interaction of a belt with a pulley, which allowed to prove the existence of an optimum of tension of a belt $2F_0$, corresponding to the minimum ψ (Fig. 3.4).

At the reduction of tension from an optimum level the effort in the following side of a belt decreases. The increase in the angle ϵ takes place. In connection with the increase

of the zones of the incomplete profile gearing and the absence of gearing, the loading on the remained teeth in the full profile gearing increases. On the contrary, at the increase of $2F_0$ in comparison with an **optimum**, when $\varepsilon \approx 0$ and all the teeth of the arc of contact are in the field of α_F , both F_2 , and F_1 , increase. The increase of F_1 promotes the increase in a step of teeth of a belt, because of the belt compliance. The gearing of a belt (with the increased step of teeth) with a pulley leads to the increase of non-uniformity of loading of teeth ψ .

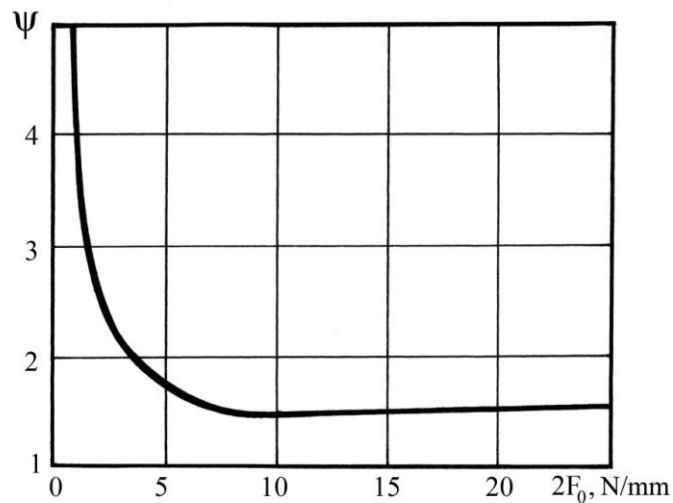


Fig. 3.4. Dependence of non-uniformity of loading of gearing of a preliminary tension of a belt

At the same time, as the analysis shows, all the above theoretical models of a toothed-belt gearing do not consider such phenomena, accompanying the work of transmission, as the dynamic effects and transmission of the part of power by the teeth, which are in the zones of the incomplete profile gearing.

3.2. Loading of the arc of contact in view of the zones of the incomplete profile gearing of teeth

As the factor of the face overlap ε_α changes during the pulley turn by one angular step, the value ψ is also changeable.

Using the results of the calculation ε_α , we get the system of the equations, defining loading of a toothed-belt gearing, accounting the zones of the incomplete profile gearing.

$$\begin{aligned}
\frac{F_{11}}{EZ_1 k_{zd}} &= \frac{F_{01}}{EZ_{01} k_{zd}} - t_p \frac{F_1 - F_{01}}{EFk_{fd}} + \Delta t, \\
\frac{F_{12}}{EZ_2 k_{zd}} &= \frac{F_{11}}{EZ_1 k_{zd}} - t_p \frac{F_1 - F_{01} - F_{11}}{EFk_{fd}} + \Delta t, \\
&\text{-----} \\
\frac{F_{1n}}{EZ_n k_{zd}} &= \frac{F_{1n-1}}{EZ_{n-1} k_{zd}} - t_p \frac{F_1 - F_{01} - F_{11} - \dots - F_{1n-1}}{EFk_{fd}} + \Delta t, \\
\frac{F_{02}}{EZ_{02} k_{zd}} &= \frac{F_{1n}}{EZ_n k_{zd}} - t_p \frac{F_1 - F_{01} - F_{11} - \dots - F_{1n} - F_{02}}{EFk_{fd}} + \Delta t, \\
F_{01} + F_{11} + \dots + F_{1n} + F_{02} &= F_1 - F_2 = F_t.
\end{aligned} \tag{3.8}$$

The first equation of the system describes an input in gearing of the first pair of teeth of an arc of contact. In the section 2.7 it is proved that the rigidity of teeth within the limits of the angle ψ_1 is changeable. At the moment of the contact of teeth their rigidity is minimal and it increases in the process of the turn of a pulley during the angle ψ_1 . Thereafter, at the pulley turn by the angle τ_2 the value $EZ_d = \text{const}$.

Thus, the first equation of the system (3.8) contains the variable EZ_{d01} , defined by the degree of gearing of teeth at the input. In the subsequent equations the value EZ_d for all the teeth is constant. The penultimate equation is solved only at $(z_0 + 2)$. It contains the decreasing member EZ_{d02} , describing the effect of the reduction of the tooth rigidity in the process of the output from gearing.

Accepting the rigidity of teeth within the limits of α_G to be constant, i.e. $EZ_1 = EZ_2 = EZ_n$, we solve the system of the equations at the given values ε_α .

For the first time the system of the equations is solved for the case of contact of pair of teeth at the input in gearing. By means of the ratio α_G / t_p° we define the position of the last pair of teeth of the arc of contact: a) full gearing (the part of the angle τ_2), when $EZ_{02} = EZ_n$; b) **partial gearing (the part ψ_2)**, in this case the value EZ_{02} is defined by the formula (2.63). The value EZ_{01} , substituted in the first equation, can be found by the dependence (2.62).

For the second time we solve the system (3.8) after the displacement of the arc by the angular value t_0° , multiple of the values t_p° and ψ_1 . For example, at $m = 5$ mm; $z_{\text{ш}} = 25$;

$t_p^\circ = 14.4^\circ$; $\psi_1 = 10^\circ \rightarrow t_0^\circ = 0.2^\circ$. According to (2.62), at the pulley turn the rigidity of belt teeth at the input in gearing increases.

Then the position of the end of the arc of contact (in the part of the angle ψ_2 or τ_2) is redefined. In the first case, according to the expression (2.63), we define EZ_{02} ; in the second case $EZ_{02} = EZ$ is substituted in the penultimate equation. Repeating the received actions X_1 times, where $X_1 = \psi_1 / t_0^\circ + 1$, we substitute the increasing value EZ_{01} in the first equation. The further calculation is made X_2 times, where $X_2 = t_p^\circ / t_0^\circ + 1 - X_1$ at constant EZ_{01} .

Thus, solving the system X_2 times, we get the values of loadings on the teeth of the arc of contact and the regularity of their variations during the pulley turn by one angular step. The further calculation is inexpedient, as during the pulley turn by the following angular step all the described processes are iterated.

The system of the equations (3.8) is solved by the method of Gauss under the developed program. The change of loading on teeth of the arc of contact for the case $m = 3$ mm; $z_0 = 5$; $z_{III} = 12$ in the process of the turn of a pulley is presented in Fig. 3.5.

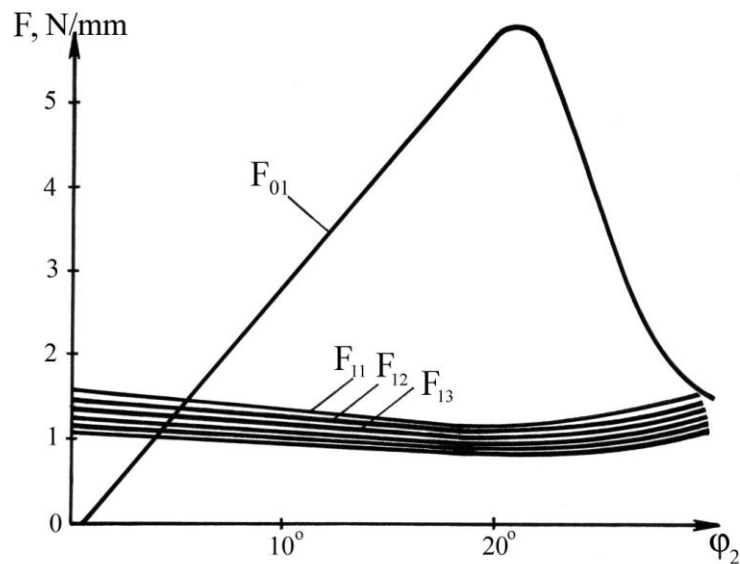


Fig. 3.5. Influence of the phase of gearing on loading of teeth of the arc of contact

The analysis of the graphs of the change of loading shows that in the process of the input in gearing of the first pair of teeth, the effort on the other teeth of the arc of contact,

located in the zone of the angle α_G , decreases (Fig. 3.6). The maximum value F_{01} is kept till the moment of the contact of the next pair of teeth inputting in gearing.

It is also established that the processes, occurring at the output from gearing (for a drive pulley) or at the input (for a driven pulley), influence little on loading of the first teeth of the arc of contact, including the first tooth from the driving side. In particular, for $z_0 = 5 \dots 30$ this influence does not exceed 5 %.

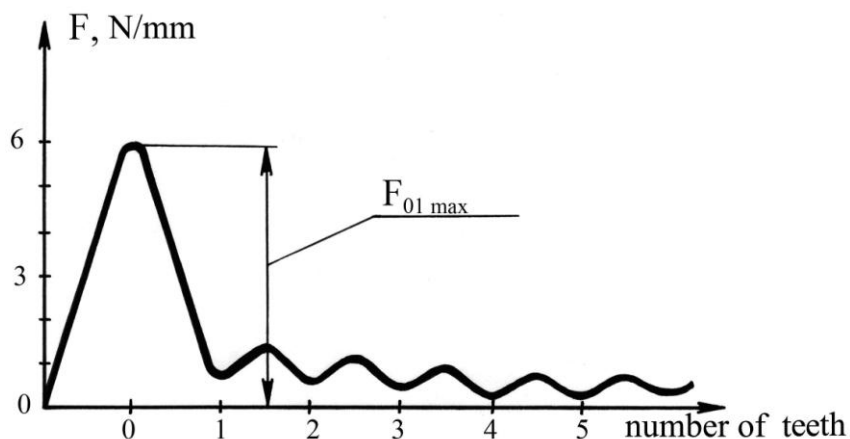


Fig. 3.6. Loading of teeth in the multiple gearing

The presented dependences of the change of loading of teeth of the arc of contact in the process of the pulley turn (Fig. 3.5, 3.6) allow to extract the maximum ψ_{\max} and minimum ψ_{\min} values of non-uniformity of loading of teeth. Their ratio ($\psi_{\max} / \psi_{\min}$) does not depend on such factors as F_i ; $2F_0$; EF ; EZ ; Δt , and it is only defined by the quantity of teeth in gearing (Fig. 3.7).

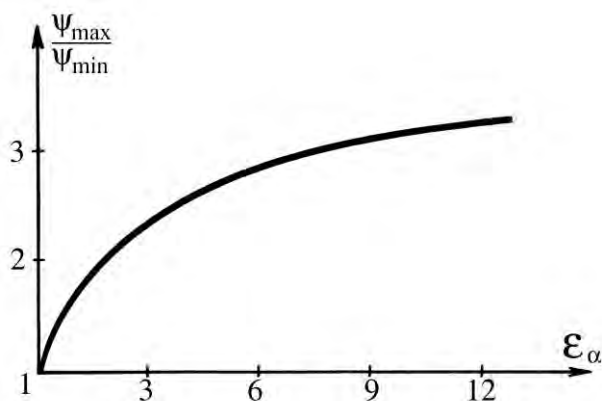


Fig. 3.7. Influence of the factor of a face overlap on non-uniformity of loading of gearing

It is seen that with the increase of z_0 the value $\psi_{\max} / \psi_{\min} = F_{01\max} / F_{01\min}$ increases non-linearly. At the same time, at $\epsilon_\alpha = 1$ this ratio is equal to 1 and at any changes of the external factors the whole loading is transferred by one tooth.

The most interesting is the change of $\psi_{\max} = F_{01\max}\epsilon_\alpha / F_t$ from the phase of the pulley turn. The analysis shows that the increase (for a drive pulley) of the values ψ **from 0** up to ψ_{\max} and the reduction (for a driven pulley) of the values ψ **from ψ_{\max}** up to 0 is followed by the mutual sliding of teeth with the velocity v_{sl} .

The increase of ψ occurs by the linear law and it is described by the equation of such a kind:

$$\psi = \psi_{\max} \frac{\varphi_2}{\psi_{1\ 2}},$$

where φ_2 – the arc of traverse of a pulley within the limits of the angle ψ_1 or ψ_2 .

Summing up the results of the calculation of the value ψ_{\max} at the different levels of the variation of the factors F_t ; $2F_0$; EF ; EZ ; Δt ; z_0 , by means of the technique of the **factorial planning**, the following equation for the calculation of ψ_{\max} is received:

$$\psi_{\max} = 0,7k_v k_F k_Z \left(0,5 \left(\frac{F_t}{F_t} \right)^2 + 1 \right) 0,53z_0 + 1 \left(1,3 - \frac{200\Delta t}{t_p} \right),$$

where k_v ; k_F ; k_Z – the factors, considering the frequency of runs of a belt, the longitudinal rigidity and the rigidity of teeth of a belt accordingly; $[F_t]$ – the allowable specific pull.

From Fig. 3.6 it is seen that the loading in the pair of the engaged teeth decreases while it is moving from the driving side to the following one. However, this reduction is not of a modulated character and it contains a harmonious component. Its amplitude for all the teeth of the arc of contact non-linearly decreases adequately to the decrease of F_{1n} in comparison with F_{01} . The number of extremes is equal to the number of the engaged pairs of teeth. Thus, the phenomenon of the changes of efforts in gearing of teeth, observed in oscillograms, is explained theoretically.

3.3. Research of loading of toothed-belt transmissions by the method of finite differences

The numerous works [3, 21, 50, 53, 56, 60, 61, 63, 98, 99] are devoted to the research of the distribution of loading in the multiple gearing, since it directly influences the load carrying capacity and durability of transmission. The analysis of a toothed-belt gearing testifies that the distribution of loading between the belt teeth corresponds to the discrete scheme by analogy to the distribution of efforts in the threaded joint, which was firstly solved by N.E. Zhukovsky [100]. After that, Zhukovsky's method was used in the other **authors' works. In particular, in the work [101] the finite number of coils** is examined and the deformation of a bending and a cut is taken into consideration; in the work [102] the question of the distribution of loading at the existence of the difference of steps is testified.

As the distribution of loading in a toothed-belt gearing corresponds to the discrete scheme, we can use the method of finite differences for the research of loading. The solution of the problem can be received by means of the canonical equations with the constant factors, solved in the closed form [77].

The problem is solved at the equality ($t_p = t_m$) and the inequality ($t_p \neq t_m$) of steps of teeth of a belt and a pulley, using the following assumptions [3, 53, 56]: 1) rigidity of pulleys, that is infinitely high in comparison with the rigidity of the belt; 2) linear dependence between the deformations and the displacements of the belt elements; 3) plane deformation of the belt at loading; 4) isolated operation of each pair of teeth; 5) equal rigidity of all the teeth and all the parts of a bearing layer along the belt length; 6) transmission of the operation effort by the lateral surfaces of teeth.

Let's study the part of a belt on the arc of contact. After applying the pull F_t , the tangential forces $P_1; P_2; P_3; \dots, P_k$ (Fig. 3.8) arise between the teeth of the belt and the pulley. The points of these **forces' application are arranged on the circle, passing through the middle of the height of the belt teeth.**

It should be mentioned that due to the **trapezoidal** forms of teeth the radial forces also operate, but their influence on the distribution of loading is not considered yet.

The pull causes the lengthening of the bearing layer of the belt in the part between $n-1$ and n teeth by the value $\Delta_{n-1; n}$. The total deformation n of a tooth in the line of the force P_n , relating to its basis, is equal to f_n , $n-1$ of a tooth in the line of the force P_{n-1} : f_{n-1} . Then the equation of the deformation compatibility in displacements is the following:

$$f_n = f_{n-1} - \Delta_{n;n-1}\rho. \quad (3.9)$$

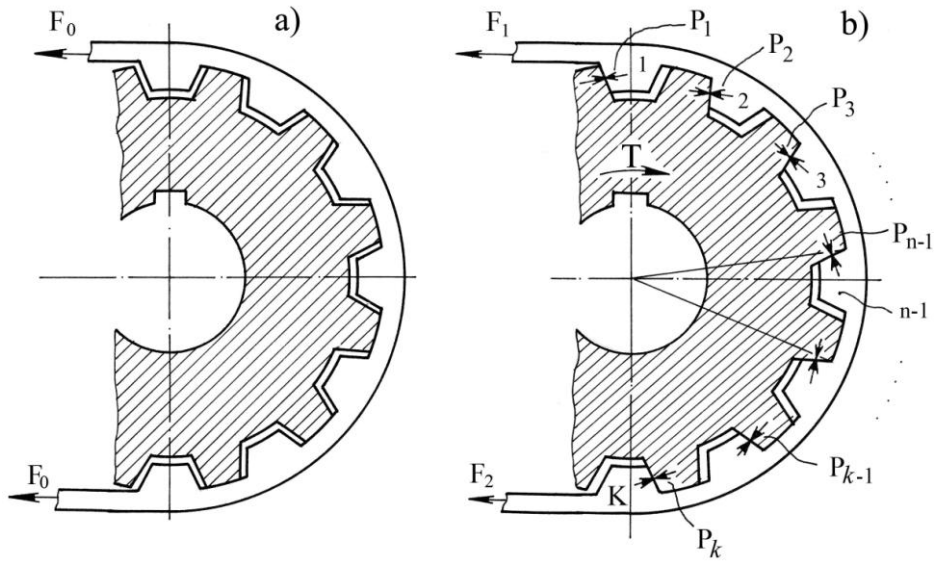


Fig. 3.8. Condition of teeth of the arc of contact: a) unloaded; b) loaded with a torque

The factor ρ displays the fact that the specified deformations correspond to cylindrical sections of various radii $\rho = R_f / R_p$, where R_f is the radius of the circle, passing through the points of the application of equivalent distributed forces; R_p is the radius of a pitch circle, coinciding with the axis of a bearing layer.

Thus, the condition of the displacement compatibility consists in the fact that the difference of the deformations of belt teeth along the arc R_f and the lengthening of the bearing layer along the arc R_p correspond to the same angle in size.

For making the law of the distribution of loading between the teeth of a belt it is necessary to proceed from the displacement to the force factors. For this aim the deformations of the tooth and the bearing layer of a belt are expressed by means of the corresponding rigidities:

$$f_n = \frac{P_n}{EZ}; \quad (3.10)$$

$$\Delta_{n-1;n} = \frac{t_p [F_t - (P_1 + P_2 + P_3 + \dots + P_{n-1})]}{EF}, \quad (3.11)$$

where EZ and EF – the rigidity of teeth and the longitudinal rigidity of a bearing layer of a belt.

Substituting the expressions (3.10) and (3.11) in (3.9), we get:

$$\frac{P_n}{EZ} = \frac{P_{n-1}}{EZ} - \frac{t_p [F_t - (P_1 + P_2 + P_3 + \dots + P_{n-1})] \rho}{EF}.$$

Having designated $\alpha = t_p EZ / EF$, we receive:

$$\begin{aligned} P_2 &= P_1 - \alpha(F_t - P_1)\rho; \\ P_3 &= P_2 - \alpha[F_t - (P_1 + P_2)]\rho; \\ &\text{-----} \\ P_n &= P_{n-1} - \alpha[F_t - (P_1 + P_2 + P_3 + \dots + P_{n-1})]\rho. \end{aligned} \tag{3.12}$$

Having received $n-1$ of the equations of the deformation compatibility for the solution of the system (3.12), we add the equation of the equilibrium condition to it. According to one of the accepted suppositions the sum of the tangential loadings, taken up by the teeth of a belt, is equal to the pull, therefore:

$$P_1 + P_2 + P_3 + \dots + P_k = F_t. \tag{3.13}$$

Thus, for the determination of the loading falling on any tooth in gearing, it is necessary to solve the system (3.12), added by the equation (3.13).

It is obvious, that in case of a large number of teeth in gearing, the solution becomes inconvenient. Therefore, we apply the differential method with the use of the solution in the finite differences. For this purpose we present (3.12) in **the difference** form. Denoting the sum of the loadings, falling on all the teeth of a belt in gearing by R_n , it can be written:

$$\begin{aligned} P_n &= R_n - R_{n-1} = \Delta R_n; \\ P_{n-1} &= R_{n-1} - R_{n-2} = \Delta R_{n-1}, \end{aligned}$$

whence it follows:

$$P_n - P_{n-1} = \Delta R_n - \Delta R_{n-1} = \Delta^2 R_n. \tag{3.14}$$

Substituting (3.14) in the general equation of the system (3.12), we get:

$$P_n - P_{n-1} - \alpha(P_1 + P_2 + P_3 + \dots + P_{n-1})\rho = -\alpha F_t \rho. \quad (3.15)$$

The simultaneous solution of the equations (3.14) and (3.15) allows receiving the following differential equation:

$$\Delta^2 R_n - \alpha R_{n-1} \rho = -\alpha F_t \rho.$$

Having transformed this equation, we get:

$$R_n - 2 - \alpha \rho R_{n-1} + R_{n-2} = -\alpha F_t \rho. \quad (3.16)$$

From (3.16) we have:

$$R_n = c_1(r_1^n - 1) + c_2(r_2^n - 1), \quad (3.17)$$

where r_1 and r_2 – the roots of the characteristic equation $r^2 - 2 + \alpha \rho r + 1 = 0$, c_1 and c_2 – constants.

Solving the characteristic equation, we receive:

$$\begin{aligned} r_1 &= 1 + 0,5\alpha\rho + 0,5; \\ r_2 &= 1 + 0,5\alpha\rho - 0,5. \end{aligned} \quad (3.18)$$

Finally, we have the following system of the equations:

$$\begin{aligned} P_1 &= R_1 - R_0 = c_1(r_1 - 1) + c_2(r_2 - 1); \\ P_2 &= R_2 - R_1 = c_1 r_1(r_1 - 1) + c_2 r_2(r_2 - 1); \end{aligned} \quad (3.19)$$

$$P_n = R_n - R_{n-1} = c_1 r_1^{n-1}(r_1 - 1) + c_2 r_2^{n-1}(r_2 - 1).$$

If to sum up all the values of the loadings in view of the formulas of the sum of the geometric progression, we receive the equation (3.17) for the value R_n .

The constants c_1 and c_2 can be defined as follows. After the substitution of the values R_n ; R_{n-1} ; R_{n-2} in the equation (3.16), we receive:

$$c_1(r_1^n - 1) + c_2(r_2^n - 1) - (2 + \alpha\rho)[c_1(r_1^{n-1} - 1) + c_2(r_2^{n-1} - 1)] + c_1(r_1^{n-2} - 1) + c_2(r_2^{n-2} - 1) = -\alpha F_t \rho.$$

Having made the transformations, we obtain:

$$c_1[r_1^2 - 2 + \alpha\rho r_1 + 1] r_1^{n-2} + c_2[r_2^2 - 2 + \alpha\rho r_2 + 1] r_2^{n-2} + \alpha\rho(c_1 + c_2) = -\alpha F_t \rho.$$

Considering the expression (3.16), it is possible to prove that the identity is carried out under the condition:

$$c_1 + c_2 = -F_t.$$

The total loading, taken up by the teeth of the arc of contact, is:

$$R_k = c_1(r_1^k - 1) + c_2(r_2^k - 1) = F_t,$$

whence we get the expressions for the constants:

$$c_1 = \frac{\left(\frac{r_2}{r_1}\right)^k}{1 - \left(\frac{r_2}{r_1}\right)^k} F_t; \quad (3.20)$$

$$c_2 = \frac{1}{1 - \left(\frac{r_2}{r_1}\right)^k} F_t. \quad (3.21)$$

Substituting c_1 and c_2 in the equation (3.19), after the transformations we receive the expression for the definition of the loading, taken by n -th tooth:

$$P_n = \frac{r_1 - 1}{r_1^k - r_2^k} \frac{r_1^{k-n} + r_2^{k-n+1}}{r_1^k - r_2^k} F_t. \quad (3.22)$$

Considering that at the real values EF , EZ and $k \leq 20$, $c_1 \rightarrow 0$, the expression (3.22) accurate to 0.01 can be presented in the following form:

$$P_n = \frac{r_1^{-1} r_1^{k-n} + r_2^{k-n+1}}{r_1^k} F_t. \quad (3.23)$$

In Fig. 3.9 the curves for the determination of the roots of the characteristic equation r_1 and r_2 and in Fig. 3.10 the curve of the distribution of loading in gearing for various designs of a belt are presented.

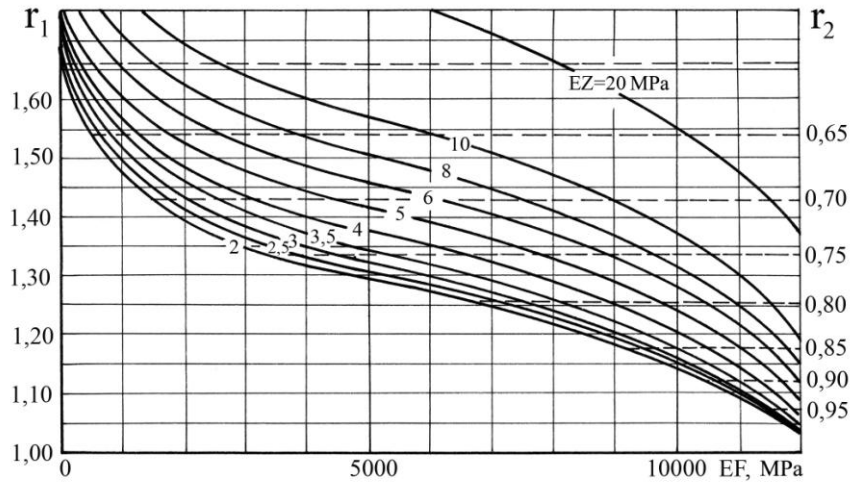


Fig. 3.9. Dependences for the determination of the roots of the characteristic equation

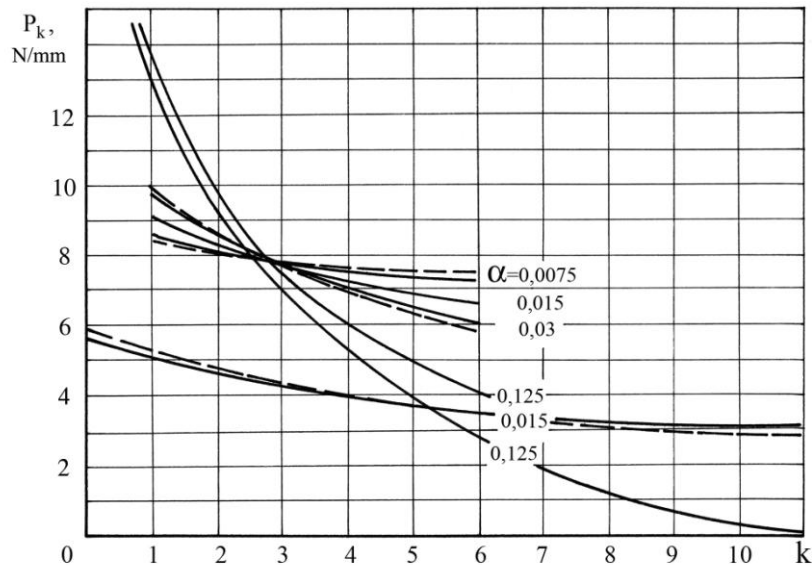


Fig. 3.10. Dependences of the distribution of loading on teeth of the arc of contact

The curves are constructed for transmission with the module $m = 7 \text{ mm}$ and the specific pull $F_t = 45 \text{ N/mm}$. Two values of the modulus of the rubber elasticity are accepted:

$E = 8.0 \text{ MPa}$ – for the rubbers with high hardness, $E = 4.0 \text{ MPa}$ – for the rubbers with average hardness, specific for **drive** belts.

For the calculation of the load carrying capacity and fatigue strength of belts it is necessary, besides the data about loading of separate teeth in gearing, to have the value of the factor of non-uniformity of the loading distribution between teeth.

In Fig. 3.11 the nomograph for the definition of ψ , depending on k , EF and EZ , is presented. In Fig. 3.12 the part of the given nomograph, corresponding to the mostly used EF and EZ , is shown.

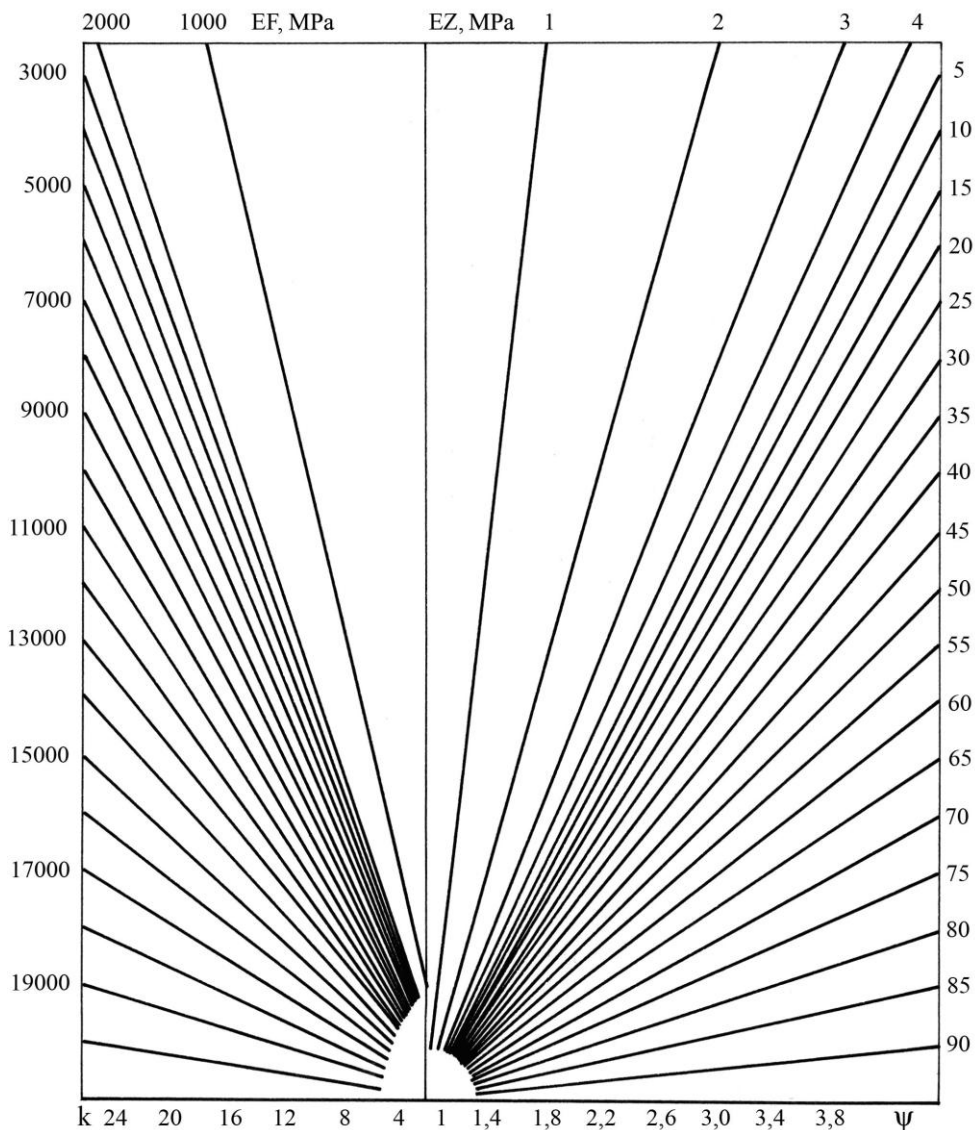


Fig. 3.11. Nomograph for the definition of the factor of non-uniformity of loading of teeth

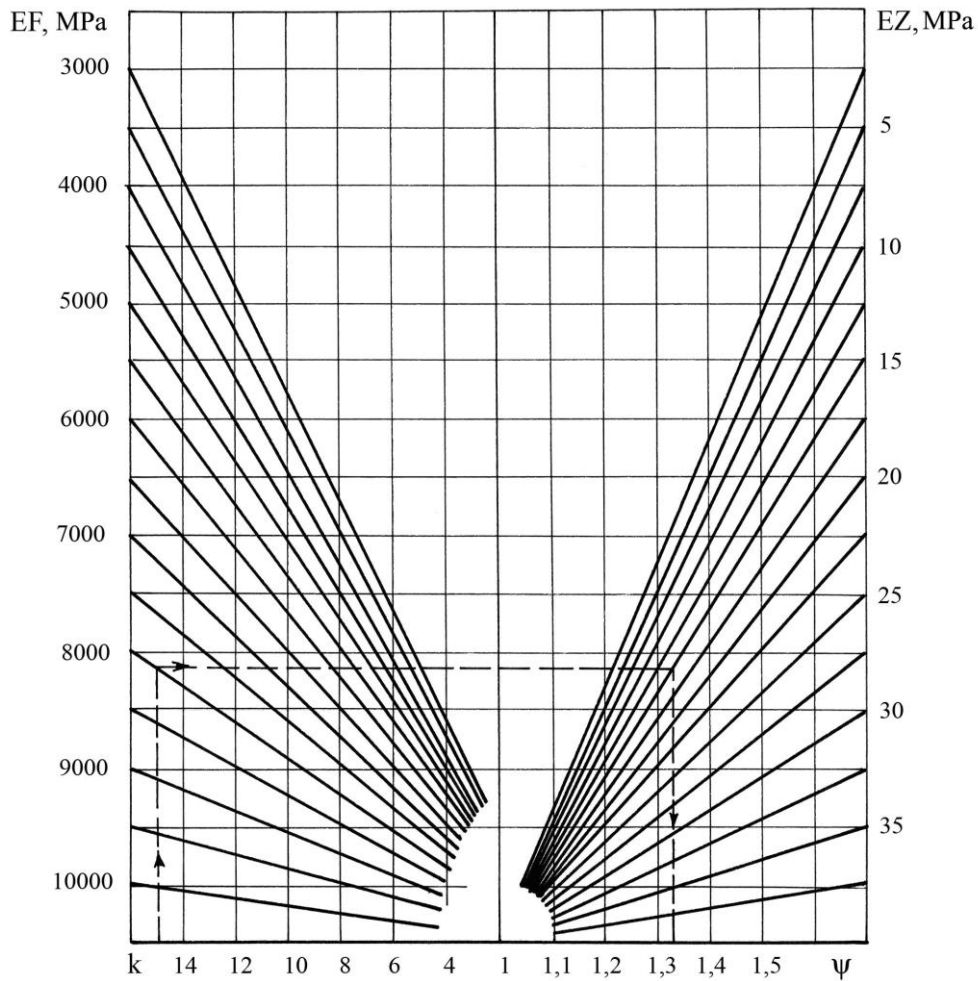


Fig. 3.12. Nomograph for the definition of the factor of non-uniformity of loading of teeth

Accounting the fact that the high longitudinal rigidity, combined with the high compliance of teeth, is characteristic for toothed belts, let's consider the case when $EF \rightarrow \infty$, and $EZ \rightarrow 0$. In this case, $\alpha = 0$ and $r_1 = r_2 = 1$. The values of the loadings on each tooth of the arc of contact represent the uncertainty. Using the rule of **Lopital**, we write:

$$P_{r_1=1; r_2=1} = \lim_{\substack{r_1 \rightarrow 1 \\ r_2 \rightarrow 0}} P_{r_1; r_2} = \lim_{r_1 \rightarrow 1} \frac{\varphi_{r_1; r_2}}{\theta_{r_1; r_2}} = \lim_{\substack{r_1 \rightarrow 1 \\ r_2 \rightarrow 0}} \frac{\frac{\partial \varphi}{\partial r_1} dr_1 + \frac{\partial \varphi}{\partial r_2} dr_2}{\frac{\partial \theta}{\partial r_1} dr_1 + \frac{\partial \theta}{\partial r_2} dr_2}.$$

From this expression for the first tooth of the arc of contact we receive:

$$\begin{aligned}
R_1 &= F_t \lim_{\substack{r_1 \rightarrow 1 \\ r_2 \rightarrow 1}} \frac{\left(\frac{r_2}{r_1}\right)^k r_1^{-1} - r_2^{-1}}{1 - \left(\frac{r_2}{r_1}\right)^k} = \\
&= F_t \lim_{\substack{r_1 \rightarrow 1 \\ r_2 \rightarrow 1}} \left(0,5 \left[r_2^{-1} r_1^{-1} \left(-\frac{k}{r_1^{k-1}} \right) + \left(\frac{r_2}{r_1}\right)^k + \frac{kr_2^{k-1}}{r_1^k} r_1^{-1} - 1 \right] + \right. \\
&\quad \left. + \frac{2+\alpha}{2\sqrt{4\alpha+\alpha^2}} \left[r_2^{-1} r_1^{-1} \left(-\frac{k}{r_1^{k-1}} \right) + \left(\frac{r_2}{r_1}\right)^k + \frac{kr_2^{k-1}}{r_1^k} r_1^{-1} + 1 \right] \right) / \\
&= 1/0,5 \left[-r_2^k \left(-\frac{k}{r_1^{k-1}} \right) - \frac{kr_2^{k-1}}{r_1^k} \right] + \frac{2+\alpha}{2\sqrt{4\alpha+\alpha^2}} \left[-r_2^k \left(-\frac{k}{r_1^{k-1}} \right) + \frac{kr_2^{k-1}}{r_1^k} \right] = \frac{F_t}{k}.
\end{aligned}$$

The similar values were received for the other teeth in gearing.

Thus, it was established that the increase in the longitudinal rigidity of a belt leads to the decrease of non-uniformity of loading of teeth in the same way as at the reduction of the rigidity of belt teeth.

The difference of the steps of a pulley and a belt is possible for the following reasons:

1) because of the mistake of manufacturing, the influence of admissions or intentional infringement of the condition $t_p = t_m$ for the creation of a favorable distribution of loading in gearing;

2) because of the operating conditions, the influence of the circumferential force, the pretension and centrifugal tension, causing the lengthening of the bearing layer of a belt.

The difference of the steps of the belt and pulley is defined by the average line of the bearing layer of the belt, i.e by the pitch diameter of the pulley.

In a general way, four cases of gearing in the presence of a regular (non-random) difference of steps $\bar{\Delta}t$ are considered (Fig. 3.13)

a) $t_p < t_m$

- 1) the even number of teeth in gearing (Fig. 3.13, a),
- 2) the odd number of teeth in gearing (Fig. 3.13, b);

b) $t_p > t_m$

- 1) the odd number of teeth in gearing (Fig. 3.13, c),

2) the even number of teeth in gearing (Fig. 3.13, d).

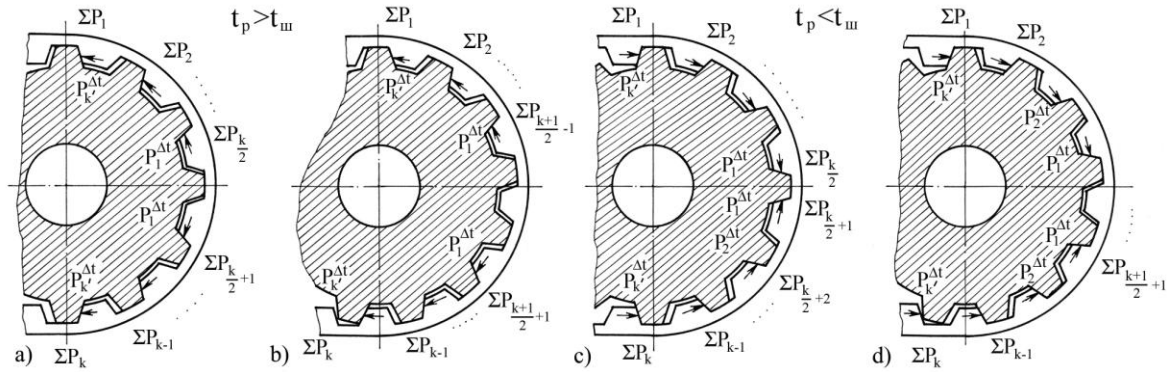


Fig. 3.13. Variants of gearing of a belt with a pulley at $t_p \neq t_m$

The problem can be solved in 2 stages:

- 1) the research of the distribution of loading, depending on the difference of steps;
- 2) the determination of the resultant loading, taken up by teeth.

The scheme of the force interaction of teeth for the first stage at $t_p < t_m$ is presented in Fig. 3.14, where the pulley and the belt are considered as symmetrically loaded combs. The half of the conditional contacts of teeth is accepted as k' . We make the condition of strain compatibilities in displacements, which can be expressed as force factors. According to Fig. 3.14, we receive:

$$\bar{\Delta}t\rho = f_n + \Delta_{n,n-1}\rho - f_{n-1}, \quad (3.24)$$

$$\Delta_{n,n-1} = \frac{t_p}{EF} P_k^{\Delta t} + P_{k-1}^{\Delta t} + \dots + P_n^{\Delta t}, \quad (3.25)$$

where $P_k^{\Delta t}; P_{k-1}^{\Delta t}; \dots; P_n^{\Delta t}$ – tangential loadings on the teeth, caused by the difference of steps.

After the substitution of (3.25) for (3.24) and some transformations we get:

$$\bar{\Delta}t\rho = \frac{1}{EZ} P_n^{\Delta t} - P_{n-1}^{\Delta t} + \frac{t_p}{EF} P_k^{\Delta t} + P_{k-1}^{\Delta t} + \dots + P_n^{\Delta t} \rho. \quad (3.26)$$

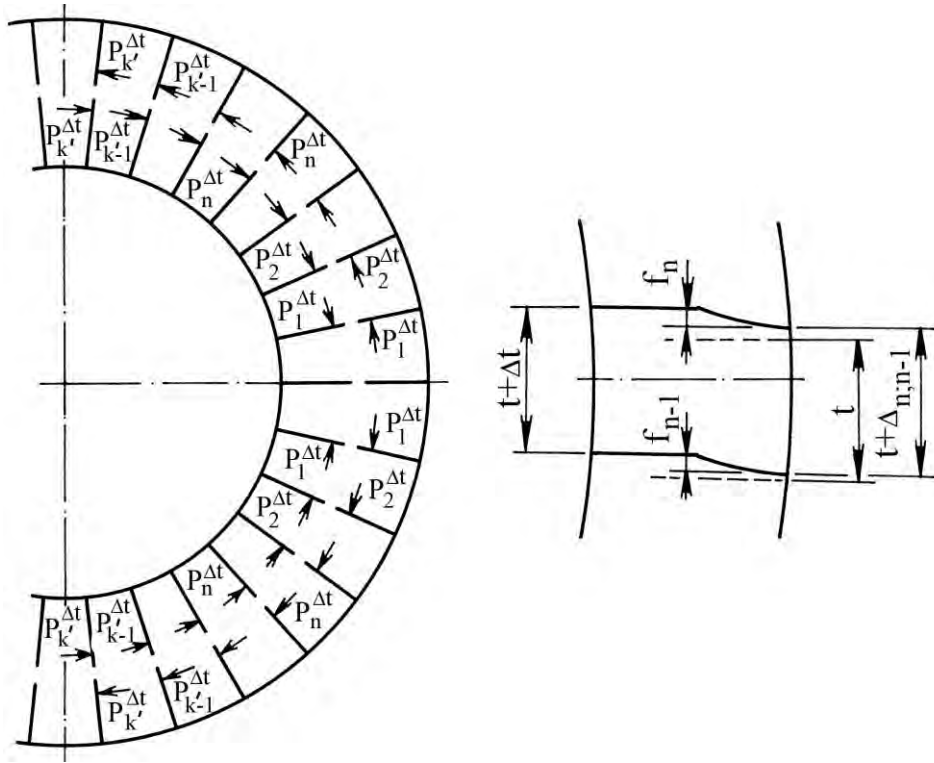


Fig. 3.14. Scheme of the force interaction of teeth of a belt and a pulley

Let's designate $\bar{Q} = EZ\bar{\Delta}t$. In this case (3.26) becomes:

$$\bar{Q}p = P_n^{\Delta t} - P_{n-1}^{\Delta t} + \alpha [P_k^{\Delta t} + P_{k-1}^{\Delta t} + \dots + P_n^{\Delta t}] \rho.$$

By means of the last expression the following system of the equations is received:

$$\begin{aligned} P_2^{\Delta t} &= P_1^{\Delta t} - \alpha [F_t' - P_1^{\Delta t}] \rho + \bar{Q}p; \\ P_3^{\Delta t} &= P_2^{\Delta t} - \alpha [F_t' - P_1^{\Delta t} + P_2^{\Delta t}] \rho + \bar{Q}p; \\ &\dots \\ P_n^{\Delta t} &= P_{n-1}^{\Delta t} - \alpha [F_t' - P_1^{\Delta t} + P_2^{\Delta t} + \dots + P_{n-1}^{\Delta t}] \rho + \bar{Q}p; \\ &\dots \\ P_k^{\Delta t} &= P_{k-1}^{\Delta t} - \alpha [F_t' - P_1^{\Delta t} + P_2^{\Delta t} + \dots + P_{k-1}^{\Delta t}] \rho + \bar{Q}p, \end{aligned} \tag{3.27}$$

where $F_t' = P_1^{\Delta t} + P_2^{\Delta t} + \dots + P_k^{\Delta t}$.

The solution of the received system is similar algorithmically to the case $t_p = t_{\text{III}}$. We rewrite the system (3.27) into the difference form. Having designated the sum of the loadings, falling on the teeth of a belt from 1 up to n as $R_n^{\Delta t}$, we receive:

$$\begin{aligned} P_n^{\Delta t} &= R_n^{\Delta t} - R_{n-1}^{\Delta t}; \\ P_{n-1}^{\Delta t} &= R_{n-1}^{\Delta t} - R_{n-2}^{\Delta t}. \end{aligned}$$

Accounting (3.27), we have:

$$P_n^{\Delta t} - P_{n-1}^{\Delta t} = R_n^{\Delta t} - 2R_{n-1}^{\Delta t} - R_{n-2}^{\Delta t} = \bar{Q}\rho - \alpha F_t' - R_{n-1}^{\Delta t} \rho$$

or

(3.28)

$$R_n^{\Delta t} - 2 + \alpha\rho R_{n-1}^{\Delta t} + R_{n-2}^{\Delta t} = \bar{Q}\rho - \alpha F_t' \rho.$$

The value $R_n^{\Delta t}$ is determined by the following expression:

$$R_n^{\Delta t} = \bar{c}_1^{-\Delta t} r_1^n - 1 + \bar{c}_2^{-\Delta t} r_2^n - 1,$$

where r_1 and r_2 – the roots of the characteristic equation, defined by the expression (3.18).

The constant factors $\bar{c}_1^{-\Delta t}$ and $\bar{c}_2^{-\Delta t}$ can be defined by the substitution of the expressions for $R_n^{\Delta t}$; $R_{n-1}^{\Delta t}$; $R_{n-2}^{\Delta t}$ to the equation (3.28), i.e.

$$\begin{aligned} \bar{c}_1^{-\Delta t} r_1^n - 1 + \bar{c}_2^{-\Delta t} r_2^n - 1 - 2 + \alpha\rho \bar{c}_1^{-\Delta t} r_1^{n-1} - 1 + \bar{c}_2^{-\Delta t} r_2^{n-1} - 1 + \\ + \bar{c}_1^{-\Delta t} r_1^{n-2} - 1 + \bar{c}_2^{-\Delta t} r_2^{n-2} - 1 = \bar{Q}\rho - \alpha F_t' \rho \end{aligned}$$

or

$$\begin{aligned} \bar{c}_1^{-\Delta t} r_1^2 - 2 + \alpha\rho \bar{c}_1^{-\Delta t} r_1 + 1 - \bar{c}_1^{-\Delta t} r_1^{n-2} + \bar{c}_2^{-\Delta t} r_2^2 - 2 + \alpha\rho \bar{c}_2^{-\Delta t} r_2 + 1 - \bar{c}_2^{-\Delta t} r_2^{n-2} + \\ + \alpha\rho \bar{c}_1^{-\Delta t} + \bar{c}_2^{-\Delta t} = \rho \bar{Q} - \alpha F_t' \rho. \end{aligned}$$

Taking into consideration the expression (3.18), we finally get:

$$\alpha \frac{-\Delta t}{c_1} + \frac{-\Delta t}{c_2} = \bar{Q} - \alpha F_t' \quad (3.29)$$

Besides the condition should be fulfilled:

$$R_k^{\Delta t} = \frac{-\Delta t}{c_1} r_1^{k-1} + \frac{-\Delta t}{c_2} r_2^{k-1} = F_t' \quad (3.30)$$

$\frac{-\Delta t}{c_1}$ and $\frac{-\Delta t}{c_2}$ are defined from the equations (3.29), (3.30) at the known F_t' .

For the definition of F_t' we use the condition of the deformation of the first tooth of the arc of contact from the line of symmetry (see Fig. 3.13, c):

$$\bar{\Delta t} p = \frac{R_1^{\Delta t}}{EZ} + \frac{t_p}{EF} R_1^{\Delta t} + R_2^{\Delta t} + \dots + R_k^{\Delta t} p$$

or

$$R_1^{\Delta t} = \bar{Q} p - \alpha F_t' p = \frac{-\Delta t}{c_1} r_1 - 1 + \frac{-\Delta t}{c_2} r_2 - 1 \quad (3.31)$$

Having solved (3.29) – (3.31), after some transformations we receive:

$$\frac{-\Delta t}{c_1} = \frac{1}{1 - \left(\frac{r_2}{r_1}\right)^{k'} \frac{r_1 - 1 - \alpha p}{r_2 - 1 - \alpha p}} \cdot \frac{\bar{Q}}{\alpha r_1^{k'}}, \quad \frac{-\Delta t}{c_2} = \frac{1}{1 - \left(\frac{r_1}{r_2}\right)^{k'} \frac{r_2 - 1 - \alpha p}{r_1 - 1 - \alpha p}} \cdot \frac{\bar{Q}}{\alpha r_2^{k'}}$$

The loadings, falling on the separate teeth of the arc of contact, in consequence of the constant difference of steps, are defined by the following expressions:

$$\begin{aligned} R_1^{\Delta t} &= \frac{-\Delta t}{c_1} r_1 - 1 + \frac{-\Delta t}{c_2} r_2 - 1 ; \\ R_2^{\Delta t} &= \frac{-\Delta t}{c_1} r_1 \frac{r_1 - 1}{r_1 - 1} + \frac{-\Delta t}{c_2} r_2 \frac{r_2 - 1}{r_2 - 1} ; \\ &\text{-----} \\ R_n^{\Delta t} &= \frac{-\Delta t}{c_1} r_1^{n-1} \frac{r_1 - 1}{r_1 - 1} + \frac{-\Delta t}{c_2} r_2^{n-1} \frac{r_2 - 1}{r_2 - 1} ; \\ &\text{-----} \\ R_k^{\Delta t} &= \frac{-\Delta t}{c_1} r_1^{k-1} \frac{r_1 - 1}{r_1 - 1} + \frac{-\Delta t}{c_2} r_2^{k-1} \frac{r_2 - 1}{r_2 - 1} . \end{aligned} \quad (3.32)$$

The analysis of the expressions testifies that the influence on $\bar{c}_1^{-\Delta t}$ and $\bar{c}_2^{-\Delta t}$ is insignificant, and at $z_{\text{III}} > 6$ it does not exceed 0.01 %. Thus, it can be neglected.

Let's simplify some computations. Since

$$\frac{(\bar{r}_1 - 1 - \alpha)}{(\bar{r}_2 - 1 - \alpha)} = -r_2; \quad \frac{(\bar{r}_2 - 1 - \alpha)}{(\bar{r}_1 - 1 - \alpha)} = -r_1,$$

the expressions for $\bar{c}_1^{-\Delta t}$ and $\bar{c}_2^{-\Delta t}$ have the following form:

$$\bar{c}_1^{-\Delta t} = \frac{\bar{Q}}{\alpha} \cdot \frac{1}{r_1^{k'} + r_2^{k'+1}}; \quad \bar{c}_2^{-\Delta t} = \frac{\bar{Q}}{\alpha} \cdot \frac{1}{r_2^{k'} + r_1^{k'+1}}.$$

Hence, the equation for the definition of the loading on n -tooth can be written in the following form:

$$P_n^{\Delta t} = \bar{c}_1^{-\Delta t} \left[r_1^{n-1} r_1^{-1} + r_2^{n-1} r_2^{-1} \frac{1}{r_1} \right] = \frac{\bar{Q}}{\alpha} r_1^{-1} \frac{r_1^{n-1} - r_2^{n+1}}{r_1^{k'} + r_2^{k'+1}}, \quad (3.33)$$

where

$$\bar{c}_1^{-\Delta t} \frac{1}{r_1} = \frac{\bar{Q}}{\alpha} \cdot \frac{1}{r_1^{k'} + r_2^{k'+1}} \cdot \frac{1}{r_1} = \frac{\bar{Q}}{\alpha} \cdot \frac{1}{r_2^{k'} + r_1^{k'+1}} \cdot \frac{1}{r_1} = \bar{c}_2^{-\Delta t}.$$

Having multiplied and divided the right part of the received equation by r_2^k , we have the following equation for k -tooth:

$$P_k^{\Delta t} = \frac{\bar{Q}}{\alpha} r_1^{-1} (r_2 - r_2^{2k+1}) / (1 - r_2^{2k+1}).$$

In case of gearing of more than one pair of teeth, i.e. at $k > 1$, and considering that $r_2 \rightarrow 0$, $\frac{r_2 - r_2^{2k+1}}{1 - r_2^{2k+1}}$ we write the following expression in the expanded form:

$$(r_2 - r_2^{2k+1}) / (1 - r_2^{2k+1}) = r_2 - 1 + r_2 - r_2^{2k+1} - r_2^{4k+2} + r_2^{6k+3} + \dots,$$

which is converging ($r_2 \ll 1$) relating to r_2 . Accounting it we get:

$$P_k^{\Delta t} = \frac{\bar{Q}}{\alpha} \left[\frac{1}{r_2} - 1 \right] r_2 = \frac{\bar{\Delta}t}{t_p} (1 - r_2) .$$

In this case the total loading, taking up by the teeth of a half of the arc of contact, is:

$$F_t' = \frac{\bar{Q}}{\alpha} \left[1 - r_2^k \frac{1 + r_2}{1 + r_2^{2k+1}} \right] .$$

The total loading on teeth is defined for each half of the arc of contact from a neutral line of transmission that is the line of symmetry.

1. If $t_p > t_{III}$:

a) up to the line of symmetry the loadings are summed up (see Fig. 3.14):

$$\Sigma P = P + P^{\Delta t} ;$$

b) after the line of symmetry the loadings are subtracted:

$$\Sigma P = P - P^{\Delta t} .$$

2. If $t_p < t_{III}$ the above-stated actions have the reverse form.

The positive or negative sign of the resultant loading corresponds to the operating (from a driving side) or a non-operating surface of teeth of a belt.

The equations (3.19) and (3.32) allow defining the resultant loadings, influencing the teeth of the arc of contact. The loading identifications, depending on their even or odd number, are presented in Fig. 3.13.

The expressions for the determination of the total loading, taken up by teeth at even k are given below:

– up to the line of symmetry: **1a** – "+"; **2a** – "-":

$$\Sigma P_n = \left(c_1 r_1^{n-1} \pm \frac{-\Delta t}{c_1} r_1^{\frac{k}{2}-n} \right) r_1^{-1} + \left(c_2 r_2^{n-1} \pm \frac{-\Delta t}{c_2} r_2^{\frac{k}{2}-n} \right) r_2^{-1} ; \quad (3.34)$$

– after the line of symmetry: 1b – "-"; 2b – "+":

$$\Sigma P_n = \left(c_1 r_1^{n-1} \mp \frac{-\Delta t}{c_1} r_1^{\frac{n-k}{2}-1} \right) r_1^{-1} + \left(c_2 r_2^{n-1} \mp \frac{-\Delta t}{c_2} r_2^{\frac{n-k}{2}-1} \right) r_2^{-1} . \quad (3.35)$$

In a similar way we get the values of the total loading, taken up by the teeth at odd k :

– up to the line of symmetry: 1a – "+"; 2a – "-":

$$\Sigma P_n = \left(c_1 r_1^{n-1} \pm \frac{-\Delta t}{c_1} r_1^{\frac{k+1}{2}-n-1} \right) r_1^{-1} + \left(c_2 r_2^{n-1} \pm \frac{-\Delta t}{c_2} r_2^{\frac{k+1}{2}-n-1} \right) r_2^{-1} ; \quad (3.36)$$

– after the line of symmetry: 1b – "-"; 2b – "+":

$$\Sigma P_n = \left(c_1 r_1^{n-1} \mp \frac{-\Delta t}{c_1} r_1^{\frac{n-k+1}{2}-1} \right) r_1^{-1} + \left(c_2 r_2^{n-1} \mp \frac{-\Delta t}{c_2} r_2^{\frac{n-k+1}{2}-1} \right) r_2^{-1} . \quad (3.37)$$

In the expressions (3.34) – (3.37) the factors c_1 and c_2 are defined by means of (3.20), (3.21); the factors $\frac{-\Delta t}{c_1}$ and $\frac{-\Delta t}{c_2}$ are defined in the following way:

k – even, $t_{\text{III}} \geq t_p$:

$$\frac{-\Delta t}{c_1} = \frac{1}{1 - \left(\frac{r_2}{r_1} \right)^{\frac{k}{2}} \frac{r_1 - 1 - \alpha}{r_2 - 1 - \alpha}} \cdot \frac{\bar{O}}{\alpha r_1^{\frac{k}{2}}}, \quad \frac{-\Delta t}{c_2} = \frac{1}{1 - \left(\frac{r_1}{r_2} \right)^{\frac{k}{2}} \frac{r_2 - 1 - \alpha}{r_1 - 1 - \alpha}} \cdot \frac{\bar{O}}{\alpha r_2^{\frac{k}{2}}};$$

k – odd, $t_{\text{III}} \geq t_p$:

$$\frac{-\Delta t}{c_1} = \frac{1}{1 - \left(\frac{r_2}{r_1}\right)^{\frac{k-1}{2}} \frac{r_1-1-\alpha}{r_2-1-\alpha}} \cdot \frac{\bar{Q}}{\alpha r_1^{\frac{k-1}{2}}}, \quad \frac{-\Delta t}{c_2} = \frac{1}{1 - \left(\frac{r_1}{r_2}\right)^{\frac{k-1}{2}} \frac{r_2-1-\alpha}{r_1-1-\alpha}} \cdot \frac{\bar{Q}}{\alpha r_2^{\frac{k-1}{2}}}.$$

Taking into account (3.22) and (3.33) the expressions (3.34) – (3.37) can be presented in the acceptable for engineering calculations form:

k – even:

$$\left(\Sigma P_1 \dots \Sigma P_{\frac{k}{2}} \right) \Sigma P_n = \left[\frac{r_1^{k-n} + r_2^{k-n+1}}{r_1^k - r_2^k} F_t \pm \frac{r_1^{\frac{k-n}{2}} - r_2^{\frac{k-n+2}{2}}}{r_1^{\frac{k}{2}} + r_2^{\frac{k+1}{2}}} \cdot \frac{\bar{\Delta t}}{t_p} EF \right] r_1^{-1}; \quad (3.38)$$

$$\left(\Sigma P_{\frac{k}{2}+1} \dots \Sigma P_n \right) \Sigma P_n = \left[\frac{r_1^{k-n} + r_2^{k-n+1}}{r_1^k - r_2^k} F_t \mp \frac{r_1^{\frac{n-k-1}{2}} - r_2^{\frac{n-k+1}{2}}}{r_1^{\frac{k}{2}} + r_2^{\frac{k+1}{2}}} \cdot \frac{\bar{\Delta t}}{t_p} EF \right] r_1^{-1}; \quad (3.39)$$

k – odd:

$$\left(\Sigma P_1 \dots \Sigma P_{\frac{k+1}{2}} \right) \Sigma P_n = \left[\frac{r_1^{k-n} + r_2^{k-n+1}}{r_1^k - r_2^k} F_t \pm \frac{r_1^{\frac{k+1-n}{2}} - r_2^{\frac{k+1-n+1}{2}}}{r_1^{\frac{k+1}{2}} + r_2^{\frac{k+1}{2}+1}} \cdot \frac{\bar{\Delta t}}{t_p} EF \right] r_1^{-1}; \quad (3.40)$$

$$\left(\Sigma P_{\frac{k+1}{2}+1} \dots \Sigma P_n \right) \Sigma P_n = \left[\frac{r_1^{k-n} + r_2^{k-n+1}}{r_1^k - r_2^k} F_t \mp \frac{r_1^{\frac{n-k+1}{2}} - r_2^{\frac{n-k+1}{2}+1}}{r_1^{\frac{k+1}{2}} + r_2^{\frac{k+1}{2}+1}} \cdot \frac{\bar{\Delta t}}{t_p} EF \right] r_1^{-1}. \quad (3.41)$$

In the expressions (3.38) – (3.41) "+" is accepted at $t_p > t_{\text{ш}}$; "-" – at $t_p < t_{\text{ш}}$.

The total diagram of the distribution of the loading in gearing develops of two diagrams – from the action F_t at $t_{\text{ш}} = t_p$ and from the difference of steps t_p and $t_{\text{ш}}$ (Fig. 3.15).

Fig. 3.16 shows the graphic dependences, constructed on the basis of (3.38) – (3.41) for the determination of the factor of non-uniformity of the distribution of the loading in the presence of the difference of steps, depending on the number of teeth in gearing, the longitudinal rigidity, the rigidity of teeth of the belt, the difference of the steps and the pull.

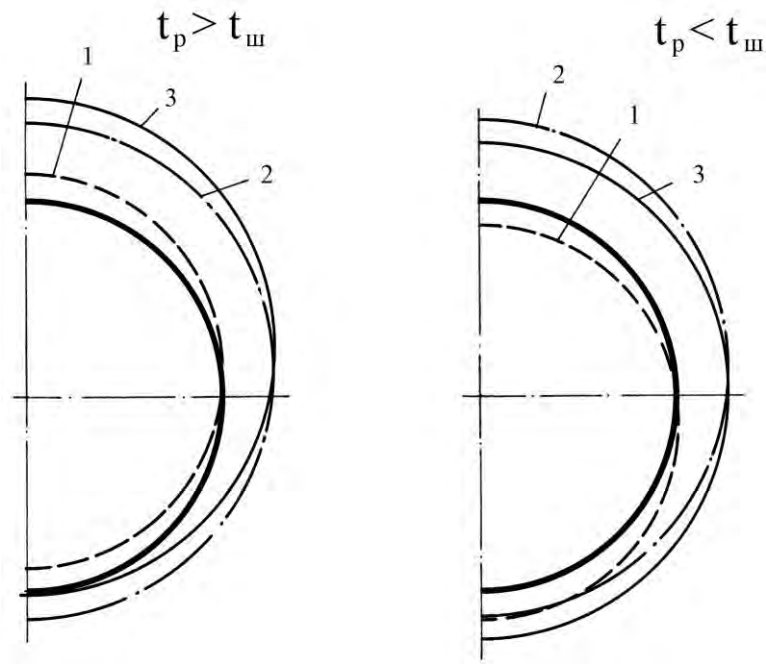


Fig. 3.15. Diagrams of the distribution of loading on the teeth of a belt:
 1 – caused by the constant difference of steps of teeth of a belt and a pulley;
 2 – from the action of a pull; 3 – resultant

The analysis shows that the existence of the difference of steps causes the essential redistribution of the loading in gearing. The received results testify that at $t_p < t_w$ the teeth are unloaded up to the line of symmetry and the part of the loading is transferred on poorly loaded teeth after the line of symmetry, and vice versa.

The choice of the certain difference of steps allows receiving practically any distribution of the loading in gearing. For example, for getting of the equilibrium distribution of the loading the difference of steps of teeth should be defined from the condition of equality of the loadings, taken up by the first and the last teeth of the arc of contact.

From (3.38), (3.39) we receive the expression for the rational value Δt [103]

$$\Delta t = \frac{F_t t_p}{EF} \cdot \frac{r_2^{k-1} - 1}{r_2 - 1} - \left(\frac{r_2}{r_1} \right)^k \frac{r_1^{k-1} - 1}{r_1 - 1} \cdot \left[\frac{\frac{k-1}{2r_1^2} - \frac{1}{r_1}}{\frac{k}{r_1^2} + \frac{k+1}{r_2^2}} + \frac{\frac{k-1}{2r_2^2} - \frac{1}{r_2}}{\frac{k}{r_2^2} + \frac{k+1}{r_1^2}} \right] \left[1 - \left(\frac{r_2}{r_1} \right)^k \right] \quad (3.42)$$

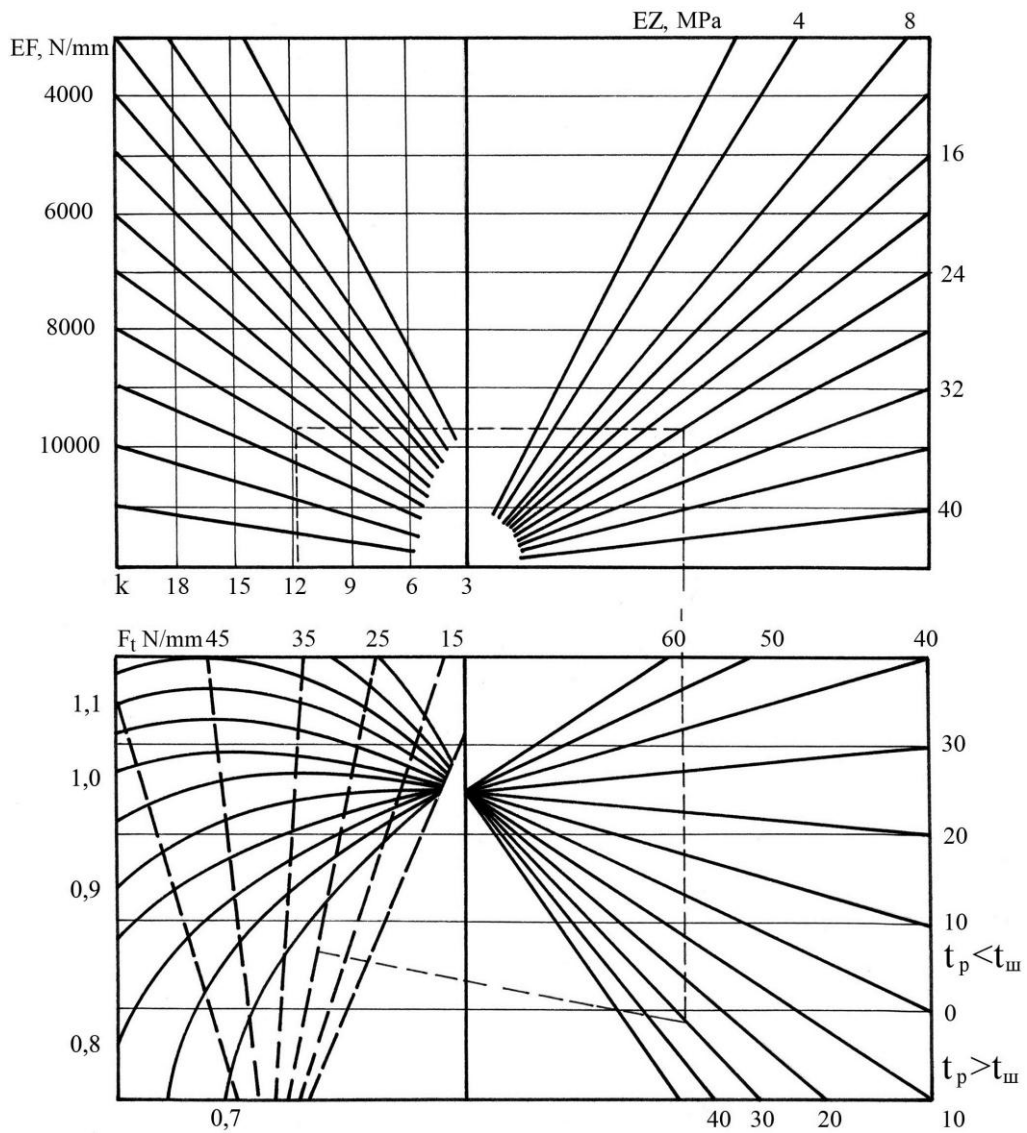


Fig. 3.16. Diagram for the determination of the factor of non-uniformity of loading of teeth

The similar dependence results from the expressions (3.40), (3.41).

On the basis of (3.42) the diagram (Fig. 3.17) is constructed. It testifies that Δt depends, to a small extent, on the number of teeth in gearing and their rigidity, and it is defined, basically, by the longitudinal rigidity of a belt and the transferred pull.

Thus, as $r_1 \gg 1$, $r_2 \ll 1$, $r_1 r_2 = 1$, the loading on the teeth, created by the difference of steps, increases from the line of symmetry of the arc of contact to its periphery. The existence of the difference causes the redistribution of the loading in gearing, and, at $(t_{\text{ш}} - t_p) < 0$ the increase in loading of the first from the driving side teeth and unloading of the last ones, is observed.

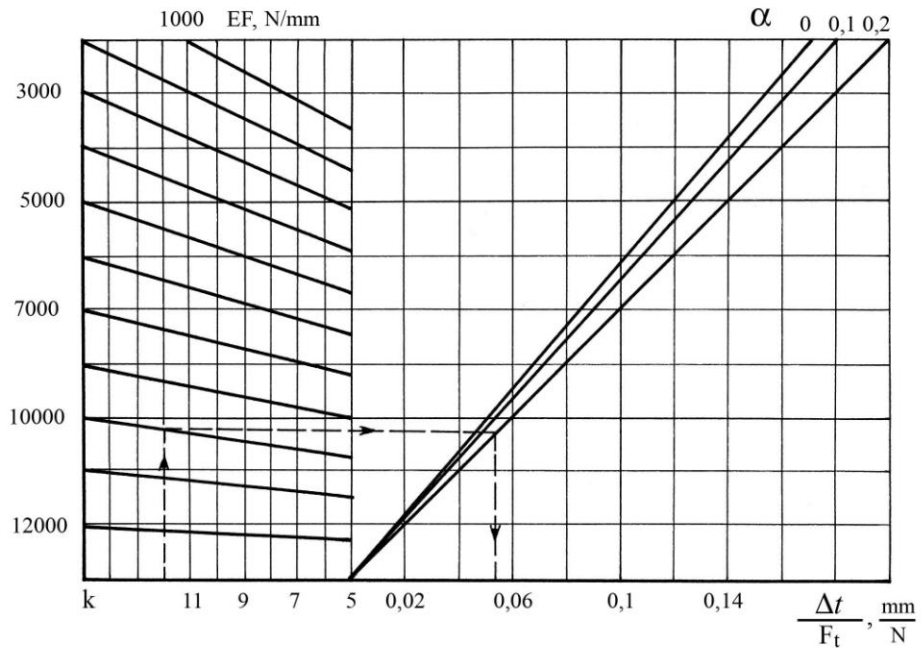


Fig. 3.17. Diagram for the choice of the correction of the step of teeth of a pulley

As a result of the conducted researches of loading of a multiple toothed-belt gearing by the method of the finite differences the dependences of the distribution of the transferred loading on the teeth from the main parameters of transmission, the conditions of gearing and physical and mechanical properties of a toothed belt were received. It was established that the most effective methodical way of control of non-uniformity of loading of gearing and, as a consequence, of the increase of the load carrying capacity and durability of toothed-belt transmissions, is the correlation adjustment of the step of the pulley teeth.

3.4. Mathematical and physical modeling of the transmission of power

At functioning of a toothed-belt transmission its elements are exposed to the complex of dynamic influences. Their classification, pointing out the systematic and random components, is offered. The random dynamic factors, connected with the non-uniformity of movement of the machine-engine or the machine-instrument, owing to their complex predictability, are not considered thereafter. The systematic dynamic loadings on teeth result from the shock character of their input in gearing and the alternate loading on the arcs of contact of pulleys, because of the successive locating of the part of the belt on the sides with different efforts, and they are also connected with the alternate bending of the belt on pulleys.

The researches established that the parameters of mechanical and physical properties of the elements of the belt in the conditions of the dynamic loading – the dynamic longitudinal rigidity EF_d and the dynamic rigidity of teeth EZ_d – essentially differ from the static values EF and EZ . For the different types of belts the excess of EF_d above EF was established: **V-belts** – 1.3 times [104]; **CVT- belts** – 1.7 times [105]; **Poly-V-belts** of the sections **K, JI, M** – 1.8; 2.0 and 2.2 times accordingly [106]; toothed belts – 1.1...1.3 times [107].

These results were received by the method of excitation of damped vibrations, which is not specific for the belt operation in transmission. As a result of the measurement of the values EF_d and EZ_d at the forced **loading with the various frequency ν of a** harmoniously changing loading, in the works [103, 108] it is offered to determine the parameters of the mechanical properties of belts by the following dependences:

$$EF_d = k_{Fd}EF; \quad EZ_d = k_{Zd}EZ, \quad (3.43)$$

where $k_{Fd} = 1.6...2.2$ at $\nu = 0...44$ Hz and $k_{Zd} = 1.2...1.6$ at $\nu = 0...22$ Hz.

It is offered to define the values k_{Fd} and k_{Zd} for toothed belts by the dependences [47]:

$$k_{Fd} = \nu^{0,096} A_F^{-0,075} F_M^{0,18+A_F}; \quad (3.44)$$

$$k_{Zd} = \nu^{0,017} A_P^{-0,56} P_M^{0,44+A_P}.$$

where F_M and P_M – average efforts of the loading cycle; $A_F = F_A / F_M$; $A_P = P_A / P_M$ – amplitude factors; F_A ; P_A – amplitude efforts on a bearing layer and belt teeth.

At the same time the use of the results EF_d and EZ_d , received by the influence of a harmonious effort on a belt, makes difficulties for the prediction of the deformations of the belt elements in a real transmission, since the loading modes of both the bearing layer and teeth are different from the sinusoidal modes. In this case, it is necessary to present the real operating mode in the form of the sum of the harmonious components and to find the deformations of the belt elements for each of them.

For the solution of the given problem it is necessary to use the visco-elastic model of a toothed belt. The bearing layer and belt teeth are replaced with equivalent elasticities and the viscosities, adequately responding to the influence of static and dynamic loadings and leading to receiving of experimentally observed k_{Fd} and k_{Zd} . In particular, for the teeth of the belts $m = 7$ mm; $B_p = 50$ mm; $P_M = 4$ N/mm the following values were received: the **visco-elastic** rigidity $E_{ve} = 0.035$ MPa; the instant (static) rigidity $E_0 = 5.479$ MPa and viscosity of the elastic after-effect $\eta_{ve} = 0.036$ MPa·s.

Using the formulas (3.43), the system of the equations (3.2) was presented in the form:

$$\frac{F_{12}}{k_{Zd} EZ} = \frac{F_{11}}{k_{Zd} EZ} - t_p \frac{F_1 - F_{11}}{k_{Fd} EF};$$

$$\frac{F_{1n}}{k_{Zd} EZ} = \frac{F_{1n-1}}{k_{Zd} EZ} - t_p \frac{F_1 - F_{11} - \dots - F_{1n-1}}{k_{Fd} EF}; \quad (3.45)$$

$$\sum F_{1n} = F_1 - F_2 = F_t.$$

The solution of the system (3.45) was made with the help of the computer by the standard program, realizing the method of Gauss [90]. At that, EF ; EZ ; F_i ; z_0 were varied and the **frequency of runs of a belt v was equal to:**

$$v = \frac{10^3 \cdot v_p}{\pi m z_p}, \text{ s}^{-1}.$$

The results of the calculation of the efforts in gearing at various frequencies of loading of a belt show that the increase in the frequency of its runs leads to the partial unloading of the teeth, adjoining to the driving side. In the examined cases for $z_0 = 4$ the reduction of the effort on the first tooth of the arc of contact makes 3.1 %, and for $z_0 = 12$ – more than 18 %.

The estimation of the influence of mechanical and physical properties of belt elements **on the distribution of the loading in gearing was made at $v = 10$ s⁻¹**. The analysis of the dependences shows that the increase in the longitudinal rigidity of the belt EF promotes the

equalization of the loading between the teeth. It, in its turn, should favorably affect the durability of a belt. The increase in the longitudinal rigidity of the belt from 1460 up to 3170 N/mm causes the reduction of ψ 1.3 times.

On the contrary, the increase in the rigidity of teeth leads to the opposite results. The increase of EZ by 13 % leads to an additional loading of the first tooth by 4.1 %.

In our opinion, the dependences k_F and k_Z from EF and EZ allow to explain the effect of the reduction of ψ from the frequency of loading. The analysis of the dependences (3.43), (3.44) shows that at the identical augment of v the value EF_d grows more quickly than EZ_d . At the same time at the increase of EF the non-uniformity of loading of teeth decreases. Thus, at the augment of v the increase of ψ (because of the growth of EZ) is unable to compensate the decrease of ψ (because of the increase of EF).

The increase in the pull, transferred by the belt, leads to the proportional increase in the loading on all the teeth which are in gearing. It is explained by the increase in the deformation of tension of the sides of the belt at the increase of F_t and the corresponding increase in the step of belt teeth t_p . The gearing of the belt with the increased step t_p with a pulley of a constant step t_{III} , leads, as it is known, to the increase of ψ .

It is necessary to note that the technique of the calculation of loading of teeth of the arc of contact, presented above, allows receiving the flattened calculated curves, which reflect the general regularities of the distribution of the loading. The experimental dependences (oscillograms), received by strain-gauging, have a characteristic harmonious profile with local extrema (Fig. 3.18), testifying to a shock input of teeth in gearing.

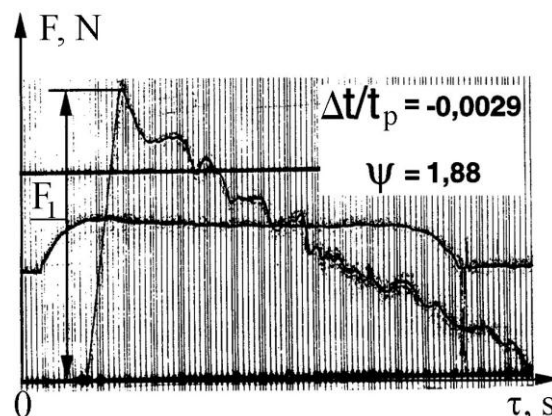


Fig. 3.18. Oscillogram of loading of a toothed-belt gearing

The author of the work [66] received the system of the differential equations, presenting torsional vibrations of a drive pulley and longitudinal vibrations of the sides of the belt, accounting the shock input of teeth in gearing. However, the main demerit of the given approach is the use of the unreasoned supposition, according to which the vibrations, arising by the action of the shock input of teeth in gearing, damp by the moment of the input in gearing of the next tooth. Thus, the shock loading is perceived by one tooth and the distribution effect of effort in the multiple gearing is not considered.

The reliable information about loading of teeth in gearing can be received on the basis of the account of non-uniformity of the distribution of shock and traction efforts on the arc of contact.

The physical and mathematical model for the research of the distribution of loading in gearing was developed. It considers: 1) shock character of loading of the first tooth of the arc of contact; 2) multiple character of gearing; 3) contact of teeth without clearance; 4) static and dynamic mechanical and physical properties of belt elements.

The developed model allows to estimate the influence of the main parameters of transmission and mechanical and physical properties of belt elements on loading of gearing and to offer the reliability methods of its uniformity [109].

According to the principle laws of mechanics the equation of motion of the system is the following [110]:

$$F_k(t) + F_c(t) + F_m(t) = 0, \quad (3.46)$$

where $F_k(t) = -k[y(t) - x(t)]$ – the elastic force; $F_c(t) = -c[\dot{y}(t) - \dot{x}(t)]$ – the damping force; $F_m(t) = -m\ddot{y}(t)$ – the inertial force; m – the weight of the system; c and k – the viscosity and rigidity of the system elements accordingly; $x(t)$, $y(t)$ – the law of motion at the input and output of the system.

Having rearranged (3.46), we get:

$$m\ddot{y}(t) + c\dot{y}(t) + ky(t) = kx(t) + c\dot{x}(t).$$

The model of the interaction of teeth in gearing can be presented in the form of the development (Fig. 3.19). The viscosity of the plastic yielding η_{pc} can be neglected, having

limited to a three-element model, since the showing of creep of a material or its relaxation [111] is not specific for the loaded teeth and an interdental part of a belt.

The pulley impacts a tooth of a belt, inputting in gearing, by the specific mass, distributed along the arc of contact:

$$m_{\text{ш}} = m_{\text{ш.g}} / z_0,$$

where $m_{\text{ш.g}}$ – generalized mass of a pulley.

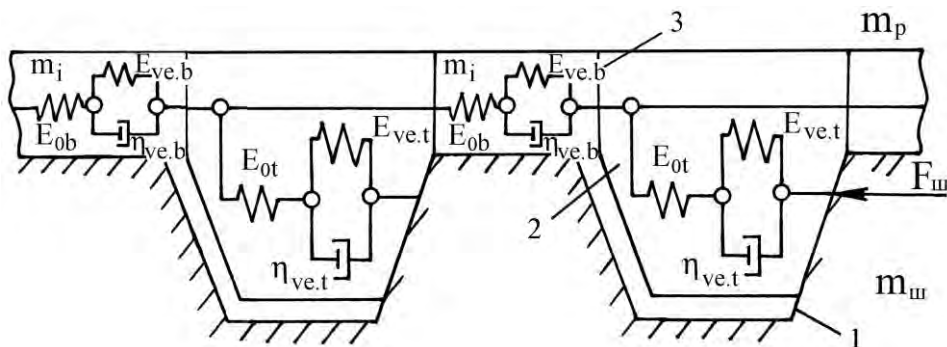


Fig. 3.19. Dynamic model of the interaction of teeth in gearing: 1 – tooth of a pulley; 2 – belt teeth; 3 – bearing layer; $E_{ve,t}$, $E_{ve,b}$ – visco-elastic rigidity of a tooth and a bearing layer; $\eta_{ve,t}$, $\eta_{ve,b}$ – viscosity of an elastic after-effect of a tooth and a bearing layer;

E_{ot} , E_{ob} – instant (static) rigidity of a tooth and a bearing layer

The distribution of loading in gearing is defined by mechanical and physical properties of belt elements. For the convenience we divide the system x – y into two elements: x – x_2 and x_2 – y (Fig. 3.20).

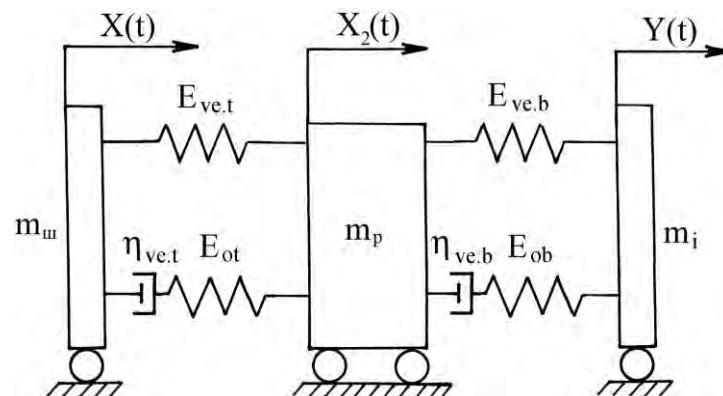


Fig. 3.20. Scheme of the calculation of loading of teeth in gearing

The equations of the movement of transmission elements can be written in the form:

$$\begin{aligned} x_2 E_{0t} &= m_p \ddot{y} + E_{0t} y, \\ x_2 &= \frac{m_p \ddot{y} + E_{0t} y}{E_{0t}} = \frac{m_p \ddot{y}}{E_{0t}} + y, \end{aligned} \quad (3.47)$$

where $m_p = m_1 m_2 / (m_1 + m_2)$, $m_2 = J / r_2^2$; m_p – the mass of a belt, considering the mass of a driving side m_1 and the moment of inertia of a driven pulley J ; m_2 – the mass of a driven pulley; r_2 – the radius of a pitch line of a driven pulley.

On the other hand:

$$E_{ve,t} x + \eta_{ve,t} \dot{x} = m_p \ddot{x}_2 + \eta_{ve,t} \dot{x}_2 + E_{ve,t} x_2. \quad (3.48)$$

After the substitution of x_2 from (3.47) into (3.48) and the transformations, the equation (3.48) becomes:

$$E_{0t} x + \eta_{ve,t} \frac{E_{0t}}{E_{ve,t}} \dot{x} = m_p \ddot{y} + E_{0t} y. \quad (3.49)$$

For the interdental part of a belt:

$$E_{0b} x + \eta_{ve,b} \frac{E_{0b}}{E_{ve,b}} \dot{x} = m_i \ddot{y} + E_{0b} y, \quad (3.50)$$

where m_i – the mass of the interdental part of a belt on the length of one step.

On the basis of the equations (3.49) and (3.50) after the transformations we receive the system of the differential equations of the distribution of loading in gearing for the case $z_0 = 2$:

$$\begin{cases} m_{\text{ш}} \ddot{x}_1 + E_{0t} x_1 = \eta_{ve,t} \frac{E_{0t}}{E_{ve,t}} \dot{x}_2 + E_{0t} x_2 + F_{\text{ш}}; \\ m_p \ddot{x}_2 + E_{0t} x_2 = \eta_{ve,t} \frac{E_{0t}}{E_{ve,t}} \dot{x}_3 + E_{0t} x_3 - F_{\text{ш}}; \\ m_i \ddot{x}_3 + E_{0b} x_3 = \eta_{ve,b} \frac{E_{0b}}{E_{ve,b}} \dot{x}_2 + E_{0b} x_2. \end{cases}$$

where $F_{\text{ш}}$ – the force of impact of a belt tooth with a tooth of a pulley.

In a similar way we make the system of the equations for n teeth in gearing, accepting that the pulley is absolutely non-deformed:

$$\left\{ \begin{array}{l} m_{\text{ш}}\ddot{x}_1 + E_{0t}x_1 = \eta_{ve.t} \frac{E_{0t}}{E_{ve.t}} \dot{x}_2 + E_{0t}x_2 + F_{\text{ш}}; \\ m_p\ddot{x}_2 + E_{0t}x_2 = \eta_{ve.t} \frac{E_{0t}}{E_{ve.t}} \dot{x}_3 + E_{0t}x_3 - F_{\text{ш}}; \\ m_i\ddot{x}_3 + E_{0b}x_3 = \eta_{ve.b} \frac{E_{0b}}{E_{ve.b}} \dot{x}_2 + E_{0b}x_2; \\ m_i\ddot{x}_4 + E_{0b}x_4 = \eta_{ve.b} \frac{E_{0b}}{E_{ve.b}} \dot{x}_3 + E_{0b}x_3; \\ \dots \\ m_i\ddot{x}_n + E_{0b}x_n = \eta_{ve.b} \frac{E_{0b}}{E_{ve.b}} \dot{x}_{n-1} + E_{0b}x_{n-1}. \end{array} \right. \quad (3.51)$$

The developed system of the differential equations (3.51) was solved numerically by Runge-Kutta method of 4-th order. The programmed solution was realized by means of *Borland Pascal 7.0* and the object-oriented programming (Application 1). The example of a graphic solution of a set of equations is presented in Fig. 3.21 (Application 2).

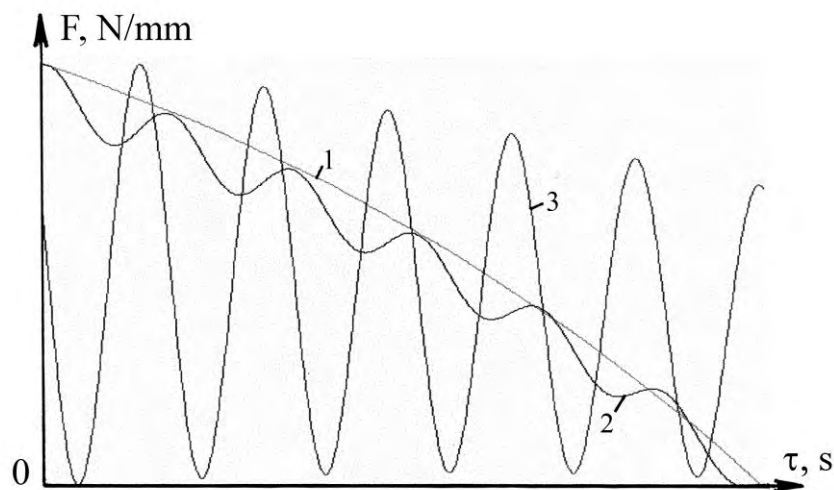


Fig. 3.21. Loading of a toothed-belt gearing:
1 – tooth of a pulley; 2 – tooth of a belt; 3 – bearing layer

As the object of the research the transmission with the following parameters was accepted: $m = 3 \text{ mm}$; $t_p = 9.42 \text{ mm}$; $z_1 = z_2 = 30$. The values of mechanical and physical characteristics of teeth and the bearing layer of the belt (static and dynamic), the number of teeth of pulleys, the value of the shock loading, the speed of the movement of a belt v_p varied.

The analysis of the received dependences testifies that the developed physico-mathematical model allows receiving the dependences of loading of gearing of a harmonious profile with the local extrema, which corresponds to the experimental curves. Hence, the developed model adequately describes the physical processes, occurring in gearing at the transmission of power.

The analysis of the received dependences shows that the increase in the static rigidity of a bearing layer and the viscosity of elastic after-effect of teeth of a belt leads to a more rigid dynamic operating mode of transmission. On the contrary, the increase in the static and visco-elastic rigidity of teeth, and also the viscosity of elastic after-effect and visco-elastic rigidity of a bearing layer of a belt contribute to more uniform loading of gearing [112].

For example, the increase of $E_{ve,t}$ from 0.015 up to 0.1 MPa leads to unloading of the first tooth of the arc of contact by 23 %, and the increase of $E_{ve,b}$ from 5 up to 50 MPa by 42.8 % (Fig. 3.22).

The influence of a high-speed operating mode of transmission on loading of gearing was investigated. As a result, the analytical dependence of the factor of dynamism of loading $k_{\psi d}$, defining the value of the dynamic factor of non-uniformity of loading of teeth $\psi_d = \psi k_{\psi d}$ from v_p , was received (Fig. 3.23).

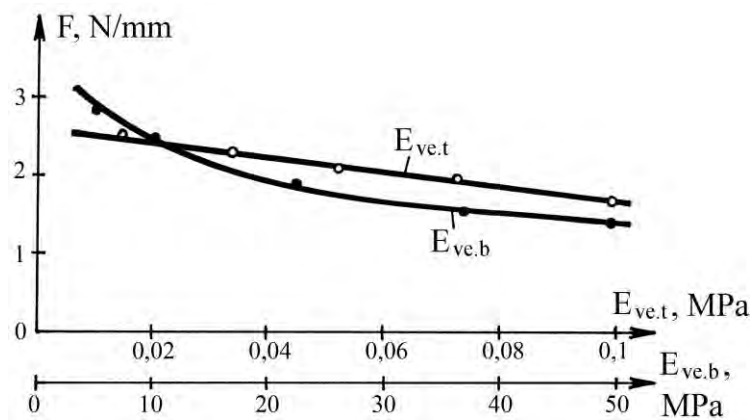


Fig. 3.22. Dependence of loading of belt teeth of mechanical and physical properties of an elastomer and a bearing layer

The non-linear increase of shock loadings on the teeth, inputting in gearing in the process of the increase of the speed of a belt, was established. In our opinion, it was caused by the non-linear increase of dynamic mechanical properties of belt elements (longitudinal rigidity and rigidity of teeth).

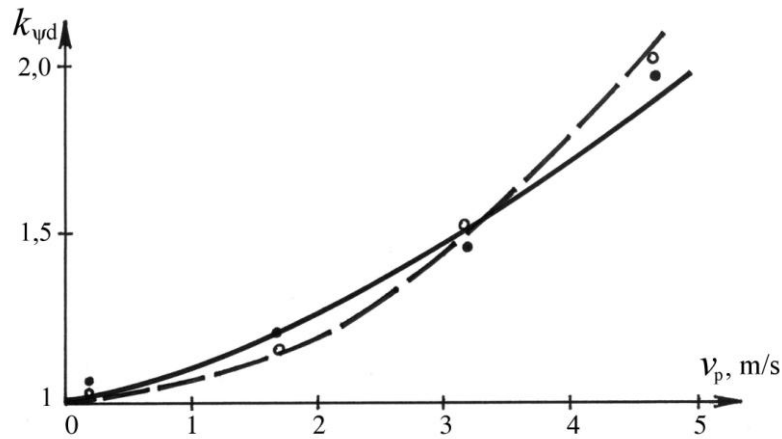


Fig. 3.23. Loading of teeth, depending on the speed of a belt:
continuous line – theoretical calculation; dashed line – experimental data

For the experimental check of the theoretical dependences the stand tests were carried out. Their main purpose was receiving of the empirical curves, reflecting the character of the distribution of loading in gearing from the speed of a belt v_p . The object of the researches were the belts $m = 7$ mm; $z_p = 71$; $B_p = 32$ and 50 mm, made by the method of diaphragm vulcanization and equipped with the wear resistant fabric coating of teeth. The technique of the carried out researches was based on the registration of the deformations of a measuring tooth of one of the pulleys of transmission (see Fig. 2.29).

The measuring tooth looked like a milled cantilever beam. The resistance strain gauges with the baseline of 10 mm were pasted on the opposite plane surfaces by the bridge circuit. The conductors from the resistance strain gauges through a current collector were connected with the unit record equipment, which was based on the light-beam oscillograph K12-22.

For carrying out of the researches the special stand (see Fig. 2.28), working on the principle of the open power contour, was made. The motor torque (800 **W**) was transferred to a drive shaft of the stand by the open tooth gearing with the transmission ratio $u = 15$.

The rotational speed of the shaft of the engine rated continuously in the range of $0...600 \text{ min}^{-1}$. The braking torque was formed on the driven shaft by means of the regulated block brake, allowing to realize the values from 0 up to 200 Nm. It provided the values $F_t = 0...57 \text{ N/mm}$ at the admissible value for $m = 7 \text{ mm}$ $[F_t] = 45 \text{ N/mm}$ at the number of teeth of pulleys of transmission $z_1 = z_2 = 20$ [70].

As a result, the oscillograms of the distribution of loading in gearing at the various belt speeds $v_p = (0.17; 1.67; 3.17; 4.67) \text{ m/s}$ were received. After the treatment of the received oscillograms (Fig. 3.24) by the method of ordinates, it was established that the value $k_{\Psi d}$ increases non-linearly while v_p increases (see Fig. 3.23). The increase of v_p from 0.17 up to 4.67 m/s leads to the increase of $k_{\Psi d}$ by 80 %.

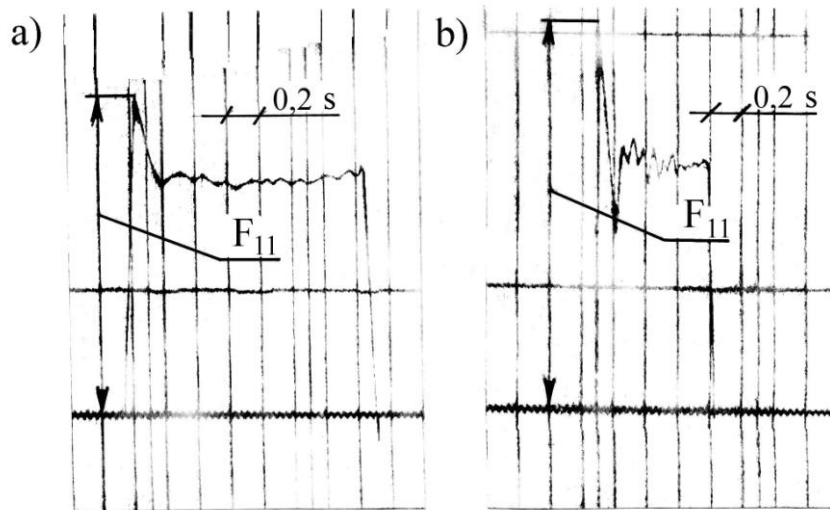


Fig. 3.24. Oscillograms of loading of a toothed-belt gearing:

a) $v_p = 1.67 \text{ m/s}$; b) $v_p = 3.17 \text{ m/s}$

The comparison of the received results showed that the theoretical dependences, defining the influence of a belt speed v_p on loading of gearing, are adequate to the empirical data. The divergence of results does not exceed 10.3 %. The similar results, presented in the section 3.6, were received in the process of the computer modeling in *ANSYS*.

Thus, the developed physico-mathematical model of the force interaction of teeth in gearing, allowed receiving the values of the working dynamic loadings, which enables to make the forecast of the durability of transmission.

3.5. Variation principles of the research of the stress-strained state

It is known that rubber (rubber-like) materials possess two excellent properties in comparison with usual design materials. Firstly, these materials are practically incompressible, i.e. their bulk moduli of elasticity essentially excel moduli of shear, and, secondly, they are capable to endure large deformations.

In view of the incompressibility of rubber materials, analyzing their stress-strained state, certain difficulties occur. It happens because the approximate calculations, based on the formulation of the problem in displacements (Navier's equation of equilibrium) can lead to the poor accuracies at the values of Poisson's ratio $\mu \approx 0.5$.

These errors arise for the reason that in the limit ($\mu = 0.5$) the usual formulation of the problem in displacements proves to be incorrect [113]. Therefore, the frequently used methods of the solution of the problem of large deformations use the expansion into series to solve linear problems. It is especially convenient when at the linear analysis the displacements are used as the basic dependent variables. In this connection, it is reasonable to make the analysis of the stress-strained state of rubber (rubber-like) materials in displacements.

There are three basic variation principles in the theory of elasticity:

- 1) principle of minimization of the potential energy, expressed by means of deformations;
- 2) principle of minimization of the complementary energy, expressed by means of stresses;
- 3) variation principle of Hellinger-Reissner, expressed by means of displacements and stresses.

The variation principle of Hellinger-Reissner causes significant difficulties for the approximate methods, as it enters the abundant number of the unknowns.

The principle of minimization of the potential energy does not allow using of the numerical methods of the solution, as it requires the choice of the system of the stresses at equilibrium, which presents significant difficulties.

The most powerful and allowing to use the numerical methods of the solution is the mixed method, based on the principle of the minimum of the potential energy and the method of Ritz.

According to the variation principle of Lagrange, the potential energy of the elastic system in an equilibrium position takes a steady-state value. This potential energy develops of the potential energy of the elastic deformation and the potential energy of outside forces.

In the basis of the solution of the problem of the theory of elasticity in displacements there is the variation principle of Lagrange, according to which, only for the true equilibrium position (of all statically possible states) the full potential energy takes the minimum value, i.e. minimization of the functional of the full potential energy.

$$\Pi = U - W, \quad (3.52)$$

where $U = \frac{1}{2} \int_V \sigma \varepsilon dV$ – potential energy of the deformation of the design; $W = \int_A P \delta dA$ – potential energy of the outside forces P ; σ – stress; ε – deformation; δ – displacement; V – volume; A – area of a design.

However, this method, even in the combination with the method of Ritz, possesses a significant error at the application to nearly incompressible materials, and it is practically unsuitable for incompressible materials.

Thus, for receiving of the method of the research of the stress-strained state, **applied** to all materials, it is necessary to use the variation principle, which is true at all acceptable values of Poisson's factor ($0 \leq \mu \leq 0.5$).

According to the work [114], the principle of the minimum of the potential energy is equivalent to the equations of the elastic field of Navier in displacements. At the same time, **Navier's formulation is wrong for incompressible materials ($\mu = 0.5$) [113]. That's why it cannot be used for such materials.** Besides, the statement of the problem in **displacements reduces the accuracy of approximate solutions, when $\mu \rightarrow 0.5$.** In order to prevent these difficulties, the variation principle, equivalent to such a statement of the problem in displacements, is necessary. Such a statement should be true both for compressible and incompressible materials.

The author of the work [114] offers the variation principle, equivalent to the equations of the elastic field, expressed by the displacement and function of the average pressure. It preserves the advantages of the principle of the minimum of the potential energy and eliminates the difficulties, arising at the usage of nearly incompressible and incompressible materials.

The author shows the method of the approximate analysis, inferred from the use of the method of Ritz together with the offered variation principle. The comparison of the results, received by this method and by the method of minimization of the potential energy, shows that the latter results are absolutely inaccurate for nearly incompressible materials,

whereas the method of the solution, based on the variation principle, yields rather exact results.

One of the most spread and adaptable methods of the research of the stress-strained state of rubber-like materials (especially for the designs of the irregular shape) is the method of the finite number of elements. The given method represents the examined design as a set of simple elements. In general, the algorithm of the finite element method is the following:

- 1) some number of the nodal points is fixed in the examined volume;
- 2) the values of an analogue quantity in each nodal point are accepted as unknowns and are the subjects to be defined;
- 3) the volume is divided into a finite number of the elements, having the common nodal points, which approximate the shape of the area in total (Fig. 3.25);
- 4) the analogue quantity is approximated on each element by some polynomial;
- 5) the solving system of the algebraic equations, presenting some condition, is made;
- 6) the received set of equations is solved by one of the known ways, the state variables are defined.

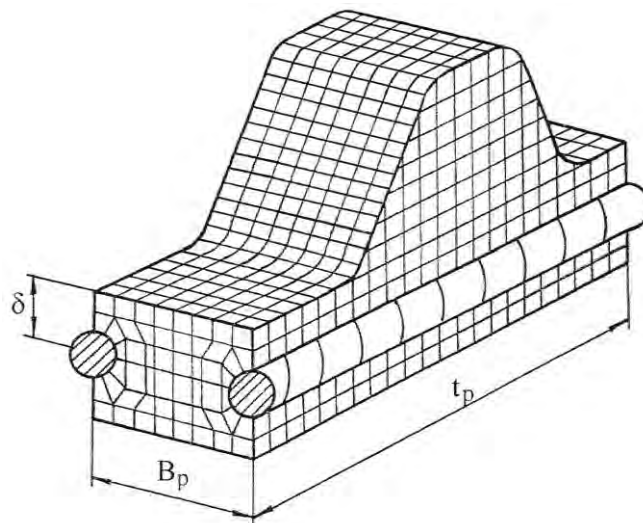


Fig. 3.25. Spatial finite-element model of a tooth of a belt

However, the method of the finite number of the elements, based on the principle of minimization of the potential energy for nearly incompressible materials, is approximate.

The above variation principles, used for the research of the stress-strained state of rubber (rubber-like) materials, with all their merits, are substantially worse than modern soft-hardware methods of modeling of loading of various designs and machines.

3.6. Hardware-software modeling of the stress-strained state

For the research of the mechanical and physical processes, occurring in gearing, the definition of the influence of the parameters of transmission on its reliability and durability, the development of the recommendations on the increase of its technical level, the complex of the computer finite-element modeling of the stress-strained state of toothed-belt transmissions in *ANSYS* [115] is fulfilled.

At modeling the concept of non-linear mechanics of continuum, the non-linear theory of thixotropic visco-elasticity, adhesive, cohesive, highly elastic and elastic-hysteresis properties of anisotropic visco-elastic systems, the principle of Mooney-Rivlin, the experimental diagrams of tension-compression of polymeric materials [43, 45, 46, 116, 117] are used.

It is known [118, 119, 120], polymeric materials and the details of engineering application, made on their basis, are visco-elastic systems and follow the fundamental laws of mechanics (Hooke, Newton, etc.) at infinitesimal speeds of the deformation. In addition, the stresses, arising in the volume of the given materials, depend not only on the value of the applied loading and also on its type, the speed of change and duration of the operation. Alongside with it, the polymeric materials display significant rheological and relaxation properties [121, 122, 123], manifested in lowering of stresses at the constant loading.

The toothed belt at the power transmission is affected by a complex of dynamic shock loadings, causing the constant change of its stress-strained state. It predetermines the intensity of the course of the destructive phenomena, leading to the loss of the workable condition and defining the load carrying capacity and durability of transmission. The researches of the stress- strained state of polymeric materials and the details of engineering application made of these materials by strain-gauge and polarization-optical methods [43, 44, 66, 124] were conducted with the tolerances and limitations, which did not allow to receive the results with the high accuracy. Besides, the quantity of defining factors and the levels of their variation are restricted, because of their high cost, complexity and the length of the experiment.

In Fig. 3.26 the developed finite-element model of a toothed-belt gearing [125] is presented. The total amount of elements is 2811 pieces. Rubber is modeled by the elements

hyper74 (1352 pieces), the toothed pulley is modeled by the elements *plane 82* (758 pieces), the bearing layer is modeled by the elements *link1* (356 pieces). The contact of teeth in gearing is modeled by the elements *target169* on the pulley (162 pieces) and *conta172* on the belt (183 pieces).

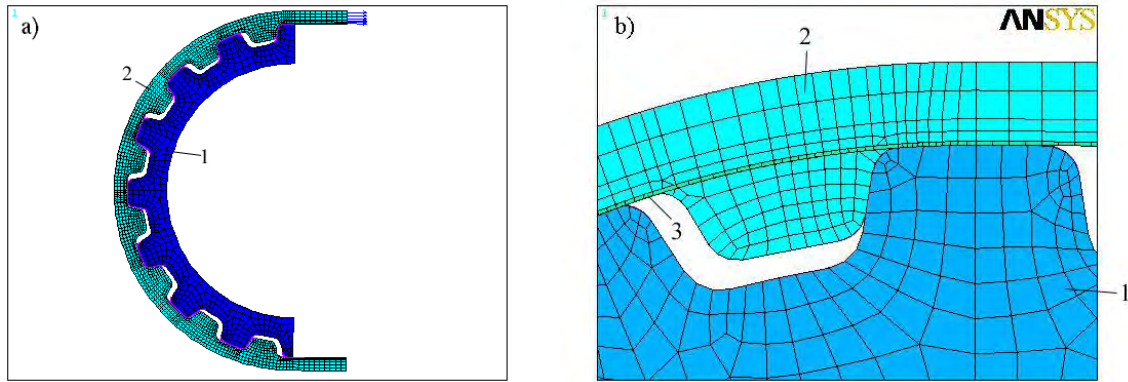


Fig. 3.26. Finite-element model of a toothed-belt gearing: a) arc of contact of a drive pulley; b) fragment of the arc of contact; 1 – pulley; 2 – belt; 3 – bearing layer

In Fig. 3.27, 3.28 the distribution of the main stress σ_1 and contact pressure in gearing of teeth on the arc of contact is shown. The maximum stress and pressure, distributed along the arc of contact, is non-uniform. Their concentration is observed in the zone of transition of a lateral surface of a tooth to the interdental space, i.e. in the area of the origination of a fatigue crack.

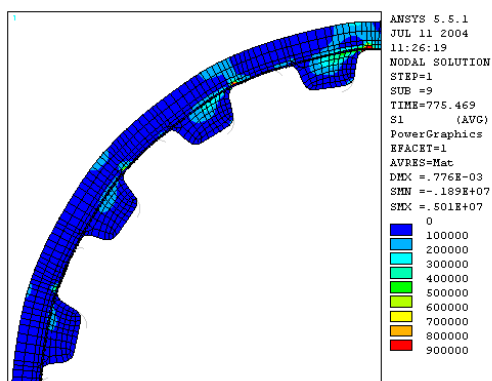


Fig. 3.27. Distribution of tension stress

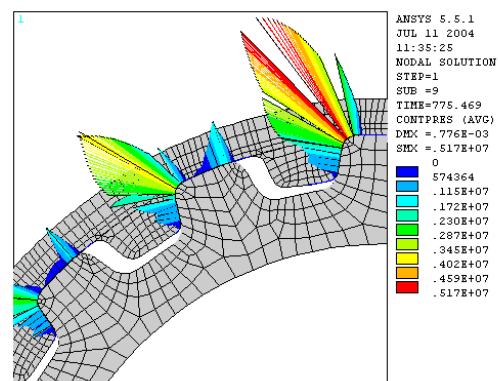


Fig. 3.28. Distribution of contact pressure

The first tooth from the driving side of a belt is the most loaded one (Fig. 3.29, 3.30).

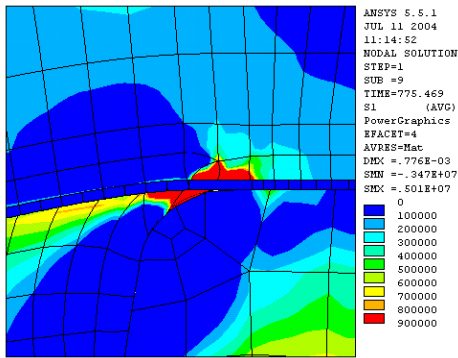


Fig. 3.29. Distribution of stresses

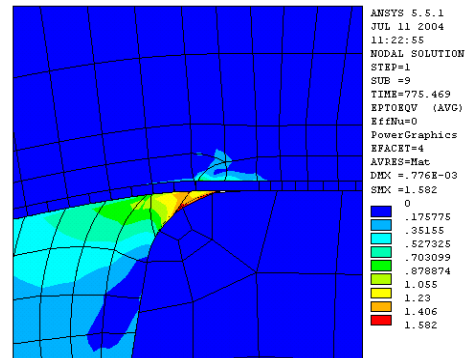


Fig. 3.30. Mises' deformations

In Fig. 3.31–3.38 the results of the finite-element computer modeling of the stress-strained state of the drive toothed belt of a **trapezoidal** profile with a step of teeth 12.57 mm ($m = 4$ mm) are presented. A belt is stretched from left to right by the force 8.0 κN . The bearing layer of the belt is considered to be inextensible. For the fixed position of the belt along the bearing layer the vertical displacements are forbidden. The pulley is considered to be motionless and absolutely rigid. The friction factor in the contact is $f = 0.5$. The material of the belt is modeled by Mooney-Rivlin's principle. The module of the elasticity of polymer is $E = 5$ MPa, Poisson's factor is $\mu = 0.499$.

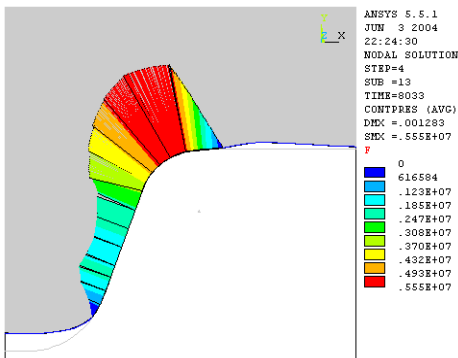


Fig. 3.31. Distribution of contact pressure

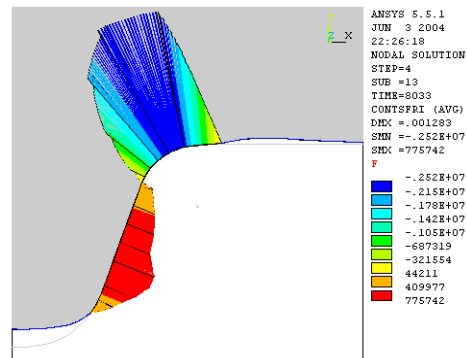


Fig. 3.32. Distribution of frictional stress

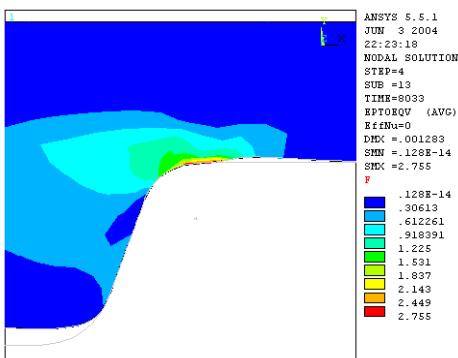


Fig. 3.33. Mises' deformations

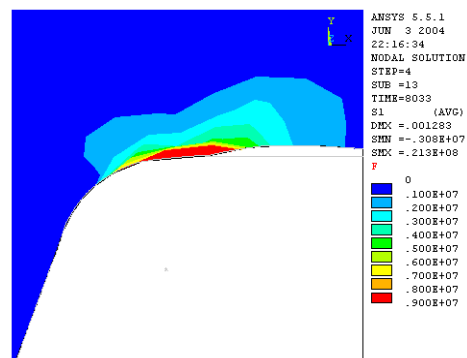


Fig. 3.34. Distribution of stresses

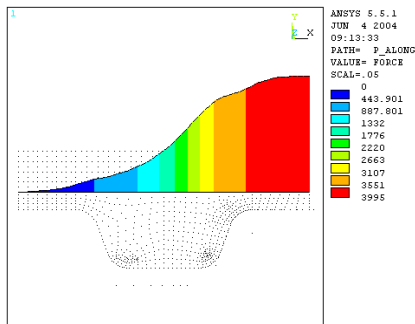


Fig. 3.35. Distribution of an effort in a bearing layer on the length of one step of teeth

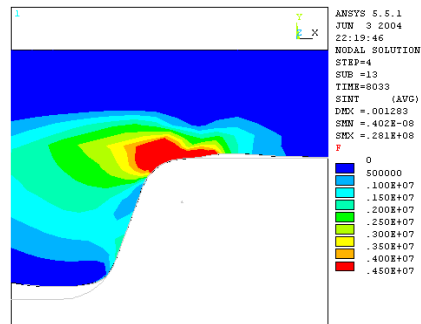


Fig. 3.36. Intensity of stresses in a belt material

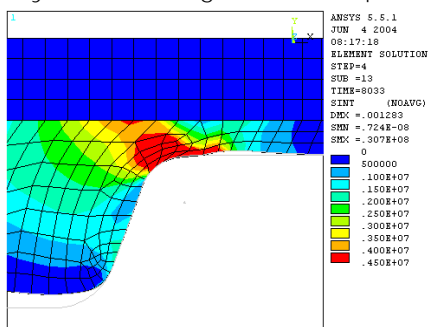


Fig. 3.37. Intensity of stresses in a belt material

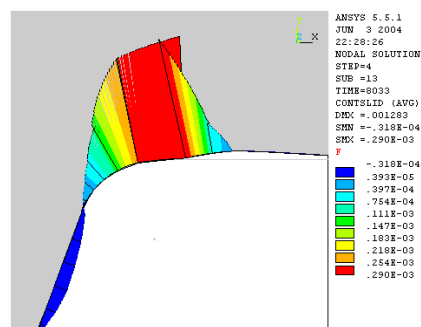


Fig. 3.38. Mutual sliding of profiles of teeth

In Fig. 3.39–3.44 the results of the finite-element computer modeling of the stress-strained state of the drive-toothed belt of the semicircular profile *HTD* with a step of teeth 14 mm are presented.

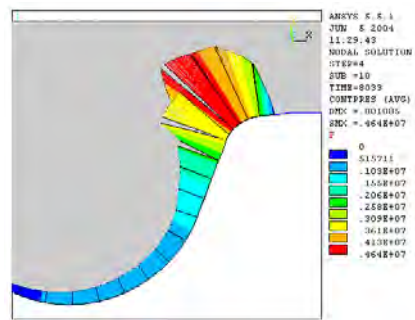


Fig. 3.39. Distribution of contact pressure

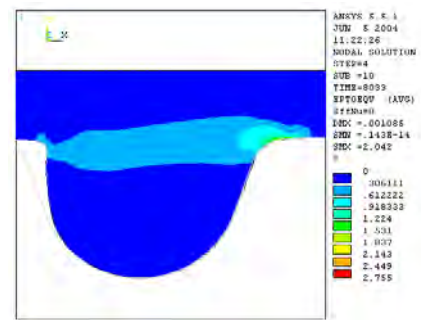


Fig. 3.40. Mises' deformations

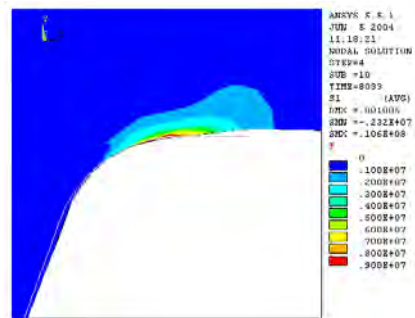


Fig. 3.41. Distribution of stresses in a belt material

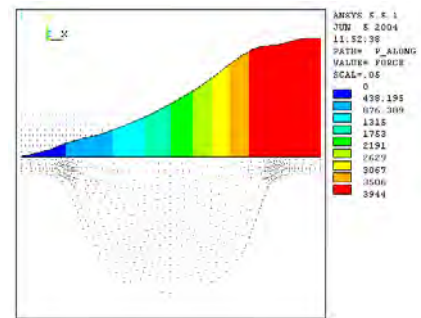


Fig. 3.42. Distribution of effort in a bearing layer

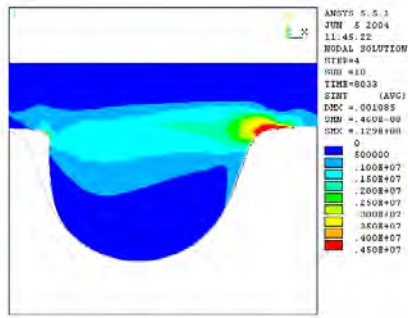


Fig. 3.43. Intensity of stresses in a belt material

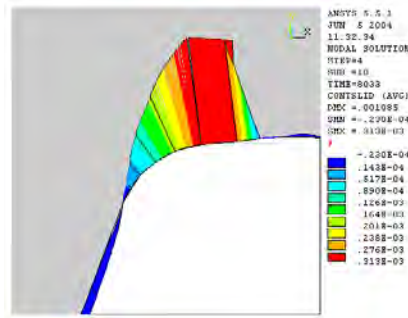


Fig. 3.44. Mutual sliding of profiles of teeth

The comparison of the results of modeling of the stress-strained state of teeth of trapezoidal and semicircular profiles, allows to make a conclusion: a semicircular profile of a tooth is more preferable. The smaller values of stresses, deformations, contact pressure and the relative sliding velocity of profiles of teeth at an input in gearing are available. It is due to the lowered profile interference of semicircular teeth in comparison with trapezoidal ones. Hence, the belts with a semicircular profile possess the higher level of load carrying capacity and durability.

In Fig. 3.45–3.49 the results of the research of the influence of a bearing layer on the stress-strained state of drive-toothed belts are presented [126].

The toothed belt with the profile *HTD*, a tooth step $t_p = 14$ mm, a specific pull $F_t = 3.2$ N/mm, applied longitudinally (horizontally), is accepted as the object of the researches. In the line of a bearing layer the lateral (vertical) restraint is lapped. The belt cannot rise up or go down. The bearing layer is accepted to be absolutely flexible laterally, but absolutely rigid longitudinally.

The solution of the problem is carried out in a flat position for a pulley of the infinitely big radius. One tooth of a belt and one interdental space of a pulley are examined. The pulley is accepted as absolutely rigid and motionless. The factor of friction between a belt and a pulley is $f_{fs} = 0.5$. Both the elastic deformation of a belt tooth and the contact interaction of a belt and a pulley are modeled. The problems are solved in the static position.

In Fig. 3.45 the distribution of the maximum main stress σ_1 (maximum tension stress) on a belt tooth in the presence of a bearing layer (cord) is presented. The cord distributes the pull along the rubber part of a belt tooth. The moderate concentration of stresses on the radius of rounding of the tooth basis is observed. The maximum level is $\sigma_1 = 1.47$ MPa.

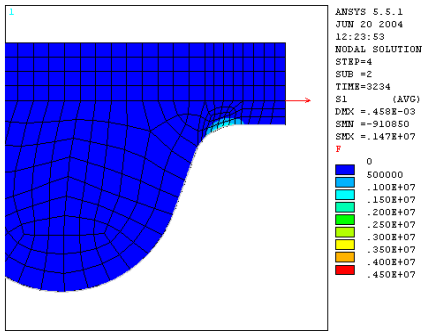


Fig. 3.45. Distribution of stresses in the presence of a bearing layer

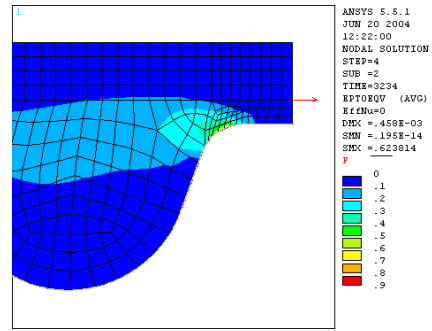


Fig. 3.46. Intensity of deformations in the presence of a bearing layer

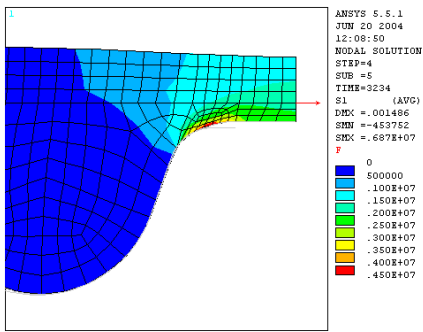


Fig. 3.47. Distribution of stresses in the absence of a bearing layer

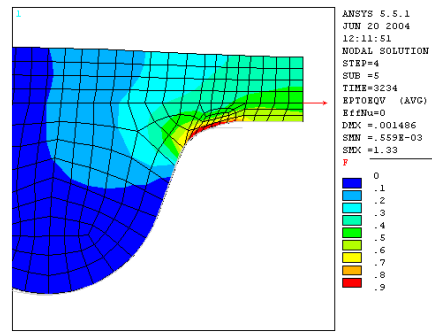


Fig. 3.48. Intensity of deformations in the absence of a bearing layer

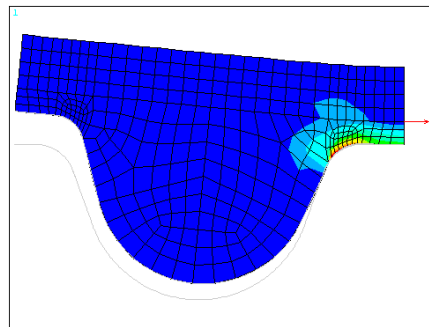


Fig. 3.49. Loss of gearing of a toothed belt with a pulley

The displacement of the right end face of a belt under the loading makes $s = 0.458$ mm, the intensity of the deformation ϵ_i (**Mises' deformation**) is also maximum on the radius of rounding of the tooth basis and it makes $\epsilon_i = 0.624$ (on the true scale; it is equivalent to 189 %) (see Fig. 3.46).

At the cord removal from a rubber part of a belt tooth the stress and deformation rise sharply. The pull from a pulley to a belt is transferred only by rubber. In Fig. 3.47 the **corresponding distribution** σ_1 is presented. The tension stresses reach the level of 6.87 MPa (increase 4.67 times). The deformation of the belt becomes visually appreciable. The dis-

placement of the right end face reaches 1.49 mm (increase 3.25 times), the intensity of the deformation reaches $\epsilon_j = 1.33$ (390 %). It increases 2.13 times (see Fig. 3.48).

The stresses and deformations in all the cases concentrate on the radius of rounding of the basis of a tooth. The comparison of the solutions shows that the existence of the cord reduces the level of stresses and deformations, arising in the body of a belt tooth at the power transmission, several times. It causes the corresponding increase in the belt durability.

The behavior of the belt in the absence of prohibition on the vertical displacement of the cord is examined (see Fig.3.49). At the pull $F_1 = 0.2$ N/mm the loss of gearing of a belt tooth with a pulley tooth takes place. On the basis of this research it is possible to define the best value of the preliminary stress of the belt, limiting the vertical displacement of the bearing layer.

The influence of a high-speed operating mode of transmission on loading of the belt bearing layer and the contact pressure in gearing of the teeth is investigated (Fig. 3.50, 3.51).

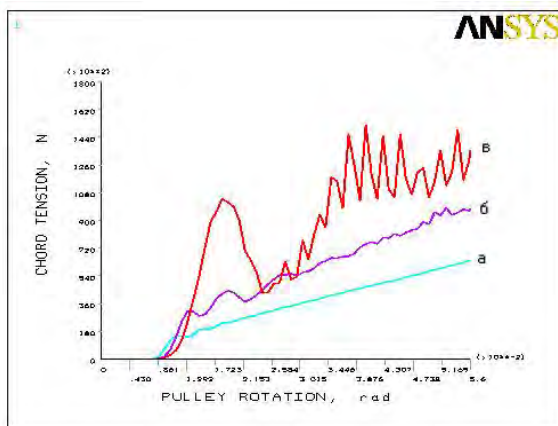


Fig. 3.50. Dependence of loading of the bearing layer of a toothed belt at an input in gearing from the frequency of rotation of a drive pulley: $n_1 = 170 \text{ min}^{-1}$; $n_1 = 550 \text{ min}^{-1}$; $n_1 = 1700 \text{ min}^{-1}$

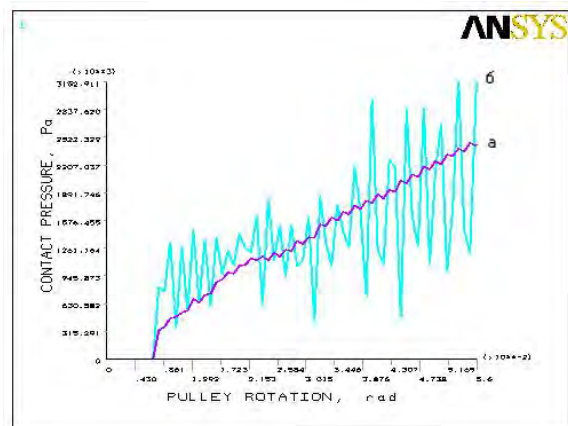


Fig. 3.51. Dependence of contact pressure at an input in gearing from the frequency of rotation of a drive pulley: $n_1 = 170 \text{ min}^{-1}$; $n_1 = 1700 \text{ min}^{-1}$

The analysis of the above-stated dependences shows that the non-linear increase of both loading of a bearing layer and the pressure in the contact of teeth along with the increase in the speed of a belt is observed. It is connected with the non-linear change of mechanical and physical properties of the elements of toothed belts at the increase in the belt speed. The received dependences are adequate to the developed theoretical dependences and experimental data.

Thus, the carried out researches allow to estimate the stress-strained state of toothed-belt transmissions; to develop the recommendations for the choice of a design, geometrical and operational parameters of transmission, the materials of elements of a toothed belt, promoting the lowering of stresses and deformations and, as a result, the substantial increase of load carrying capacity and durability of toothed-belt transmissions.

The computer modeling, which results are adequate to the theoretical development and experimental data, allows coming to a qualitatively new level of designing of toothed-belt transmissions with the improved technical characteristics.

3.7. Experimental research of the dynamic rigidity and the factor of damping of vibrations of a toothed-belt transmission

At the research of the dynamics of a toothed-belt transmission it is necessary to have the values of mechanical characteristics at the dynamic modes of loading. The researches of a toothed-belt transmission at a static mode of loading [127] and also the definition of its dynamic rigidity and the factor of damping by the method of free damped vibrations at the equal tension of belt sides [128] do not reflect the valid work of transmission. The offered technique with the use of the forced resonant vibrations allows setting up the stated characteristics for a case of a real loading of a belt.

The basic scheme of the stand is presented in Fig. 3.52, a. The forced torsion vibrations of pulleys of a toothed-belt transmission are created by the cam-driven generator. The eccentricity of a cam is 0.5...1.0 mm at the length of the lever 350 mm. For the stabilization of the frequency of generated vibrations the drive with a magnetic amplifier PMU 6P-1A is used.

The examined transmission and the generator of torsion vibrations have the vibration isolation from the plate of the stand. One pulley of a toothed-belt transmission is rigidly slow-downed on a support, another one is connected with a flywheel, receives the variable torque from the vibration generator through the flange coupling and change torsion shaft 2.

The variable values of the moment of inertia of the vibration system J are received, changing the mass of the flywheel. The own frequency of the vibration system is changed, using the torsion shafts of the various rigidity.

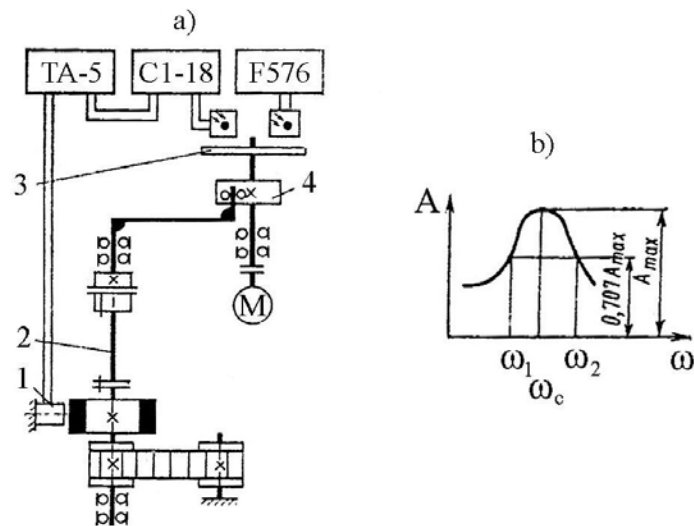


Fig. 3.52. Scheme of the stand for the determination of the dynamic rigidity and the factor of damping of vibrations in a toothed-belt transmission (a) and the general view of an amplitude-frequency characteristic (AFC) (b)

For the fixation of the shear of phases of the vibration system and the generator, and also the frequency of generated vibrations two photo elements and a disk 3, fixed on the axis of the generator, are used. Through the apertures in a disk the first photo element sets a signal on the digital frequency meter **F-576** for the determination of the frequency of vibrations, and the second element sets the signal on the first channel of the two-beam oscillograph **C1-18**. The disk is fixed on the shaft in such a way that the hole for the second photo element is opposite to the certain point, corresponding to the maximum radius of the cam 4.

For the determination of torsion vibrations of a flywheel the wire strain gauges, pasted on the elastic beam 1, are used. The first end of the beam is closed rigidly and the other one makes vibrations together with the flywheel. The signal is transmitted to the amplifier **TA-5**, and then to the second channel of the oscillograph **C1-18**. The kind of the signal confirms the harmonious character of the raised vibrations.

The preliminary tension of the belt is adjusted by screws; the set preliminary tension is controlled along the bending deflection of a belt under the action of the effort. The loading by the moment is carried out by the demountable lever and the load. The difference of tension of the transmission sides is provided with the elastic deformation of the torsion shaft.

The relative amplitude of the torsion vibrations of the flywheel is displayed on the screen of the oscillograph. At the shear of phases by $\pi / 2$ the resonance of the torsion vi-

brations is observed. Measuring consistently relative amplitude at the corresponding circular frequency of the generator, the amplitude-frequency characteristic (AFC) is determined.

The calculation dependences are presented for one-mass vibration system. At the linear dependence between the elastic force and the deformation the equation of the forced angular vibrations of the flywheel looks like [129]:

$$J\varphi'' + \xi\varphi' + c_{all}\varphi = c_s\delta_t,$$

where c_s and c_{all} – torsion rigidity of the torque shaft and the whole system; ξ – the factor of damping of vibrations in a toothed-belt transmission; δ_t – the law of the displacement of the end of the torque shaft; $c_s\delta_t$ – the law of change of the exciting force; φ – the angle of deflection of the flywheel.

The solution of this equation with the known value of frequency of its free vibrations ω_c allows defining the dynamic rigidity of a toothed-belt transmission:

$$c = J\omega_c^2 - c_s.$$

It is possible to consider the moment of inertia of the vibration system equal to the moment of inertia of the flywheel $J = 1.1 \text{ N}\cdot\text{m}\cdot\text{s}^2$, since the moments of inertia of other details of the stand are negligible. The torsion rigidity of the torque shaft is $c_s = 780 \text{ Nm/rad}$.

The damping in the torque shaft can be neglected as it is less than the damping in a toothed-belt transmission. By relative AFC we define Q-quality of the vibration system, which is equal to the ratio of the free circular frequency to the width of a resonant curve at the amplitude $0,707A_{\max}$. Comparing the received value of Q-quality with its value, expressed by the ratio of inertial reactive impedance on the resonant frequency to the loss resistance, we receive the calculation formula for the factor of damping:

$$\xi = J \omega_2 - \omega_1 ,$$

where ω_1 and ω_2 – see Fig. 3.52, b.

Thus, for the calculations it is necessary to know only the kind of a resonant curve, which allows lowering of the labor content of the experiment, having excluded the calibration of the flywheel absolute deflection. At the change of the frequency of free vibrations

of the system, which is received by the various combinations of the values J and c_s , we get AFC, showing the insignificant non-linearity of the vibration system.

Investigating the dynamic characteristics of a toothed-belt transmission, two maxima AFC are observed. The first maximum corresponds to the shear of the phases by $\pi / 2$, the second maximum appears at the exciting vibrations, which circular frequency is twice less than the circular frequency of the first maximum AFC (at that, shear of the phases is approximate to zero). During this moment the intensive lateral vibrations of the following side of a belt are observed. The calculation of the dynamic characteristics is made, using the first maximum AFC.

The significant difference of partial frequencies of torsion vibrations of pulleys of transmission and lateral vibrations of belt sides is confirmed experimentally. The dynamic characteristics of a toothed-belt transmission of the machine tools of the models 1D340 and 1P416F3 ($z_{\text{ш}} = 20$ and 22; module $m = 5$ mm, $B_p = 50$ mm, $z_p = 71$) are investigated on the stand.

The dependences of the dynamic rigidity and the factor of damping of a toothed-belt transmission from the preliminary tension of a belt are presented in Fig. 3.53. The graphs show that the dynamic rigidity of the toothed-belt transmission, used in the machine tools of the models 1D340 and 1P416F3, averages $c = 2...3.5 \cdot 10^4$ Nm/rad, and the factor of damping is $\xi = 2.5...4.5$ Nms/rad. The static rigidity of transmission is $c_{st} = 1$ Nm/rad.

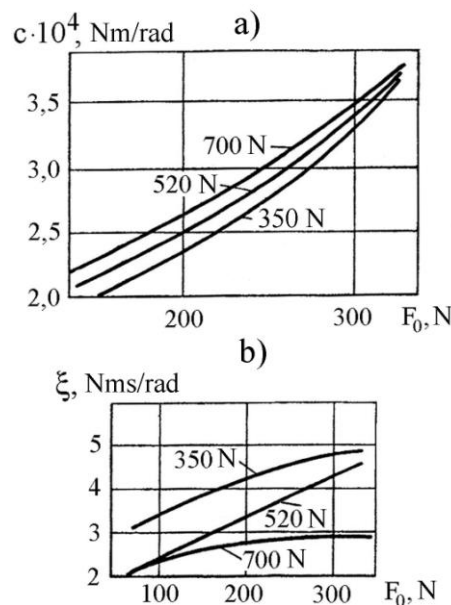


Fig. 3.53. Dependences of the dynamic rigidity c (a) and the factor of damping ξ (b) of a toothed-belt transmission of the preliminary tension of a belt F_0 at various values of a pull F_t

The moment of inertia of a drive of the machine tool can be modeled on the stand, changing the moment of inertia of a flywheel for the determination of resonant frequencies of a drive.

The analysis of the received dependences testifies that with the increase in a preliminary tension of a belt the dynamic rigidity and the factor of damping of vibrations increase. Hence, the unfounded increase in a preliminary tension of a belt leads to the increase in the internal losses and decrease in the efficiency of transmission. In the work [53] the similar conclusion at the research of efficiency of a toothed-belt transmission was received. At the same time both the increase in the dynamic rigidity with the reduction of the factor of damping and the growth of the pull in transmission at the constant preliminary tension take place.

The change of the length of a toothed belt influences its dynamic characteristics. At the research of two belts $B_p = 40$ mm in width with a number of teeth $z_p = 78$ and 154 it is established that the value of the dynamic rigidity (in relation to a step) for a longer belt increases 1.5 times [130].

3.8. Conclusions

1. The research of loading of a multiple toothed-belt gearing by the method of the finite differences testifies that the distribution of the loading corresponds to the discrete scheme.

2. At the research of loading of gearing it is necessary to consider the change of the factor of the overlap ε_α in the process of various phases of gearing and transmission of a part of power by the teeth, which are in the zone of the incomplete profile gearing.

3. As a result of the carried out researches of loading of the multiple toothed-belt gearing by the method of the finite differences the dependences of the distribution of transferred loading on teeth from the main parameters of transmission, the conditions of gearing and mechanical and physical properties of a toothed belt have been received. It has been established that in the most effective methodical way of control of non-uniformity of loading of gearing and, as a consequence, of the improvement of load carrying capacity and durability of toothed-belt transmissions, is the correlation adjustment of the step of pulley teeth.

4. The physico-mathematical model of the multiple toothed-belt gearing has been developed. It allows to define its dynamic loading, depending on the main parameters of transmission and mechanical and physical properties of a belt. The system of the differential equations, describing the distribution of the loading in gearing, has been solved by the numerical method. The solution is presented in the form of the graphic dependences, having a harmonious profile with the local extrema, which corresponds to the experimental curves, received on the developed stand by the method of oscillometry. The divergence of the results does not exceed 10 %, which confirms the adequacy of the model to the mechanical and physical processes, occurring in gearing.

5. The complex of the theoretical and computer finite-element modeling of the stress-strained state of toothed-belt transmissions in *ANSYS* has been lead. The results of modeling have shown the adequacy of the developed theoretical theses to the carried out experimental researches. It allows providing of a qualitatively new level of designing of the toothed-belt transmissions, characterized by the high accuracy and the lowered labor costs.

6. The experimental research of the dynamic rigidity and the factor of damping of vibrations of a toothed-belt transmission have been carried out on the developed stand. It has been established that with the increase in a preliminary tension of a belt the dynamic rigidity and the factor of damping of vibrations increase. Hence, the unfounded increase in a preliminary tension of a belt leads to the increase in the internal losses and the decrease in the efficiency of transmission. At the same time both the increase in the dynamic rigidity with the reduction of the factor of damping and the growth of the pull in transmission at the constant preliminary tension take place. The increase in the length of the toothed belt leads to the significant increase in its dynamic rigidity.

Chapter 4. DESIGN-ENGINEERING METHODS OF THE IMPROVEMENT OF THE TECHNICAL LEVEL OF TRANSMISSIONS OF POWER BY FLEXIBLE LINK

4.1. Energy and resource saving ecologically-safe technology of drive toothed belts

The basic aspects of the technology of drive toothed belts are widely presented in the works [131, 132, 133]. It should be noted that the manufacturing techniques include the following complexes of the working operations:

- assembly of a blank of a belt on a sprocket drum, using cord, fabric and unvulcanized elastic materials;
- vulcanization of blanks under heat and pressure;
- blank cutting (rolled-up stock) into separate belts;
- quality control of belts.

The assembly of blanks of locked belts consists in placing of one or several layers of facing fabric on an assembly profile drum, coiling of a cord thread in the helical line, laying and rolling on the necessary quantity of elastomer. The fabric, put on an assembly drum, looks like a cylindrical sleeve, sewed or stuck together on the moving line.

The operation of a cord coiling is the most important thing at this engineering stage. The uniformity of loading of separate coils of a cord and the load carrying capacity of a belt mostly depend on the quality of its fulfillment. The uniformity of a cord coiling is provided by two requirements: the constants of a step and tension of coiling. The stable step of coiling is provided with the application of one or several rollers for directing of a cord. **The clearance between a roller and an assembly drum should be minimal (2...10 mm).**

The set effort of tension is provided by means of brake mechanisms, influencing the spool with a cord. The tension of the cord is supported by the constant periodic of the braking torque, carried out by hand.

At coiling of a cord thread on the assembly drum the additional spinning or spinning away take place. As a result, the step of a thread coiling changes. The belts with the metal cord, received an additional twisting, deform inadvertently in a free state, getting "eight-fold twisting". The operation of such belts in transmission is accompanied by their intensive friction on rims. For the elimination of this phenomenon the assembly machine tool is equipped with an extra attachment, which carries out the rotation of a unit of fas-

tening of the spool together with the spool to the side, which is opposite to the direction of the rotation of the assembly drum [134].

After cutting of a rolled-up stock there are certain difficulties with sealing of the ends of a belt of a cord. The problem is very actual for the belts with a metal cord, which ends can cause traumas and damage the details of transmission. The simplest way of the elimination of such a phenomenon consists in giving of the larger angle of coiling to a cord thread in the places of the future cutting. Such coiling is carried out by means of the additional support, placed on the basic support of the assembly machine tool and bearing a roller for the direction of a cord. The interrupted motion is given to the additional support, therefore in the places of the future cutting of a rolled-up stock the speeds of both supports are summed up. As a result, the deflection angle of spirals of the cord increases. The additional support is motionless relating to the basic support in the places of usual coiling [135].

The vulcanization of drive belts is carried out in autoclaves. Such a method of vulcanization is specific for lengthy (up to 3150 mm) toothed belts. The longer belts are vulcanized in open-side presses or in the vulcanizers of the periodic action, carrying out the vulcanization of a belt by parts.

The toothed belts of a small length without fabric facing are made by the method of molding in moulds with hydraulic presses with flat heated plattens.

The method of molding consists in coiling of a cord on a sprocket drum and the installation of the drum in the heated mould. (Fig. 4.1).

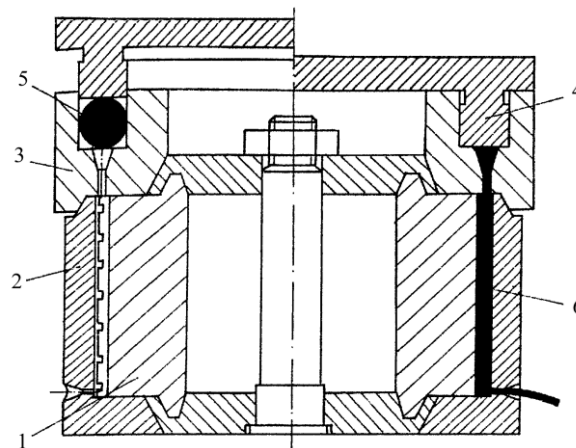


Fig. 4.1. Scheme of a mould for molding of toothed belts: 1 – sprocket drum; 2 – frame; 3 – cylinder; 4 – piston; 5 – raw compound; 6 – blanks of belts

The mould is closed by the cylinder, the toroidal fragment of raw rubber is put into the circular groove, and the piston is established. The mould is placed between flat heated

plattens of the hydraulic press. At the rapprochement of the plattens raw rubber fills the form, forming the body of a blank of a belt. After the process of vulcanization the plattens of the press are separated, the mould is taken out, and an internal sprocket drum is pressed out together with a blank. The drum is taken out in parts from the blank, which is cut into separate belts.

Mould belts are characterized by the exact sizes and a high quality of surfaces, since they are formed by the precisely and qualitatively processed surfaces of a mould. The high pressures of pressing (15...25 MPa) provide dense structure of belts, the absence of pores, holes, etc. For these reasons a cord of mould belts possesses the raised adhesion to elastomer. The lack of the method is the impossibility of getting of a wear resistant fabric coating of teeth, **that's why mould belts are made, as a rule, of polyurethane, that is 3...10 times more expensive than chloroprene rubbers, mostly used for manufacturing of toothed belts.**

Pressing in a diaphragm autoclave provides producing of toothed belts with a wear resistant fabric facing of teeth due to the uniform drafting of a rubber blank on a sprocket drum. **The durability of such belts exceeds the durability of the similar mould belts 5...7 times.** The blank, consisting of the layers of facing fabric, consequently put on a drum, a cord and a raw compound in a sheet form, is put into the operating zone of an autoclave (Fig. 4.2). The zone represents a curing bag, located inside the massive frame, consisting of an external steel cylinder and an internal elastic rubber diaphragm.

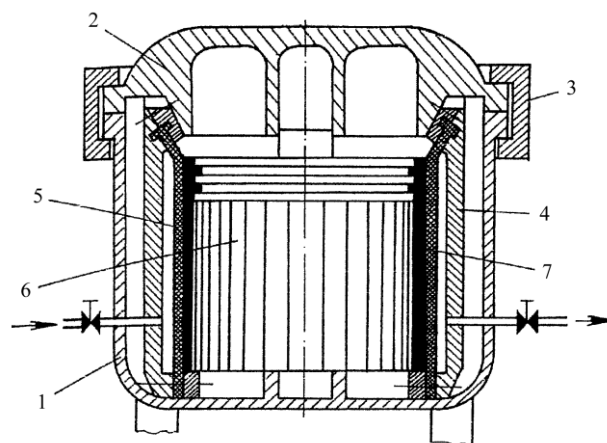


Fig. 4.2. Scheme of an autoclave for manufacturing assembly belts: 1 – frame; 2 – cover; 3 – shutter; 4 – curing bag; 5 – diaphragm; 6 – sprocket drum; 7 – blank

The diaphragm looks like a rubberized-fabric pipe with flanges and its thickness is 5...12 mm. The over-heated steam is moved into the space between a wall of the cylinder

and a diaphragm. The steam has the temperature of vulcanization of a blank and the pressure 0.6...1.5 MPa. The diaphragm drafts and uniformly covers and presses the blank on the sprocket drum. After the process of vulcanization the drum with the blank is taken out of an autoclave, the blank is taken off and cut into separate belts.

At the same time the technology of vulcanization in an autoclave has its demerits, which do not allow realizing the maximum durability of the produced belts. First of all, it is connected with the low pressures of pressing in comparison with the method of molding.

The low pressures of pressing cause the low parameters of durability of adhesion of a cord to elastomer, the presence of porosity, holes, etc. in a finished article. At the use of rigid rubbers poor-quality pressing of the profile of teeth is frequently observed. Beside, pressing in an autoclave is carried out by the flexible pressing element – the rubber-cord diaphragm. The presence of the non-rigid pressing element does not allow receiving of the **demanded thickness of belts, that's why they should be ground off.**

The new progressive highly effective technology of producing of drive toothed belts [136] has been developed. The technology is based on the pressing of a blank of a belt by rigid elements (PRE), synchronously approaching in a radial direction. The flow of a vulcanized elastomer in a radial direction provides the qualitative implementation of the process of fabric facing on a working surface of a belt, excluding the formation of folds. The presence of rigid elements (sectors) allows to receive the belts of the pre-set thickness with the demanded quality of surfaces just in the mould. The method does not demand power-intensive autoclaves and it is carried out in the hydraulic vulcanization presses with heated plattens.

The equipment for manufacturing of belts by the method of PRE represents a mould with a vertical axis of rotation (Fig. 4.3).

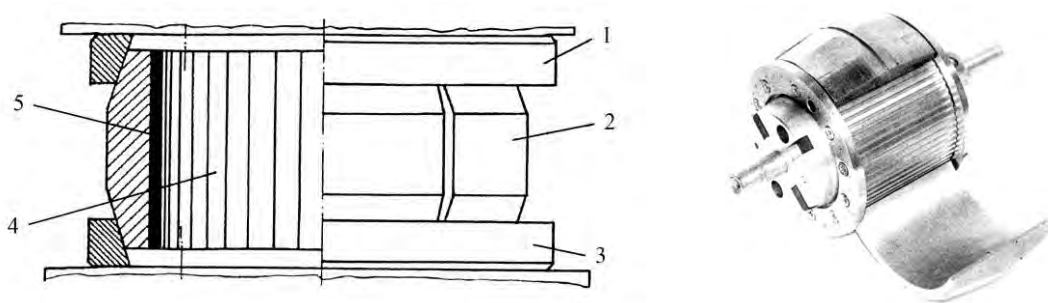


Fig. 4.3. Scheme and physical form of a sector mould for manufacturing of toothed belts:
1, 3 – top and bottom of cones; 2 – sector; 4 – gear core; 5 – blank of belt

Let's consider the operation process of such a mould. At the removed top cone 1 and the sectors 2 the gear core 4 with a blank of a belt 5, consisting of facing fabric, a bearing layer and non-vulcanized rubber, is installed into the bottom cone 3 and is preliminary centered. Then in the bottom cone 3 the set of sectors 2 is established and covered with the top cone 1. At the vertical compression of cones 1 and 3 the sectors 2 approach, pressing the blank on the core. The pressure in the mould is 20...25 MPa.

The carried out experimental researches on the stand equipment (the belt breaking strength; the resistance of the belt tooth to the shear; the strength of adhesive links; the resource) showed that the application of the method of PRE allows providing high parameters of mechanical and physical properties of a belt [137]. It leads to the improvement of the load carrying capacity and the operational resource of drive toothed belts.

Thus, the developed technology of drive toothed belts has the following advantages:

- 1) raised transferred power and durability of toothed belts in comparison with mould and autoclave analogues;
- 2) application of the unified equipment and the absence of finishing operations;
- 3) raised productivity in view of the absence of finishing operations of the backing-off surface of a belt;
- 4) minimization of industrial wastes due to the application of hydraulic presses instead of autoclaves and the absence of the grinding equipment;
- 5) raised ecological cleanliness of manufacture due to minimization of technological waste and exclusion of formation of a rubber dust;
- 6) high (up to 95 %) operating ratio of the basic materials;
- 7) low specific energy intensity of the technological process.

The disadvantages of the method are the following:

- 1) limited length of belts, defined by the dimensions of a mould and a working zone of the technological equipment;
- 2) low mechanization and automation of the technological process.

Some equipment modifications have been developed. It allows to automate manufacturing techniques, to improve the quality of products and simplify the design and manufacturing techniques of the details of moulds.

The analysis of the process of pressing of belts in the sector moulds shows that filling of shape-generating grooves of equipment is carried out not only due to the mechanical movement of the plastic rubber mass by means of the sectors. Heating of the vulcanized

mass is accompanied by its nonreversible thermal expansion up to 5...12 %. Thus, filling of the mould takes place due to the increase in the volume of a vulcanizate, which allows to create the progressive designs of the equipment, where the displacement of the sectors corresponds to the radial direction, and a shape-generating groove pressurizes at the closed-ended pressing elements.

The given equipment has a horizontal axis of the gear core and two pressing sectors (Fig. 4.4). For the realization of the operating cycle the gear core 1 with a pre-assembled blank 2 is located into the bottom half-mould 3, where it is centered on the flange 4. The core is covered with the same top half-mould and is placed between the plattens of the press. At the approach of the plattens the half-moulds also approach up to the contact, closing the blank of a belt in a shape-generating groove of a mould. For preventing of the heavy pressure in a mould the scraps of a rubber mixture run out into the orifice hole 5 by the diameter 0.2...1 mm or into flaps [138].

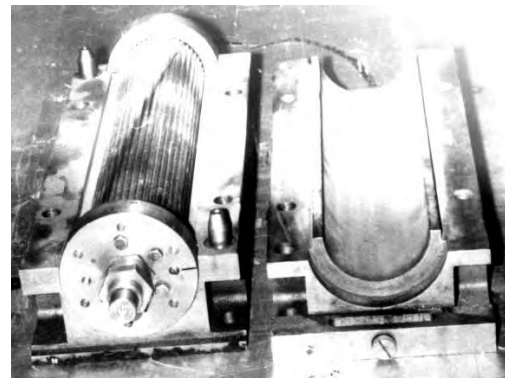
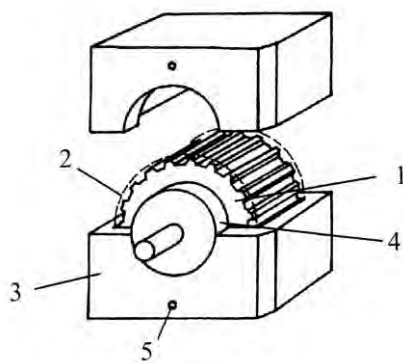


Fig. 4.4. Scheme and physical form of a horizontal mould:

1 – gear core; 2 – blank of belt; 3 – half-mould; 4 – flange; 5 – orifice hole

One of the ways of updating of the equipment consists in giving universal properties to it. To avoid manufacturing of expensive sets of moulds for the belts of about the same sizes, one unified frame of two sectors, equipped with a set of gear cores for each of the standard sizes of belts and the set of the changeable elastic sleeves of the identical diameter, is manufactured. The internal surface of the sleeve performs shape-generating functions, the external one interacts with the internal boring of the sectors (Fig. 4.5) [139].

The progressive design of a mould for manufacturing of the double-sided toothed belts, characterized by the raised reliability of work and the quality of products, is developed (Fig. 4.6) [140].

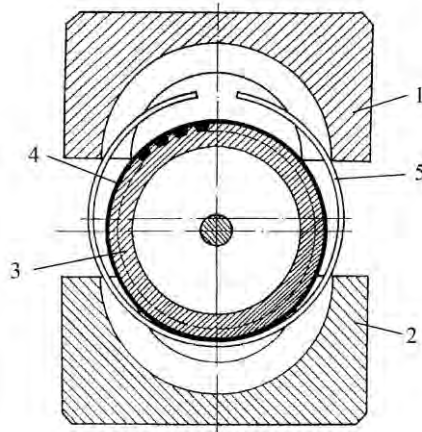


Fig. 4.5. Universal mould for manufacturing of toothed belts: 1,2 – top and bottom half-moulds; 3 – gear core; 4 – blank of belt; 5 – elastic sleeve

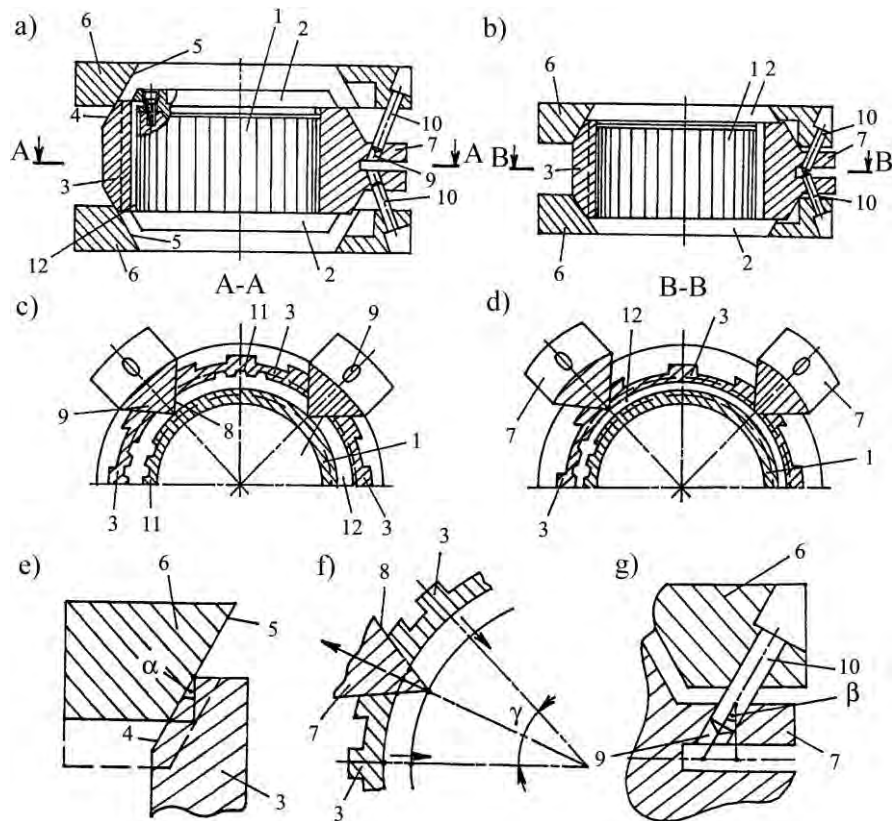


Fig. 4.6. Mould for manufacturing of double-sided toothed belts: a) general view of a mould, a longitudinal section along a plane of symmetry in an initial phase of pressing; b) the same in the final phase of pressing; c) the same, the section A-A; d) the same, the section B-B; e) scheme of interaction of the mechanism of radial movement with the sectors of the first group; f) scheme of interaction of the sectors of the first and second groups; g) scheme of interaction of the mechanism of radial movement with the sectors of the second group; 1 – sprocket drum; 2 – aligning flanges; 3 – molding sectors of the first group; 4 – external conic surfaces of the sectors of the first group; 5 – internal conic surfaces of the cones of the mechanism of radial movement; 6 – cones of the mechanism of radial movement; 7 – sectors of the second group; 8 – lateral planes of the sectors of the second group; 9 – angular holes; 10 – guide pins; 11 – teeth; 12 – circular clearance, a shape-generating double-sided toothed belt

The mould for manufacturing of double-sided toothed belts contains a toothed collapsible core 1 with the removable aligning flanges 2, the molding sectors 3 of the first group with the external conic surfaces 4, interacting with the internal conic surfaces 5 of the cones 6 of the mechanism of radial movement. The sectors 7 of the second group in the form of the ground wedges with the flat lateral planes 8 are placed between the sectors 3 of the first group. The sectors 7 have the angular holes 9 with the guide pins 10, pressed into the cone 6. On the external surface of the core 1 and the internal cylindrical surface of the sectors 3 the teeth 11, corresponding to the interdental spaces of the made double-sided belt, pressed in the circular clearance 12, are cut.

Let's consider the working process of such a mould. Wear resistant fabric coating is overlaid sequentially on the toothed collapsible core, preliminary taken out of the mould. Then the bearing layer in the form of a cord is coiled in the helical line. After that the layer of the sheet non-vulcanized elastomer and one more layer of fabric coating are overlaid on the coiled cord. The sectors 3 of the first group, alternating with the sectors 7 of the second group (the sectors of both groups are placed in a vertical clearance between aligning flanges 2) are set round the core with the assembled blank. The core 1 with the blank and the sectors 3, 7 go down on the bottom cone 6. The conic surfaces 4 of the sectors 3 start interacting with the conic surfaces 5 of the cones 6, and the pins 10 input into the holes 9 of the sectors 7. The angle of deflection of a guide pin to the axis of rotation of the mould is determined by the ratio:

$$\operatorname{tg}\beta = \operatorname{tg}\alpha \cdot \cos \frac{\gamma}{2},$$

where α – the angle of deflection of the external conic surface of molding sectors of the first group to the axis of rotation of the mould; γ – the angle of a wedge of molding sectors of the second group, $\gamma = 360^\circ/z$; z – the number of sectors in each group.

Then the core 1 is covered with the top cone 6, the working surfaces of the cone interact with the surfaces of the sectors 3 and 7 in the same way.

The design of the mould allows to keep the size of clearances between the movable sectors, excluding the occurrence of significant friction forces between them, which provides the improvement of durability and reliability of a mould and minimization of a flash on a toothed part of belts. It promotes the increase of their quality.

4.2. Parameters of the technological process of the manufacture of drive toothed belts

The basic parameters of the technological process of the manufacture of **rubber-technical** products and, in particular, drive toothed belts are the pressing pressure, temperature and duration of vulcanization [141, 142].

4.2.1. Pressing pressure

The transmission of a pull from teeth to the bearing layer of a belt is carried out by means of the mechanical and chemical adhesive forces, arising during the vulcanization on the border "bearing layer – elastomer".

The pressing pressure p causes the strength of adhesive bonds σ_{ad} , the presence or absence of porosity and holes, i.e. the solidity of a finished article. The load carrying capacity and durability of a belt depend on the value σ_{ad} . Between p and σ_{ad} there is a regression link. It is caused by the fact that the bearing layer is not a monolithic rod, but a set of elementary rods (wires, fibers).

The value σ_{ad} depends on the degree of the penetration of a filler (rubber) between the wires or fibers. The higher is p the better is the filling of the section of a bearing layer with rubber and the area of their contact.

For the determination of an optimum level p the experimental researches were carried out. According to [70] σ_{ad} is defined by the effort F that is necessary for the extraction of the bearing layer from the samples, representing the fragments of a belt (Fig. 4.7).

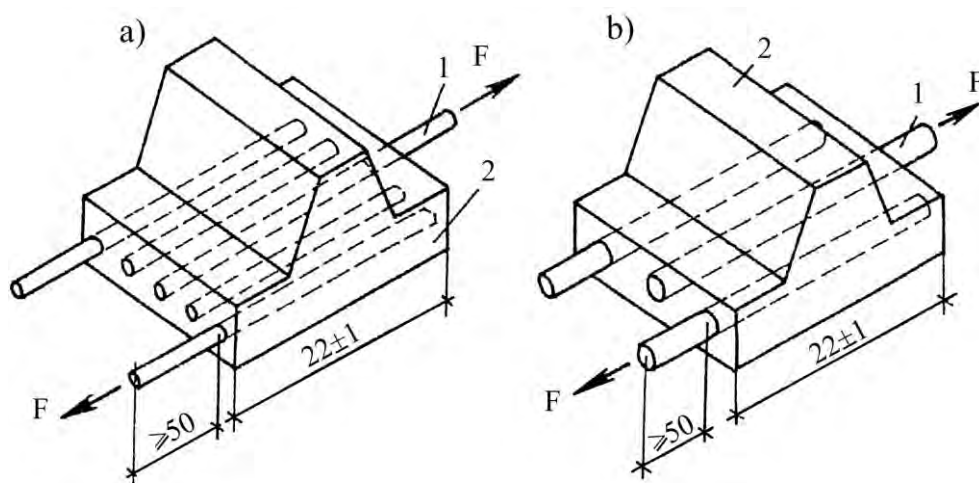


Fig. 4.7. Configuration of the samples of toothed belts for the determination of the strength of adhesion: 1 – bearing layer; 2 – sample

For the metal cord 5JI15 (Fig. 4.7, a) (5 brass wires, twisted together, Ø0.15 mm) and 7JI12 is $F \geq 50$ N, for 15JI15 (Fig. 4.7, b) (15 wires Ø0.15 mm) and 12JI12 is $F \geq 150$ N.

Practically, F is determined with the help of the machine of tension, supplied by a special vice for fixing of bared cables. At moving apart of the jaws the highest value F , which corresponds to the destruction of the adhesive combination, is fixed.

The value σ_{ad} is calculated by the dependence:

$$\sigma_{ad} = F / \pi d_c L,$$

where L – the length of the vulcanized part of a bearing layer.

The investigations are carried out by means of the special frame of a mould (Fig. 4.8) with a chord aperture in the central part. The manometer, representing a spring-loaded rod is placed in the aperture. The free end of the rod interacts with the displacement indicator of a clock type IH-1.

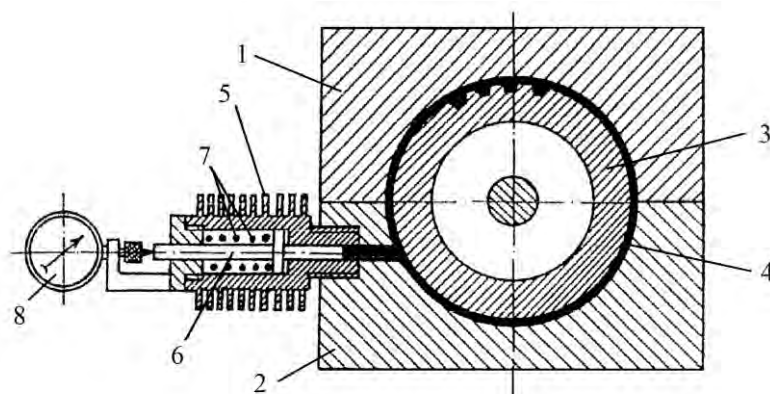


Fig. 4.8. Scheme of the pressure measurement of pressing: 1,2 – top and bottom half-moulds; 3 – gear core; 4 – blank of a belt; 5 – manometer; 6 - rod; 7 – spring; 8 – displacement indicator

The pressure in the mould is varied by the quantity of rubber mixture, by the change of the section of the orifice holes, and also by the regulation of effort of compression of plattens of a press.

The belts with the module $m = 3$ mm and the number of teeth $z_p = 48$ are the objects of the researches. The filler material is the rubber 1453, made on the basis of chloro-

prene rubber. The facing is the fabric of the article 56320, gum-dipped by №420 or a rubber mixture 1453. The bearing layer is the metal cord 5JI15, 15JI15.

Thus, 4 types of samples are investigated: 1 – 5JI15+420; 2 – 5JI15+1453; 3 – 15JI15+420; 4 – 15JI15+1453.

The investigations show that in the beginning σ_{ad} increases non-linearly with the increase of p . After filling of the whole bearing layer with elastomer σ_{ad} is stabilized, and the further increase of p does not lead to the change of σ_{ad} (Fig. 4.9).

The analysis of the received dependences $\sigma_{ad} = f(p)$ shows that receiving of σ_{admax} is possible under the condition when $p \geq 4$ MPa. The realization of such a level of p is carried out at pressing of a belt by the rigid elements or sectors.

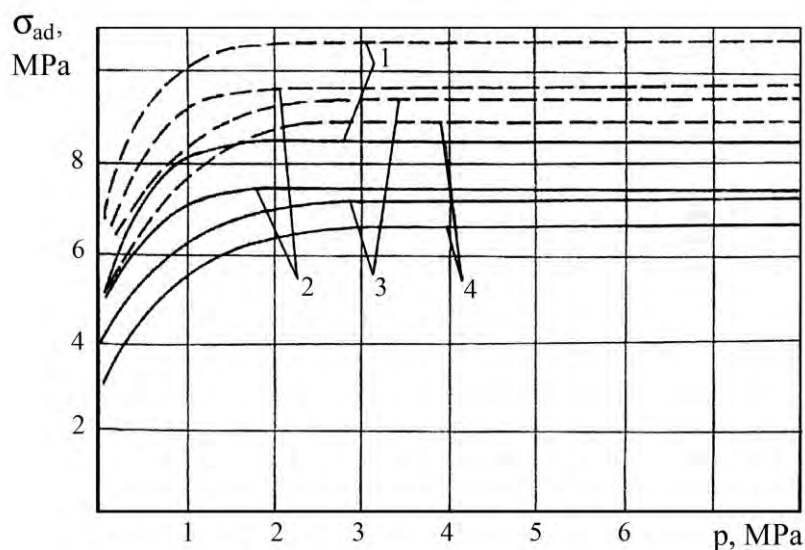


Fig. 4.9. Influence of the pressing pressure on the strength of adhesion of metal cord to a rubber mass of a toothed belt (the explanatory notes are in the text)

4.2.2. Temperature of vulcanization

The majority of **rubber-technical** products are vulcanized at the temperature 140...170°C [141]. The use of higher temperatures allows to reduce the duration of vulcanization and, hence, to raise labor productivity. The raise of the temperature by 10°C allows to reduce the duration of vulcanization practically 2 times [142]:

$$\frac{\tau_1}{\tau_2} = k^{\left(\frac{t_2 - t_1}{10}\right)},$$

where τ_1 – the duration of vulcanization at the temperature t_1 ; τ_2 – the duration of vulcanization at the temperature t_2 ; k – the temperature factor of the speed of vulcanization ($k \approx 2$).

However, the deterioration of mechanical and physical properties of a finished article is observed, if the rubbers are used for a belt manufacture at the temperature above 140°C.

It is connected with the fact that during vulcanization, alongside with the basic process (the formation of cross linkage of macromolecules of rubber and spatial vulcanized cross-linking structure), the chemical processes of cyclization and modification of polymer chains, a rearrangement of the vulcanization bonds, thermal and oxidative destruction of polymer chains take place (Fig. 4.10) [46, 142]. In this case, over-vulcanization (reversion) of a vulcanizate occurs.

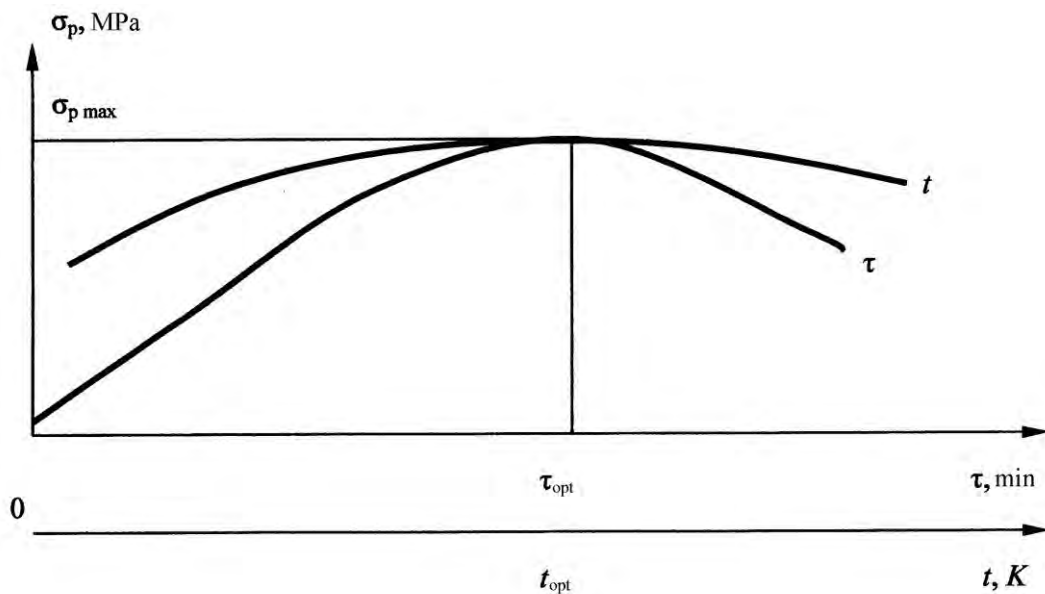


Fig. 4.10. Dependence of the strength of a belt at tension of time τ and temperature t of vulcanization

4.2.3. Duration of vulcanization

The optimality of the technological process of the manufacture of belts is defined by the least duration of vulcanization, at which the maximum values of the basic mechanical and physical properties of a vulcanizate (the strength at tension, the friction resistance, the ageing resistance) are achieved (see Fig. 4.10).

Examining the mechanical characteristics of rubbers and raw rubbers, it is established that under-vulcanized samples [46, 142] have the following higher parameters: the tear resistance, the formation and growth of fatigue cracks at cyclic loading.

The authors explain this phenomenon by the fact that while the **rubber-technical** products are in service, the heat energy, formed inside a vulcanizate due to the internal friction, mechanical and chemical processes, is firstly spent for the ending of the process of vulcanization up to the optimum level of the formation of polymer chains and the vulcanization bonds, and, secondly, the heat energy activates, stimulates or accelerates the processes of the thermal and mechanical destruction of polymeric material.

For the experimental testing of the influence of duration of vulcanization on the durability two experimental batches of belts (10 pieces in each one) are made. The vulcanization medium represents the rigid pressing sectors; the vulcanization pressure (5 MPa); the temperature of vulcanization (140°C); the duration of vulcanization of belts from the first batch (20 minutes) and from the second batch (17 minutes).

The belts are brought to the experimental-industrial durability testing. The average lifetime of the belts from the first batch is 120 h., the second batch is 200 h.

Let's define the dependence of the duration of tests and the number of the cycles of loading of belt teeth.

The belt is inseparable, making the cyclic runs along the contour of transmission between drive and driven pulleys. During one run one separate tooth of a belt experiences one loading on each pulley. The gearing of teeth does not allow elastic sliding and slippage of a belt.

Thus, the product of the rotation frequency of a pulley by the ratio of the length of a pulley circle to the length of a belt represents the quantity of loadings of one separate tooth of a belt a minute on a corresponding pulley, which are designated as N_1 and N_2 :

$$N_1 = n_1 \frac{\pi d_1}{t_p z_p}; \quad N_2 = n_2 \frac{\pi d_2}{t_p z_p}.$$

The total quantity of loadings of one separate tooth of a belt a minute on both pulleys is:

$$N_{\Sigma} = N_1 + N_2 = n_1 \frac{\pi d_1}{t_p z_p} + n_2 \frac{\pi d_2}{t_p z_p} = \frac{\pi(n_1 d_1 + n_2 d_2)}{t_p z_p}.$$

Considering that $t_p = \pi m$, $n_2 d_2 = n_1 d_1$, $d_1 = m z_1$, we receive:

$$N_{\Sigma} = \frac{\pi(n_1 d_1 + n_2 d_2)}{t_p z_p} = \frac{2\pi n_1 m z_1}{\pi m z_p} = \frac{2n_1 z_1}{z_p}.$$

The total number of cycles of loading of one separate tooth of a belt during the tests is:

$$N_n = \frac{2n_1 z_1}{z_p} t,$$

where t – the total duration of the resource test, expressed in minutes.

The frequency of rotation of a drive pulley of the examined transmission is $n_1 = 10000 \text{ min}^{-1}$, the number of teeth of a drive pulley is $z_1 = 12$, the number of teeth of a belt is $z_p = 90$, the average resource of belts from the first batch is $t_1 = 7200$ minutes, the second is $t_2 = 12000$ minutes.

Hence, the durability of the belts from the first batch makes $N_{n1} = 1.92 \cdot 10^7$ cycles, the second – $N_{n2} = 3.2 \cdot 10^7$ cycles.

Thus, the choice of rational modes of the technological process of the manufacture is an effective means of the increase in the durability of drive toothed belts. The realization of the technological process of the manufacture of toothed belts with optimization of a mode by the parameters of pressure, temperature and the time of vulcanization allows to **increase the durability of belts by 65...70 % and to lower the labor cost by 10 %** [143].

4.3. Progressive designs of the reinforced toothed belts

The design of a toothed belt with sleeve-loopback reinforcement has been developed (Fig. 4.11).

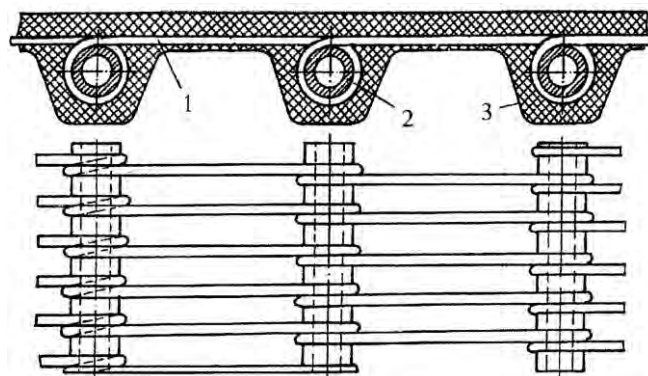


Fig. 4.11. Longitudinal section of a belt with sleeve-loopback reinforcement:
1 – bearing layer; 2 – sleeve; 3 – tooth of a belt

In the given belt the loops of a bearing layer 1 enclose the sleeves 2, placed along the teeth 3, and they have the same direction of coiling, which provides a high adaptability to assembling of blanks of a belt. The experimental toothed belts with sleeve-loopback reinforcement with a step of teeth 50.8 mm are manufactured (Fig. 4.12).

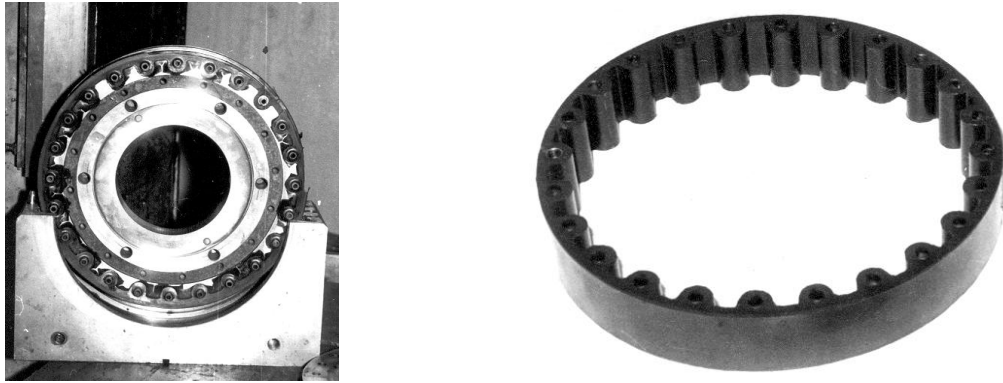


Fig. 4.12. Technological mould and a toothed belt with sleeve-loopback reinforcement

In the given design of a toothed belt the pull is transferred directly from the teeth to a bearing layer without the occurrence of shearing stress in elastomer.

For carrying out of the comparative analysis of the stress-strained state of the reinforced and non-reinforced toothed belts, the computer finite-element modeling in ANSYS is made. In Fig. 4.13, 4.14 the results of the modeling of a non-reinforced design of a toothed belt of a semicircular profile are presented [144].

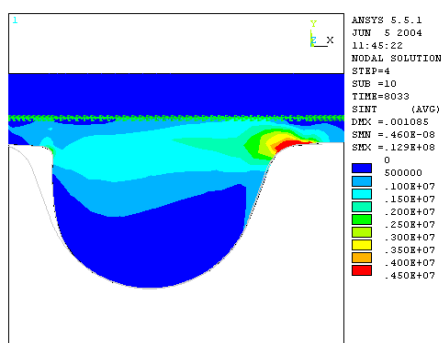


Fig. 4.13. Distribution of stresses

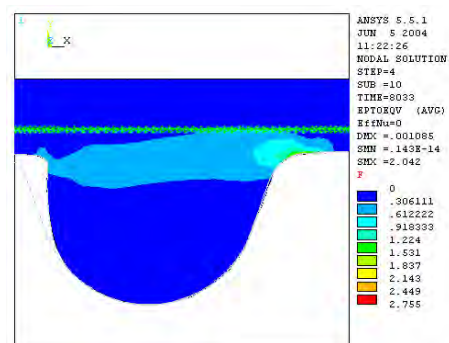


Fig. 4.14. Mises' deformations

The results of the modeling show that the maximum values of the tension stress σ_1 and the intensity of the deformation (**Mises' deformation**) ϵ_j are observed on the radius of transition of a lateral surface of the tooth to the surface of an interdental space. Thus $\sigma_1 = 12.9 \text{ MPa}$, $\epsilon_j = 2.042$.

In Fig. 4.15-4.20 the results of the modeling of the reinforced toothed belts are presented:

- 1) reinforcement by a sleeve $\varnothing 10$ mm (Fig. 4.15, 4.16);
- 2) reinforcement by a sleeve $\varnothing 12$ mm (Fig. 4.17, 4.18);
- 3) sleeve-loopback reinforcement by a sleeve $\varnothing 12$ mm (Fig. 4.19, 4.20).

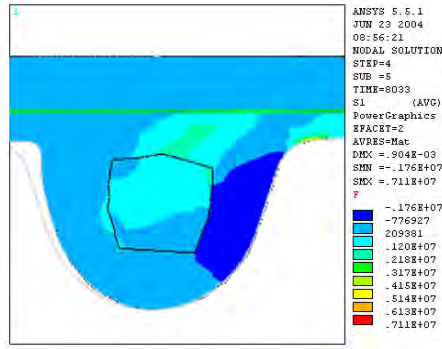


Fig. 4.15. Distribution of stresses

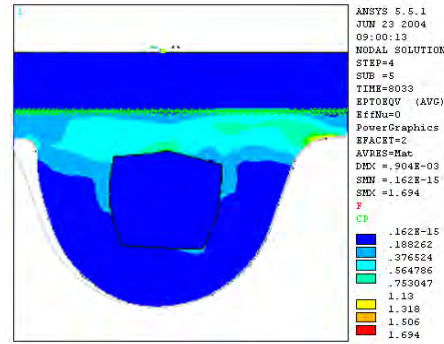


Fig. 4.16. Mises' deformations

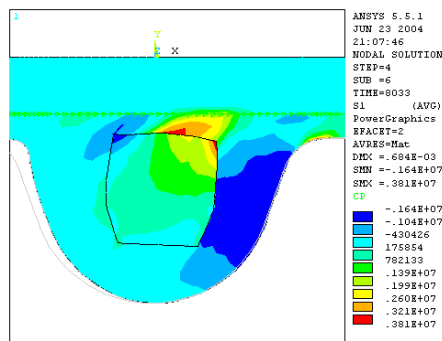


Fig. 4.17. Distribution of stresses

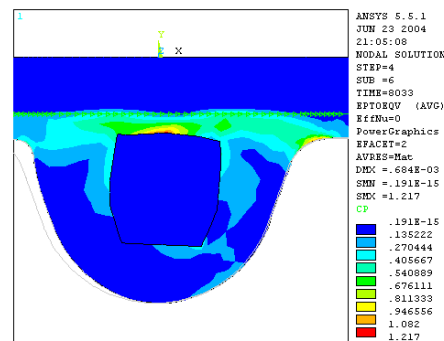


Fig. 4.18. Mises' deformations

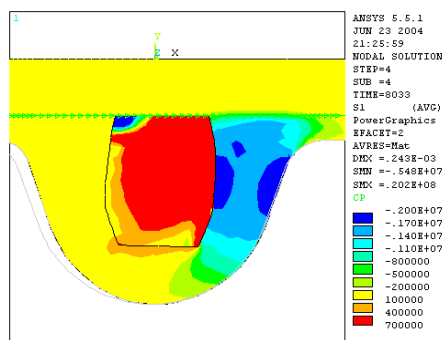


Fig. 4.19. Distribution of stresses

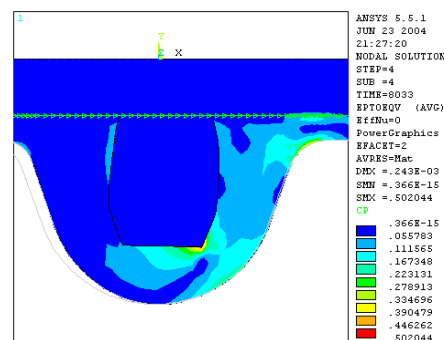


Fig. 4.20. Mises' deformations

The following conclusions can be made:

- 1) reinforcement by a sleeve $\varnothing 10$ mm allows to lower σ_1 up to 7.1 MPa (45 %) and ϵ_1 up to 1.694 (17 %);

2) reinforcement by a sleeve $\text{Ø}12$ mm allows to lower σ_1 up to 3.8 MPa (70 %) and ϵ_i up to 1.217 (40 %);

3) sleeve-loopback reinforcement by a sleeve $\text{Ø}12$ mm, fulfilling the mechanical link of armature with a bearing layer, allows to lower σ_1 up to 1.7 MPa (87 %) and ϵ_i up to 0.502 (75 %). It allows to raise the load carrying capacity and durability of transmission considerably.

The high engineering level of the given **toothed**-belt transmissions, alongside with the other advantages, allows to use them in energy-intensive drives of the processing equipment.

The technology of the assembly of belts with sleeve-loopback reinforcement differs in the special ways of coiling of the bearing layer, allowing to carry out looping around armature. The assembly of belt blanks is carried out on the special assembly machine tool (Fig. 4.21).

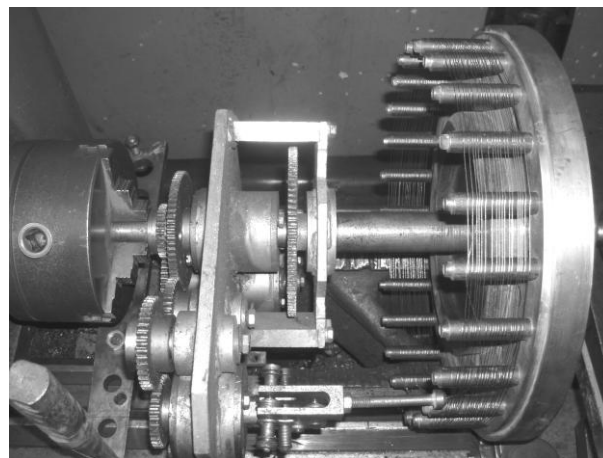
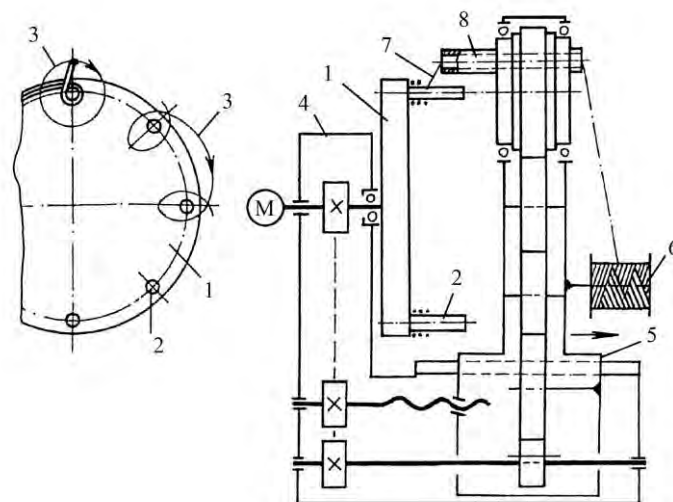


Fig. 4.21. Kinematic scheme and the physical form of the device for the assembly of toothed belts with sleeve-loopback reinforcement: 1 – faceplate; 2 – pin; 3 – trajectory of the thread carrier; 4 – frame; 5 – support; 6 – bobbin carrier; 7 – bearing layer; 8 – thread carrier

The basic units of the machine tool are a faceplate with the rods for the fixation of reinforcement sleeves and the thread carrier. The thread carrier moves along the closed prolate cycloid relative to the sleeves. Per revolution of the faceplate the thread carrier makes the number of the revolutions about the axis, which is equal to the number of belt teeth. Besides, per revolution of a faceplate the thread carrier is displaced axially (relating to the faceplate) by the size of a step of coiling of a bearing layer.

Thus, the direction of coiling of a bearing layer on all the sleeves is equal, and the thread carrier makes the full length winding of all the sleeves.

4.4. **Toothed**-belt transmissions with the improved technical and ecological parameters

The practice of designing of **toothed** transmissions shows that the use of helical wheels allows to increase the transmitted loading essentially or to increase the durability of transmission at the constant mass and dimension parameters. Alongside with it, the smoothness of the operation of transmission raises and its acoustic radiation decreases by 50 % [145].

The helical toothed-belt transmission was patented in 1983. [146]. However, the elastic toothed belt can be only herringbone in contrast to the rigid toothed wheels, capable to perceive axial effort (Fig. 4.22).

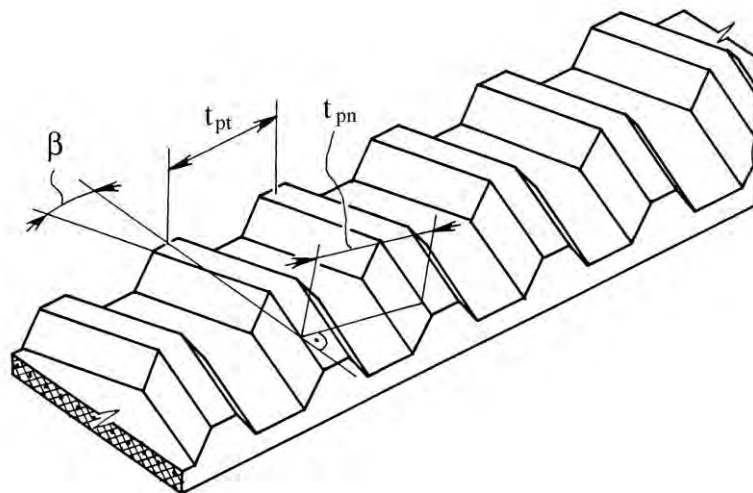


Fig. 4.22. Basic geometrical parameters of toothed belts with herringbone teeth

The profile of teeth in a herringbone design [147] provides the decrease in the noise level by 17...19 dB in comparison with the similar spur design [148].

The design of the belt with helical teeth, which symmetric halves are displaced in a longitudinal direction, relating to each other, is developed (Fig. 4.23) [149].

By analogy to the helical wheels it is advisable to predetermine the basic geometrical parameters in the normal section, which is perpendicular to the tooth line (see Fig. 4.22).

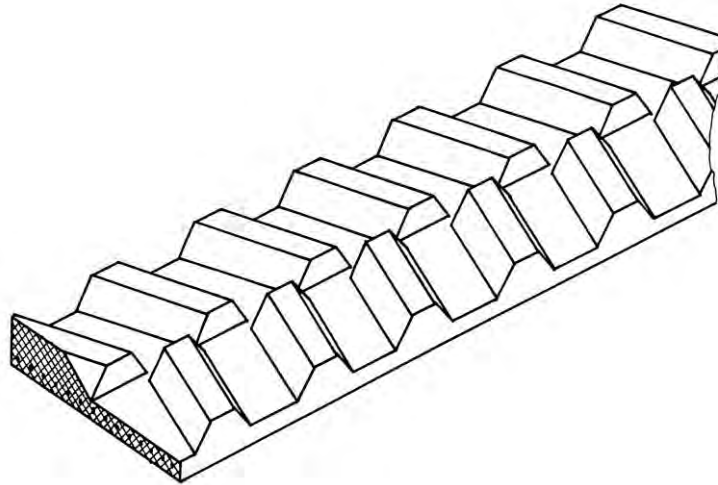


Fig. 4.23. Modified herringbone toothed belt

The longitudinal (circular) step of teeth is determined by the formula:

$$t_{pt} = \frac{t_{pn}}{\cos \beta}, \quad (4.1)$$

where t_{pn} – the normal step of teeth; β – the slope of teeth.

According to (4.1) the length of the belt L_p is determined by the expression:

$$L_p = t_{pt} Z_p = \frac{Z_p t_{pn}}{\cos \beta}.$$

The similar expressions can be received for toothed pulleys. Their type corresponds to the dependences for the calculation of the geometrical parameters of helical (herringbone) cog-wheels.

The helical belts are not standardized, but the producer companies regulate the values of a normal step of teeth t_{pn} (5.08; 9.525; 12.7; 10 and 20 mm) and their sizes in the normal section. However, the given geometrical calculation does not provide the demanded parameters of the working ability of transmission.

It is known that the toothed belt possesses compliance under the operating loads. The working deformations of belts exceed the deformations of cog-wheels approximately by 2 orders of the absolute magnitude. For the realization of the maximum possible durability of a belt the value of non-uniformity of loading of teeth is 0.7...0.9, and it is provided with the correction of pulleys, i.e. the increase in their external diameter by the following value:

$$\Delta d = \frac{\Delta t \cdot z_{III}}{\pi}, \quad (4.2)$$

According to the modern conceptions, the value Δt , providing the maximum durability of a belt in the set operational conditions, is determined by the following semi-empirical dependence:

$$\psi = \left[\frac{\left(\frac{25h_p z_0}{F_t \sqrt{\frac{G}{2}}} \right)^5}{\frac{400h_f z_0}{F_t \omega_1 f_{fs} \left(\frac{F_1}{c+2} + \frac{F_2}{2} \right)^{\chi_p}} (1 + 0,00005(HS - 60))^2} \right]^{\frac{1}{S + \chi_p}},$$

where HS – Shore hardness of elastomer A; χ_p – the exponent, describing the wear of elastomer.

The amendment Δd (4.2) is determined by the solution of the following equation relating to Δt at the known ψ and the parameters of mechanical and physical properties of the belt elements:

$$\psi = 1,3 \left[\left(\frac{F_t}{m^2} \right) \left(\frac{2F_0}{F_t} \right)^{-0,6} e^{\left(\frac{2F_0}{F_t} \right)^{0,5}} \left(\frac{1}{EF} + 0,001 \right) 0,25 + EZ \ 8334 + z_0^3 \left(\frac{-\Delta t}{t_p} + 0,0065 \right) \right]^{0,167}$$

The use of the given technique allows to receive one of the basic parameters of a **toothed**-belt transmission, i.e. the external diameter of the pulley, providing the maximum possible durability of a belt for the given conditions. However, it is obvious that in **toothed**-belt transmissions with herringbone teeth the belt is deformed both in longitudinal and cross-sectional sections.

The analysis of the force interaction of a toothed belt with pulleys shows (Fig. 4.24) that the axial forces cause the tension of a belt in a cross direction on a drive pulley and the compression on a driven pulley.

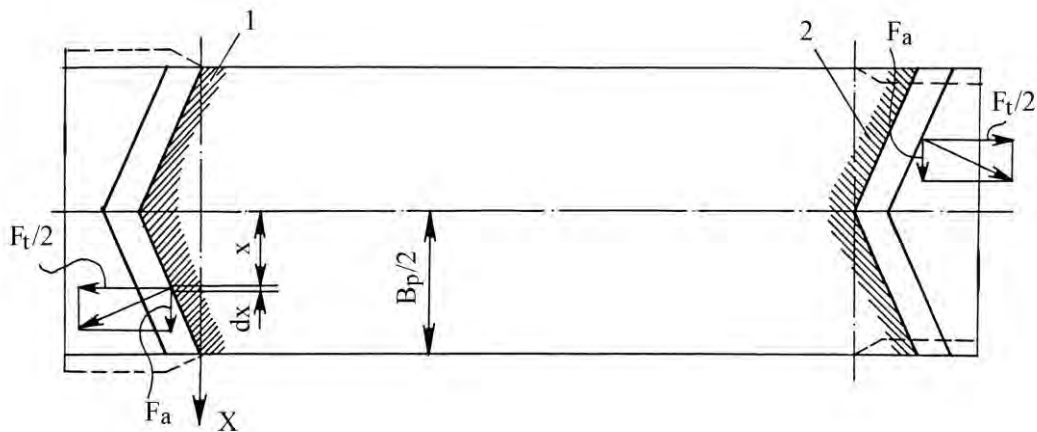


Fig. 4.24. Distribution of efforts on the arcs of contact in a **toothed**-belt transmission with herringbone teeth: 1, 2 – teeth of a drive pulley and a driven pulley

It causes the distortion of geometry of belt teeth and, in particular, the change of the slope of teeth $\Delta\beta$. The correction of the slopes of teeth of the drive $\Delta\beta_1$ and driven $\Delta\beta_2$ pulleys is necessary for the axial load compensation, the increase of the uniformity of distribution of loading along the length of the tooth, the lowering of the concentration of stresses, and for the raising of the load carrying capacity and the durability of the belt.

Let's receive the expressions for the calculation of the values of the amendments $\Delta\beta_1$ and $\Delta\beta_2$. For this purpose we allocate the elementary section dx in the tooth of a belt (see Fig. 4.24), where the elementary force $dF_a = dF_t / 2\text{tg}\beta$ acts. Within the limits of the given part the deformation of the belt tooth is considered to be parallel to the axis X and equal to:

$$\Delta d_x = \frac{dF_a}{E}.$$

At the uniform distribution of the pull along the width of the belt the absolute deformation of its end faces is equal to:

$$\Delta B = \int_0^{\frac{B_p}{2}} \Delta d_x = \int_0^{\frac{B_p}{2}} \frac{dF_a}{E} = \frac{F_a}{E} = \frac{F_t}{2E \cdot \operatorname{tg}\beta}.$$

On the basis of the features of the distribution of circumferential and axial loadings on the drive and driven pulleys of transmission (Fig. 4.25), after some transformations, we receive:

$$\operatorname{tg}(\beta - \Delta\beta_1) = \frac{\frac{B_p}{2} \operatorname{tg}\beta}{\frac{B_p}{2} + \Delta B_1}, \quad \operatorname{tg}(\beta + \Delta\beta_2) = \frac{\frac{B_p}{2} \operatorname{tg}\beta}{\frac{B_p}{2} + \Delta B_2}.$$

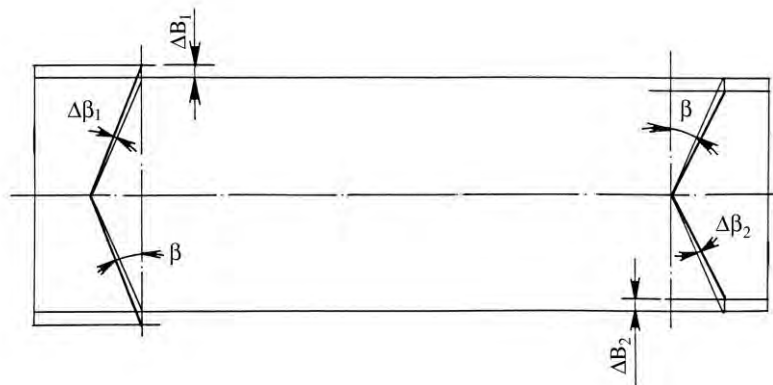


Fig. 4.25. Deformation of the belt on the arcs of contact of herringbone pulleys

After a number of transformations we receive the expressions for the calculation of the angular amendments of the pulleys [150]:

$$\Delta\beta_1 = \operatorname{arctg}\left(\frac{F_t \cdot \operatorname{tg}\beta}{B_p E \cdot \operatorname{tg}\beta + F_t}\right); \quad \Delta\beta_2 = \operatorname{arctg}\left(\frac{F_t \cdot \operatorname{tg}\beta}{B_p E \cdot \operatorname{tg}\beta - F_t}\right).$$

Let's consider the importance of these amendments. For a toothed belt with the module $m = 3$ mm, $B_p = 45$ mm, $E = 5$ MPa, $F_t = 10$ N/mm and $\beta = 20^\circ$, the slopes of teeth of pulleys should be: $\beta_1 = \beta - \Delta\beta_1 = 17,73^\circ$; $\beta_2 = \beta + \Delta\beta_2 = 22,9^\circ$.

In practice, it means that the correction of the slopes of teeth of herringbone pulleys makes 10...15 % of a slope of belt teeth.

4.5. Lowering of the contact pressure in a **toothed**-belt gearing by the method of optimization of geometry of teeth

The results of the research of distribution of the contact pressure in a toothed-belt gearing, combined with the data about the endurance of a material of teeth, make the basis of the resource designing of drive toothed belts. Thus, it is necessary to consider that the contacting bodies (a belt and a pulley) are made of dissimilar materials. Hence, the condition of the contact consists in coincidence of the displacement of each point of a surface of teeth in the part of contact.

Thus, it is possible to accept the proved assumption that the loading along the length of a tooth is distributed uniformly and it is symmetric in relation to its center. The errors of manufacturing and installing, and also the elastic deformations of other details of transmission (shaft, bearings, etc.) are not considered.

For the research of the distribution of the contact pressure along the length of teeth the following technique can be used. According to it, an absolutely rigid beam, laying on the elastic basis and being under the action of the symmetric loading, is considered [151, 152]. A number of absolutely rigid connections (cores) between a beam and a basis is located (Fig. 4.26, a).

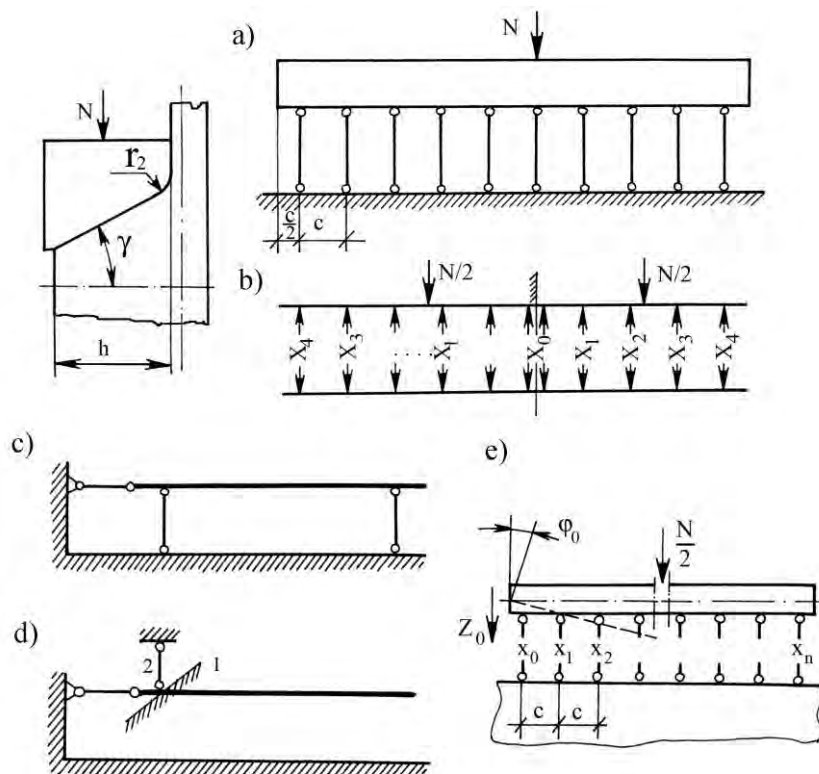


Fig. 4.26. Schemes of loading of teeth in gearing

The condition of the contact of the beam and the basis in the points of installation of rods consists in coincidence (continuity) of vertical displacements of a sole of a beam and elastic basis. As the beam is symmetric, the problem can be simplified, accepting the rigid fixing in the middle of the beam (Fig. 4.26, b).

If the given statically indeterminate problem is solved by the method of forces with the use of a beam on two supports, connected with the basis (Fig. 4.26, c), it is necessary to consider the compliance of the basis from the forces, applied to them and the beam. It complicates the determination of the factors in the initial equations of the method of forces considerably. Therefore, it is appropriate to solve the given problem in the following way. The vertical rods are replaced with the connections 1 and 2, forbidding the turn and the vertical movement of a beam, which provides its balance (Fig. 4.26, d). It is obvious that the beam is subjected to the force influence (the external loading N and the forces x_i) and to **the kinematic influence (the turn φ_0 and the vertical movement z_0)** (Fig. 4.26, e).

Using the symmetry, the turning angle **in fixing is $\varphi_0 = 0$** . In this case, only the forces $x_1; x_2; x_3; \dots; x_n$ influence the elastic base. The corresponding reactive forces in the rods are accepted to be even-distributed in the parts $c_1; c_2; c_3; \dots; c_n$. Hence, $x_i = \rho_i c_i$. It is natural that for receiving of the solution in quadratures, the value i should be finite. $i \leq 10$ is recommended [153]. In this case, there are 11 equations in this system.

Besides, the use of symmetry allows to exclude 6 unknowns. The forces x_i are equal on the left and on the right and the turning angle **in fixing is $\varphi_0 = 0$** . The equations of the mixed structure, considering the conditions of the contact of the elastic base and the rigid beam ($i = 1, 2, 3, \dots$) **and the balance of the beam as a whole, are made for the determination of the unknowns.** After a number of transformations, the above-examined equations can be written in the form:

$$\begin{aligned}
 & x_1 \delta_{11} + x_2 \delta_{12} + x_3 \delta_{13} + \dots + x_n \delta_{1n} + z_0 + \Delta_{1\rho} = 0; \\
 & x_1 \delta_{21} + x_2 \delta_{22} + x_3 \delta_{23} + \dots + x_n \delta_{2n} + z_0 + \Delta_{2\rho} = 0; \\
 & \text{-----} \\
 & \quad -x_1 \quad -x_2 \quad -x_3 \quad \dots -x_n + \Sigma N = 0; \\
 & \quad -x_1 a_1 - x_2 a_2 - x_3 a_3 - \dots - x_n a_n + \Sigma M = 0,
 \end{aligned} \tag{4.3}$$

where δ_{nn} – the displacement in the direction of the force x_n from the force $\bar{x}_n = 1$; Δ_m – the load displacement; a_i – the distance from the point 0 to the point $i = 1, 2, 3, \dots, n$; M – the moment from the external loading relating to the point 0; N – the projection of the external loading on the vertical axis.

The displacement δ_{ni} is defined by the yielding of the elastic base from the unit force, as the assumption about the absolute rigidity of the tooth of the pulley is accepted, i.e. $\delta_{ni} = \omega_{ni}$.

After the determination of the contact displacement, their values are inserted in the equation (4.3) and the forces $x_1; x_2; x_3; \dots; x_n$ are defined. If the value of the force x_j is divided into the value of the elementary area of contact, we receive the intensity of the reactions with a lattice diagram, which can be approximated by the equivalent curve. In this case, the pressure in any point on the effective length of the belt tooth B is determined under the formula:

$$P_y = \frac{N}{B \cdot b_p} \psi_y,$$

where N – the normal force, influencing the tooth: $N = P/\cos\gamma$; P – the quantity of the pull, taken up by the belt tooth; b_p – the calculation width of a beam; $\psi(y)$ – the dimensionless factor of the concentration of the contact pressure.

Let's accept $b_p = 1$, after that, the intensity of the distribution of the contact loading is:

$$P_y = \frac{N}{B} \psi_y. \quad (4.4)$$

If we replace $y/B = v$ in the expression (4.4), expressing N in terms of P , we get:

$$P_y = \frac{P}{B \cdot \cos\gamma} \psi_v. \quad (4.5)$$

The graphs of the change of the factor of concentration of the contact pressure along the length of a tooth, depending on the calculation width and length of a part of the contact, constructed according to (4.5), are resulted in Fig. 4.27. The value, received on the

basis of the standard geometrical parameters of a belt tooth, is accepted as the calculation width of the part of contact.

$$b_p = \frac{0,06 [h_p - R(1 - \sin \gamma)]}{\cos \gamma}$$

The analysis of the curves in Fig. 4.27 shows that the contact pressure at the end faces decreases with the increase in the length of a tooth. It is also established that the contact pressure at the end faces of a tooth is 1.3...2.5 times more than in the middle part.

Thus, the increase in the width of a belt is considered to be the rational approach in designing of **toothed**-belt transmissions, providing the lowering of the contact pressure in gearing of teeth. The use of the belt of a smaller module with the equivalent increase in its width is also rational.

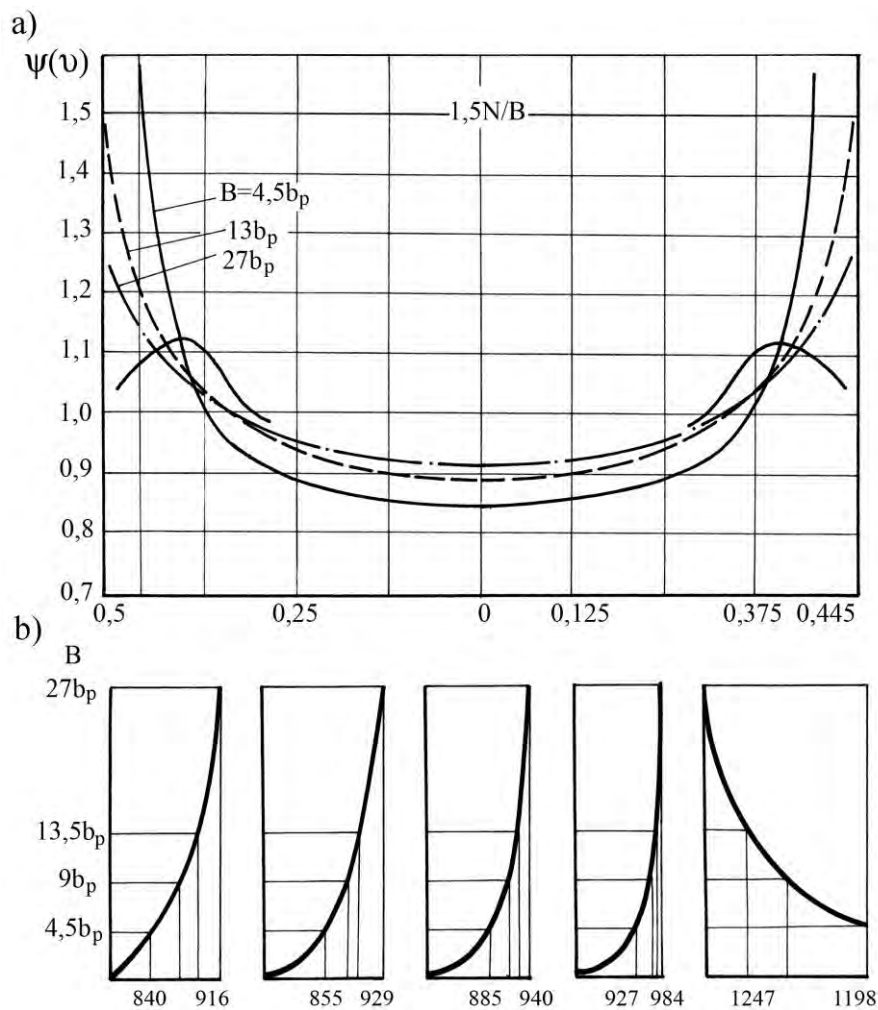


Fig. 4.27. Dependences of the change of the contact pressure along the length of the tooth

In Fig. 4.27, b the graphs of the change of coordinates of the curves in the parts, depending on the ratio b_p / c , are constructed. The graphs show that at $b_p / c = 1 / 3$ the coordinates of the curve points in all the parts do not practically change and the set of the curves can be presented by a generalized curve. Besides its generalized character, the given curve corresponds to the belts with the length of the teeth, having the prevailing practical application. Thus, $\psi(v) = 1.3 \dots 1.5$.

However, due to the increased compliance of the end faces of the belt tooth the concentration of the loading in these places is less. The influence of the increased compliance of the end faces of the tooth extends to 0.2 of the length of the belt tooth.

Thus, the diagram of the distribution of the contact loading of the belt teeth in the form of a rigid beam has a saddle-shaped form, which corresponds to the general technical concepts about the distribution of the contact pressure in connections [154, 155].

The distribution of the contact pressure along the length of belt teeth can be defined by the representation of the tooth of a pulley in the form of a rigid press tool, acting on the elastic half-plane. The problems of such a type are examined in the works [156, 157, 158].

During the research it is accepted that the contact pressure depends on the form of the part, which is in contact. If the press tool has the rectangular flat basis $2a'$ in width, corresponding to the lateral side of the belt tooth, and it is loaded by the normal force N (Fig. 4.28), the law of the pressure distribution is represented by the following equation:

$$p_x = \frac{N}{x\sqrt{d'^2 - x^2}} \quad (4.6)$$

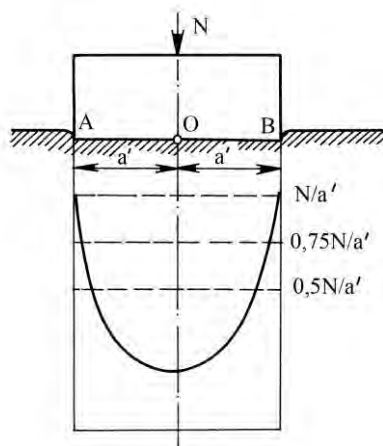


Fig. 4.28. Calculation scheme

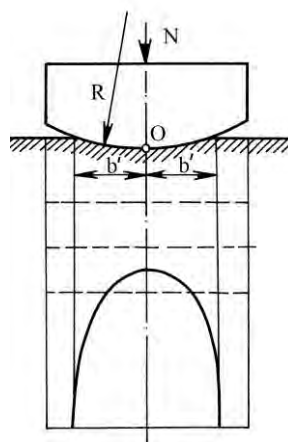


Fig. 4.29. Calculation scheme

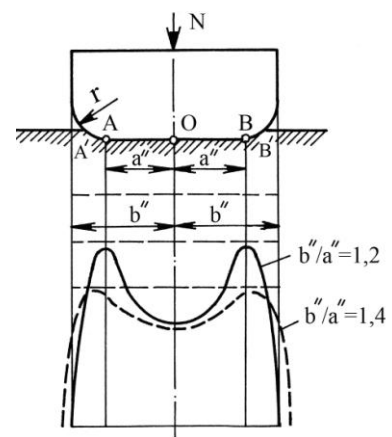


Fig. 4.30. Calculation scheme

If the press tool has the form of a cylinder with curvature $1/R$ (Fig. 4.29), the expression (4.6) becomes:

$$p_x = \frac{E\sqrt{b'^2 - x^2}}{2R(1-\mu^2)}, \quad (4.7)$$

where E – the module of elasticity of the material of a belt tooth; μ – Poisson's factor; b' – the half-width of an area of contact:

$$b' = 1,128\sqrt{\frac{NR(1-\mu^2)}{E}}. \quad (4.8)$$

In the case of the application of the press tool with the rectangular flat basis $2a''$ in width and the rounded edges $1/r$ (Fig. 4.30) we receive:

$$p_x = \frac{2N\sin\varphi_0 \left[\pi - 2\varphi_0 \cos\varphi + \sin\varphi \ln \left| \frac{\sin\varphi + \varphi_0}{\sin\varphi - \varphi_0} \right| + \sin\varphi_0 \ln \left| \operatorname{tg} \frac{\varphi + \varphi_0}{2} \operatorname{tg} \frac{\varphi - \varphi_0}{2} \right| \right]}{\pi d'' \pi - 2\varphi_0 - \sin 2\varphi_0}, \quad (4.9)$$

where $\varphi_0 = \arcsin a''/b''$; $2b''$ – the width of the area of contact after compression; $\varphi = \arcsin x\sin\varphi_0 / d''$.

As in the intermediate phases of an input of teeth in gearing and also in the transmissions with the uneven teeth their lateral surfaces are not parallel, it is necessary to get $p(x)$ for the press tool with an inclined basis. Thus, the expression for $p(x)$ should be explained as the most general case of the formula (4.7) or, in other words, be analogous to the case of the action of the asymmetrical loading on the base of the press tool with a horizontal basis. Such a loading is presented in the form of the force N , equal to N and passing through the point C , and also by the moment M equal to N , multiplied by the lever of OC (Fig. 4.31).

As a result, the base of the press tool turns and moves vertically. Such a case should be considered in two variants.

1) The press tool is in the contact with the base to an elastic counterbody (see Fig. 4.31):

$$\rho(x) = \frac{N}{\pi \sqrt{d'^2 - x^2}} + \frac{E \cdot dx}{2(1-\mu^2) \sqrt{d'^2 - x^2}}. \quad (4.10)$$

From the theory of the strength of materials [159] it is known that the dependence of the turning angle of the section of the moment is as follows:

$$\alpha = \frac{4M(1-\mu^2)}{\pi E d'^2}. \quad (4.11)$$

According to (4.10) $\rho(x) \rightarrow \pm \infty$ at $x = \pm a$. However, the diagram of the contact pressure differs by its asymmetry (in comparison with Fig. 4.28).

2) The press tool is not in the contact with the elastic base by one of its end faces, which corresponds to the condition of a limited contact (Fig. 4.32, 4.33):

$$\rho(x) = \frac{2N}{\pi(d' - a_1)} \sqrt{\frac{x + a_1}{d' - x'}} \quad (4.12)$$

where a_1 defines the boundary of the contact and represents the function M at the constant N .

In the point of the boundary of contact, i.e. at $x = a_1$, $\rho(x) = 0$.

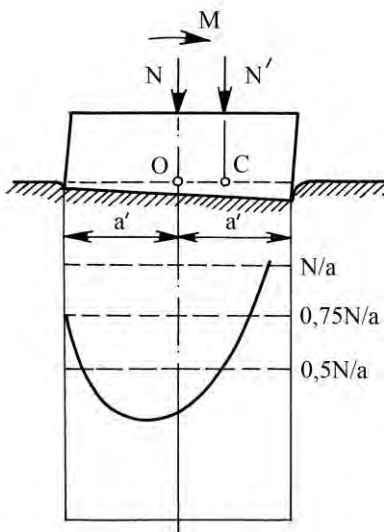


Fig. 4.31. Calculation scheme

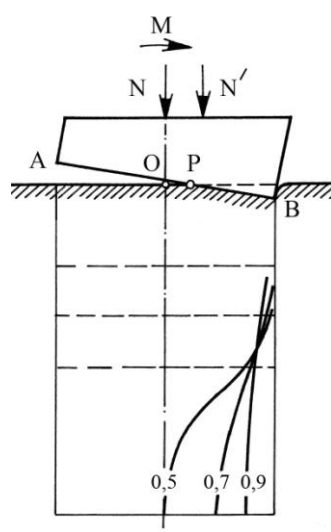


Fig. 4.32. Calculation scheme

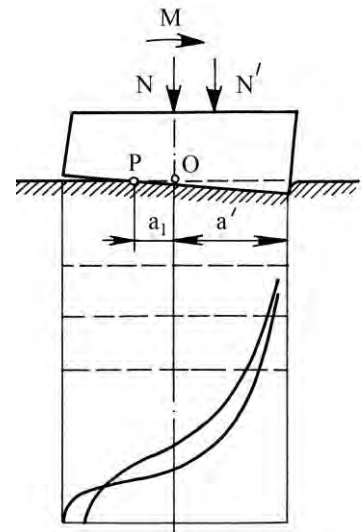


Fig. 4.33. Calculation scheme

Thus, the expressions, describing the typical loadings of the elastic base by a rigid counterbody (press tool), are received. It enables to consider the contact of teeth in a **toothed**-belt gearing. There are three variants of their standard design implementation:

1) a tooth of a pulley is made by the radius ρ_e (Fig. 4.34, a), which leads to taking of the transmission with a semicircular profile at its increase, and to a trapezoidal profile at its lowering to the minimal standard values;

2) a tooth of a belt is made in a straight line, approximating an involute (Fig. 4.34, b) and the angle of a pulley space is less than the angle of the profile of a belt tooth, which corresponds to the standardized transmissions of the type *STS (STPD)*. Thus, the lateral side of the tooth of a pulley is at the alternate angle $\Delta\gamma$ with the lateral side of the tooth of the belt, which is called a preliminary slope;

3) a tooth of a pulley has a straight-sided profile, providing its contact with the tooth of a belt along the whole lateral side (Fig. 4.34, c).

For the choice of the **calculation scheme let's consider each variant in case of the absence of rounding of a tip of a pulley tooth and the basis of a belt tooth**, i.e. $r_2 = 0$.

The variant of the contact of teeth of a pulley and a belt at the scheme in Fig. 4.34, c can be narrowed down to an axisymmetrical problem at the scheme in Fig. 4.33, i.e. the conditions in the boundary points of the press tool are similar to the conditions in the point of the contact of the angular points of a root and the point of a tooth of a belt with the lateral side of a tooth of a pulley.

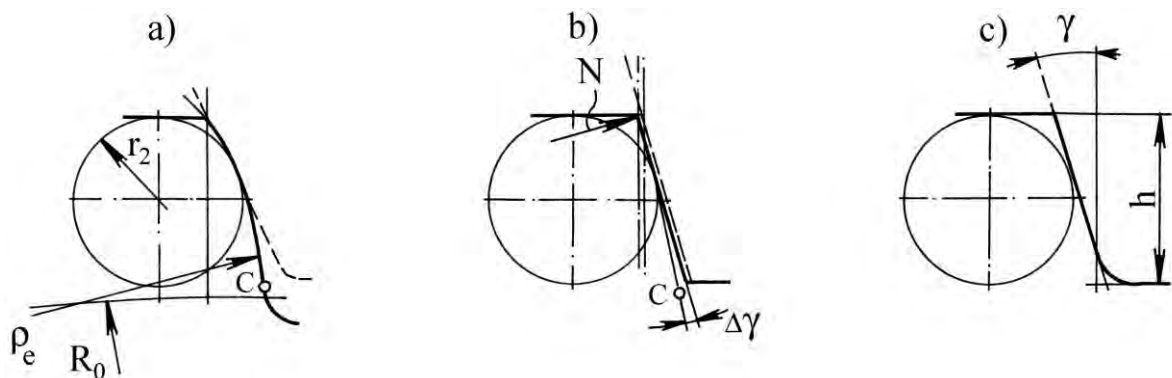


Fig. 4.34. Possible configurations of trapezoidal teeth of a belt

The variant of the contact of teeth at the scheme in Fig. 4.34, **b at presence of $\Delta\gamma$** also presents an axisymmetrical problem at the scheme in Fig. 4.33, and the conditions in a

boundary point are similar to the conditions in the point of the contact of the lateral side of a tooth of a belt with the lateral side of a tooth of a pulley.

The position of the given point depends on $\Delta\gamma$ and the effort, taken up by a belt. In a limiting case it coincides with an angular point of the base or the tip of the tooth of a belt. In the last case the contact of teeth is identical to the third variant (Fig. 4.34, c).

The relationship between the loading and α is found at the scheme in Fig. 4.31. Under the stipulation that the force is applied to the angular point of the tooth of a pulley, after some transformations of the expression (4.11) with the replacement $N = P/\cos\gamma$, we receive:

$$P = \frac{\pi E \alpha d' \cos \alpha}{4 (1 - \mu^2)}, \quad (4.13)$$

where $\alpha = \Delta\gamma$.

Assuming $d' = \frac{b}{2} = \frac{h_p - r_2}{2} \frac{1 - \sin \gamma}{\cos \gamma}$, we have $P = (2.2 \dots 2.6)m$ at the values

$\Delta\gamma = 3 \dots 4^\circ$ and $\gamma = 20 \dots 25^\circ$.

At $k < 10$ the absence of the complete contact is possible at $\Delta\gamma = 6 \dots 8^\circ$.

Thus, the variant of the contact of teeth at the scheme in Fig. 4.34, b can be replaced by the variant at the scheme in Fig. 4.34, c. The difference is in the fact that the penetration of the tooth of a pulley into the mass of the belt tooth is deeper. It happens, because the profile of the tooth of a pulley is located at the angle $\Delta\gamma$ to the lateral side of the tooth of a belt before an input in gearing.

For the estimation we compare two variants of the interaction of a rigid press tool with an elastic base, presented in Fig. 4.28 and 4.31. In both cases the press tool is in contact with the elastic base by the whole contact area, but the diagrams of the contact pressure are different.

Comparing (4.6) and (4.10), we get the factor, characterizing the asymmetry of the diagrams of the contact pressure:

$$\varepsilon = 1 + \frac{\pi E \alpha x \cos \gamma}{2 (1 - \mu^2) P}. \quad (4.14)$$

According to the scheme in Fig. 4.34, it is possible to introduce a variant of the contact of teeth by a half of the rigid press tool with the curvilinear base ρ_e . Let's define the dependence between the loading and the width of the area of contact, accepting the application of force in the angular point of the tooth of a pulley.

Using the method of mapping, we can assume that, if the rigid press tool (tooth of a pulley) is cut by the plane, passing through the force vector, the loading of a pushed back part, taken up by the remained part and its yielding, according to the formula (4.8), is $\sqrt{2}$ times more. As we proceed from the constant value of yielding, the true loadings are 2 times less because of the symmetry.

On the basis of the expression (4.8), after the substitution of $P/\cos\gamma$ for N and ρ_d for R , we get:

$$P = \frac{b^2 E}{2,55\beta (1-\mu^2)}. \quad (4.15)$$

From (4.15) it follows that at $b' = b(h_p - r_2(1-\sin\gamma)) / \cos\gamma$ and $z_{III} < 20$ we have $P = 7m$.

At the transmission of the pull $F_t = F_{tmax} = 65m$ it corresponds to nine teeth on the arc of contact under the condition of the uniform distribution of the loading between them. Hence, at the pseudoinvolute profile of teeth of a pulley the complete and incomplete contacts with the belt teeth across the width of a lateral side, are possible. It means that the use of the diagram in Fig. 4.29 is possible only in the first case.

Thus, the variant of the contact of teeth of the pseudoinvolute profile can be resulted in the axisymmetrical problem at the scheme in Fig. 4.33. The initial localized contact should be considered by means of a preliminary slope, the value of which is defined by the expression:

$$\alpha_e = \frac{8b'}{2,45\pi\beta}. \quad (4.16)$$

The expression (4.16) can be received in the result of the combined solution of the dependences (4.13) and (4.15) under condition of $\alpha = \beta'/2$.

At $z_{III} < 20$, $\alpha_e \approx 10^\circ$.

Hence, the scheme of the limited contact of the press tool with the elastic base in the form of a semi-infinite plane (Fig. 4.33) is accepted as a calculation scheme. The initial linear or point contact is considered by means of the factor of asymmetry ε (4.14).

Whereas the tooth of a belt represents a semi-infinite plane, the contact pressure on the part of the unit length is defined by the formula (4.12).

In Fig. 4.35 the scheme of the interaction of teeth of a belt and a pulley is shown. According to the designations, accepted in Fig. 4.35, the formula (4.12) becomes:

$$p(x) = \frac{2N}{\pi\varepsilon} \sqrt{\frac{e-x}{x}}, \quad (4.17)$$

where e – the width of the area of the contact of teeth of a belt and a pulley

$$0 < e < \frac{h_p - r_2}{\cos \gamma} \frac{1 - \sin \gamma}{\cos \gamma}.$$

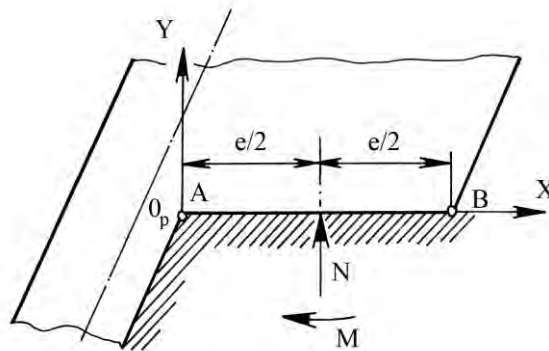


Fig. 4.35. Scheme of the contact of lateral sides of teeth of a belt and a pulley

The tooth of a belt inputs in gearing with the tooth of a pulley with the significant resistance, caused by the friction force, which is necessary to be considered. We accept the factor of friction to be constant in all the points of the contact and the following boundary conditions: in the unloaded parts of the boundary of a half-plane ($x < 0$ and $x > e$) $\sigma_y = 0$; $\tau_{xy} = 0$; in the loaded part ($0 < x < e$) $u = 0$; $\sigma_y = p(x)$; $\tau_{xy} = -f p(x)$; $dx = \text{const}$.

Assigning u and $v = -dx$ the specific meaning of the elastic displacement along the axes X and Y , accounting the above-stated boundary conditions and the fact that in the point B $p(x) = 0$, we receive the following expression for the determination of the contact pressure in

view of the friction:

$$p(x) = \frac{2N \cos \chi \rho}{x e^{1-2\rho}} \left(\frac{e-x}{x} \right)^{0.5-\rho}, \quad (4.18)$$

where $\rho = \frac{1}{\pi} \arctg f \frac{1-2\mu}{2(1-\mu)}$; f – the factor of friction in the pair "tooth of a belt – tooth of a pulley": $f = F/N$.

In the case of the absence of friction, i.e. at $F = 0$, we receive $\rho = 0$, and (4.18) becomes (4.17). In other words, the expression (4.17) is a special case of the expression (4.18), which is convenient to be written in a parametric form:

$$p(x) = P_e \psi(x), \quad (4.19)$$

where P_e – the average pressure in the part of the unit length:

$$P_e = \frac{P}{e \cdot \cos \gamma},$$

P – the effort, taken up by the tooth of a belt; $\psi(x)$ – the dimensionless factor of concentration of the contact pressure, depending on the linear factor X :

$$\psi(x) = \frac{2 \cos \pi \rho}{\pi (1-2\rho)} \left(\frac{e-x}{x} \right)^{0.5-\rho}. \quad (4.20)$$

Substituting $\eta = \frac{x}{e}$, we receive:

$$\psi(\eta) = \frac{2 \cos \pi \rho}{\pi (1-2\rho)} \left(\frac{1-\eta}{\eta} \right)^{0.5-\rho}. \quad (4.21)$$

Expressing the average pressure as the whole width of a rectilinear part of a lateral side of the tooth of a belt at $b = \frac{h_p - r_2}{\cos \gamma} \frac{1 - \sin \gamma}{\cos \gamma}$, i.e.

$$P_b = \frac{P}{h_p - r_2} \frac{1}{1 - \sin \gamma}, \quad (4.22)$$

the expression (4.19) can be written in the following way:

$$p(x) = P_b \psi_1(x), \quad (4.23)$$

where $\psi_1(x) = \psi \eta \frac{b}{e}$.

The expression (4.23) characterizes the distribution of the contact pressure independent of the length of a belt tooth. The curves $\psi_1(x)$ at $e = b$ at the various factor of friction are given in Fig. 4.36.

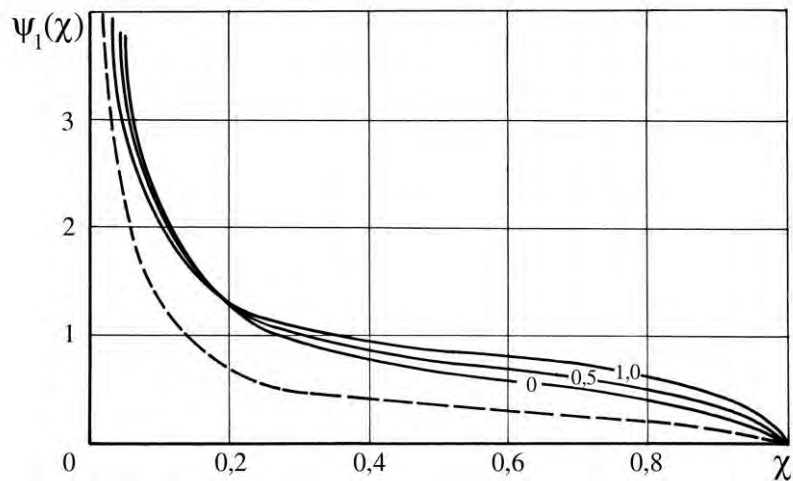


Fig. 4.36. Dependence of the factor of concentration of the contact pressure along the length of the tooth at various values of the friction factor

The presented dependences show that along with the increase of f the part of the high contact pressure near the tip of the tooth of a pulley decreases. The pressure on the rest part of the contact increases. However, for the values ($0.3 < f < 0.7$), observable in the contact of **teeth of toothed-belt transmissions**, these changes are absolutely insignificant, and they can be neglected.

On the other hand, the essential factor, influencing the distribution of the contact pressure, is the radius of rounding of the tip of the tooth of a pulley. For the estimation of its influence we can use the scheme of the contact of the rigid press tool, having the round-

ed end faces, with the elastic base (see Fig. 4.30), and the expression (4.9), describing the law of the pressure distribution.

In Fig. 4.37 the scheme of the contact of teeth with rounding is shown.

Hereafter, we shall consider the tooth with rounding as a half of the rigid press tool with the rounded end face, i.e. the part of AO (see Fig. 4.30), which corresponds to the part EB (see Fig. 4.37). We designate the part of the contact of teeth up to the application of loading $EB = a''$.

According to the setting of the problem, at the use of the formula (4.9) it is necessary to increase the received values two times. The value $p(x)$ in the point B is different from zero and, hence, it is a little bit overestimated in comparison with the true value, in the point E it is underestimated. Therefore (4.9) is used for the approximate calculation of the contact pressure in the part near the point E .

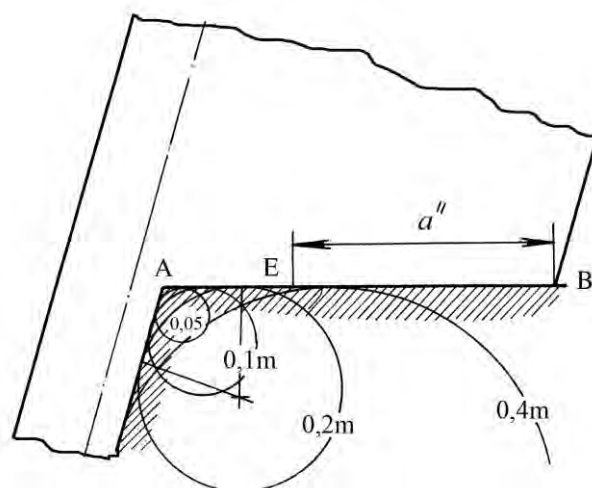


Fig. 4.37. Interaction of the tooth of a belt with the tip of the tooth of a pulley

The received solutions are summed up. It leads to receiving of the diagram with the step curve, replaced by the equivalent smooth graph.

From the constructions, presented in Fig. 4.37, the width of the initial part of the contact of teeth is determined by the expression:

$$a'' = \frac{h_p - r_2 + r_{2p} \cdot 1 - \sin \gamma}{\cos \gamma}. \quad (4.24)$$

The width of the part of contact after the application of the loading can be defined by the graph in Fig. 4.38.

The contact pressure in each point across the width of the area of contact can be expressed as follows:

$$p(x) = P_a'' \psi(\xi), \quad (4.25)$$

where P_a'' – the average pressure in the part of the unit length

$$P_a'' = \frac{P}{a'' \cdot \cos \gamma},$$

$\psi(\xi)$ – the factor of the change of the contact pressure in the function $\xi = \frac{x}{a''} s$:

$$\psi(\xi) = \frac{4 \sin \varphi_0 \left[x - 2\varphi_0 \cos \varphi + \sin \varphi \ln \left| \frac{\sin \varphi + \varphi_0}{\sin \varphi - \varphi_0} \right| + \sin \varphi_0 \ln \left| \operatorname{tg} \frac{\varphi + \varphi_0}{2} \operatorname{tg} \frac{\varphi - \varphi_0}{2} \right| \right]}{\pi (\pi - 2\varphi_0 - \sin 2\varphi_0)}.$$

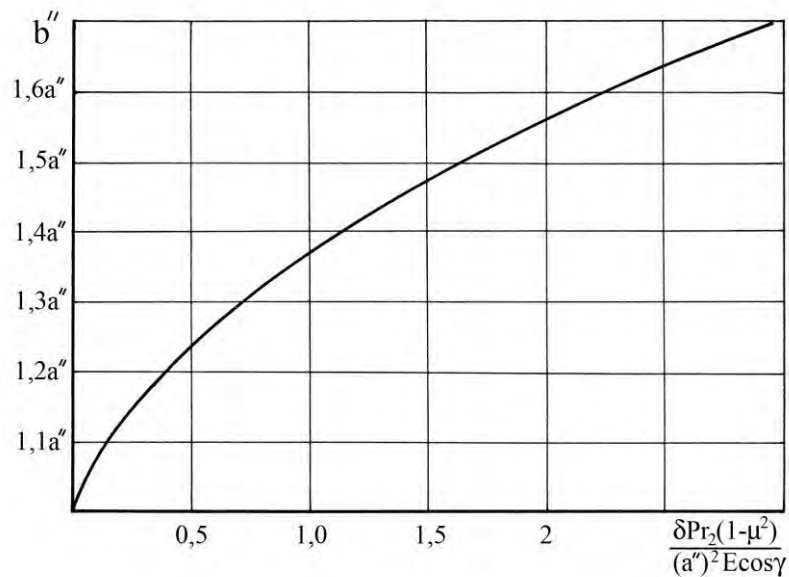


Fig. 4.38. Dependence of the width of the area of contact of the value of the loading

If the average pressure across the whole width of a linear part of the lateral side of the tooth of a belt is expressed by the formula (4.22), in this case, the expression (4.25) has the following form:

$$p_x = P_b \psi_2 x,$$

where $\psi_2 x = \psi \xi \frac{b}{a''}$.

Hereafter, considering the expressions, defining b and a'' , we finally receive:

$$\psi_2 x = \psi \xi \frac{h_p - r_{2p} \cdot 1 - \sin \gamma}{h_p - r_2 + r_{2p} \cdot 1 - \sin \gamma}. \quad (4.26)$$

It is obvious, that the length of the tooth and the radii of rounding of its tips can be expressed as a module or a step of teeth, and the ratio b/a'' does not depend on the module. The factor $\psi(\xi)$ is also independent of the module, if the force P is expressed in the ratio $[8Pr_2(1-\mu^2)] / (\cos \gamma (a'')^2 E)$, defining the value of an abscissa of the graph in Fig. 4.39, by the dimension factor and the module, i.e. $P = um$. The graphs are constructed at the following parameters: $\gamma = 20^\circ$; $h_p = 0.6m$; $r_2 = (0.05 \dots 0.5)m$; $u = 5, 10$ and 20 N/mm.

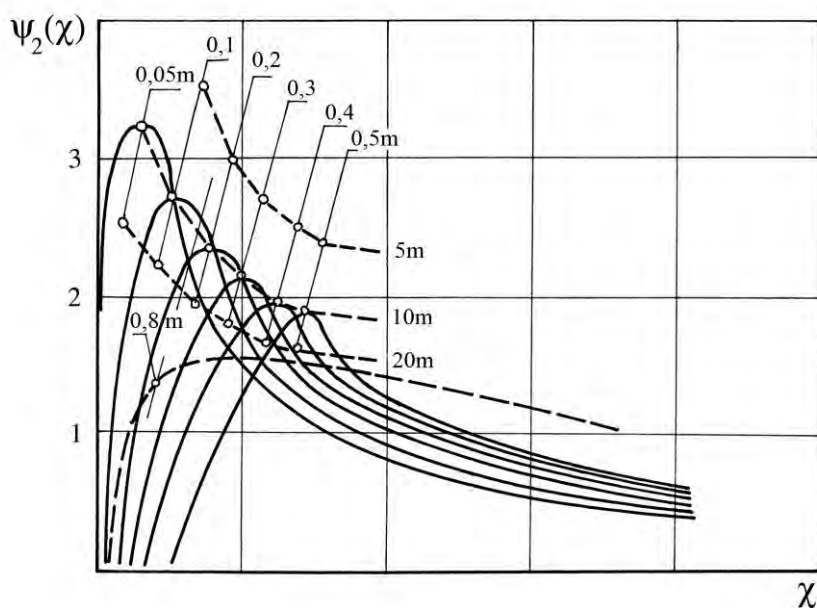


Fig. 4.39. Dependences of the factor ψ_2 of the dimensionless coordinate and loading

The change of γ , h_0 and E for one module practically does not influence $\psi(\xi)$ at the constant r_2 . At the increase of h_0 the ratio b'' / a'' decreases, which causes the increase of $\psi(\xi)$, but in a less degree than a simultaneous reduction of the average contact pressure. At the same time, the increase in the module of elasticity causes the increase of $\psi(\xi)$, and the values $\psi_2(\chi)$ for the existing designs of belts at the equal r_2 practically coincide. Therefore the change of $\psi_2(\chi)$ is presented by one curve for every r_2 .

The increase of $\psi_2(\chi)$ at the lowering of u can be explained by the fact that the reduction of the area under a smaller loading leads to the reduction of the ratio b'' / a'' and to the increase of $\psi(\xi)$. Besides, the graphs show that at the increase in the radius of rounding of the tip of the tooth the maximum values of $\psi_2(\chi)$ firstly decrease, and then they increase again. It is explained by the fact that at small values of r_2 the slope $\psi_2(\chi)$ is larger than the slope b / a'' (Fig. 4.40). From the certain moment the slopes equalize and the situation reverses.

Thus, at $r_2 > 0,35m$ the increase in the maximum contact pressure occurs. Firstly, it is caused by the reduction of the resultant area of the contact of teeth under the loading.

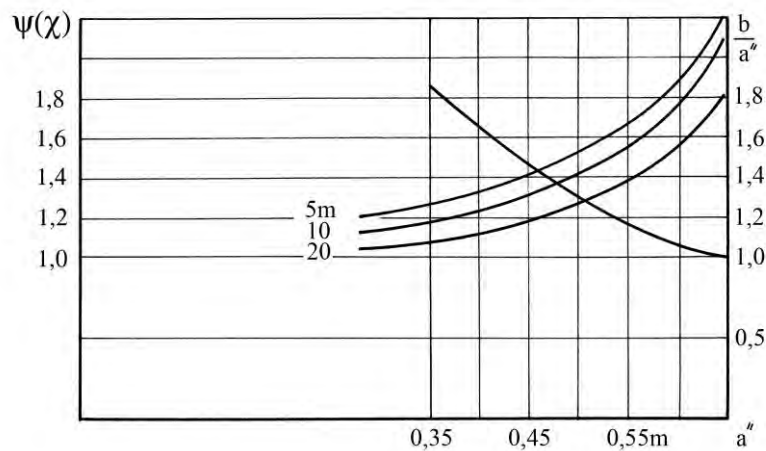


Fig. 4.40. Dependence of the factor ψ of the sizes of the contact area pattern

On the basis of the above-stated researches we find a rational variant of rounding of the tip of the tooth of a pulley (Fig. 4.41).

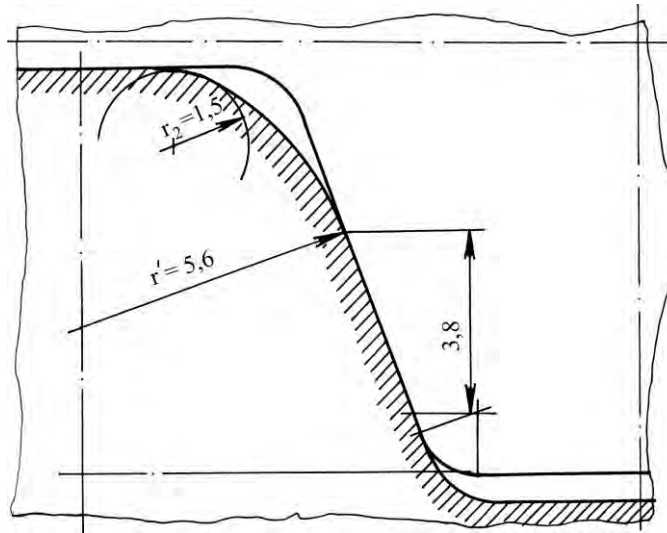


Fig. 4.41. Rational geometry of transmission with trapezoidal teeth

The basic precondition of such a choice consists in the fact that at $b'' / a'' > 1.7$, $\psi(\xi)_{\max} = 1.1$, and it does not practically change. Let's introduce the supplementary condition $b'' < b$ in order not to cause a sharp rising of pressure, as the edge of the tip of the tooth of a pulley under the loading should not contact with the tooth of a belt.

We receive $a'' = (0.32 \dots 0.34)m$. On the basis of Fig. 4.38, at $b'' / a'' = 1.7$ we have: $\delta P r_2' (1 - 2\mu) / (a'')^2 E \cos \gamma = 3, 2$. From this expression, at the existing value of the module of elasticity of rubber and $\gamma = 20^\circ$, we receive: 1) $P = 5m - r_2' = 2, 4m$; 2) $P = 10m - r_2' = 1, 2m$; 3) $P = 20m - r_2' = 0, 6m$.

We accept $r_2' = 0, 8m$ on the basis of the maximum loadings, taken up by the teeth of a belt. The graph of the distribution of the contact pressure for the given case is represented with a dashed line in Fig. 4.39.

Whereas the area of the contact of teeth is larger, the lowering of the maximum contact pressure occurs. The comparison of the curves shows that the offered variant of rounding of the tip of the tooth of a pulley is optimum, especially for the transmissions with the module $m < 5$ mm, since the contact pressure is 1.2...1.5 times less in comparison with the standard geometry. The resultant value of the contact pressure can be found from the simultaneous solution of the expressions for the parts of the tip of the tooth of a belt (4.23), taking preliminary $e = a''$ in (4.20) and (4.24), and of the tip of the tooth of a pulley (4.26).

In Fig. 4.42 the dependences of the resultant factor of concentration of the contact pressure $\psi(\chi)$ of the dimensionless coordinate X and the loading on the tooth $P = um$ are pre-

sented. The curves are received by the approximation in the points of discontinuity on the boundaries of the above-stated parts.

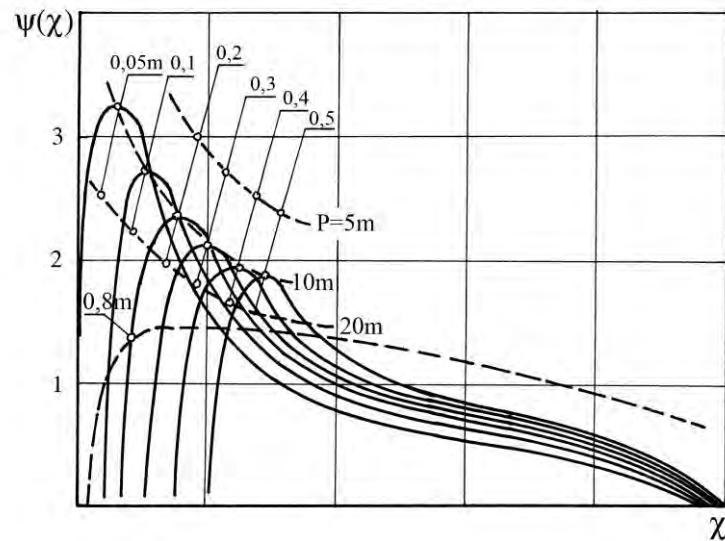


Fig. 4.42. Dependences of the factor ψ of the dimensionless coordinate and loading

As well as the graphs in Fig. 4.36 and 4.39, the received dependences are comprehensible to the transmissions with any module or step of teeth. On their basis the dependences $\psi(\chi)$ of the loading P and the radius r_2 are constructed (Fig. 4.43).

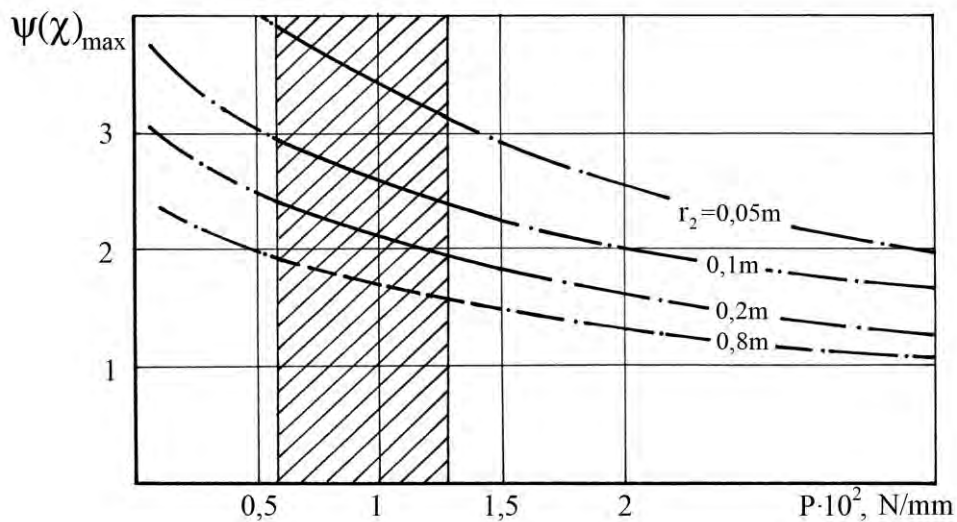


Fig. 4.43. Dependences of the maximum factor $\psi(\chi)_{max}$ of the loading and the radius of rounding of the tip of the tooth of a pulley

The marked zone corresponds to the operational interval of loadings on the teeth of a belt. The analysis of the received dependences shows that the least value $\psi(\chi)$ is observed at $r_2 = 0.3m$ or at $r_2' = 0.8m$ (as it has been established above). At $r_2 < 0.3m$ $\psi(\chi)$ starts increasing quickly.

In the process of designing and modernization of **toothed-belt transmissions** the values $\psi(\chi)$ should be chosen in the following way: at $r_2 = (0.1...0.3)m$, $\psi(\chi) = 1.8...2.5$; at $r_2 < 0.1m$, $\psi(\chi) = 2.5...4$.

The problem of the determination of rational geometrical parameters of teeth in the case of a complete adjoining of their lateral sides has been considered before. For the incomplete profile or partial gearing at non-parallelism of lateral sides the factor of asymmetry ε (4.14) should be introduced.

If it is necessary to receive gearing with a complete contact of lateral sides in unloaded transmission at the absence of the lateral clearance between teeth, the angle of a pulley space is equal to the angle of the profile of a belt tooth and the preliminary slope $\Delta\gamma = 0$. In this case, the law of the distribution of the contact pressure is defined with the help of the factor $\psi(\chi)$.

The most actual profile (from the practical point of view) is the straight-sided (trapezoidal) profile of the tooth of a pulley with the angle of a space, which is more than the angle of the profile of a belt tooth, or a round profile (Fig. 4.34, a).

There is an angle of a preliminary inclination of lateral sides of teeth $\Delta\gamma$ for the given variants of a design. For the variant in Fig. 4.34, b at $\Delta\gamma = 3 \dots 4^\circ$ the width of the area of contact is equal to the width of a straight-line part of the lateral side of the belt tooth δ at $r_2 = 0$ and $P > (2...3.5)m$, N/mm. The analysis of the expression (4.14) shows that the change across the width of the area of contact at $P = \text{const}$ is linear with the angular factor:

$$\theta = \frac{\pi E \alpha \cos \gamma}{2(1 - \mu^2) P}$$

In this case, the maximum value $\psi(\chi)_{\text{max}}$, depending on the angle $\alpha = \Delta\gamma$ and loadings P at $r_2 = 0$, is determined. In Fig. 4.44 the dependences of $\psi(\chi)_{\text{max}}$ at $r_2 = 0$ are given (dashed lines).

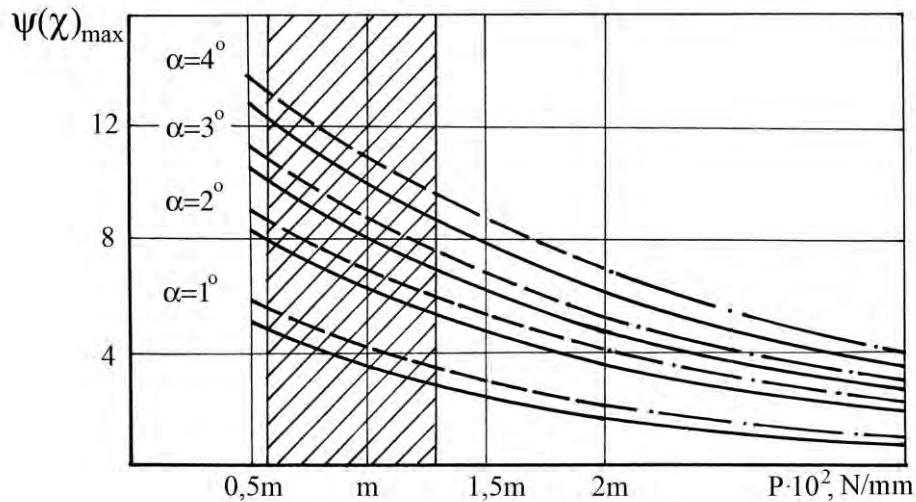


Fig. 4.44. Dependences of the factor $\psi_{\max}(\chi)$ at the presence of the difference of the profile angles of teeth

$X = 0,25(b'' + a'')$ is accepted as a maximum X , where b'' is defined by means of the graph in Fig. 4.38 at the existence of the radius of rounding of the tip of the tooth of a pulley. The dependences of $\psi_{\max}(\chi)$ at $r_2 = 0,3m$ (continuous lines) are also constructed in Fig. 4.44. The marked zone corresponds to the operational loadings, taken up by the belts.

The analysis of the received dependences testifies to the significant influence of the slope of lateral sides on the concentration of the contact pressure in the base of the tooth of a belt. In the case of a straight-sided (trapezoidal) profile of teeth at $\Delta\gamma = 1^\circ$ the maximum pressure in the indicated zone increases by 30...40 %.

Thus, the reduction of the angle of a space of a pulley in comparison with the angle of the profile of the tooth of a belt, on the one hand, improves gearing conditions, i.e. the profile interference decreases, on the other hand, it leads to the substantial increase of the concentration of the contact pressure in the base of the tooth of a belt. The maximum difference of the angles should be no more than 10° at $\gamma_{\text{ш}} > \gamma_{\text{п}}$ and at the absence of clearance.

As it was mentioned above, the complete physical contact of teeth at $P = 7 \text{ N/mm}$ for the transmissions with the module $m = 4$ and 5 mm is observed up to the complete geometrical contact, corresponding to the ending of the input in gearing. The similar situation is observed for the profile *HTD*, which can be replaced by the straight-sided profile with a conventional slope $\alpha_e = 10$ and $\epsilon_{\max} = 3$.

Abstracting from the representation of a tooth of a belt in the form of a contacting half-plane, we evaluate the influence of the actual geometry of a profile. For the solution of the given problem we use the conformal transformation of the right angle on a half-plane with the use of the function of a complex variable. The half-lines, parallel to the sides of the right angle, are transformed to semiparabolas with the common focus O' (Fig. 4.45).

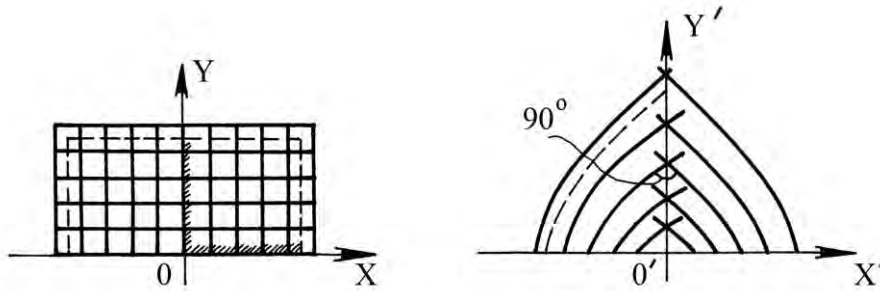


Fig. 4.45. Explanatory notes are given in the text

The figures are deformed, but the angles between two curves are remained. Thus, the coordinate lines are transformed into two classes of the focused parabolas. If the angle of the profile is $2\gamma = 50^\circ$ or 40° , which corresponds to the standard geometry of trapezoidal teeth, the mapping function is not expressed as the elementary one.

For the given case the contact of teeth can be presented as the contact of the rigid press tool with the elastic half-strip, having a rigid sealing (Fig. 4.46).

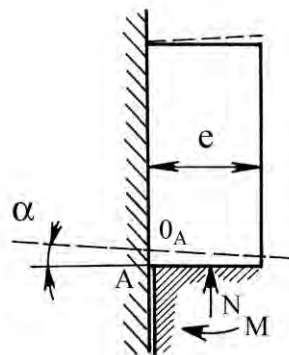


Fig. 4.46. Explanatory notes are given in the text

The boundary conditions on an area of the contact remain unchanged. Missing some transformations, we receive the following expression for the accepted calculation scheme:

$$p_x = \frac{N}{e} \cdot \frac{\cos \pi \rho}{\left(\operatorname{ch} \frac{\pi e}{S_{\max}} + 1 \right)^{0,5-\rho}} \left[\frac{\operatorname{ch} \frac{\pi e}{S_{\max}} - \operatorname{ch} \frac{\pi x}{S_{\max}}}{\operatorname{ch} \frac{\pi x}{S_{\max}} - 1} \right]^{0,5-\rho}, \quad (4.27)$$

where S_{\max} – the largest conventional width of the tooth of a belt (the width of the base of the belt tooth without taking into account the roundings).

If the expression (4.27) is written down in the form of the formula (4.18) and $\chi = \eta e$ is accepted, after the simplifications, we receive:

$$\psi_\eta = \frac{\cos \pi \rho}{\operatorname{ch} \pi \rho} \left[\frac{\operatorname{ch} \pi q - \operatorname{ch} \pi q \eta}{\operatorname{ch} \pi q \eta - 1} \right]^{0,5-\rho}, \quad (4.28)$$

where $q = e / S_{\max}$.

It follows from the expression that at the constant factor of friction the distribution of the contact pressure depends only on the value q , which is the geometrical characteristic of the deformed area.

Thus, the rigidity of the half-plane is equal in all the points and depends on the elastic constants; the rigidity of the half-strip decreases in the process of the removal from the fixed end.

Substituting the values $e = b$ and S_{\max} , expressed as the module (step) for all the types of belts with trapezoidal teeth, to the expression (4.28) we receive $q = 0.515$.

In Fig. 4.36 the dependence (dashed line) of the change of the contact pressure in the dependence (4.28) at the factor of friction $f = 0.5$ is presented. The comparison of the given dependence with the similar one, constructed according to (4.21) with the same factor of friction, testifies to their insignificant divergence, especially in the part, adjoining an angular point of the belt tooth A .

As the length of the contact is insignificant and the ratio $e / S_{\max} \rightarrow 0$, the rigidity of the tooth of a belt in the zone of the tip is lowered not in such a degree, that the nature of a curve of the contact pressure near the point B differs greatly from the received one at the interaction of teeth in the form of a rigid press tool and a half-plane.

Thus, the calculation technique of the contact pressure in a **toothed**-belt gearing is developed. The main factors, promoting its lowering, are defined. It is theoretically estab-

lished that the existence of rounding of the tip of trapezoidal teeth of a pulley reduces the contact pressure of teeth of a belt. The optimum value of the radius $r_{2III} = (0.32 \dots 0.34)m$, at which the contact pressure decreases 1.2...1.3 times, is determined.

At the same time, optimization of a working profile of trapezoidal teeth of pulleys **of toothed**-belt transmissions does not allow to reach high parameters of the working ability, and, first of all, the transferred power and durability. The reason is the interference of the compliant **elastomer** trapezoidal teeth of a toothed belt and, as a consequence, the significant non-uniformity of the distribution of normal and tangential stresses on the volume of teeth. It follows that the engineering methods of optimization of the working profile of trapezoidal teeth with the purpose of increasing of their working ability, considered in the theory and practice of toothed-belt transmissions, are practically exhausted.

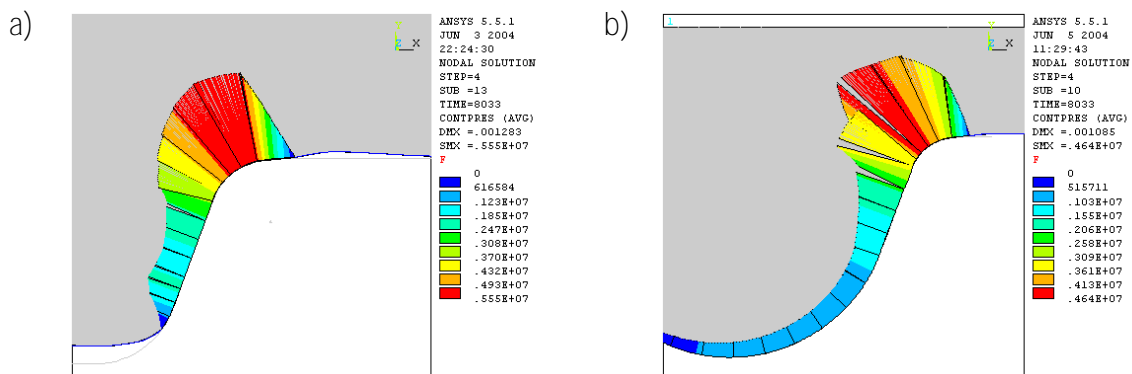


Fig. 4.47. Distribution of the contact pressure in gearing of trapezoidal (a) and semicircular (b) teeth

The computer modeling of the stress-strained state of the optimized trapezoidal (Fig. 4.47, a) and semicircular teeth (Fig. 4.47, b) in ANSYS shows that the maximum contact pressure in gearing of the semicircular teeth (under otherwise equal conditions) decreases by 19.6 % [160].

Therefore, the **toothed**-belt transmissions with the semicircular profile of teeth *HTD*, outlined in the end section by the arc of a circle with the radius of tips r_{2III} are more progressive with the raised engineering level.

4.6. Conclusions

1. The modern technology of toothed belts by the method of pressing of the rigid elements, characterized by the lowered energy and materials consumption, the raised characteristics of belts and ecological cleanliness has been developed.

2. The rational parameters of the engineering process of the belt manufacture (pressure, temperature and duration of vulcanization), allowing to increase their operational resource by **65...70 % and to lower the labor cost by 10 %, have been offered.**

3. The modern designs and the technology of the assembly of toothed belts with sleeve-loopback reinforcement have been presented. The stress-strained state of the developed belts by the method of the finite elements in ANSYS has been investigated. It has been established that the sleeve-loopback reinforcement allows to lower stresses and **deformations by 75...85 % in the** dangerous section, which allows to recommend the given **toothed**-belt transmissions instead of the chain ones in the energy-intensive drives of the processing equipment.

4. The herringbone toothed-belt transmission with the raised technical and ecological characteristics, having the correction of the slopes of teeth of pulleys relating to the slope of teeth of the belt, defined by the kinematic and force features of gearing of teeth, has been developed. The correction of slopes of teeth of herringbone pulleys **makes 10...15 % of a slope** of belt teeth.

5. The calculation technique of the contact pressure in a toothed-belt gearing has been developed and the main factors, promoting its decrease, have been defined. It has been established theoretically that the existence of rounding of the tip of trapezoidal teeth of a pulley reduces the contact pressure of the belt teeth. The optimum value of the radius $r_{2III} = (0.32...0.34)m$, at which the lowering in contact pressure 1.2...1.3 times occurs, has been defined. On the basis of the computer finite-element modeling in ANSYS it has been established that the more effective profile (from the point of view of minimization of the contact pressure in gearing) is a semicircular profile of teeth *HTD*. The maximum contact pressure in gearing of the latter ones (under the equal conditions) decreases by 19.6 % in comparison with the optimized trapezoidal profile.

Chapter 5. LOAD CARRYING CAPACITY AND OPERATIONAL RESOURCE OF TRANSMISSIONS OF POWER BY FLEXIBLE LINK

5.1. Wear resistance of toothed belts

It is shown in the work [24] that the most acceptable for the calculation of the durability of teeth of a belt by the tribological criterion is the power method, based on the following dependence:

$$l = l_0 P_{fr}^{\chi}, \quad (5.1)$$

where l – the intensity of deterioration; l_0 – the intensity of deterioration at the unit power of friction; P_{fr} – power friction; χ – the parameter, depending on the material, characteristics of a counterbody and the conditions of loading.

Differentiating (5.1) by time, we receive:

$$\frac{dl}{dt} = \frac{dl_0}{dt} P_{fr}^{\chi}. \quad (5.2)$$

The power of friction at an input of teeth in gearing is not constant, since the force F_{11} and the speed of sliding of teeth v_{sl} change during the turn of a pulley by the angle ψ_1 : F_{11} – increases linearly, v_{sl} – decreases non-linearly. The instant value of the power of friction, corresponding to the turn of a pulley by the angle φ_x within the limits $0 \leq \varphi_x \leq \psi_1$, can be written in the form:

$$P_{fr.x} = F_{fr.x} v_{sl.x}. \quad (5.3)$$

In view of the linear increase of F_{11} **we can find the** force of friction $F_{fr.x}$, proceeding from the ratio:

$$F_{fr.x} = F_{11x} f_{fs} = F_{11} \frac{\varphi_x}{\psi_1} f_{fs} = \frac{F_1 \psi f_{fs} \varphi_x}{z_0 \psi_1}. \quad (5.4)$$

According to the expressions (2.34) and (5.4), the dependence (5.3) becomes:

$$P_{fr.x} = \frac{F_t \omega \psi f_{fs} \Phi_x}{z_0 \psi_1} \left[F_1 \left(\frac{\Phi_x}{\psi_1} \right)^c + F_2 \right]. \quad (5.5)$$

We receive the total work of the friction force for one cycle of an input in gearing by the time integration (5.5):

$$A_{fr} = \int_0^t P_{fr.x} dt = \int_0^{\psi_1} \frac{P_{fr.x} d\varphi}{\omega} = \frac{F_t \psi f_{fs} \psi_1 k_{vsl}}{z_0}.$$

where $k_{vsl} = \left(\frac{F_1}{c+2} + \frac{F_2}{2} \right)$ – the factor, considering the speed of the relative sliding of teeth in contact (Tab. 5.1).

Tab. 5.1. Values of the factor of the sliding velocity of teeth

Type of teeth	Module m , mm	k_{vsl}
semicircular	3.0	1.71
	4.0	2.26
	5.0	4.48
trapezoidal	1.0	1.0
	1.5	1.19
	2.0	1.59
	3.0	1.83
	4.0	2.15
	5.0	4.29
	7.0	6.11
10.0	9.13	

Considering the power of friction and averaging the received value, we have:

$$P_{fr} = \frac{F_t \psi f_{fs} \omega k_{vsl}}{z_0}. \quad (5.6)$$

The values (5.2) of intensity of deterioration **and the figure χ can be defined on the basis of empirical results.** It is necessary to start with the fact that the rules of deterioration of facing and rubber are different.

The above-mentioned parameters for a rubber mass of the tooth are defined by the author [24]. Meanwhile the wear of facing precedes the wear of rubber. Hence, the above-named technique is good for the definition of the durability of teeth, deprived of fabric facing. All the above considered, the durability of a belt by the criterion of wear of teeth is defined by the dependence:

$$N_w = N_1 + N_2, \quad (5.7)$$

where N_1 , N_2 – the durability of facing and the rubber mass of the tooth of a belt, cycles.

For the mould belts at $N_1 = 0$ the expression (5.7) is transformed into the following form:

$$N_w = N_2.$$

The durability of facing is defined by the dependence:

$$N_1 = \frac{h_f}{h_{1f}}, \quad (5.8)$$

where h_f – the thickness of facing; h_{1f} – the thickness of facing, wearing for one cycle of loading.

Coming to the unit power of friction, the value h_{1f} is defined from (5.1):

$$h_{1f} = h_{1f} P_{ff}^{\chi_f}, \quad (5.9)$$

where h_{1f} – the thickness of facing, wearing at the unit power of friction for one cycle of loading.

In the works [43, 46] **the values** $\chi = 0.9...1.4$ for rubbers or **rubber-cord** designs, for example, auto-tyres, are resulted. In the work [24] **it is recommended that** $\chi = 1.2$ for toothed belts. It is obvious that the given values cannot be used for the fabric facing, which is not made of rubber. Nevertheless, the facing is made of polymeric material and the gen-

eral rules of wear of polymers, including rubbers, can be used for the description of wear of fabric.

On the basis of (5.9) the expression (5.8) can be presented in the form:

$$N_1 = \frac{h_f}{h_{11f} P_{ff}^{\chi_f}}. \quad (5.10)$$

In such a form the expression (5.10) is unsuitable for calculations. At the known value h_f ; and the value P_{ff} , determined by (5.6), this expression contains two unknowns h_f and χ_f .

For the determination of h_f and χ_f we write down (5.10) for two modes of tests, characterized by the kinematic similarity, i.e. $v_{p(1)} = v_{p(2)}$; $Z_{1(1)} = Z_{1(2)}$; $u_{(1)} = u_{(2)}$. In other words, for both modes of tests the parameters, defining kinematics of an input of teeth in gearing, should be constant. The transferred specific circumferential force F_t should be changed.

The tests are carried out up to the complete wear of facing. In the moment of denudation of rubber mass of teeth the durability of facing for both modes $N_1^{(1)}$ and $N_1^{(2)}$ is registered. Having defined $P_{ff}^{(1)}$ and $P_{ff}^{(2)}$, the system of the equations can be solved:

$$\begin{cases} N_1^{(1)} = \frac{h_f}{h_{11f} P_{ff}^{(1) \chi_f}}; \\ N_1^{(2)} = \frac{h_f}{h_{11f} P_{ff}^{(2) \chi_f}}. \end{cases} \quad (5.11)$$

Two lots (six pieces in each one) of belts are subjected to resource tests. The parameters of transmission: $m = 3$ mm; $z_p = 60$; $z_0 = 8$; the modes of tests: 1) $F_t = 6$ N/mm, $\psi = 1.2$; 2) $F_t = 12$ N/mm, $\psi = 1.76$. It is established that $N_1^{(1)} = 1.85 \times 10^7$ cycles; $N_1^{(2)} = 2.85 \times 10^6$ cycles. In the result of the solution (5.11) we have $h_{11f} = 2.5 \times 10^{-13}$ mm; $\chi_f = 1.75$.

At the determination of N_2 the limiting wear division of a tooth by the thickness of the layer, wearing for one cycle of loading, is not correct. The similar approach is acceptable to the calculation of N_1 , when the reduction of thickness of facing slightly influences mechanical and physical properties of teeth, in particular, its rigidity.

The rigidity of teeth decreases non-linearly, depending on the thickness of the wearing layer [90]. As a result, the moment comes when the teeth become unable to transfer the pull. The "jump" of teeth of a belt on teeth of pulleys takes place and non-synchronization of transmission begins.

The value of a wearing layer of the mass of teeth of a belt h_{1r} increases constantly, because of the increase of their compliance and the augment of the tangential displacement Δ (Fig. 5.1) [161].

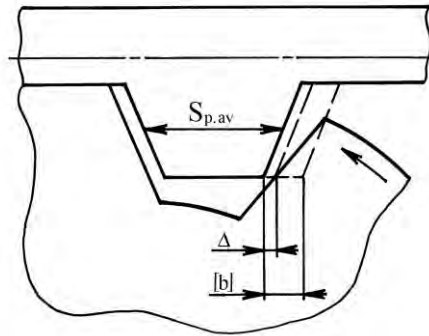


Fig. 5.1. Tangential displacement of teeth of a belt

Let's write the expression (5.8) for the rubber mass of teeth of a belt at the absence of fabric facing on them:

$$N_2 = \frac{h}{h_{1r}}, \quad (5.12)$$

where $[h]$ – the limiting wear of the teeth of a belt.

The use of the technique of finding of the parameters of the equation, describing the wear of rubber of a belt tooth by the technique, offered for the definition of the wear of facing, is impossible. Actually, from (5.12) we receive:

$$N_2 = \frac{h}{h_{11r} P_{fr}^{\chi_r}}, \quad (5.13)$$

where h_{11r} – the thickness of a layer of the belt teeth, wearing at the unit power of friction for one cycle of loading; χ_r – the exponent, describing the wear of rubber.

The value of the limiting wear can be defined from the condition of preservation of gearing. In the work [21] it is established that at the limiting tangential displacement of teeth $[b] = (1.6...1.95)\Delta$ (see Fig. 5.1) their durability does not exceed several hundred cycles. The real observable tangential displacement b is defined by the deformation of the first tooth of an arc of contact, which is in the full gearing b_1 , and by the lengthening of a belt in the part between the examined teeth Δt_p :

$$b = b_1 + \Delta t_p. \quad (5.14)$$

The expression (5.14) can be written in the expanded form:

$$b = \frac{F_t \Psi}{EZ_d z_0} + \frac{F_{11}^{1-k} t_p}{a},$$

where k , a – the parameters of the equation.

As $[b] = (1.6...1.95)\Delta$ is maximum permissible, we equate $[b] = b$, and find the minimum permissible rigidity of the worn out tooth [162]:

$$EZ^{(w)} = \frac{F_t \Psi}{z_0 \left(b - \frac{F_{11}^{1-k} t_p}{a} \right) k_{Zd}}.$$

We accept $[b] = 1.6\Delta$, where

$$\Delta = m \left[\sin \gamma \left(\frac{z_{\text{ш}}}{2} - k_1 \right) + k_2 \operatorname{tg} \beta_p - z_{\text{ш}} \frac{\gamma}{2} \right];$$

$$\gamma = \arccos \left(1 - \frac{2k_2}{z_{\text{ш}}} - k_1 \right); \quad k_1 = \frac{\delta}{m}; \quad k_2 = \frac{h_p}{m}.$$

After the transformations we get:

$$b = S_p \left(\sqrt[1,5]{0,91 \left[1 - \frac{F_t \psi}{z_0 \left(b - F_{11}^{1-k} t_p / a \right) EZ_d} \right]} \right),$$

The influence of wear on the rigidity of teeth of a trapezoidal profile is defined in the work [90]:

$$EZ^{(w)} = EZ \left(1 - 1,1 \left(\frac{h}{S_p} \right)^{1,5} \right). \quad (5.15)$$

In particular, $[h] = 2.2 \text{ mm}$ or $0.687 S_p$ is received for the belts with the module $m = 3 \text{ mm}$; $z_0 = 8$; $F_t = 6 \text{ N/mm}$ and $\psi = 1.2$ $[h] = 2.2 \text{ mm}$ or $0.687 S_p$. Under the same conditions and at $F_t = 10 \text{ N/mm}$, $[h] = 1.31 \text{ mm}$ or $0.410 S_p$.

The value h_{1r} is defined on the basis of the results of the stand resource tests. The average thickness of teeth $S_{p.av}$ of the assembly belts with the removed facing (3-60-16) and mould belts (3-60-16) is measured with the help of the tool microscope MMI-2. Then the **belts are established on the stand for resource tests. The tests are carried out during $3 \cdot 10^4$ cycles of loading at the fixed value of the pull.** After that the average thickness of teeth $S_{p.av(w)}$ is measured again, and their wear $h_1 = S_{p.av} - S_{p.av(w)}$ is defined.

In such conditions the wear is described by the system of the equations:

$$\begin{cases} N_2^{(1)} = \frac{h_1}{h_{1r} P_{fr}^{(1)} \chi_r}; \\ N_2^{(2)} = \frac{h_2}{h_{1r} P_{fr}^{(2)} \chi_r}. \end{cases}$$

In view of the equal duration of tests we have:

$$\frac{h_1}{h_{1r} P_{fr}^{(1)} \chi_r} = \frac{h_2}{h_{1r} P_{fr}^{(2)} \chi_r} \quad (5.16)$$

The values of power of the friction from the expression (5.16) are determined by means of the expression (5.6).

As a result of the researches it has been established that the values h_{1r} and χ_r do not depend on manufacturing techniques of the belts, and are basically determined by the hardness of rubber. For the rubber mixtures, used at manufacturing of toothed belts, the dependences h_{1r} and χ_r on the hardness of material are presented in Fig. 5.2. The analysis of the dependences testifies that the increase of the hardness of belt teeth considerably increases their durability. The increase of HS from 64 to 85 units results in the increase of N_2 2.8 times.

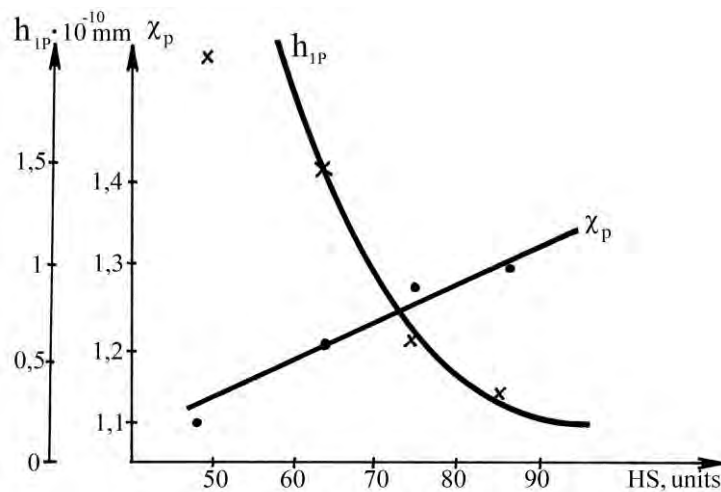


Fig. 5.2. Dependence of the parameters of wear of belt teeth on their hardness

The carried out researches show that the developed method of determination of the durability of teeth of toothed belts by the tribological criterion allows to predict it with the satisfactory accuracy [163].

5.2. Fatigue strength of toothed belts

Nowadays the calculation of the fatigue strength of belt teeth is based on the results of resource tests of toothed-belt transmissions, which are statistically processed.

In the work [24] the adhesive model of the formation of a fatigue crack in the base of teeth of a belt is offered. However, in this case, only a shear component is taken from the complex of operating loadings (shear, compression, bending).

At first, such an approach seems justified, since in general the shear deformations make more than 30 % [21, 23]. Nevertheless, the authors have not received the explanation of the fact that the fatigue crack is formed from the belt tooth side, contacting with a driven pulley. The role of adhesion in the formation of a fatigue crack has not found its acknowledgement either.

Actually, the volume of a bearing layer in the volume of a belt is minor. Taking it into account, the expression for the calculation of durability, caused by adhesive forces, is possible only for toothed belts, which teeth are vulcanized to the bearing layer in the form of a metal or polymeric tape.

In order to prove that the fatigue life of belt teeth is defined by the complex of factors, but not only by the adhesion of rubber to the bearing layer, we show the following causes.

Let's consider the process of formation of a fatigue crack. The analysis of the reasons of the loss of the working ability of toothed belts testifies that the crack arises in the zone of transition of an interdental space to a lateral surface of a tooth. On the assumption that the occurrence of the fatigue crack is the consequence of the destruction of the adhesive connection, it would arise not on a surface of a tooth, where there are no adhesive connections, but in its base, contacting with a bearing layer.

Thus, the formation of the fatigue crack is the consequence of the action of not only shear forces. Analyzing the diagrams of the distribution of the tangential stresses in the material of belt teeth and on the interface "tooth – bearing layer" [34, 89], it is established, that their maximum values are observed in the zone of crossing of the straight lines, which make up the continuation of a lateral surface of the belt tooth and the surface of the thread of a bearing layer, which is the nearest to the base of the tooth. Hence, the concentration of shear stresses is inside of the volume of the tooth, but not on its surface.

Let's make the following example. The results of the researches of the stress-strained state of teeth testify to the non-uniform distribution of tangential stresses in the bases of trapezoidal teeth and practically uniform distribution in the bases of semicircular teeth. In this case, the localization of the maximum stresses and deformations in the teeth of a semicircular profile is observed in the zone, which is near the axis of symmetry of a tooth.

However, the results of resource tests of belts *HTD* testify to the similar character of the fatigue failure. The crack appears on the surface of a tooth and progresses along a normal to the radius of rounding up to the denudation of a bearing layer [164]. The crack extends at the angle 25...30 with the axis of a bearing layer (Fig. 5.3, a) and its length is $(0.2...0.3) S_{p.av}$.

About 30...35 % of the tested belts have shown the modified fatigue failure of teeth (Fig. 5.3, b), consisting in the distribution of a crack on some distance from the surface of a bearing layer. The similar destruction is fixed for the belts with trapezoidal teeth [57, 164].

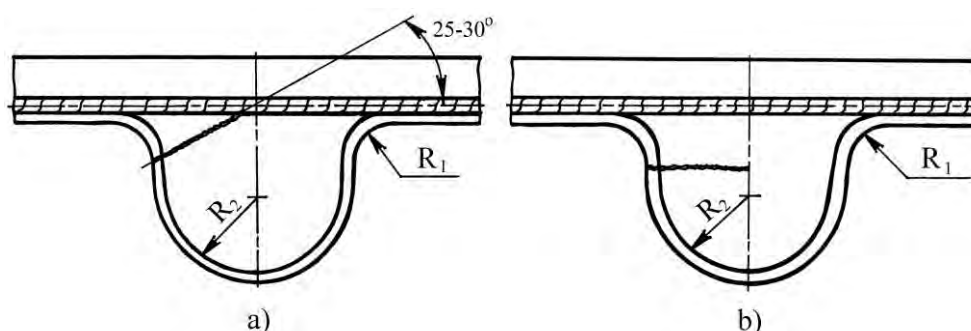


Fig. 5.3. Kinds of the distribution of a fatigue crack of teeth *HTD* of a profile

Thus, the fatigue failure of teeth of a belt is cohesion-adhesive with a prevalence of the first factor and the absence of the second one in some cases. The insignificant influence of the adhesive factor follows from the circumstance that the period of time from the occurrence of the crack up to its distribution along the length, corresponding to the loss of the load **carrying capacity of teeth, makes only 5...8 % of the durability N_f** . First of all, it is connected with a sharp increase in the concentration of stresses in the tip of the crack in comparison with the rounded part of transition of an interdental space to a lateral surface of a tooth. Hence,

$$N_f = N_b + N_d, \quad (5.17)$$

where N_b ; N_d – the fatigue durability of belt teeth before the origin of a crack and its distribution up to the limiting condition of teeth accordingly.

Accounting the above-stated calculations the expression (5.17) becomes $N_f \approx (1.05...1.08)N_b$. At the same time, the destruction of an adhesive layer between the

elastomer and the cord is observed at the stage, corresponding to N_d . Hence, the account of the adhesive factor of the destruction of teeth does not apply essential correction in the accuracy of the definition of the value N_f . The greatest interest, from the practical point of view, is presented by the stage N_b , where the durability of teeth should be defined on the basis of the equations of the durability of rigid bodies.

In this connection we can consider the formation of a fatigue crack from the tooth side, interacting with a driven pulley, as the existing techniques of prediction of the durability do not allow to explain this fact.

At an input of teeth in gearing the friction force F_{fr11} promotes the compression of a lateral surface of the belt tooth (Fig. 5.4). The opposite side of the belt tooth lengthens. It also lengthens at an output from gearing with a driven pulley, since the friction force F_{fr12} has an opposite direction. The friction forces in gearing of teeth, located at the following side, cause smaller deformations of the tension-compression of teeth (in view of $F_2 < F_1$).

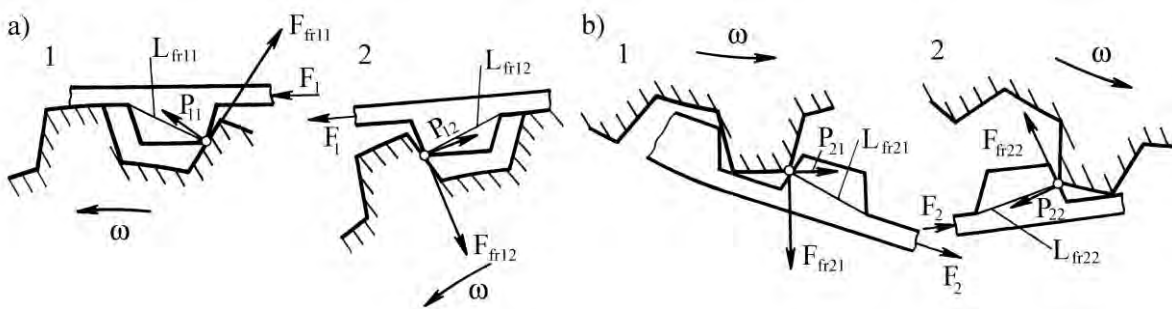


Fig. 5.4. Direction of friction forces in a **toothed**-belt transmission:
a) driving side; b) following side; 1 – drive pulley; 2 – driven pulley

Besides, the given forces create bending moments, various in size, influencing the belt tooth. The values of the arms of the influence of the friction forces F_{11} (F_{12}) and F_{21} (F_{22}) are equal accordingly:

$$L_{fr11} = L_{fr12} \approx \frac{h_p \cos^2 \beta_p}{\sin \left[\arctg \frac{\frac{h_p}{\cos \beta_p} - S_p}{\frac{h_p}{\cos \beta_p} + S_p} \operatorname{ctg} \left(\frac{90^\circ + \beta_p}{2} \right) + 90^\circ - \frac{90^\circ + \beta_p}{2} \right]}; \quad (5.18)$$

$$L_{fr21} = L_{fr22} \approx S_p + 2h_p \operatorname{tg}\beta_p. \quad (5.19)$$

Having the values of the loadings, influencing the teeth, we receive the expressions for the determination of stresses, acting in their material. In this case, the effort, acting on the belt tooth, can be put not in the middle of its lateral side, but in the tip (see Fig. 5.4), contrary to the approach, offered in the work [165]. It corresponds to the kinematic features of an input trajectory. Chapter 2 shows that the initial contact of teeth occurs in the point, located in the rounded part of transition of the tip of the belt tooth to its lateral side.

The results of the researches in the work [166] allow to make the following conclusion: the disconnection of teeth at an output from gearing with a driven pulley takes place in the point at a height of $(0.3...0.4)h_p$ from the surface of an interdental space. Hence, at the output from gearing with a drive pulley the application of the loading in the middle part of the lateral surface of teeth of a belt can be justified.

Let's make the calculation scheme for the receiving of the dependences of the basic stresses, acting in the belt teeth, of the main parameters of transmission (Fig. 5.5).

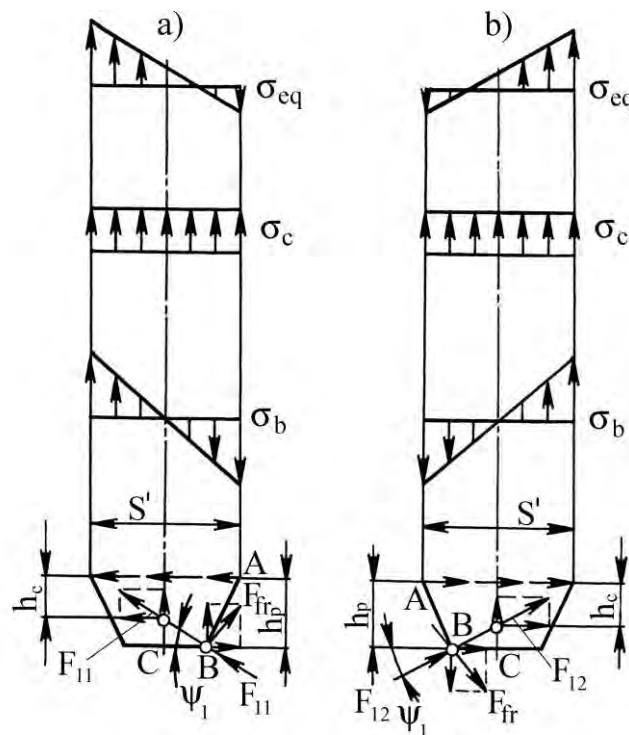


Fig. 5.5. Distribution of stresses in the material of belt teeth:
a) at an input in gearing; b) at an output from gearing

At an input of teeth in gearing we have the following values of stresses:

– bending stress:

$$\sigma_b = \frac{6F_{11}}{S_p + 2h_p \operatorname{tg}\beta_p} \left[\cos \psi_1 h_p - \sin \psi_1 \left(\frac{S_p}{2} + f_{fs} h_p \right) \right]; \quad (5.20)$$

– compression stress:

$$\sigma_c = \frac{F_{11}}{S_p + 2h_p \operatorname{tg}\beta_p} \left[\sin \psi_1 + f_{fs} \cos \psi_1 \right]; \quad (5.21)$$

– shear stress:

$$\tau = \frac{F_{11}}{S_p + 2h_p \operatorname{tg}\beta_p} \left[\cos \psi_1 - f_{fs} \sin \psi_1 \right]. \quad (5.22)$$

The normal resultant pressure in the point B ($\sigma_{pr} = \sigma_b + \sigma_c$) depends on the ratio of the values f_{fs} and ψ_1 . The existence of the tension of bending in the point B is connected with the fulfillment of the condition:

$$\frac{1}{f_{fs} + \frac{S_p}{2h_p}} \geq \operatorname{tg}\psi_1. \quad (5.23)$$

Thus, for example, at $\psi_1 = 10^\circ$; $m = 7$ mm and $f_{fs} = 0.1$ and 0.4 , according to (5.23), we receive $1.304 > 0.176$ and $0.937 > 0.176$ accordingly. Hence, the occurrence of the tension stresses in the point B at an input in gearing is practically inexplicable.

The shear of the belt tooth in the direction of the action of the force F_{11} will dominate over the shear from the friction forces in the case of the fulfillment of the condition:

$$\frac{1}{f_{fs}} \geq \operatorname{tg}\psi_1. \quad (5.24)$$

We receive the following values of stresses for the output from gearing (see Fig. 5.5):

–bending stress:

$$\sigma_b = -\frac{6F_{12}}{S_p + 2h_p \operatorname{tg}\beta_p} \left[\cos \psi_1 h_p + \sin \psi_1 \left(\frac{S_p}{2} + f_{fs} h_p \right) \right]; \quad (5.25)$$

–compression stress:

$$\sigma_c = \frac{F_{12}}{S_p + 2h_p \operatorname{tg}\beta_p} \left[\sin \psi_1 - f_{fs} \cos \psi_1 \right]; \quad (5.26)$$

– shear stress:

$$\tau = \frac{F_{12}}{S_p + 2h_p \operatorname{tg}\beta_p} \left[\cos \psi_1 + f_{fs} \sin \psi_1 \right]. \quad (5.27)$$

The presence of the compression or tension in the point B depends on the ratio of ψ_1 and $\operatorname{arctg}f_{fs}$. At $\psi_1 > \operatorname{arctg}f_{fs}$ the stress of the compression from the force F_{12} dominates over the compression by the friction forces.

The ratio σ_b and σ_c is of interest at the various $F_{11(12)}$ and f_{fs} . So, at any $F_{11(12)}$ and the increase of f_{fs} from 0.1 up to 0.2; 0.3; 0.4 the ratio σ_b / σ_c changes in the following way: 9:1; 6.6:1; 5:1; 4:1. It can be explained by the fact that at the relatively constant values of σ_b the vertical component of the friction force $F_{11}f_{fs}\cos\psi_1$ increases and σ_c increases too. The ratio σ_b / τ is approximately constant and equal to 2.5:1. Thus, the bending stress has the largest value at an input in gearing and the compression stress has the minimum value. At the increase of ψ_1 from 10° up to 20 and 30° the value σ_{pr} increases 1.17 and 1.44 times accordingly.

The similar ratios are also observed at an output of teeth from gearing. Thus, the increase of ψ_2 from 10° up to 20 and 30° promotes the growth of σ_{pr} 1.25 and 1.76 times accordingly. The more intensive growth of σ_{pr} with the increase of ψ is connected with the opposite direction of σ_b and σ_c .

According to the maximum strain energy theory the equivalent stress in the basis of teeth of a belt is equal to:

$$\sigma_{eq} = \sqrt{\sigma_b + \sigma_c^2 + 3\tau^2}. \quad (5.28)$$

The analysis of the dependence (5.28) for the point B at an input in gearing and an output from it shows that the values σ_{eq} are practically equal. The increase of σ_{eq}^{in} over σ_{eq}^{out} by 2...5 % is found. At the same time, the given values have different signs: σ_{eq}^{in} is the compression stress, σ_{eq}^{out} is the tension stress.

It is known that the fatigue crack (for the majority of machine-building details) arises in the part with prevailing tension stresses. It is characteristic of cog-wheels, fixing details, etc. [167]. Therefore, the occurrence of the fatigue crack from the belt tooth side, interacting with a driven pulley, becomes obvious. At an output from gearing with the given pulley in the zone of the point B of the belt tooth the maximum tension efforts act.

The corresponding pressure arising in teeth of a semicircular structure:

$$\sigma_b = \frac{1,5F_{11}}{R_2^2} h_c (\cos \psi_1 - \sin \psi_1 f_{fs}) - \sin \psi_1 R_2 ;$$

$$\sigma_c = \frac{F_{11}}{2R_2} (\sin \psi_1 + f_{fs} \cos \psi_1);$$

$$\tau = \frac{F_{11}}{2R_2} (\cos \psi_1 - f_{fs} \sin \psi_1),$$

where $h_c = h_p + R_2(\sin \psi_1 - 1)$; h_p, R_2 – see Tab. 1.8.

The analysis of the given dependences shows that in both cases the equivalent pressure to a great extent depends on the geometrical parameters of teeth of a belt defining the area of dangerous section.

Let's define the equivalent pressure arising in the basis of teeth of a belt with a trapezoidal structure at their input in gearing with teeth of a drive pulley. We shall accept the following parameters of transmission: $F_{11} = 50$ N/mm; $t_p = 14$ mm; $f_{fs} = 0.5$. Thus, $\sigma_{eq} = 23.07$ MPa. At similar parameters of toothed-belt drive with teeth of a semicircular

structure $\sigma_{eq} = 12.85$ MPa. Thus, use of a semicircular structure of teeth instead of trapezoidal allows lowering equivalent pressure in dangerous section by 44.3 %.

At hardware-software modeling of the stress-strained state of teeth of belts of trapezoidal and semicircular structures in *ANSYS* the results similar to theoretical calculation are received. For a trapezoidal structure $\sigma_{eq} = 23.1$ MPa, for semicircular $\sigma_{eq} = 12.9$ MPa. The received results testify to adequacy of the developed theoretical physical and mathematical models of the stress-strained state of teeth of belts of various structures to the real physico-mechanical processes occurring in gearing by transmission of capacity.

As all the force factors (bending, shearing and compressing loadings) act on the teeth of a belt together, there is no necessity to indicate the destruction criteria, corresponding to each kind of loading.

The equation of the durability of belt teeth in a general form can be written in the following way [168]:

$$\left(\frac{\sigma_{eq}}{[\sigma_{eq}]} \right)^{m_N} = \frac{N_b}{N_f},$$

where $[\sigma_{eq}]$ – the stress in the material of the belt tooth, corresponding to the basic level of durability N_b ; m_N – the exponent of the curve of fatigue of teeth.

If $m_N = 1$, $[\sigma_{eq}]_1$ corresponds to the stress at the single loading. Thus, the data **about the breaking strength of teeth** $\sigma_1 = [\sigma_{eq}]_1$ are necessary for the determination of N_f . **The value** σ_1 is determined by the dependence (5.28) with the help of the substitution of the value F_{12p} , corresponding to the minimum effort, causing the breaking off of the belt tooth at a single loading, into the formulas (5.25) – (5.27) (Tab. 5.2).

Taking it into account, the fatigue durability of the belt teeth is:

$$N_f = N_b \left(\frac{\sigma_r}{\sigma_{eq}} \right)^{m_N}, \quad (5.29)$$

where σ_r – the limit of endurance of teeth.

Tab. 5.2

Type of belt	Hardness of teeth HS	F_{12p} , N/mm
$m = 1$ mm (1-112)	77.2	17.4
$m = 1.5$ mm (1.5-53)	64.1	30.7
$m = 2$ mm (2-68)	75.0	33.5
$m = 3$ mm (3-48)	64.2	50.0
$m = 4$ mm (4-48)	73.7	56.5
$m = 5$ mm (5-100)	70.8	81.8
$m = 7$ mm (7-71)	70.5	142.0
$m = 10$ mm (10-96)	67.0	218.5
XL (130 XL)	69.3	30.8
XL (210 XL)	90.0	24.8
L (300 L)	71.6	43.9
L (210 L)	88.5	36.9
H (300 H)	71.9	52.9
H (300 H)	90.5	43.8

In figures 5.6, 5.7 dependences $\sigma_{eq} = f(F_{11})$ for toothed belts with a trapezoidal and semicircular structure of teeth of standard sizes existing now on a global scale are presented.

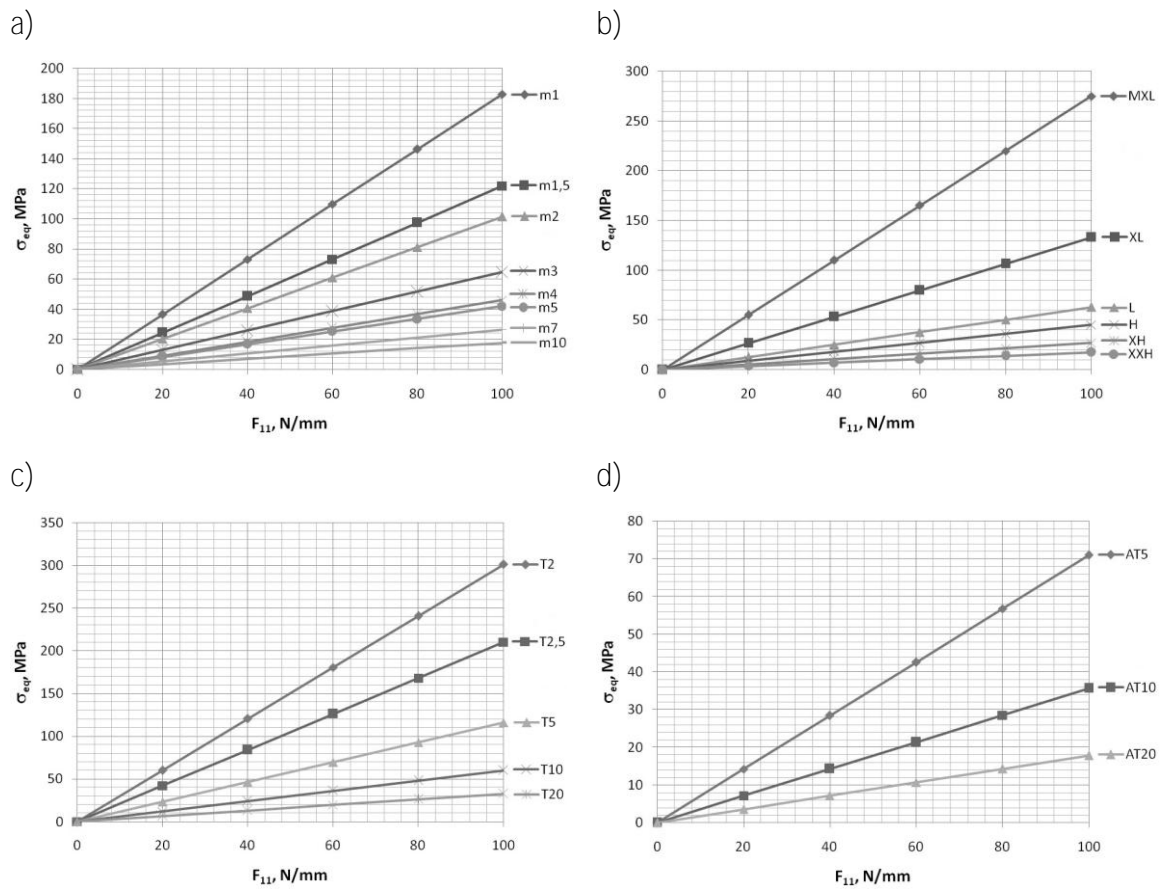


Fig. 5.6. Loading of teeth of belts with trapezoidal teeth: a) TU RB 00149438-073-95; b) ISO 5296; c) DIN 7721; d) AT (Automobile Transmission)

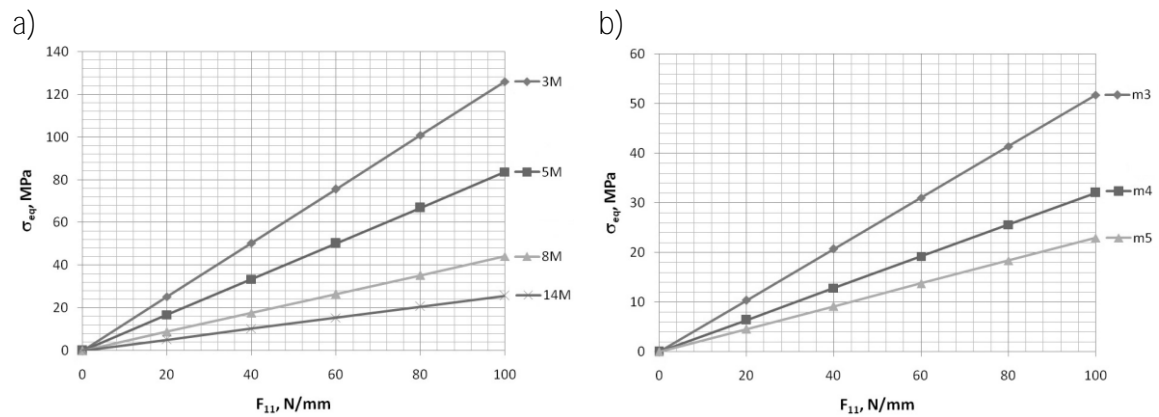


Fig. 5.7. Loading of teeth of belts with semicircular teeth:

a) HTD (ISO 13050); b) TU 38405560-84

It is necessary to note that the purpose of existing engineering techniques of design calculation of toothed-belt drives is a definition of the minimal width of the toothed belt meeting shown requirements to conditions of transmission of capacity and its size.

In a basis of the given techniques there is a choice of geometry of a working part and a step of teeth which is carried out on the basis of initial data about transferred capacity and frequency of rotation of a drive shaft by means of diagrams. In this connection the comparative analysis of a loading of teeth of belts of various standard sizes and structures with equal or close step of teeth represents significant practical interest. The results of a loading of teeth of toothed belts of various standards with step of teeth of a belt $t_p = 5$ and (8...10) mm are presented in figure 5.8.

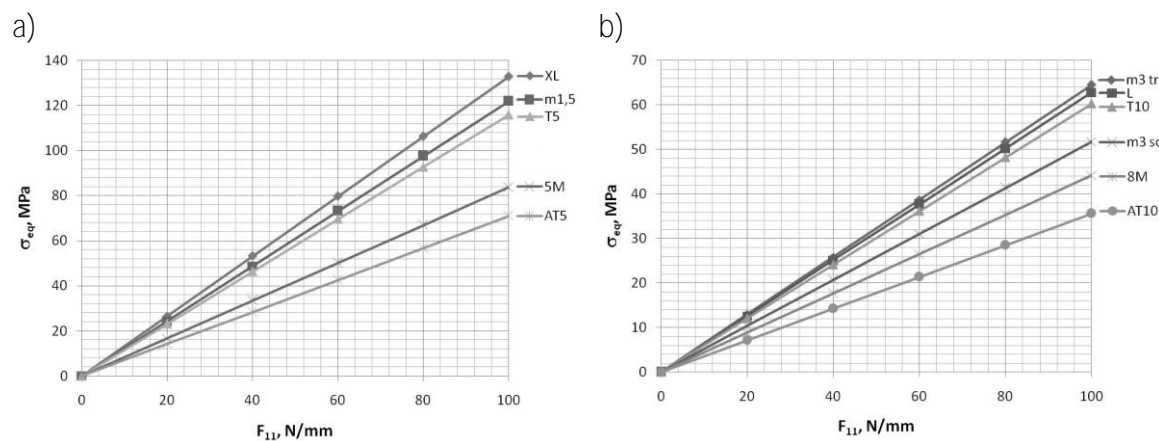


Fig.5.8. Loading of teeth of belts: a) $t_p = 5$ mm; b) $t_p = 8...10$ mm

The analysis of diagrams testifies that application of toothed belts with structure AT or a semicircular structure of teeth (instead of trapezoidal) allows lowering considerably

equivalent pressure in dangerous section, hence, in a corresponding measure it allows raising transferred capacity and an operational resource of toothed belts.

At preservation of the given parameters at the former level it is possible essential decrease in weight and dimensions of toothed-belt drive, hence, its dynamic loading, noise, vibrations and, at last, cost prices of manufacturing. We shall analyse the reasons for the given superiority of toothed belts with structure **AT** and a semicircular structure of teeth.

It has been above noted that the major factors defining a stress-strained state of teeth of a belt are its geometrical parameters. For the comparative analysis of the given parameters of toothed belts of various structures and standard sizes we shall enter relative scale factors: $k_1 = S_p / t_p$; $k_2 = h_p / t_p$; $k_3 = h_p / S_p$ and $k_4 = h_p / H_p$, where S_p , h_p , t_p and H_p – see Tab. 1.6-1.8. The results of calculation of scale factors are presented in Tab. 5.3.

Tab. 5.3. Scale factors of toothed belts

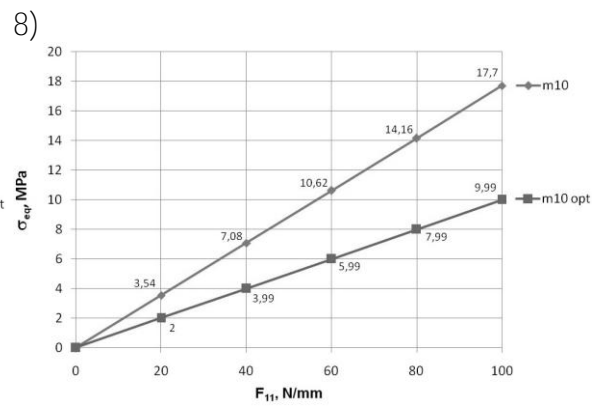
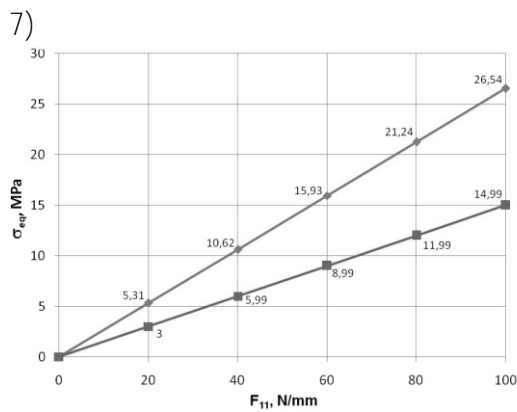
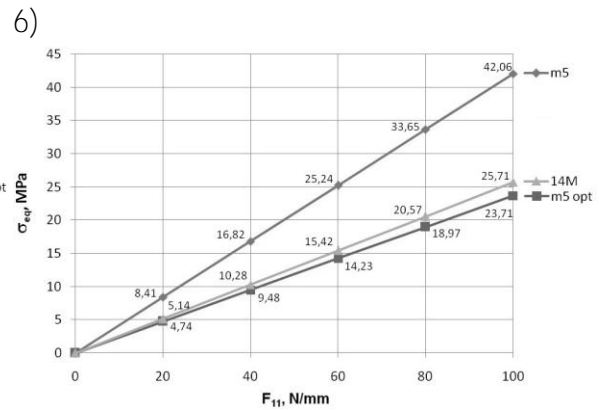
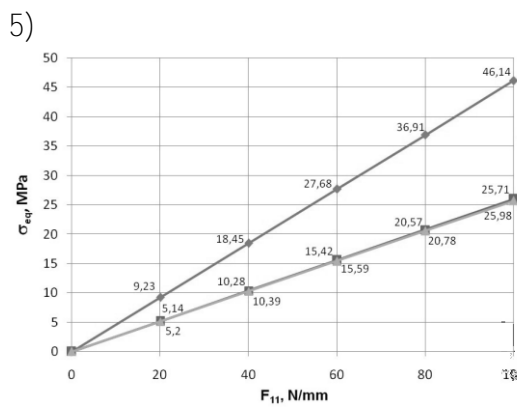
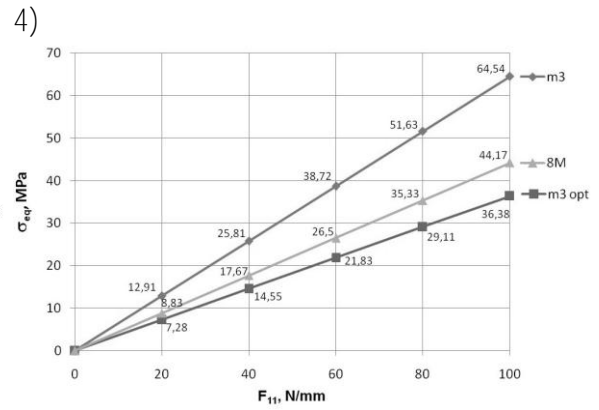
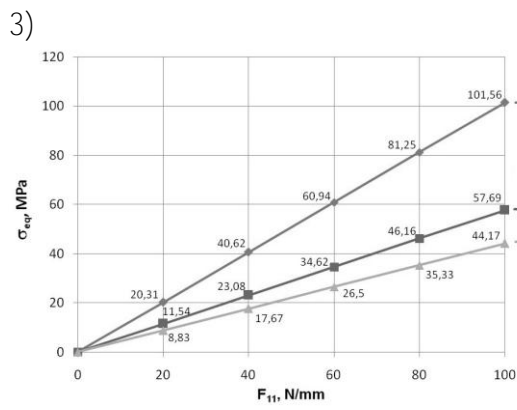
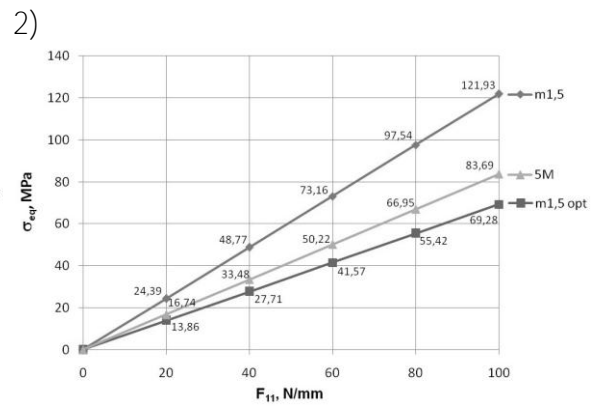
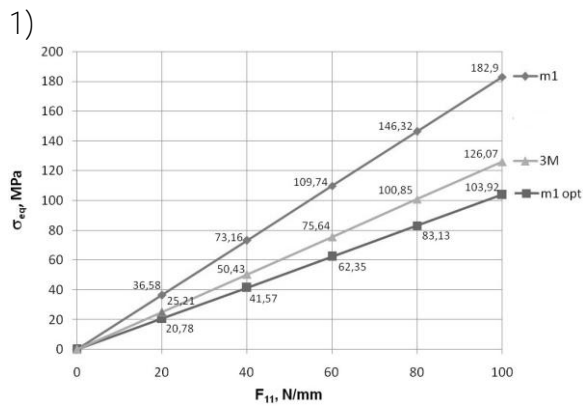
Standard	Marks	t_p , mm	Scale factors			
			k_1	k_2	k_3	k_4
<i>Trapezoidal structure</i>						
OST 3805114-76, TU RB 00149438-073-95	m1	3.14	0.318	0.255	0.80	0.5
	m1.5	4.71	0.318	0.254	0.80	0.546
	m2	6.28	0.286	0.238	0.83	0.5
	m3	9.42	0.339	0.212	0.625	0.5
	m4	12.57	0.350	0.198	0.568	0.5
	m5	15.71	0.318	0.222	0.70	0.534
	m7	21.99	0.364	0.279	0.75	0.545
	m10	31.42	0.382	0.286	0.75	0.6
<i>Average value</i>			<i>0.334</i>	<i>0.243</i>	<i>0.725</i>	<i>0.528</i>
ISO 5296	MXL	2.032	0.374	0.251	0.671	0.464
	XL	5.08	0.265	0.250	0.927	0.552
	L	9.525	0.336	0.200	0.585	0.531
	H	12.7	0.346	0.180	0.520	0.534
	XH	22.225	0.357	0.286	0.8	0.567
	XXH	31.75	0.384	0.3	0.781	0.607
<i>Average value</i>			<i>0.344</i>	<i>0.244</i>	<i>0.714</i>	<i>0.542</i>
DIN 7721	T2.0	2.0	0.35	0.25	0.714	0.454
	T2.5	2.5	0.4	0.28	0.7	0.538
	T5	5.0	0.36	0.24	0.667	0.545
	T10	10.0	0.35	0.25	0.714	0.555
	T20	20.0	0.325	0.25	0.769	0.625
<i>Average value</i>			<i>0.357</i>	<i>0.254</i>	<i>0.713</i>	<i>0.543</i>
AT (Automobile Transmission)	AT5	5.0	0.5	0.24	0.48	0.444
	AT10	10.0	0.5	0.25	0.5	0.555
	AT20	20.0	0.5	0.25	0.5	0.625
<i>Average value</i>			<i>0.5</i>	<i>0.247</i>	<i>0.493</i>	<i>0.541</i>
<i>Semicircular structure</i>						
TU 38405560-84	m3	9.42	0.531	0.425	0.8	0.667
	m4	12.57	0.557	0.398	0.714	0.667
	m5	15.71	0.573	0.382	0.667	0.667
<i>Average value</i>			<i>0.554</i>	<i>0.402</i>	<i>0.727</i>	<i>0.667</i>
HTD (ISO 13050)	3M	3.0	0.567	0.390	0.688	0.434
	5M	5.0	0.564	0.412	0.730	0.458
	8M	8.0	0.612	0.423	0.689	0.564
	14M	14.0	0.616	0.430	0.698	0.602
<i>Average value</i>			<i>0.589</i>	<i>0.413</i>	<i>0.701</i>	<i>0.515</i>

The analysis of the received results shows that toothed belts of various standard sizes and structures do not possess geometrical similarity of teeth. Alongside with it teeth of toothed belts with structure **AT** and a semicircular structure are more massive with the increased height, width or a corner of a structure in comparison with teeth of a trapezoidal structure.

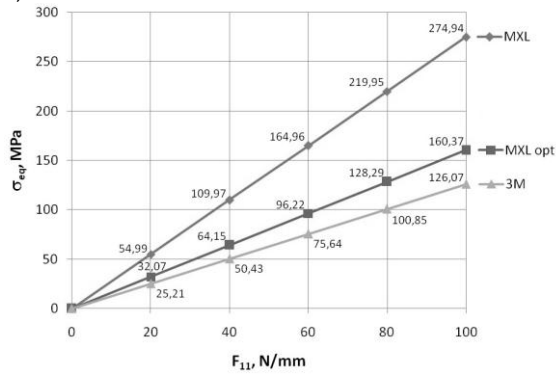
Besides in toothed-belt drives with a semicircular structure of teeth practically there is no radial backlash between teeth of a belt and a pulley in gearing. It leads to more uniform distribution of pressure and deformations on all volume of the teeth of a belt and significant decrease in a loading of the dangerous section which is in the field of transition from a lateral surface of the teeth to an interdental hollow. Alongside with it significant **(15...20 %) decrease in contact pressure upon a surface** of the bearing layer adjoining to an interdental surface of a belt occurs what, in turn, raises fatigue durability of a bearing layer. Let's assume, that teeth of a trapezoidal structure have the same scale factors $k_1 = S_p / t_p$ и $k_2 = h_p / t_p$ as well as teeth of a semicircular structure at a constant step of teeth. Thus, we shall hypothetically increase height and width of teeth of belts due to decrease in similar parameters of pulleys of transmission, lateral and radial backlashes in gearing teeth. Considering that rigidity and durability of metal teeth of pulleys of toothed-belt drive is non-comparable more rigidity and durability of elastomer teeth of a belt such reduction will lead to decrease in weight and dimensions of pulleys. The results of researches are shown in figure 5.9 (pages 222...224).

The analysis of the received graphic dependences shows that increase in geometrical parameters of teeth of a trapezoidal structure up to a level of similar parameters of teeth of a semicircular structure allows **considerably (on 30...45 %) lowering equivalent** pressure and deformations in their dangerous section and providing loading ability and fatigue durability of teeth of a trapezoidal structure practically equal to the given parameters of teeth of a semicircular structure. Alongside with it there is an essential decrease in weight and dimensions of toothed-belt drive.

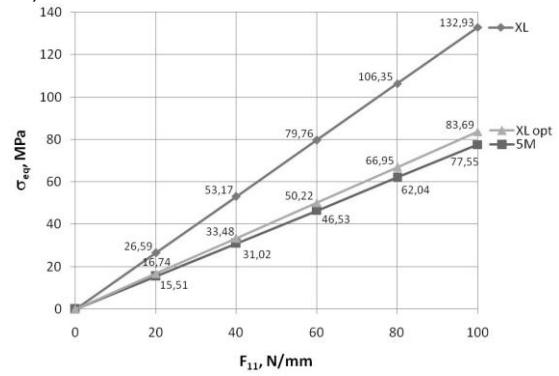
At the same time it is necessary to note that teeth of a semicircular structure possess a number of the advantages not peculiar to teeth of a trapezoidal structure to which first of all it is necessary to refer their minimal profile interference, the raised wear resistance due to lowered capacities of friction and speed of mutual sliding of teeth of a belt and a pulley at an input in the gearing, the raised smoothness of the work, lowered noise and vibrations. In aggregate it allows ascertaining unequivocally higher technological level of toothed-belt drives with teeth of a semicircular structure.



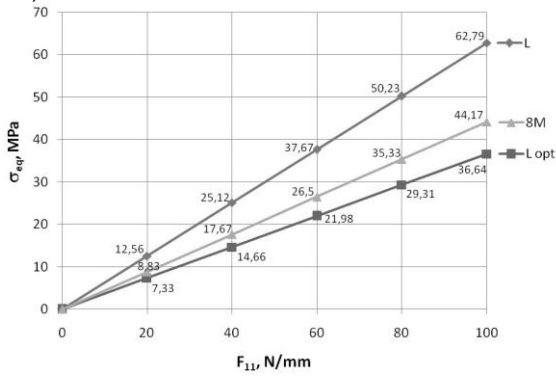
9)



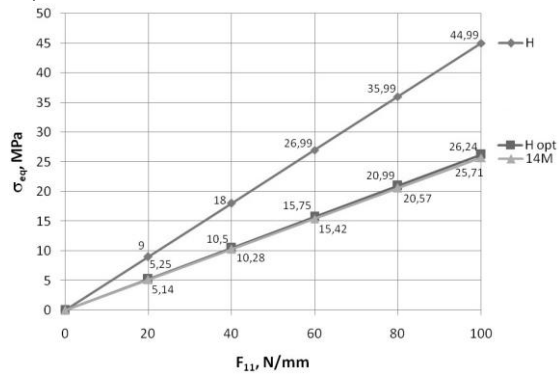
10)



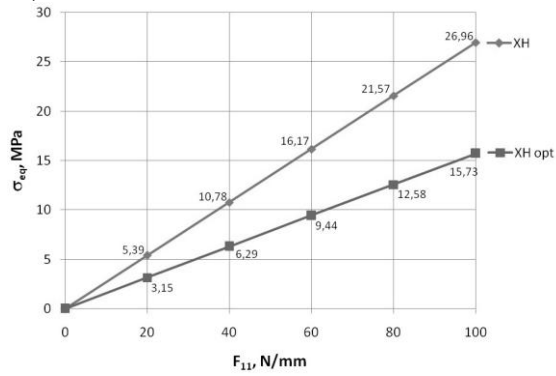
11)



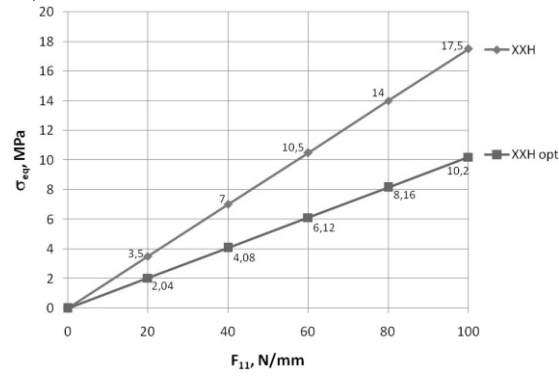
12)



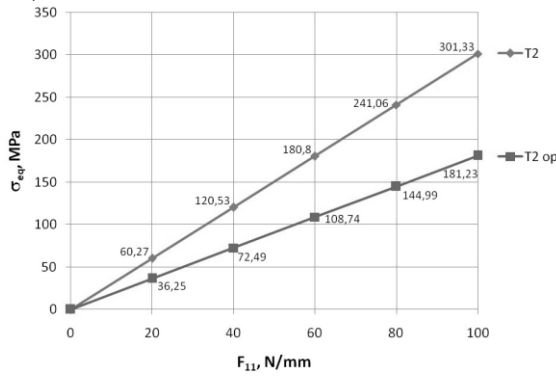
13)



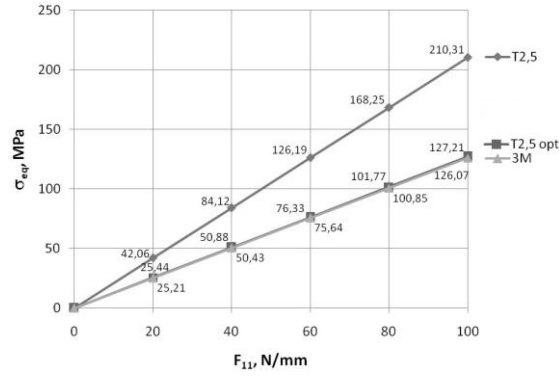
14)



15)



16)



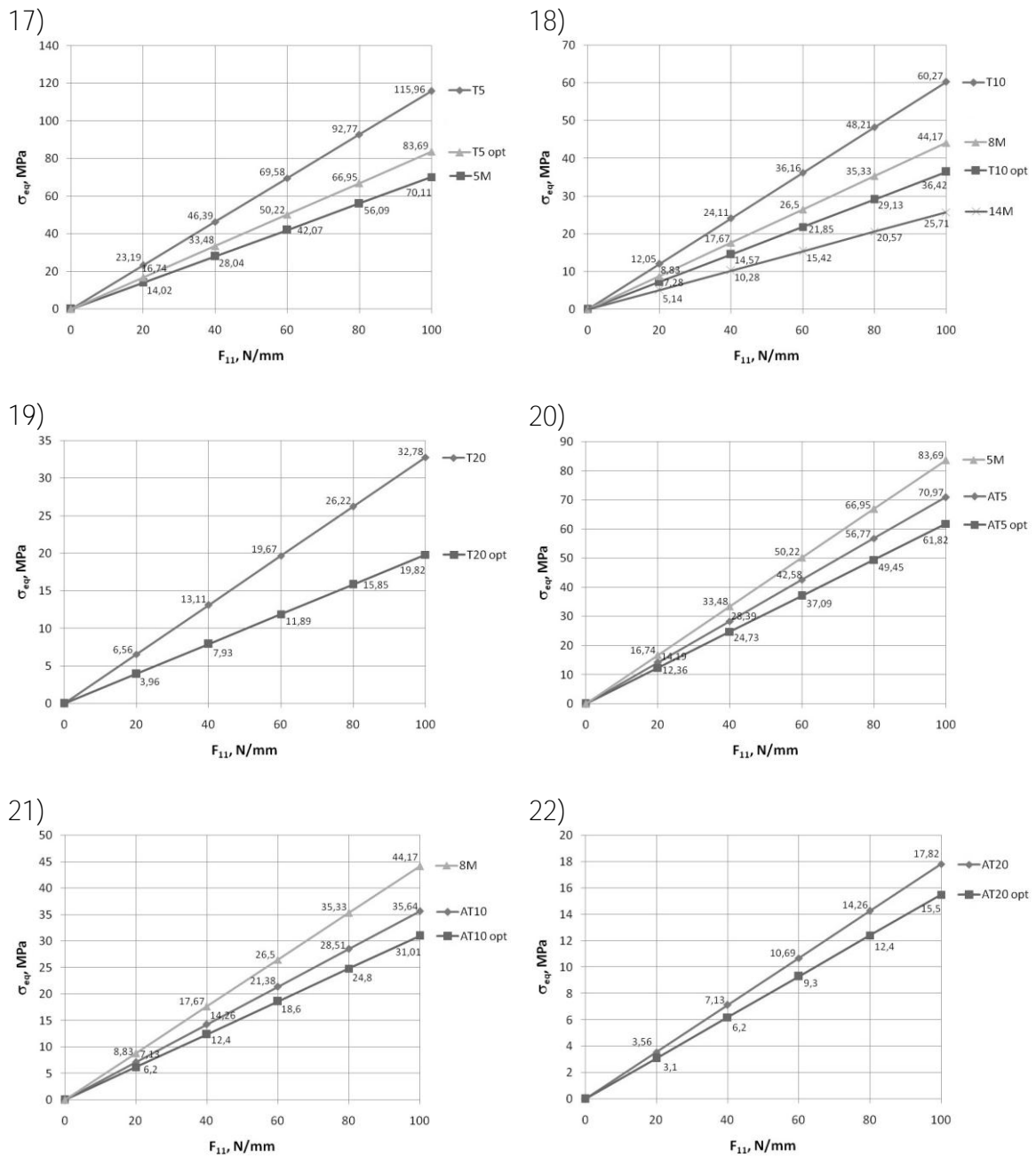


Fig. 5.9. Loading of teeth of toothed belts

The carried out comparative analysis of the international standards existing now, concerning standard sizes and structures of drive toothed belts (Tab. 5.4) has shown their imperfection regarding unreasonably wide nomenclature of them with close or equal step of teeth – the parameter being a basis of design engineering calculation of toothed-belt drives.

Tab. 5.4. Matrix of standard sizes and structures of toothed belts of the international standards

Standard	Standard size Step of teeth t_p , mm								
	<i>Trapezoidal structure</i>								
OST, TU RB		m1 3.14	m1.5 4.71	m2 6.28	m3 9.42	m4 12.57	m5 15.71	m7 21.99	m10 31.42
ISO 5296	MXL 2.032		XL 5.08		L 9.525	H 12.7		XH 22.225	XXH 31.75
DIN 7721	T2 2	T2.5 2.5	T5 5		T10 10			T20 20	
AT			AT5 5		AT10 10			AT20 20	
<i>Semicircular structure</i>									
TU 38405560-84					m3 9.42	m4 12.57	m5 15.71		
HTD (ISO 13050)		3M 3	5M 5		8M 8		14M 14		

Therefore, with the purpose of increase of a technological level of toothed-belt drives, observance of the general rules of standardization, unification, the international division of labour and cooperation it is offered to develop the new international standard «Belts drive toothed and pulleys. Basic sizes» using the results of researches received in the present work.

5.3. Lowering of the sliding friction of teeth in gearing

The given above dependences (§5.1 and §5.2) testify to the significant influence of the sliding friction of teeth on the durability of a belt. For the experimental check of the influence of friction on loading of gearing the computer modeling of its stress-strained state in ANSYS is carried out.

In Fig. 5.10 and 5.11 the results of the modeling of the stress-strained state of teeth of a semicircular profile with a step $t_{III} = 14$ mm at the various values of the factor of friction in the contact of teeth are presented.

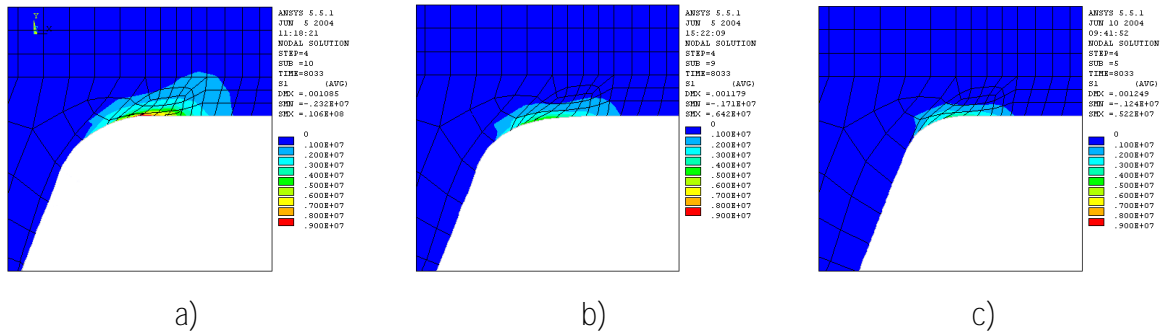


Fig. 5.10. Distribution of stresses in the belt tooth material:

a) $f_{fS} = 0.5$; b) $f_{fS} = 0.2$; c) $f_{fS} = 0.1$

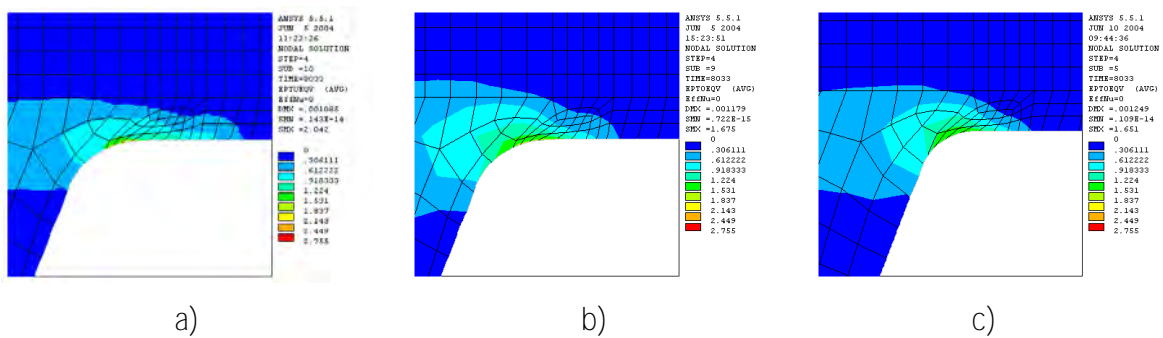


Fig. 5.11. Intensity of deformations in the belt tooth material:

a) $f_{fS} = 0.5$; b) $f_{fS} = 0.2$; c) $f_{fS} = 0.1$

The results of the modeling show that the maximum tension stresses σ_{1max} and the deformation intensity (Mises' deformation) ϵ_{imax} are observed on the radius of transition of a lateral surface of a tooth to the surface of an interdental space. At $f_{fS} = 0.5$: $\sigma_{1max} = 10.6 \text{ MPa}$, $\epsilon_{imax} = 2.042$. The lowering of the friction factor up to the value $f_{fS} = 0.2$ (under all other equal conditions) allows to reduce σ_{1max} up to 6.42 MPa (39.4 %) and ϵ_{imax} up to 1.675 (18.7 %). The further lowering of f_{fS} up to 0.1 leads to the reduction of σ_{1max} up to 5.22 MPa (50.7 %) and ϵ_{imax} up to 1.651 (19.1 %).

Thus, the numerical modeling with the use of the modern hardware-software means confirms the fact that the decrease in the sliding friction of teeth in a **toothed**-belt gearing is an effective method of the increase of the durability and load carrying capacity of toothed belts. The reduction of roughness of the working surfaces of a belt and pulleys of a **toothed**-belt transmission is offered as the methods of the decrease in friction in the contact of teeth.

The working surface of teeth of toothed belts is covered with a special fabric facing, which promotes the increase of their rigidity and wear resistance. The facing durability **makes 75...80 % of the general durability of teeth**. It is made of kapron or nylon, and it is impregnated with special adhesive chemical compositions on the basis of latex or rubber for the improvement of the adhesion strength to the components of a belt.

The measurement of the friction force between the belt tooth, covered with fabric facing, and the steel penetrator ($Ra = 1.6$ microns) is lead by means of a hardware-software complex on the basis of a tribometer ПД1 (Fig. 5.12).

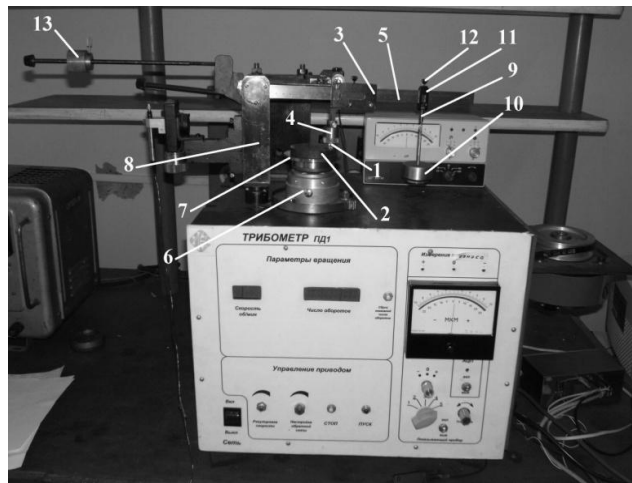


Fig. 5.12. Tribometer PD1: 1 – holder of the upper specimen; 2 – holder of the down specimen; 3 – carriage; 4 – screw nut; 5 – traverse; 6 – case; 7 – supporting cylinder; 8 – rotary rack; 9 – damper; 10 – basin; 11 – load carriage; 12 – screw; 13 – counter-weight

For **the** belts with the teeth covered by nylon fabric "Nuela-120", gum-dipped with 88CA TU381051760-89, $f_{fS} = 0.38 \pm 0.02$.

For the less roughness the fabric is additionally impregnated with some special adhesive compositions on the basis of graphitic dust. The measurement of the friction force shows that $f_{fS} = 0.25 \pm 0.01$.

The resource tests of the toothed belts, made with the use of two above mentioned kinds of fabric coating of teeth, show that the operational resource of belts increases from $1.9 \cdot 10^7$ to $2.1 \cdot 10^7$ cycles (10.5 %) at the average, providing that the fabric is additionally impregnated with adhesive compositions on the basis of graphitic dust.

It is known that the roughness of working surfaces of pulleys **of a toothed**-belt transmission has no decisive importance, as they are exposed to grinding by a belt in operation. However, at $Ra > 1.6$ microns the opportunity of running-in of a belt and a pulley

is practically excluded. The belt breaks down quickly due to the intensive **abrasion of** its working surfaces. The recommended values of roughness are $Ra = 1.25 \dots 1.6$ microns.

The electro-pulse polishing is used as the finite stage of the operation of steel pulleys **of a toothed**-belt transmission [169]. The pulleys *HTD 22-5M-32* (with the teeth of a semicircular profile, $t_{\text{III}} = 5$ mm, $z_{\text{III}} = 22$, $b_{\text{III}} = 32$ mm, $d_e = 33.87$ mm), 45 GOST 1050-88 made of steel (32 pieces) are processed. Electro-pulse polishing is carried out in 2 %-th water solution of ammonium chloride for 1.5 minutes at the temperature of electrolyte 70°C and stress 300 V.

The measurement of roughness is carried out by a standard technique (GOST 2789-73) on a **profilograph-profilometer M2** "Mahr GmbH", the length of burrs is defined with the help of a microscope "**PMT-3**".

Before processing the pulleys have the roughness of the working surfaces $Ra = 1.75 \dots 2.5$ microns and the burrs on the edges with the height $0.2 \dots 0.35$ mm. After electro-pulse polishing the burrs on the edges of the details are taken off completely, the roughness of the working surfaces of pulleys lowers up to $Ra = 1.25 \dots 1.6$ microns, which corresponds to the requirements of the design documentation. The physical form of the pulleys is presented in Fig. 5.13.

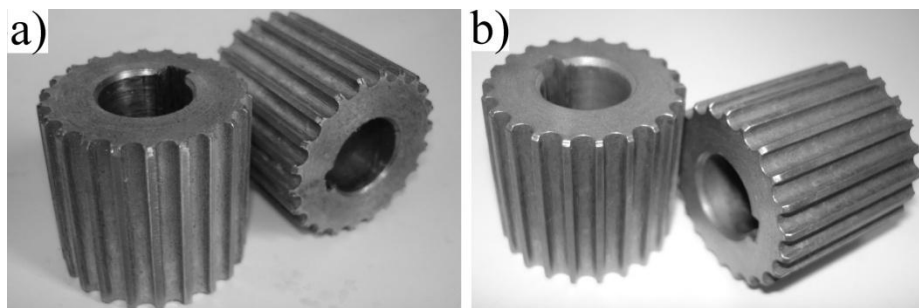


Fig. 5.13. Physical form of pulleys **of a toothed**-belt transmission:
a) before processing, b) after electro-pulse polishing

The resource tests of toothed belts "*ContiSynchroforce CXP III HTD 1500-5M-32*" (Germany) in the drive of the experimental **parquet-polishing** machine "**CO-318**" ($P = 2.2$ kW, $n = 600$ min⁻¹, $d = 200$ mm) show that after the electro-pulse polishing of pulleys **the durability of toothed belts increases by 20...22 %**. In such a case, the estimated cost of manufacturing of pulleys at their series production increases slightly (no more than 5 %).

On the basis of the carried out complex of the theoretical and experimental researches, including numerical modeling of loading of a **toothed**-belt gearing in a real-time mode, the following conclusions and recommendations [170] are made. They are recommended for the use in the theory and practice of designing and operation of **toothed**-belt transmissions:

- electro-pulse polishing, providing the fulfillment of the requirements of the technical documentation and a normative operational resource with the minimum **energy** and labor costs, should be used as the final operation of the technological process of manufacturing of steel pulleys of transmission;

- wear-resistant fabric coating of working surfaces of teeth with its additional impregnation with the adhesive compositions on the basis of graphitic dust, which allows to increase the durability of belts by 10.5 % at the average, should be used in manufacturing of drive toothed belts;

- the results of the computer finite-element modeling of the stress-strained state, adequate to the developed theoretical dependences and the results of the industrial tests of transmission, should be used for the design of **toothed**-belt transmissions.

5.4. Probabilistic methods of prediction of the durability of toothed belts

Probabilistic methods of the estimation of **wear-fatigue** strength make the basis of the resource designing of **toothed**-belt transmissions.

The analysis of the results of fatigue tests of the pieces of materials and machine elements show that the exact description of the dependence of the number of loadings before the failure N from the **maximum stress of the cycle** σ of the regular loading at the constant factor of asymmetry r gives the following equation [171]:

$$N = \frac{Q}{\sigma} \ln \left\{ 1 + \left[\exp \left(\frac{\sigma - \sigma_r}{\nu_0} \right) - 1 \right]^{-1} \right\}, \quad (5.30)$$

where Q – the factor of endurance, equal to the product of a limit of endurance σ_r by the number of cycles up to the point of the lower knee of the fatigue curve N_0 ; ν_0 – the equation parameter equal to the ratio of the product of a limit of endurance by the characteristic of the slope of the fatigue curve ν to their difference: $\nu_0 = \sigma_r \nu / (\sigma_r - \nu)$.

The reason of the dissipation of the fatigue resistance is the dissipation of the values of the limit of endurance, which can be estimated with the use of the function of the normal distribution. In the case of the normal distribution of the values of the endurance limit, the expression (5.30) becomes:

$$N = \frac{Q}{\sigma} \ln \left\{ 1 + \left[\exp \left(\frac{\sigma - \sigma_{rp}}{v_0} \right) - 1 \right]^{-1} \right\},$$

where $\sigma_{rp} = M(\sigma_r) + tS(\sigma_r)$ – the particular value of the limit of endurance, corresponding to the probability P ; $M(\sigma_r)$ and $S(\sigma_r)$ – mathematical expectation and a square deviation of the values of the limit of endurance of the set of details; t – the quantile of the normal distribution, corresponding to the probability P [172].

The estimation of the dependence of the number of cycles before the failure of the value of the stress, made with the account of probability of non-failure, gives the idea of the resistance of machine elements to the fatigue. Such the estimation allows determining of non-varying parameters of the equation of the fatigue curve and the parameters of the distribution of the values of the endurance limit.

The object of the experimental researches is the toothed belts, made by the method of pressing by the rigid elements. The standard sizes of the belts (module-number of teeth) are 2-68; 3-60; 4-48. The belts have a wear-resistant coating of teeth with kapron fabric, gum-dipped, and they are made with the different types of a bearing layer (Tab. 5.5).

Tab. 5.5. Mechanical and physical properties of a bearing layer

Type of bearing layer	Diameter d_c , mm	Quantity of unit threads, pieces	Diameter of unit threads, mm	"Alive" section, mm ²	Module of elasticity E , MPa	Breaking strength, kg (MPa)
5JI15	0.4	5	0.150	0.089	$4.5 \cdot 10^4$	20(2247)
15JI15	0.75	15	0.150	0.265	$5.7 \cdot 10^4$	60(2260)
20CT	0.35	1600	0.009	0.102	$4.58 \cdot 10^4$	11(1147)
35CT	1.0	2400	0.009	0.152	$5.2 \cdot 10^4$	24
75CA	1.25	8000	0.009	0.509	$3.64 \cdot 10^4$	65

For the researches the stand with the open force contour, allowing to test two belts at the frequency of the rotation of the pulleys $n_{\text{ш}} = 1800$ and 2200 min^{-1} , is used (Fig. 5.14)

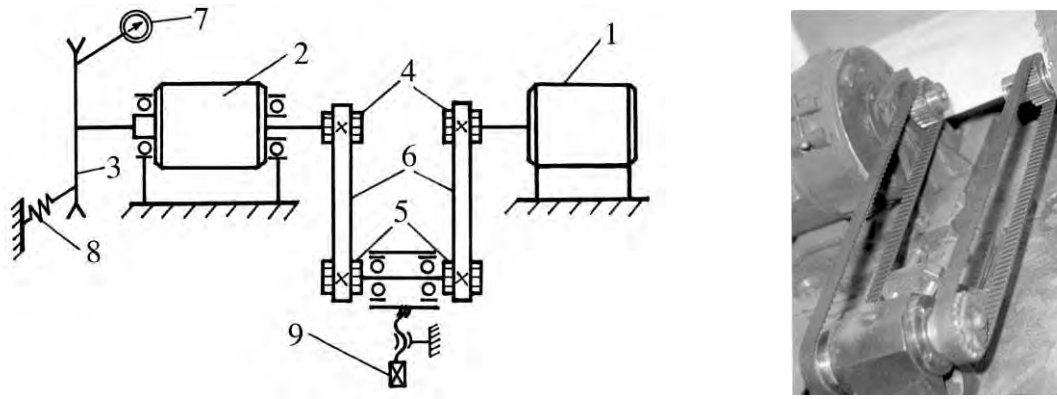


Fig. 5.14. Kinematic scheme and physical form of the stand for the research of the durability of toothed belts: 1 – electric motor; 2 – brake machine; 3 – disk of the balancer; 4 – drive pulley; 5 – driven pulley; 6 – belt; 7 – indicator of replacement; 8 – elastic element; 9 – tension device

Stresses in a bearing layer at bending are:

$$\sigma_b = \frac{Ed_c}{2\rho},$$

where ρ – the radius of the curvature of a pulley.

The minimum and maximum stresses of the cycle are:

$$\sigma_{\min} = \sigma_{2F_0}; \quad \sigma_{\max} = \sigma_b + \sigma_{2F_0}.$$

The average stress of the cycle is:

$$\sigma_{av} = \sigma_{2F_0} + \frac{\sigma_b}{2}.$$

As a result of the researches, it is established, that the fatigue strength of all the types of a bearing layer decreases exponentially with the increase of the operating stresses (Fig. 5.15–5.19).

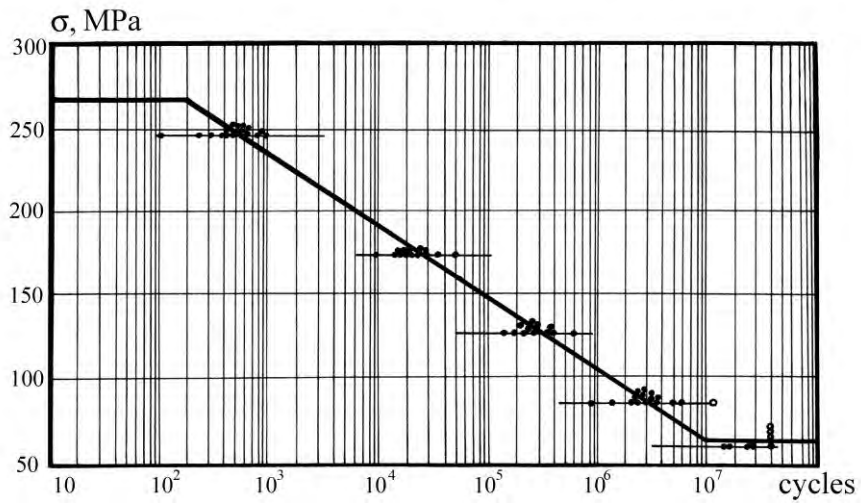


Fig. 5.15. Diagram of a fatigue of toothed belts with a metal cord 5JI15

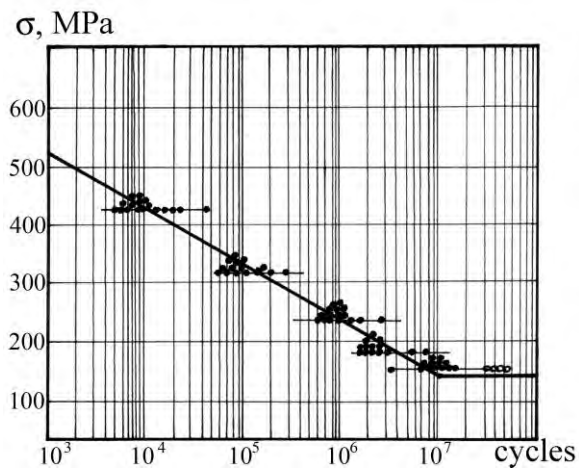


Fig. 5.16. Diagram of a fatigue of toothed belts with a metal cord 15JI15

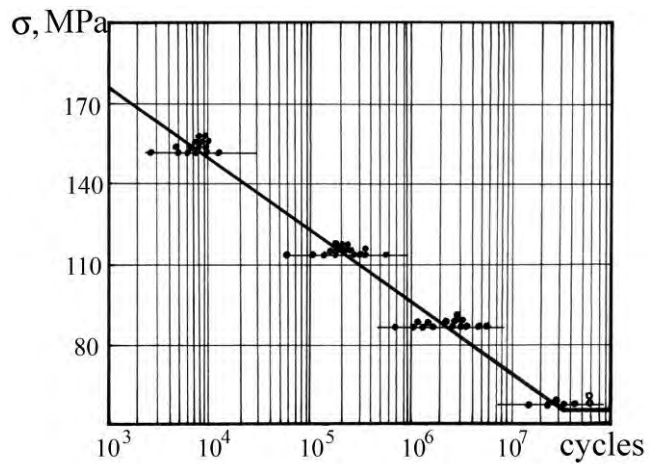


Fig. 5.17. Diagram of a fatigue of toothed belts with a glass-fiber cord 20CT

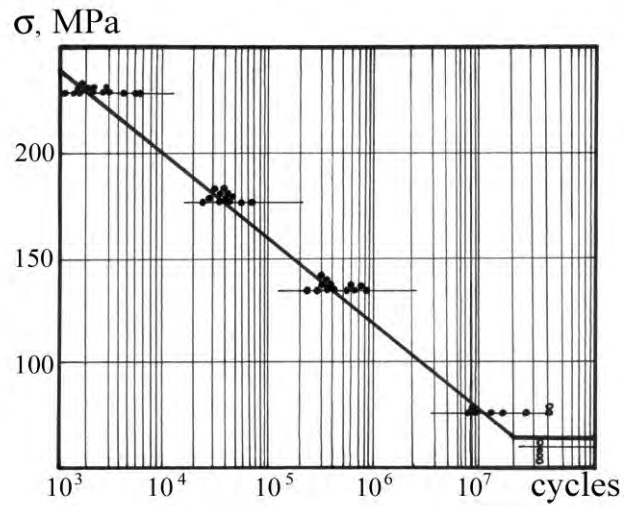


Fig. 5.18. Diagram of a fatigue of toothed belts with a glass-fiber cord 35CT

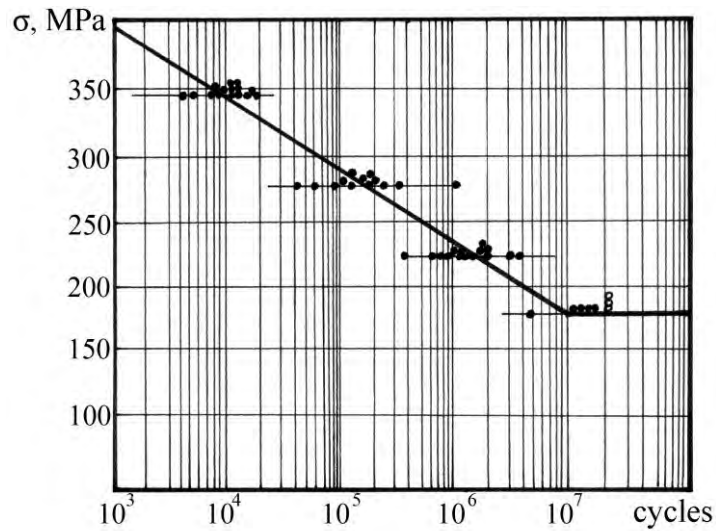


Fig. 5.19. Diagram of a fatigue of toothed belts with a glass-fiber cord 75CA

Characteristics of the fatigue resistance of different types of a bearing layer are presented in Tab. 5.6.

Tab. 5.6

Bearing layer	$\bar{\sigma}_r$, MPa	v_0 , MPa	S_r , MPa	Q , MPa·cycle
5J115	65	22.1	8.75	$6.25 \cdot 10^8$
15J115	140	23.5	19.6	$1.4 \cdot 10^9$
20CT	55	13.5	9.05	$1.5 \cdot 10^8$
35CT	64.5	22.8	10.93	$1.05 \cdot 10^8$
75CA	168.1	28.2	17.67	$1.45 \cdot 10^8$

The results of the carried out researches can be used at the choice of a bearing layer. For example, both the glass-fiber cord 20CT and the metal cord 5JI15 can be used for the spline toothed belts ($m = 1, 2, 3$ mm).

The analysis of the diagrams of the fatigue of the above-mentioned types of a bearing layer shows that the average value of the limit of endurance $\bar{\sigma}_r$ is equal to 65 and 55 MPa accordingly, the number of cycles up to the point of the lower knee of the fatigue curve $N_0 = 10^7$ and 3×10^7 cycles accordingly. The glass-fiber cord can endure 3 times more loadings at the equal value of the average limit of endurance. It allows using of the belts with a glass-fiber cord 20CT on the pulleys of a small diameter.

Let's draw a comparison between $\bar{\sigma}_r$ and N_0 for a metal cord 15JI15 and a glass-fiber cord 75CA. For the metal cord 15JI15: $\bar{\sigma}_r = 140$ MPa, $N_0 = 10^7$ cycles; for the glass-fiber cord 75CA: $\bar{\sigma}_r = 168.1$ MPa; $N_0 = 10^7$ cycles. At the equality of N_0 the glass-fiber cord 75CA has a larger value $\bar{\sigma}_r$. It allows using of the belts with the glass-fiber cord 75CA for more loaded transmissions.

The characteristics of the fatigue resistance of teeth of toothed belts are also defined. The tests are made on a stand-pulsor (Fig. 5.20).

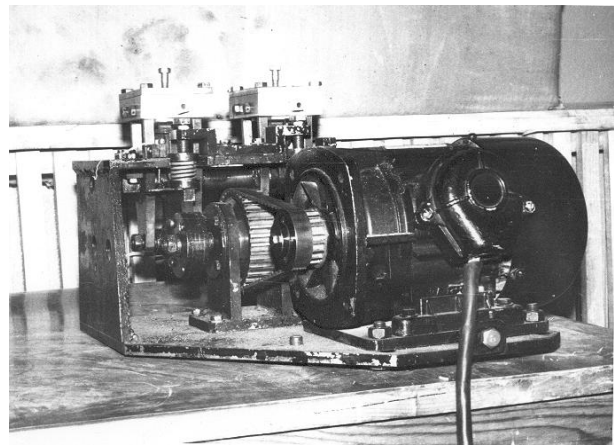
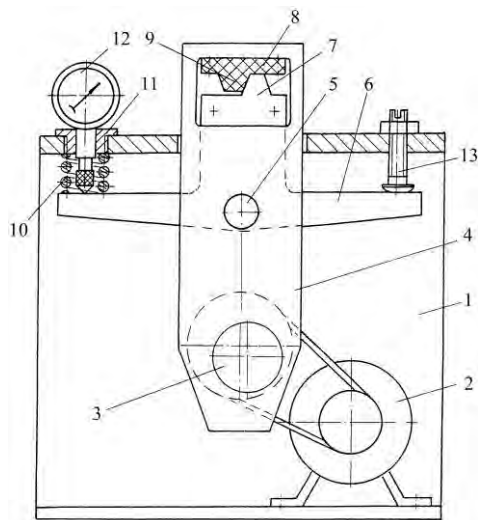


Fig. 5.20. Kinematic scheme and physical form of a stand-pulsor: 1 – frame; 2 – electric motor; 3 – eccentric shaft; 4 – lever; 5 – axis; 6 – rocker; 7 – penetrator; 8 – specimen of a belt; 9 – tooth of a belt; 10 – spring; 11 – adjusting screw; 12 – indicator of replacement; 13 – fixing screw

In the given stand the working loading is periodically put on the lateral surface of the tooth by means of the penetrator, representing the tooth of a pulley of transmission. The frequency of loading is 12 Hz. Four lots of toothed belts are tested.

The belts of the first lot ($m = 2$ mm) consist of: a) mould; b) assembly; c) assembly, reinforced with copper wire $\text{Ø}0.6$ mm (Fig. 1.17). The analysis of the diagrams of the fatigue (Fig. 5.21) testifies that the assembly and reinforced belts have the increased values $\bar{\sigma}_r$ and N_0 .

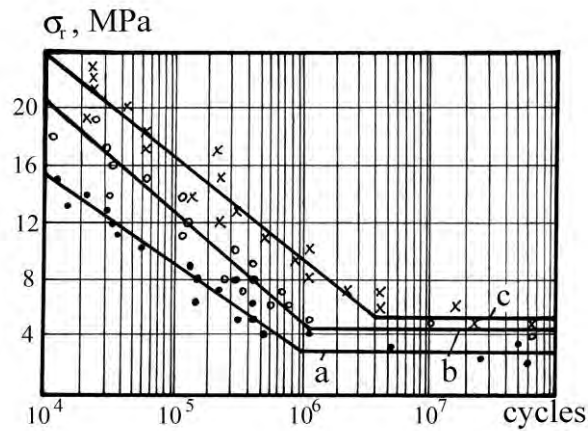


Fig. 5.21. Diagrams of the fatigue of toothed belts: a) mould; b) assembly; c) assembly reinforced

In this case, a) $\bar{\sigma}_r = 3$ MPa, $N_0 = 10^6$ cycles; b) $\bar{\sigma}_r = 4.5$ MPa, $N_0 = 1.2 \times 10^6$ cycles; c) $\bar{\sigma}_r = 5.5$ MPa, $N_0 = 4 \times 10^6$ cycles. Thus, the presence of fabric facing and reinforcement of belt teeth leads to the increase of $\bar{\sigma}_r$ 1.5 and 1.8 times accordingly.

The second lot includes the following belts: a) assembly, the pressure of vulcanization $P = 0.6$ MPa; b) assembly, $P = 20$ MPa; c) assembly, micro-reinforced (Fig. 1.16). The analysis of the diagrams of the fatigue (Fig. 5.22) shows that the increased pressure of vulcanization and micro-reinforcement increase the durability of toothed belts. Thus, for: a) $\bar{\sigma}_r = 15$ MPa, $N_0 = 1.4 \times 10^6$ cycles; b) $\bar{\sigma}_r = 16$ MPa, $N_0 = 2.2 \times 10^6$ cycles; c) $\bar{\sigma}_r = 19.5$ MPa, $N_0 = 3.5 \times 10^6$ cycles.

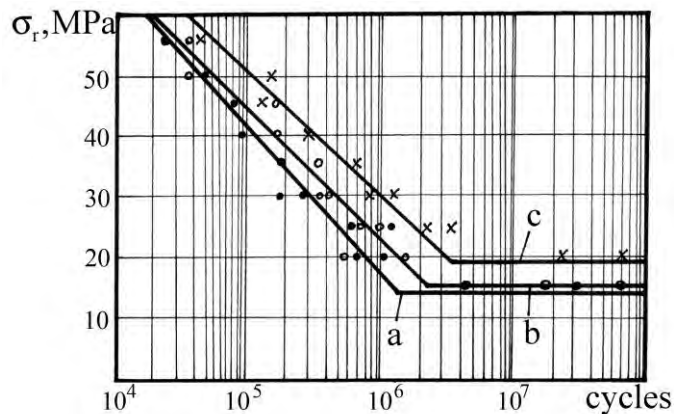


Fig. 5.22. Diagrams of the fatigue of toothed belts: a) assembly, $P = 0.6$ MPa; b) assembly, $P = 20$ MPa; c) assembly micro-reinforced

The belts of the third lot have different **Shore** hardness A of teeth (HS): 58.6; 64.2; 74.3; 85.2 units accordingly. On the basis of the diagrams of the fatigue (Fig. 5.23) the dependences $\bar{\sigma}_r$ and Q of the hardness are constructed (Fig. 5.24).

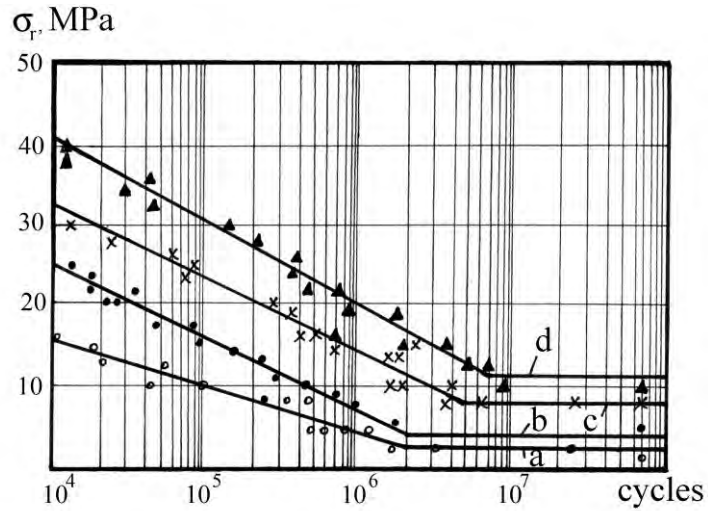


Fig. 5.23. Diagrams of the fatigue of toothed belts with different Shore hardness A of teeth
HS: a) 58.6; b) 64.2; c) 74.3; d) 85.2 units

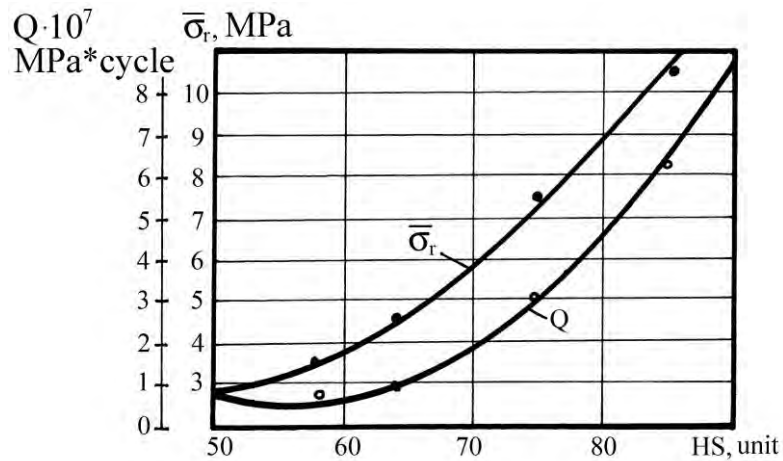


Fig. 5.24. Dependence of an average limit of endurance and the factor of endurance of the hardness of teeth

The analysis of the dependences testifies that the increase of the hardness of teeth from 58.6 to 85.2 units leads to the augmentation of $\bar{\sigma}_r$ 3 times, which promotes the corresponding increase of the life time of toothed belts.

The belts of the fourth lot have different degrees of reinforcement of teeth, which represents the ratio of the diameter of a spring d to the length of a tooth h_p (Fig. 1.20): 0; 0.3; 0.5; 0.7; 1.0.

On the basis of the diagrams of the fatigue (Fig. 5.25) the dependences of the characteristics of the fatigue resistance of the degree of reinforcement of teeth (Fig. 5.26) are constructed. The graphs show that the augment of the degree of reinforcement of teeth from 0 to 1 leads to the increase of the fatigue resistance of toothed belts 3.1 times.

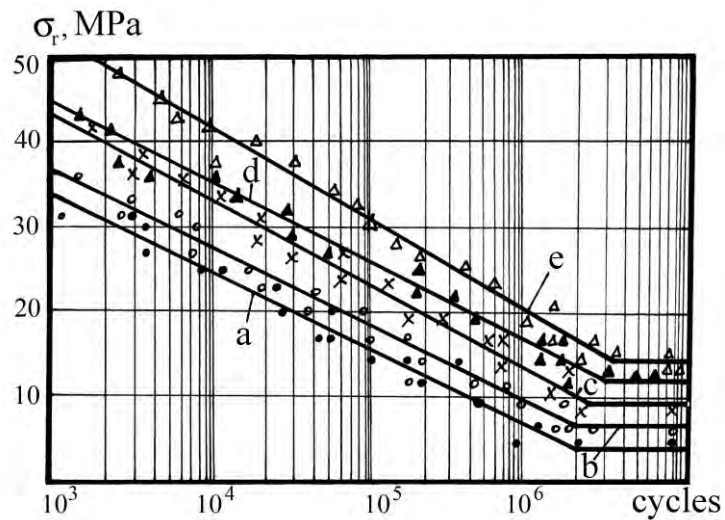


Fig. 5.25. Kinetic diagrams of the fatigue of toothed belts with different degrees of reinforcement of teeth: a) 0; b) 0.3; c) 0.5; d) 0.7; e) 1.0

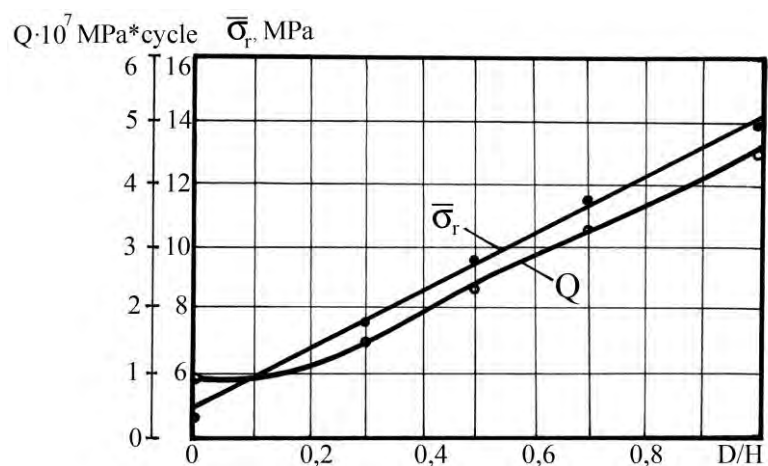


Fig. 5.26. Dependence of an average limit of endurance and the factor of endurance of the degree of reinforcement of teeth

Thus, the results of the researches on the dissipation of characteristics of the fatigue resistance and predicting of an operational resource of drive toothed belts are generalized by means of the kinetic theory of the mechanical fatigue. The techniques of fatigue tests, probabilistic resource designing of drive toothed belts and the basics of diagnosing of the fatigue at the operation are developed [173].

On the basis of the diagrams of the fatigue the curves of equal probability of non-failure of the elements of toothed belts, allowing to specify the permissible pull, depending on the set operational resource, are constructed.

5.5. Design method of the improvement of technical characteristics of toothed-belt transmissions

As it has been stated above, the increase of a step of belt teeth t_p is observed at a constant step of pulley teeth t_w in the process of transmission of power. In this case, the interference of teeth increases considerably, but the load carrying capacity and durability of a toothed belt decrease. Therefore, one of the main aspects of a design calculation of transmission is the determination of a step correction of teeth of a pulley.

The analysis of the world scientific and technical literature has shown that there are some contradictory recommendations for the calculation of correction. The authors of the works [49, 61] recommend increasing of the external diameter of a pulley d_a by $0.001 t_p$. For the belts of the "modular" system the value of the correction is defined by means of the tables, depending on the reference diameter of a pulley. In this case, the external diameter of a pulley is:

$$d_a = mz_1 - 2\delta + k_1,$$

where k_1 – the correction (Tab. 5.7) [174].

Tab. 5.7.

mz_1 , mm	k_1 , mm	mz_1 , mm	k_1 , mm
up to 50	0.08	120...198	0.13
50...78	0.10	200...318	0.15
80...118	0.12	320...500	0.18

The given technique does not consider the influence of mechanical and physical properties of a belt on non-uniformity of loading of teeth. Therefore, in the work [175] the value k **can be** found by the dependence:

$$k_{1(2)} = 0,2 \frac{F_t}{B_p} \lambda z_{1(2)}, \quad (5.31)$$

where λ –the compliance of a bearing layer on the length of one step (Tab. 5.8).

Tab. 5.8.

$m, \text{ mm}$	1.0	1.5	2.0	3.0	4.0	5.0	7.0	10.0
$\lambda, \text{ mm}^2/\text{N} \cdot 10^{-4}$	7	8	9	10	11	13	14	16

In the work [176] it is offered to consider not only the sizes of a pulley, but also the value of the transferred loading. For example, at $10 < z_0 \leq 30$:

$$k_1 = \frac{0,0005}{\pi} z_1 z_0 - 10. \quad (5.32)$$

The analysis of the expression (5.32) shows that at $z_0 < 10$ a step of teeth of a pulley is not corrected, which is inconsistent with the laws of the distribution of loading in gearing, at the reduction of z_0 loading of teeth increases, and at $z_0 < 6$ the value of the allowable circumferential force is corrected. Thus, at the reduction **of** z_0 the value k_1 increases.

In the work [177] it is offered to determine the value of the correction of a step on the basis of mechanical and physical properties of a belt in view of the length of the arc of contact:

$$\Delta t = t_m - t_p = \frac{0,4 z_0^{0,2} k_\alpha F_t B_p}{E_z}, \quad (5.33)$$

where k_α – the ratio of the compliances of a belt frame and its teeth.

To the authors' point of view, the expressions (5.31) – (5.33) allow to get $\psi = 1$, which predetermines the maximum possible durability of a belt. At the same time, it is proved, that at the reduction of ψ the durability of belts increases [178].

Hence, $\psi = 1$ is not a universal parameter, providing the maximum durability of a belt.

In view of the influence of the frequency of belt runs ν on its mechanical and physical properties and the distribution of the loading in gearing, the author of the work [47] offers the dependence Δt of ν .

Meanwhile, the value Δt , corresponding to the predetermined value ψ , can be found by the following dependence [179]:

$$\Delta t = \frac{t_p}{200} \left[1,3 - \frac{\psi}{k_\nu k_F k_Z \left(0,5 \left(\frac{F_t}{F_t} \right)^2 + 1 \right) 0,53z_0 + 1} \right], \quad (5.34)$$

where k_ν , k_F , k_Z – the factors, considering the frequency of belt runs, longitudinal rigidity and rigidity of belt teeth.

In the work [90] it is offered to achieve the maximum possible level of an operational resource of toothed belts by means of supporting of the equivalence of both criteria of the working ability. Therefore, the pressures on the teeth of the arc of contact are equated.

At the same time, in the given work the values of ψ , providing the maximum level of the durability of a belt by the criteria of wear of the profile N_w and the fatigue failure of teeth N_f , are not given.

For receiving of the dependence N_f of ψ a numerical experiment is carried out. In such a case, according to the technique of orthogonal planning [180] the factors, defining the fatigue durability of belt teeth, vary. It is established that the durability can be determined by the dependence:

$$N_f = \left(\frac{25h_p z_0}{F_t \psi \sqrt{\frac{G}{2}}} \right)^5. \quad (5.35)$$

The durability of a belt by the criterion of wear of teeth is:

$$N_w = 1,25 \frac{h_f}{h_{1f}} \left(\frac{F_t \omega \psi f_{fs} k_{Vsl}}{z_0} \right)^{1,75}. \quad (5.36)$$

The analysis of the dependences (5.35), (5.36) shows that the ratios $dN_w / d\psi$ and $dN_f / d\psi$ are less than zero. Thus, the dependences N_w and N_f of ψ have no extrema, and the value ψ cannot be found by the methods of common optimization. Hence, it is possible to determine the value ψ , corresponding to non-maximal possible, but to some definite predetermined level of the durability.

The comparison of the dependences (5.35) and (5.36) testifies that at any values of the argument $dN_w / d\psi < dN_f / d\psi$. Therefore, there is a condition, at which $N_w = N_f$. The value ψ for the given case is determined by equating of (5.35) and (5.36):

$$\psi_{opt} = \frac{z_0}{F_t} \left(\frac{h_{1f}}{1,25h_f} \right)^{0,3} \left(\frac{25h_p}{\sqrt{G}} \right)^{1,5} \omega f_{fs} k_{vsl}^{0,5}. \quad (5.37)$$

For example, at $m = 3$ mm; $\omega = 15.7$ s⁻¹; $F_t = 6$ N/mm the value $\psi_{opt} = 0.45$. At $\psi < \psi_{opt}$ the durability of a belt is determined by the processes of wear, and at $\psi > \psi_{opt}$ the operational resource depends on the intensity of the behavior of the fatigue failure.

Thus, at the predetermined value of the durability of a belt N_p by the formula (5.37) the value ψ_{opt} is found, the value of the durability N_m is determined by (5.35) or (5.36). If $N_f > N_m$, the value of non-uniformity of loading of teeth is found by the expression:

$$\psi = \frac{z_0}{F_t \omega f_{fs} k_{vsl}} \left(\frac{1,25h_f}{N_p h_{1f}} \right)^{0,57}.$$

In the case $N_f < N_m$ the value ψ is determined by the dependence:

$$\psi = \frac{25h_p z_0}{F_t \sqrt{G}} \left(\frac{1}{N_m} \right)^{0,2}.$$

The value Δt can be found by the dependence (5.34) at the known ψ .

The complex of stand tests is carried out for the experimental check of the developed dependences. The object of the researches is toothed belts with the module $m = 7 \text{ mm}$; $z_p = 71$; $B_p = 32 \text{ mm}$, made by the method of pressing by rigid elements and equipped with a wear-resistant fabric coating of teeth. The technique of the researches is based on the registration of the deformations of the strain-gauge tooth of one of the pulleys of transmission (see Fig. 2.29) of the special stand (see Fig. 2.28).

The kind of the distribution of loading in gearing at the various values of a step correction is found in the following way. The strain-gauge pulley is made with the external diameter 139.0 mm , $\Delta t / t_p = +0.00433$ and $\psi = 0.43$ (Fig. 5.27, a).

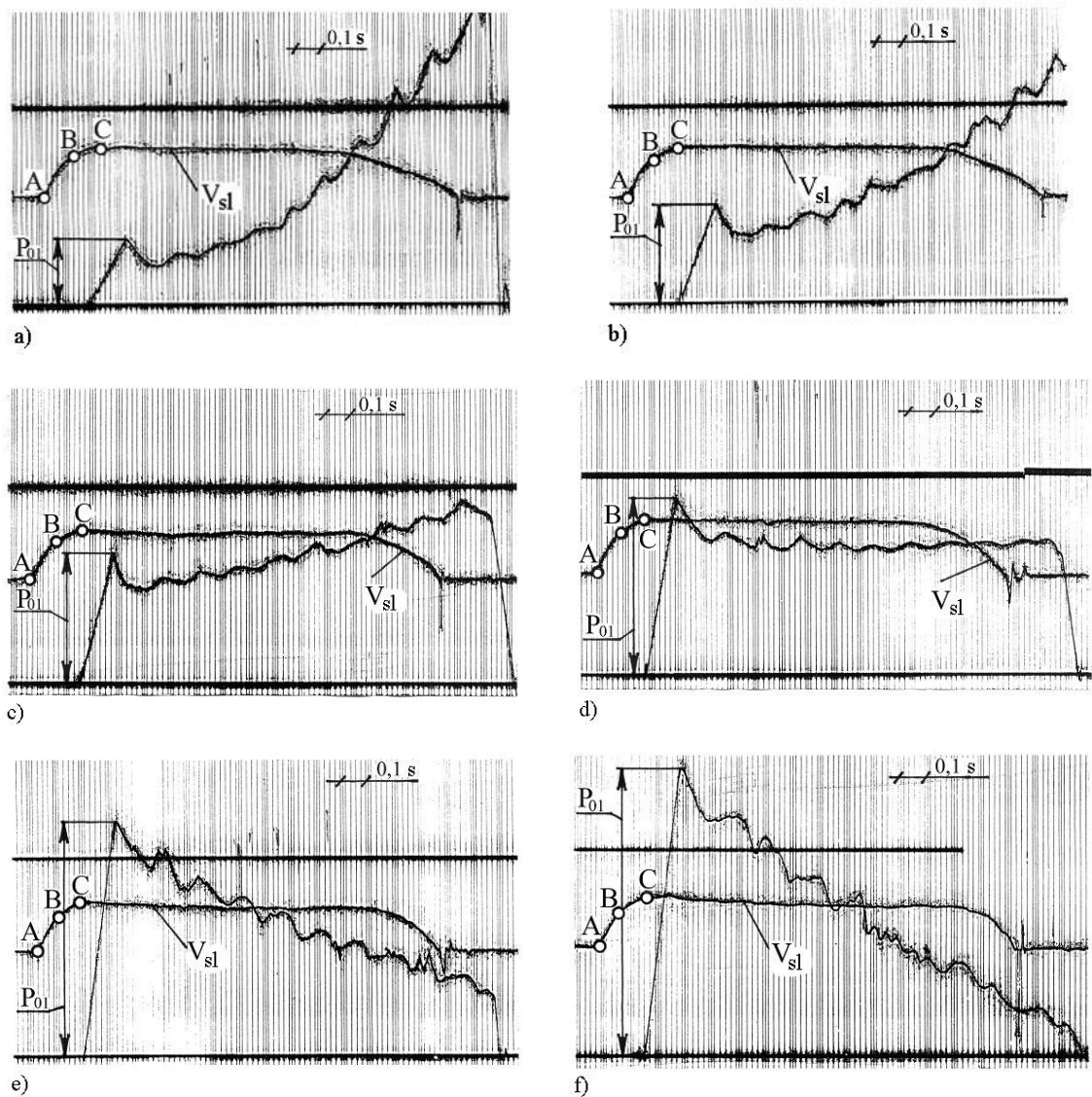


Fig. 5.27. Oscillograms of the distribution of loading in gearing

After the oscillogram recording the external diameter of a pulley is ground up to 138.8 mm, at which $\Delta t / t_p = +0.0029$ and $\psi = 0.72$ (Fig. 5.27, b). After carrying out the next series of tests the pulley is consistently ground up to the diameters: 138.6 mm ($\Delta t / t_p = +0.00143$; $\psi = 1.02$) (Fig. 5.27, c); 138.4 mm ($\Delta t / t_p = 0$; $\psi = 1.30$) (Fig. 5.27, d); 138.2 mm ($\Delta t / t_p = -0.00143$; $\psi = 1.59$) (Fig. 5.27, e); 138.0 mm ($\Delta t / t_p = -0.0029$; $\psi = 1.88$) (Fig. 5.27, f).

As a result of the processing of the received oscillograms by the method of ordinates it is established, that ψ decreases linearly in the process of increasing of the correction of a step of teeth of a pulley (Fig. 5.28). In the examined range of the change of $\Delta t / t_p$ the discrepancy between the theoretical and experimental results does not exceed 14.3 %.

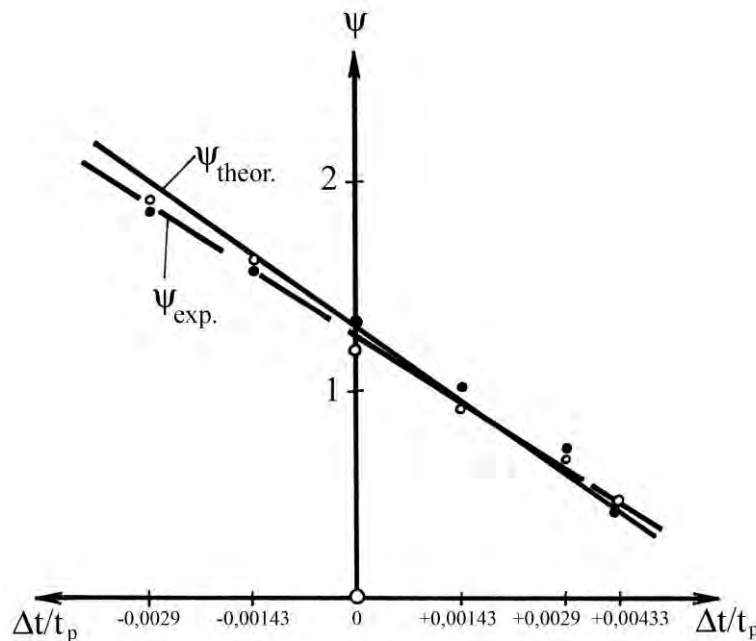


Fig. 5.28. Dependence of the factor of non-uniformity of loading of teeth of a belt of the correction of a step of teeth of a pulley:
 • – theoretical calculation; o – experimental data

The analysis of the dependences ψ of Δt shows that the greatest discrepancy between them is observed in the field of high values of the ratio $\Delta t / t_p$. It is caused by the fact that the partial output of teeth from gearing, located at the following side, is not considered in the theoretical calculation of ψ .

At $\Delta t / t_p < 0$ the loading on the given teeth is rather insignificant, and in the case of the significant correction of a step of pulley teeth, the main part of the transferred pull is

redistributed in the zone, adjacent to the following side. In view of the trapezoidal form of teeth along with the increase of the effort the radial force, pushing out teeth from gearing, also increases. The insufficient tension of the following side is unable to neutralize the action of the radial forces, so, some teeth output from gearing partially. As their rigidity decreases, in this case, the pull is redistributed in the zone at the following side. The loading **on the teeth in this zone increases, which does not lead to the decrease of ψ** . The elimination of the given phenomenon takes place at the increase of the preliminary tension of a belt by the value $\Delta 2F_0$, according to the dependence [181]:

$$\Delta 2F_0 = 0,2 F_t \left(\frac{0,00143 \Delta t}{t_p} \right)^2.$$

Thus, the technique of the determination of the rational value of the correction of a step of pulley teeth, providing uniform loading of gearing and the improvement of the load carrying capacity and durability of toothed belts, is developed. On the basis of the carried out complex of the theoretical and experimental researches the modern technique of the design-engineering calculation **of toothed**-belt transmissions with the improved characteristics is developed [182].

5.6. Conclusions

1. The technique of the resource design **of a toothed**-belt transmission by the criterion of wear of the working profile of belt teeth on the basis of the power approach has been developed. It allows specifying of the value of the operational resource and predicting of it with a reasonable accuracy.

2. The technique of the resource design **of a toothed**-belt transmission by the criterion of a fatigue failure of belt teeth, considering kinematic and force features of the interaction of teeth in gearing, has been developed. The calculation of the fatigue life is based on the results of the analysis of the complex stress-strained state and the developed models of the loss of the working ability and the main principles of the destruction of teeth.

3. The loading of teeth of drive toothed belts of standard structures on the basis of the developed physical and mathematical models of the complex is stress-strained state, kinematic and power features of interaction of teeth in gearing is investigated. The equivalent pressure in the dangerous section, defining fatigue durability of teeth of a belt is estab-

lished, that, depends, basically, from their geometrical parameters. On the basis of the received results of researches recommendations on increase of a technological level of toothed-belt transmissions are developed.

4. The technique of a probabilistic estimation of the fatigue strength of a bearing layer and belt teeth on the basis of the results of their resource tests and the kinetic theory of mechanical fatigue has been developed. The results of the researches on the dissipation of the characteristics of the fatigue resistance of the elements of toothed belts have been generalized.

5. The recommendations on the choice of the optimum materials, designs and manufacturing techniques of drive toothed belts by the criterion of the highest load carrying capacity and the operational resource have been developed. It has been established that the belts, made by the method of pressing by the rigid elements, in comparison with the mould ones have a raised limit of endurance $\bar{\sigma}_r$ 1.5 times and a base number of cycles of loading N_0 1.2 times; **the reinforcement of belt teeth with copper wire Ø0.6 mm** augments $\bar{\sigma}_r$ 1.22 times and N_0 – 3.33 times in comparison with a non-reinforced design. The increase of mould pressure from 0.6 up to 20 MPa leads to the increase of $\bar{\sigma}_r$ 1.1 times and N_0 – 1.57 times. Micro-reinforcement of belt teeth by the cuts of viscose fiber increases $\bar{\sigma}_r$ 1.29 times and N_0 – 1.59 times. The increase of the tooth hardness, defined by the material of the belt filler, from 58.6 up to 85.2 units, according to Shore A, leads to the increase of $\bar{\sigma}_r$ 3 times and N_0 – 3.5 times. The increase of the degree of reinforcement of belt teeth from 0 up to 1 leads to the increase of $\bar{\sigma}_r$ 3.1 times and N_0 – 2.25 times.

6. The results of the computer finite-element modeling of the stress-strained state **of a toothed-belt** gearing, depending on the tribological characteristics of the transmission elements, have been given. The methods of lowering of friction in the contact of teeth have been offered and checked experimentally.

7. The technique of the calculation of the rational parameters **of a toothed-belt** transmission, providing uniform loading of gearing and the increase of the load carrying capacity and the operational resource of transmission, has been developed. It has been established that the loading distribution in the multiple gearing depends on the correction of a step of pulley teeth and the factor of non-uniformity of loading. The rational value of the factor is in the interval 0.8...1.1, depending on the conditions of the operation and the parameters of transmission.

CONCLUSION

The theoretical and experimental research of mechanical transmissions of power by flexible link, of the belt and toothed-belt transmissions in particular, has made it possible to solve an important scientific and technical problem of improving technical level by design, engineering and manufacturing methods.

The model of the interaction of flexible link with the pulleys has been developed. It allows considering the action of shear deformations at the transmission of power. The influence of shear deformations of flexible link on the value of its relative sliding has been defined. The received theoretical results are adequate to the experimental data, which makes it possible to recommend the developed technique for the estimation of sliding in a belt transmission, depending on its traction ability. As a result of the research of kinematics of a toothed-belt transmission, based on a matrix transformation of coordinates, the sliding velocity of teeth and the zones of their incomplete profile gearing have been defined. The developed theoretical dependences are also adequate to the received experimental data.

The research of a multiple toothed-belt gearing loading by the method of finite differences testifies that the distribution of loading corresponds to the discrete scheme. The carried out research shows the dependences of the distribution of transmitted loading on the teeth of the main transmission parameters, the conditions of gearing and mechanical and physical properties of a toothed belt have been received. It has been discovered that the most effective methodical way of gearing loading non-uniformity control and, as a consequence, raising the load carrying capacity and durability of toothed-belt transmissions level, is the correlation adjustment of a step of pulley teeth.

As a result of the investigation of dynamics and loading of a toothed-belt gearing on the basis of the developed physical and mathematical and virtual models the calculated dependences of the distribution of loading in gearing of the main parameters of transmission, the mechanical and physical properties of the elements of toothed belts have been received. It has allowed predicting their operational resource objectively. The analytical dependences have been confirmed experimentally.

On the basis of the experimental research it has been established that with the increase in a preliminary tension of flexible link its dynamic rigidity and the damping factor of vibrations increase. Therefore, the unreasonable increase in a preliminary tension leads to an increase in intrinsic losses and decrease in transmission efficiency. At the same time, along with the growth of a transmitted pull (at a constant preliminary tension of flexible

link) an increase in the dynamic rigidity and reduction of the damping factor take place. The increase in the length of flexible link leads to the significant increase of its dynamic rigidity.

The hardware-software finite-element modeling of the stress-strained state of the components of toothed-belt transmissions has been carried out. On its basis the optimum geometrical and operational parameters, which allowed essentially to raise the load carrying capacity and durability of transmission, have been defined. The results of the modeling have shown the adequacy of the worked out theoretical statements to the carried out experimental researches, which allows to ensure a qualitatively new level of designing of the toothed-belt transmissions, described by the high reliability and lowered labor cost.

The technique of the calculation of the contact pressure in a toothed-belt gearing has been developed, and the main factors promoting its lowering, have been defined. It has been established that the rounding of the tip of the trapezoidal teeth of pulleys reduces contact stresses of belt teeth considerably. The optimum value of the radius of rounding has been determined. On the basis of the computer modeling it has been established that the semicircular profile of teeth is more effective from the point of view of minimization of the contact pressure in gearing.

The modern technique and equipment for the manufacture of drive toothed belts have been developed. The technique is characterized by the reduced power, material and labor costs and by the increased ecological cleanliness. The rational parameters of the technological process have been offered.

The chevron toothed-belt transmission with the raised engineering and ecological characteristics, having the correction of the slopes of teeth of pulleys relating to the slope of belt teeth, defined by the kinematical and force features of gearing of teeth, has been developed.

It has been established that the most effective design method of the improvement of operational characteristics of toothed-belt transmissions is macro-reinforcement of toothed belts. The designs and engineering of toothed belts with sleeve-loopback reinforcement of teeth have been presented. As a result of the research of the stress-strained state the significant lowering of stresses and deformations in the dangerous section in comparison with the standard non-reinforced design has been established. The techniques of drive toothed belts durability prediction, based on the models of their destruction due to the wear and fatigue failure have been developed and confirmed experimentally. On the basis of the resource tests, probability methods of the estimation of the fatigue strength and kinetic theory of

mechanical fatigue the results of the investigations in the dispersion of characteristics of resistance of the fatigue of flexible links have been generalized.

The modern technique of the design calculation of a toothed-belt transmission with the improved operational characteristics has been developed.

The received investigation results have been introduced in some industrial enterprises of the Republic of Belarus and the Russian Federation with a significant economical efficiency.

The research works, presented in the monography, were awarded a silver medal and a diploma at III International Innovation and Investment Exhibition in Moscow.

APPENDICES

Appendix 1. The program of the solution of the system of the differential equations of the dynamic model of the force interaction of teeth in gearing (object-oriented programming)

Uses Objects, Graph, Crt, GrDTop, Mouse, GrafMatr;

```
const
{GraphDeskTop}
ExitFl : Boolean = False;
const
{model const}
M = 46.2;
mm = 4;
mv = 0.076;
Kc = 5;
Kd = 0.035;
c = 0.0036;
cv = 0.5;
F = 10.00;
Kvc = 700;
Kvd = 10;

type
UndoRec = Record
    TStart: Real;
    Tend: Real;
end;

var
{GraphDeskTop}
CurColor      : Byte;
DeltaT         : Real;
Time           : Real;
IsCount        : Boolean;
TStart         : Real;
TEnd           : Real;
RCoord         : RealCoordType;
grDriver       : Integer;
grMode         : Integer;
ErrCode        : Integer;
```

```

_str      : String;
OutStr    : String;
LTCoord   : PointType;
RBCoord   : PointType;
MouseRec  : TMouseRec;
OldMouseRec : TMouseRec;
UndoArray : Array[1..5] of UndoRec;
UndoArrPtr : Byte;

```

```

LeftPanel : PPanel;
DownPanel : PPanel;
ZoomInBtn : PButton;
ZoomOutBtn : PButton;
ReDrawBtn : PButton;
UndoBtn    : PButton;
ExitBtn    : PButton;

```

```
type
```

```
{modelling types}
```

```
  Glnarray = ARRAY[1..10] OF real;
```

```
var
```

```
{modelling Variables}
```

```
  t,h      : Real;
```

```
  x,dxdt,xout : GlnArray;
```

```
  s,ds     : Real;
```

```
{DataFiles}
```

```
  fModel : text;
```

```
  fPModel : text;
```

```
  MazFile : text;
```

```
Function IsMouseChange : Boolean;
```

```
begin
```

```
  IsMouseChange:=False;
```

```
  MsRead(MouseRec.x,MouseRec.y,MouseRec.MBut);
```

```
  With MouseRec Do Begin
```

```
    IF (OldMouseRec.X <> X) or (OldMouseRec.Y <> Y) Then Begin
```

```
      Str(MouseRec.x:4,OutStr);
```

```
      Str(MouseRec.y:4,_str);
```

```
      OutStr:= OutStr +_str;
```

```
      setcolor(7);
```

```

    setfillstyle(1,7);
    Bar(GetMaxX-69,GetMaxY-10,GetMaxX-6,GetMaxY-2);
    setcolor(0);
    OutTextXY(GetMaxX-75,GetMaxY-10,OutStr);
    IsCount:=False;
end
else begin
    If not IsCount then Begin
        Time:=TStart + MouseRec.X/(GetMaxX-76-3)*DeltaT;
        RetRealcoord('Model',Time,RCoord);
        setfillstyle(1,7);
        Bar(3,GetMaxY-11,GetMaxX-76,GetMaxY-2);
        setcolor(0);
        Str(Time:7:3,OutStr);
        OutTextXY(GetMaxY-120,GetMaxY-11,'t:'+OutStr);
        setcolor(14);
        Str(RCoord.sq:8:4,OutStr);
        OutTextXY(3,GetMaxY-11,'s:'+OutStr);
        setcolor(11);
        Str(RCoord.sqt:8:4,OutStr);
        OutTextXY(120,GetMaxY-11,'v:'+OutStr);
        setcolor(4);
        Str(RCoord.sqtt:8:4,OutStr);
        OutTextXY(240,GetMaxY-11,'a:'+OutStr);
        IsCount :=True;
    end;
end;
IF (OldMouseRec.MBut <> MBut) Then IsMouseChange:=True;
end;
OldMouseRec:=MouseRec;
end;

```

```

Procedure DrawGraphics(TStart,TEnd : Real);

```

```

Begin
{DrawGraphics}
GraphEl('Model',          {File.Dat}
        1,                  {EINum}
        3,2,GetMaxX-76,GetMaxY-16,{Coord}
        False,              {ClearFlag}
        ",                  {avStr}
        false,              {ZeroLine}
        0,                  {ZeroNum}

```

```

        False,          {AllGrFI}
        2,TStart,TEnd);
GraphEl('Model',      {File.Dat}
        2,              {EINum}
        3,2,GetMaxX-76,GetMaxY-16,{Coord}
        False,         {ClearFlag}
        ",             {avStr}
        false,         {ZeroLine}
        0,              {ZeroNum}
        False,         {AllGrFI}
        1,TStart,TEnd);
GraphEl('Model',      {File.Dat}
        3,              {EINum}
        3,2,GetMaxX-76,GetMaxY-16,{Coord}
        False,         {ClearFlag}
        ",             {avStr}
        false,         {ZeroLine}
        0,              {ZeroNum}
        False,         {AllGrFI}
        4,TStart,TEnd);
end;

```

Procedure ReDrawProc;

```

Begin
  SetViewPort(2,3,GetMaxX-76,GetMaxY-16,False);
  SetBkColor(15);
  ClearViewPort;
  SetViewPort(0,0,GetMaxX,GetMaxY,False);
  UndoArray[UndoArrPtr].TStart:=TStart;
  UndoArray[UndoArrPtr].TEnd:=TEnd;
  DrawGraphics(Tstart,TEnd);
  UndoArrPtr:=UndoArrPtr+1;
  IF UndoArrPtr>5 Then UndoArrPtr:=5;
  DeltaT:=RetDeltaT;
  Tstart:=RetTStart;
  TEnd :=TStart+DeltaT;
End;

```

Procedure UndoProc;

```

Begin
  UndoArrPtr:=UndoArrPtr-2;
  If UndoArrPtr<=0 then UndoArrPtr:=1;

```

```

TStart := UndoArray[UndoArrPtr].TStart;
TEnd := UndoArray[UndoArrPtr].TEnd;
RedrawProc;
end;

```

```

Procedure PushLeftButton;

```

```

Begin

```

```

IF ZoomInBtn^.PushButton(MouseRec.X,MouseRec.Y,False) Then TEnd:=TEnd*0.3;

```

```

IF ZoomOutBtn^.PushButton(MouseRec.X,MouseRec.Y,False) Then

```

```
TEnd:=TEnd/0.3;

```

```

IF ReDrawBtn^.PushButton(MouseRec.X,MouseRec.Y,False) Then ReDrawProc;

```

```

IF UndoBtn^.PushButton(MouseRec.X,MouseRec.Y,False) Then UndoProc;

```

```

IF ExitBtn^.PushButton(MouseRec.X,MouseRec.Y,False) Then ExitFl:=True;

```

```

IF (MouseRec.X>3) and (MouseRec.X<(GetMaxX-76)) Then TStart:=TStart + Mouse-
eRec.X/(GetMaxX-76-3)*DeltaT;

```

```

end;

```

```

Procedure PushRightButton;

```

```

Begin

```

```

If (MouseRec.X>3) and (MouseRec.X<(GetMaxX-76)) Then

```

```

If TStart < (TStart + MouseRec.X/(GetMaxX-76-3)*DeltaT) Then

```

```

TEnd:=TStart + MouseRec.X/(GetMaxX-76-3)*DeltaT;

```

```

end;

```

```

Procedure EventInterpretator;

```

```

begin

```

```

MsHide;

```

```

Case MouseRec.MBut of

```

```

1: PushLeftButton;

```

```

2: PushRightButton;

```

```

end;

```

```

MsShow;

```

```

end;

```

```

Procedure ShowDeskTop;

```

```

Begin

```

```

{Panels}

```

```

LTCoord.X:=GetMaxX-75;

```

```

LTCoord.Y:=1;

```

```

RBCoord.X:=GetMaxX-5;

```

```

RBCoord.Y:=GetMaxY-1;

```

```

LeftPanel := New(PPanel,Init(LTCoord,RBCoord,7));

```



```

LTCoord.X:=1;
LTCoord.Y:=GetMaxY-15;
RBCoord.X:=GetMaxX-75;
RBCoord.Y:=GetMaxY-1;
DownPanel := New(PPanel,Init(LTCoord,RBCoord,7));

{Buttons}
LTCoord.X:=GetMaxX-70;
LTCoord.Y:=10;
RBCoord.X:=GetMaxX-10;
RBCoord.Y:=30;
ZoomInBtn := New(PButton,Init(LTCoord,RBCoord,7,'>>'));

LTCoord.X:=GetMaxX-70;
LTCoord.Y:=45;
RBCoord.X:=GetMaxX-10;
RBCoord.Y:=65;
ZoomOutBtn := New(PButton,Init(LTCoord,RBCoord,7,'<<'));

LTCoord.X:=GetMaxX-70;
LTCoord.Y:=80;
RBCoord.X:=GetMaxX-10;
RBCoord.Y:=100;
ReDrawBtn := New(PButton,Init(LTCoord,RBCoord,7,'ReDraw'));

LTCoord.X:=GetMaxX-70;
LTCoord.Y:=115;
RBCoord.X:=GetMaxX-10;
RBCoord.Y:=135;
UndoBtn := New(PButton,Init(LTCoord,RBCoord,7,'Undo'));

LTCoord.X:=GetMaxX-70;
LTCoord.Y:=GetMaxY-60;
RBCoord.X:=GetMaxX-10;
RBCoord.Y:=GetMaxY-40;;
ExitBtn := New(PButton,Init(LTCoord,RBCoord,7,'Exit'));

{DeskTop}
Line(1,GetMaxY-1,1,1);
Line(GetMaxX-1,1,1,1);

LeftPanel^.ShowPanel;

```

```

DownPanel^.ShowPanel;
ZoomInBtn^.ShowEnableButton;
ZoomOutBtn^.ShowEnableButton;
ReDrawBtn^.ShowEnableButton;
UndoBtn^.ShowEnableButton;
ExitBtn^.ShowEnableButton;
end;
Procedure ReleDeskTop;
begin
  Dispose(LeftPanel,Done);
  Dispose(DownPanel,Done);
  Dispose(ZoomInBtn,Done);
  Dispose(ZoomOutBtn,Done);
  Dispose(ReDrawBtn,Done);
  Dispose(UndoBtn,Done);
  Dispose(ExitBtn,Done);
end;

```

```

{-----}
{Include modelling files}
  {$I SaveFile.inc}
  {$I Derivs.inc}
{-----}

```

```

{Main}
Begin
  {Open File of output results}
  Assign(fModel,'Model.dat');
  ReWrite(fModel);
  Assign(fPModel,'PModel.dat');
  ReWrite(fPModel);

  {Road variables}

  {Start conditions}
  x[1]:=0;
  x[2]:=0;
  x[3]:=0;
  x[4]:=0;
  x[5]:=0;
  x[6]:=0;
  h:=0.001;

```

```

t:=0;
While t < 1 Do
  Begin
    model;
    t := t + h
  End;
Close(fModel);
Close(fPModel);

{GraphDeskTop}
grDriver := Detect;
InitGraph(grDriver, grMode, ' ');
ErrCode := GraphResult;
if ErrCode <> grOk then
  Begin
    WriteLn('Graphics error:', GraphErrorMsg(ErrCode));
    Halt(2);
  end;

UndoArrPtr:=1;
ShowDeskTop;
InitGraphics;
ReDrawProc;
{Mouse}
MsShow;
{DeskTopEventInterpretator}
Repeat
  IF IsMouseChange Then EventInterpretator;
Until (MouseRec.MBut=3) or ExitFl ;
CloseGraph;
DoneGraphics;
ReleDeskTop;
end.

{ Integration of Ordinary }
{ Differential Equations }
{ Runge-Kutta Method }

PROCEDURE rk4(y,dydx : glnarray; n: integer; x,h : real;
              Var yout: glnarray);

{ Programs using routine RK4 must provide a }

```

```

{ PROCEDURE derivs(x:real;y:glnarray;VAR dydx:glnarray); }
{ which returns the derivatives dydx at location      }
{ x,given both x and the                          }
{ funtion values y.The calling program must also define  }
{ the types                                         }
{ TYPE                                             }
{   glnarray = ARRAY[1..nvar] OF real;           }
{ where nvar is the number of variables y.        }

```

```

VAR

```

```

    i      : integer;
    xh,hh,h6 : real;
    dym,dyt,yt : glnarray;

```

```

BEGIN

```

```

    hh:=h*0.5; h6:=h/6.0; xh:=x+hh;
    FOR i:=1 TO n DO BEGIN
        yt[i]:=y[i]+hh*dydx[i] END;
    derivs(xh,yt,dyt);
    FOR i:=1 TO n DO BEGIN
        yt[i]:=y[i]+hh*dyt[i]  END;
    derivs(xh,yt,dym);
    FOR i:=1 TO n DO BEGIN
        yt[i]:=y[i]+h*dym[i]; dym[i]:=dym[i]+dym[i] END;
    derivs(x+h,yt,dyt);
    FOR i:=1 TO n DO BEGIN
        yout[i]:=y[i]+h6*(dydx[i]+dym[i]+2.0*dym[i]) END
END;

```

```

Procedure Derivs(t:real; x: glnarray; var dxdt: glnarray);

```

```

Begin

```

```

    dxdt[1] := x[4];
    dxdt[2] := x[5];
    dxdt[3] := x[6];
    dxdt[4] := (-Kc*x[1]+c*Kc/Kd*x[5]+Kc*x[2]+F)/M;
    dxdt[5] := (-Kc*x[2]+c*Kc/Kd*x[6]+Kc*x[3]-F)/mm;
    dxdt[6] := (-Kvc*x[3]+cv*Kvc/Kvd*x[5]+Kvd*x[2])/mv;

```

```

End;      { derivs }

```

```

{$I Rk4.inc}

```

```

Procedure Model;

```

```

Begin

```

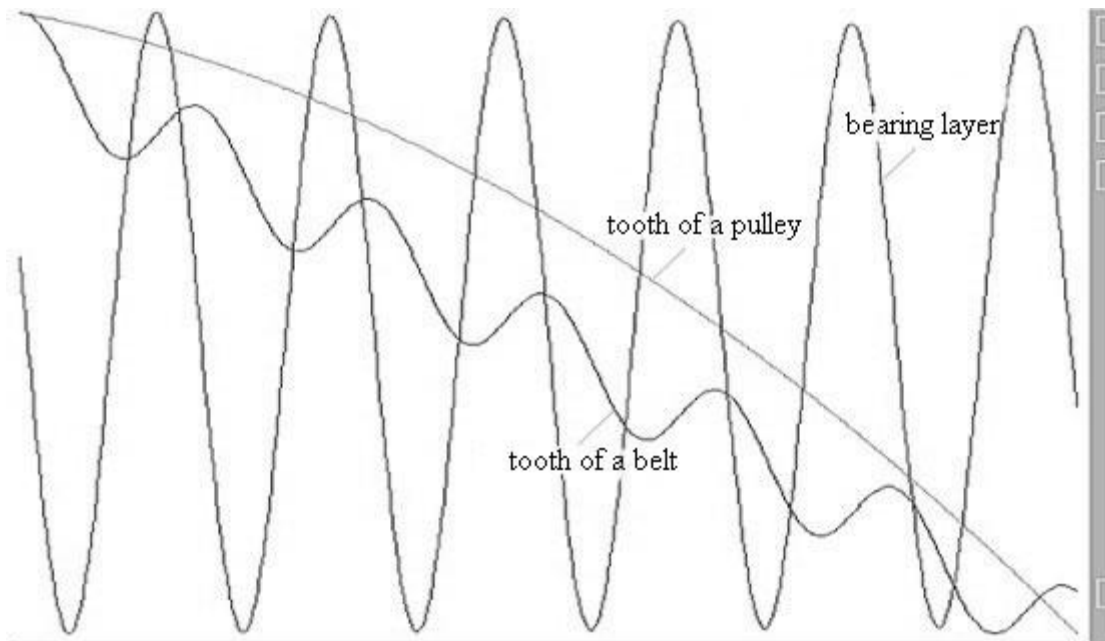
```

    {Equation & Runge_Kutta method }
    Derivs(t,x,dxdt);

```

```
Rk4(x,dxdt,6,t,h,xout);  
{Save result on current step}  
SaveFile(t,dxdt[4]*M,dxdt[5]*mm,dxdt[6]*mv,dxdt[2],x[3],dxdt[3]);  
x := xout;  
end;
```

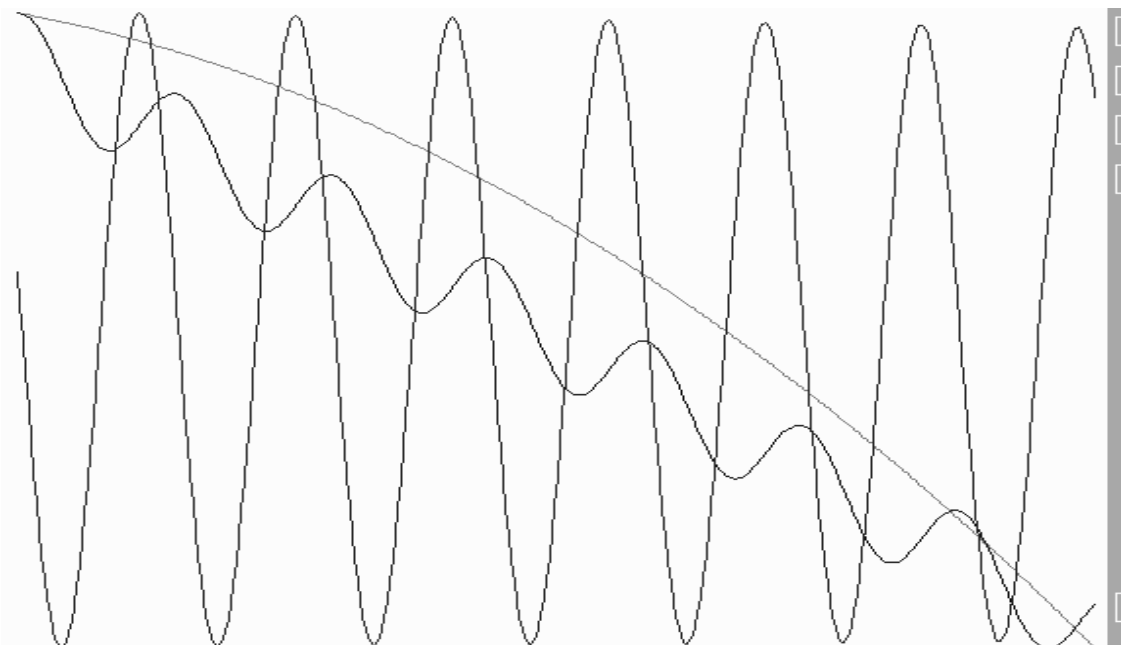
Appendix 2. Distribution of loading in a toothed-belt gearing



$$m_{\text{ш}} = 46,2; m_{\text{п}} = 4; m_l = 0,076; k_c = 5; k_d = 0,035; c = 0,0036;$$

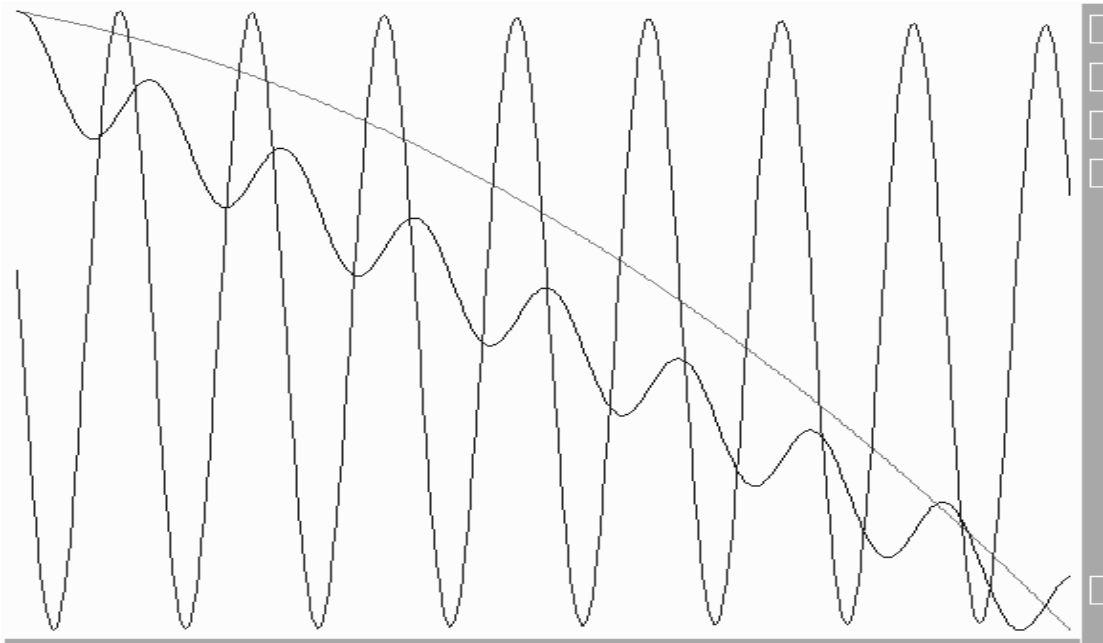
$$c_v = 0,5; F = 10; k_{vc} = 700; k_{vd} = 10; m = 3; t_p = 9,42; z_1 = z_2 = 30$$

Fig. A.1. Loading of elements of a toothed-belt gearing



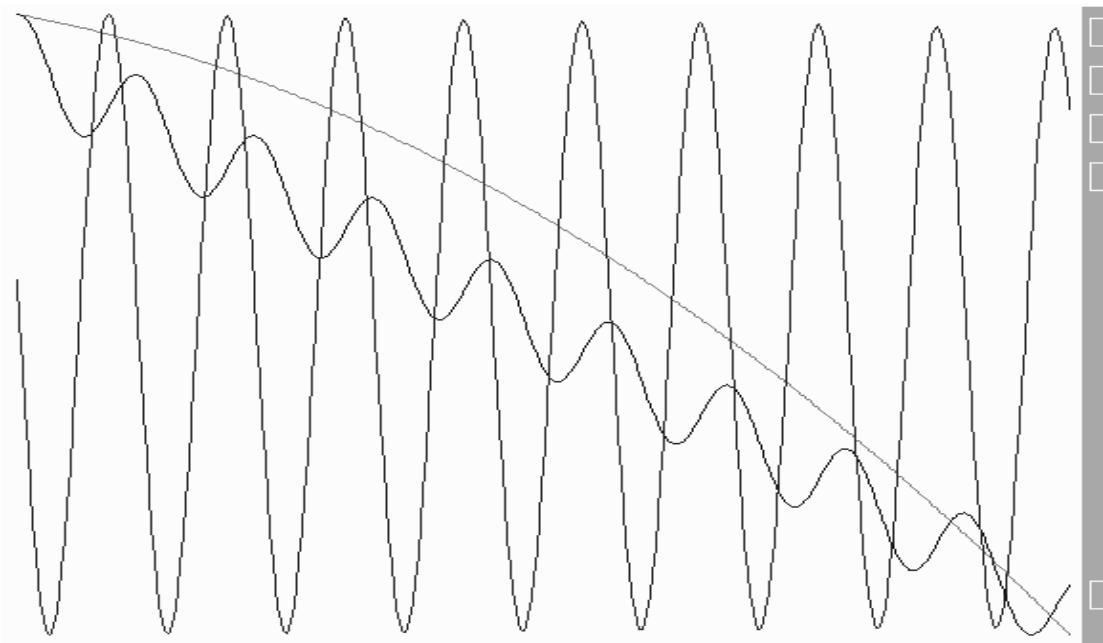
$$k_{vc} = 900$$

Fig. A.2. Loading of elements of a toothed-belt gearing



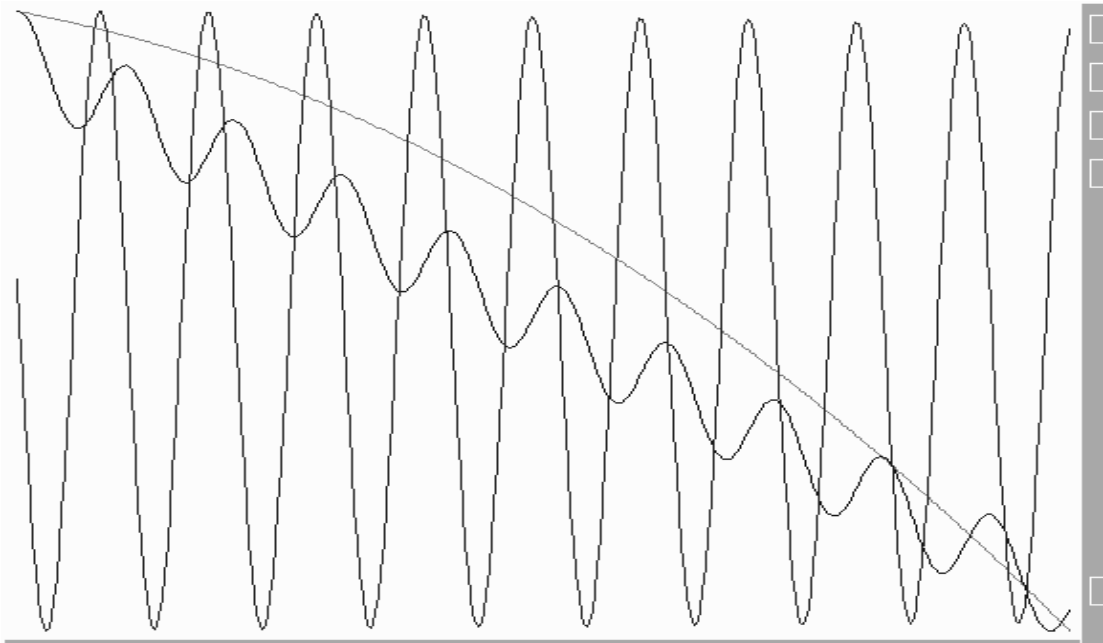
$$k_{vc} = 1200$$

Fig. A.3. Loading of elements of a toothed-belt gearing



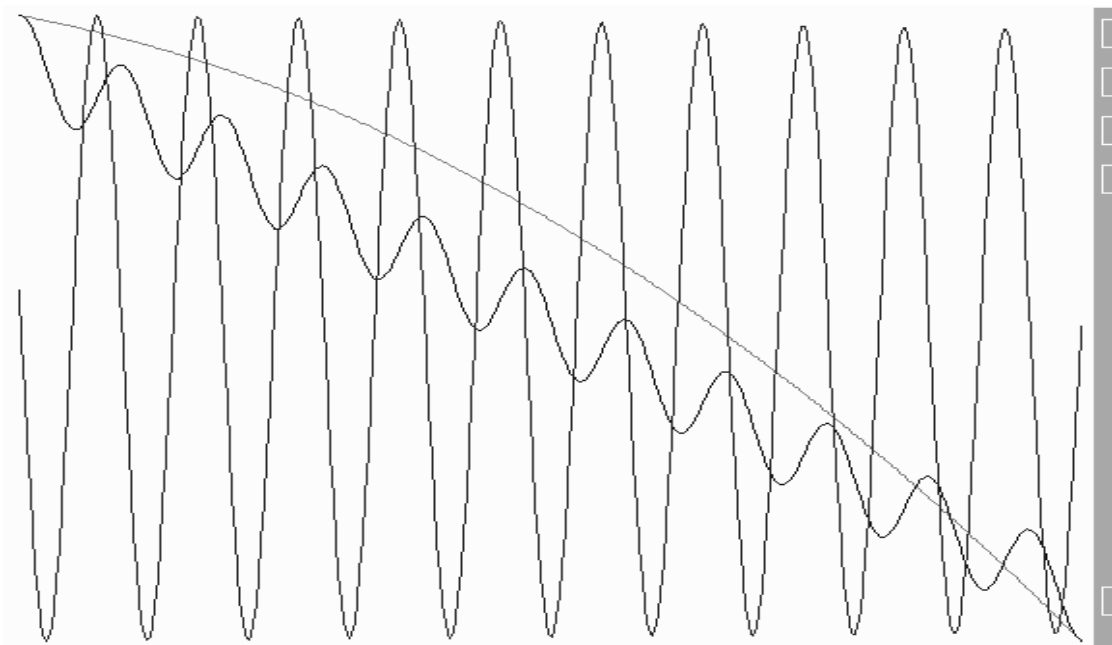
$$k_{vc} = 1500$$

Fig. A.4. Loading of elements of a toothed-belt gearing



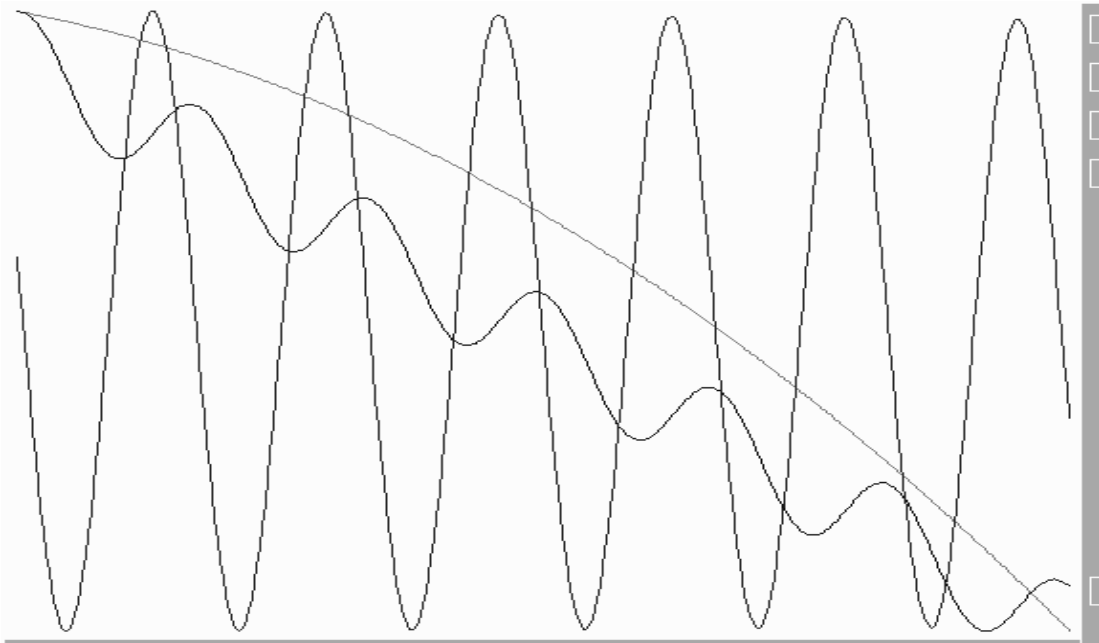
$$k_{vc} = 1800$$

Fig. A.5. Loading of elements of a toothed-belt gearing



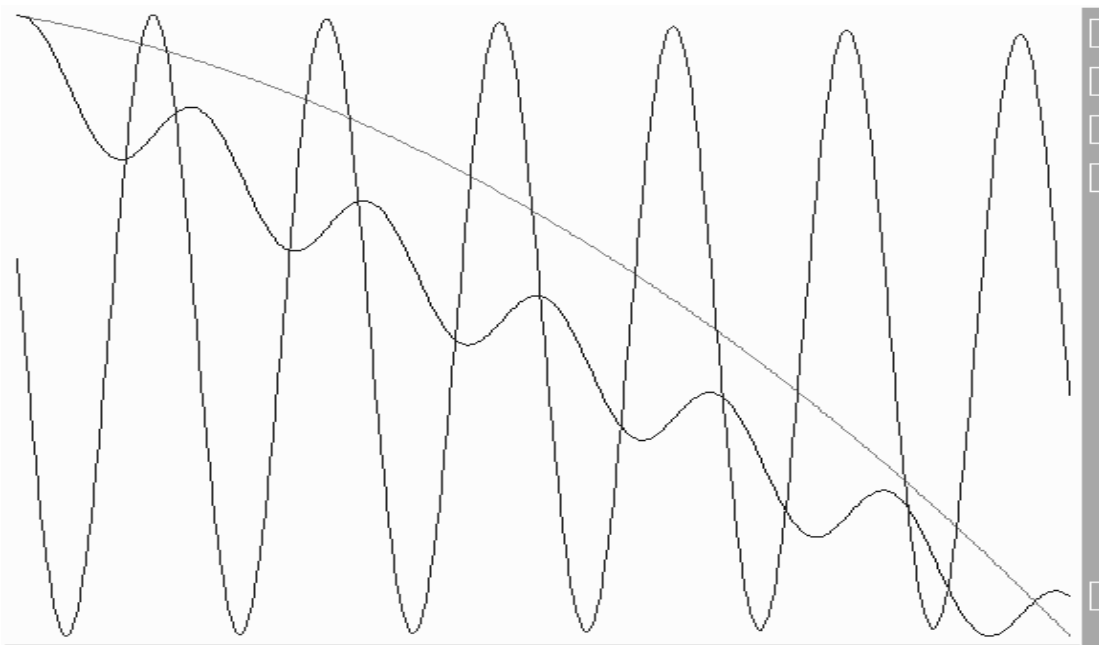
$$k_{vc} = 2100$$

Fig. A.6. Loading of elements of a toothed-belt gearing



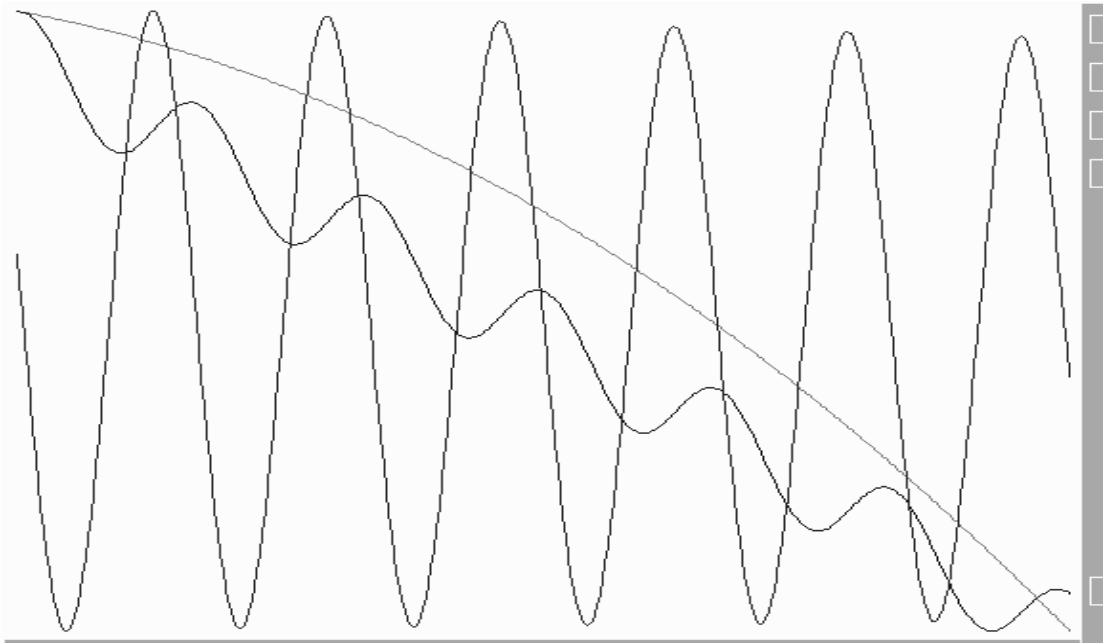
$$k_c = 3$$

Fig. A.7. Loading of elements of a toothed-belt gearing



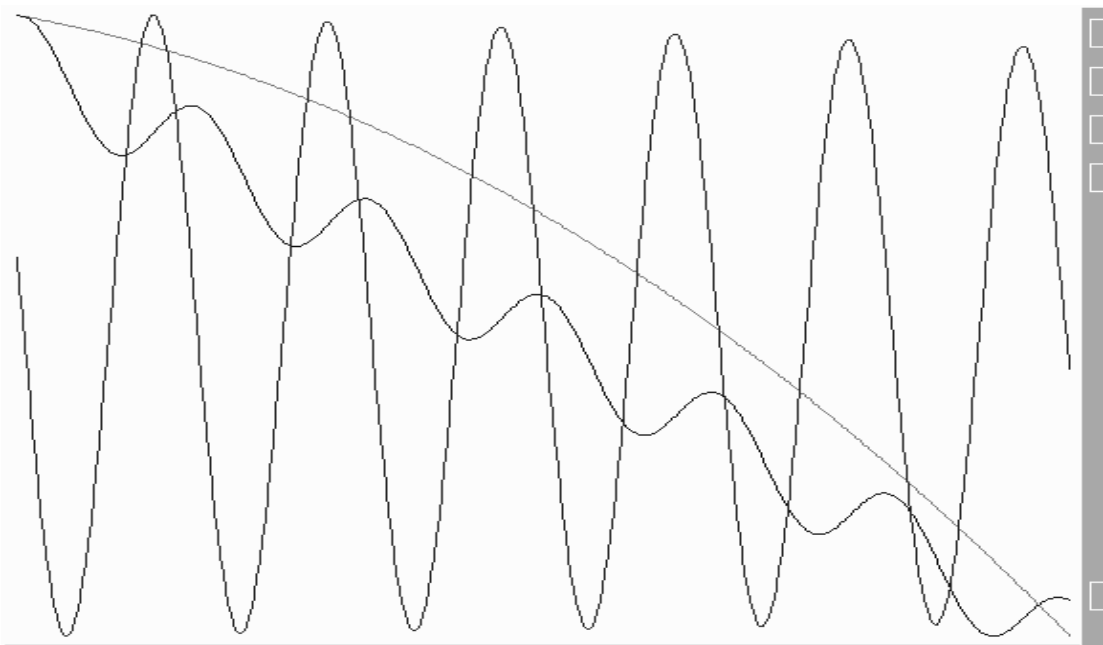
$$k_c = 7$$

Fig. A.8. Loading of elements of a toothed-belt gearing



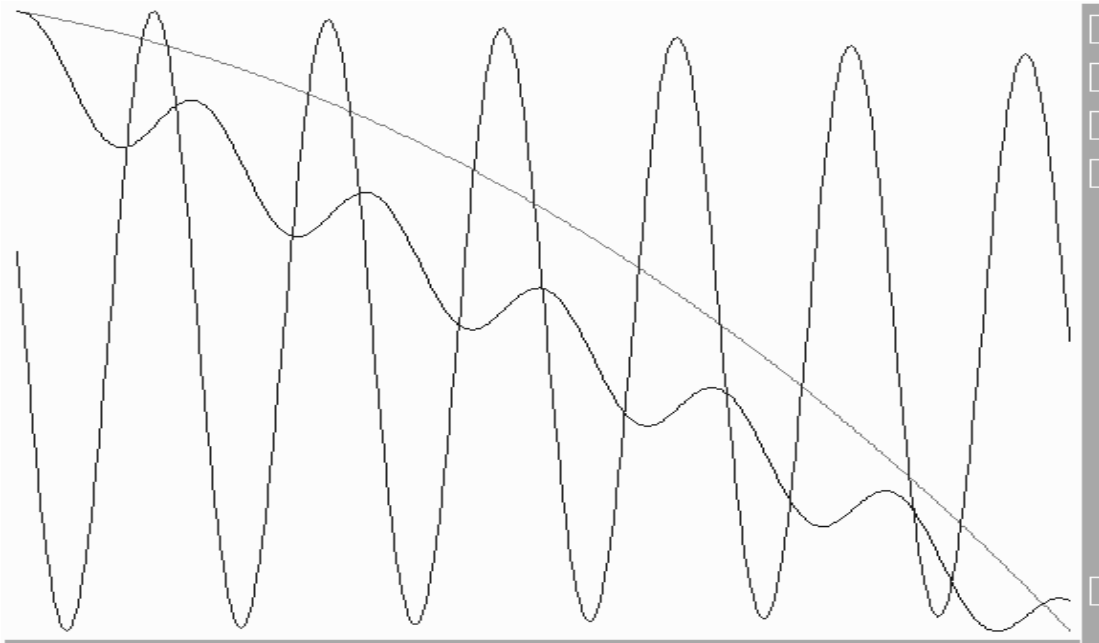
$$k_c = 9$$

Fig. A.9. Loading of elements of a toothed-belt gearing



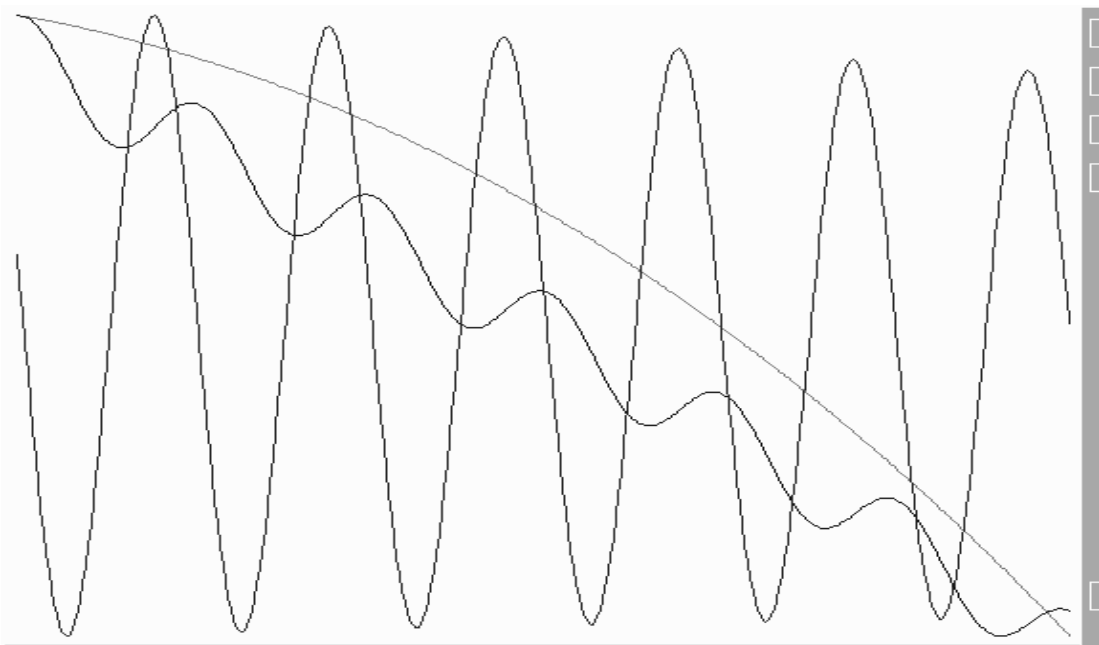
$$k_c = 11$$

Fig. A.10. Loading of elements of a toothed-belt gearing



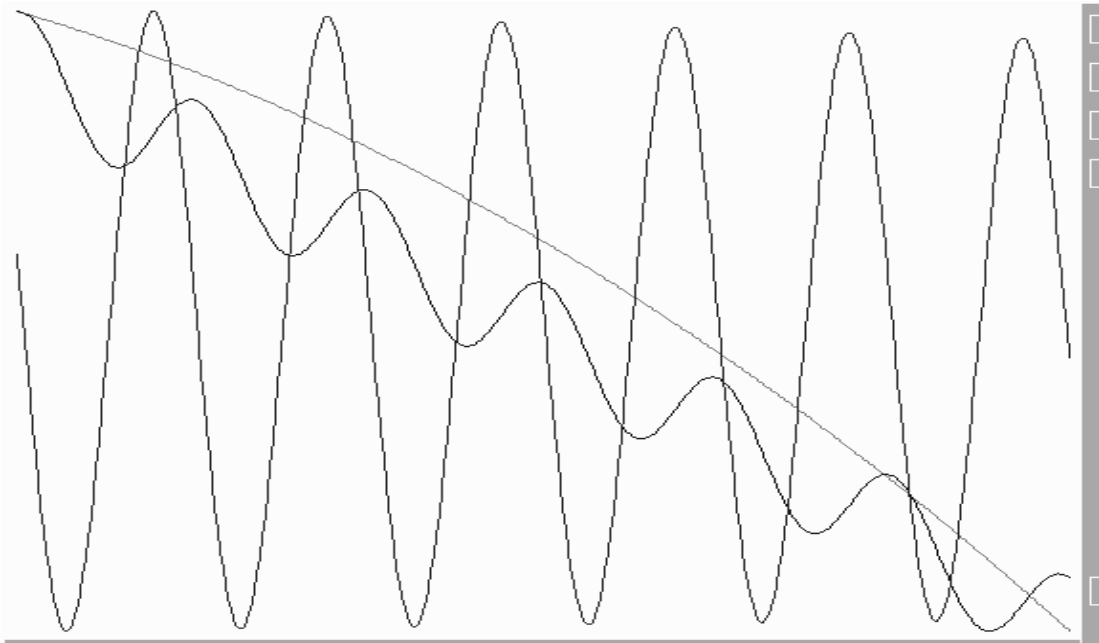
$$k_c = 15$$

Fig. A.11. Loading of elements of a toothed-belt gearing



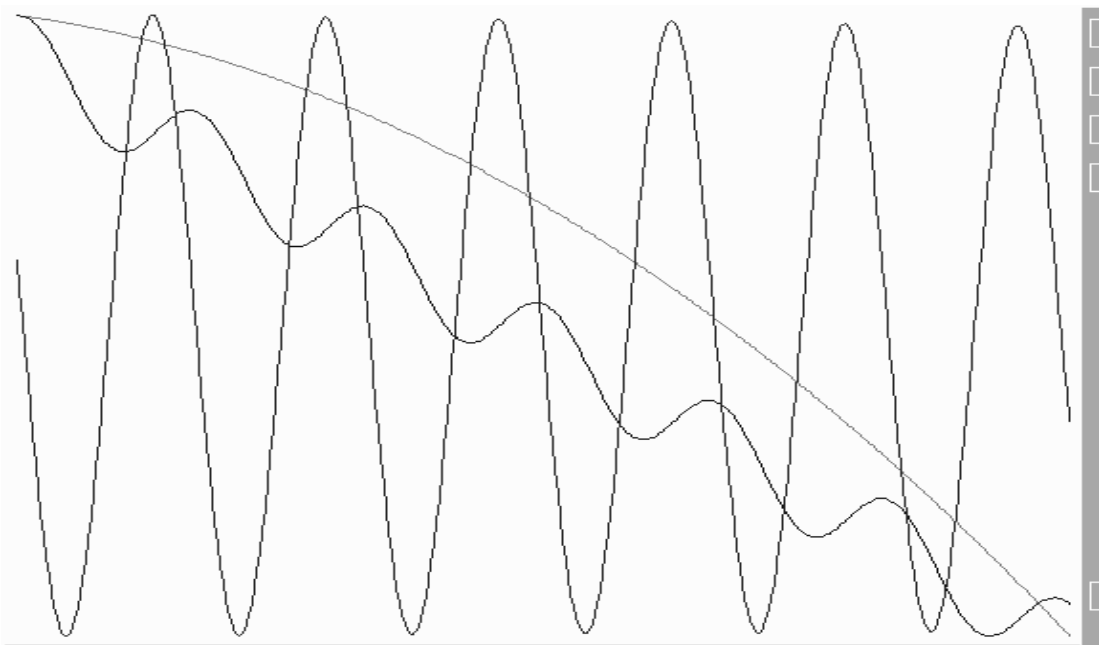
$$k_c = 19$$

Fig. A.12. Loading of elements of a toothed-belt gearing



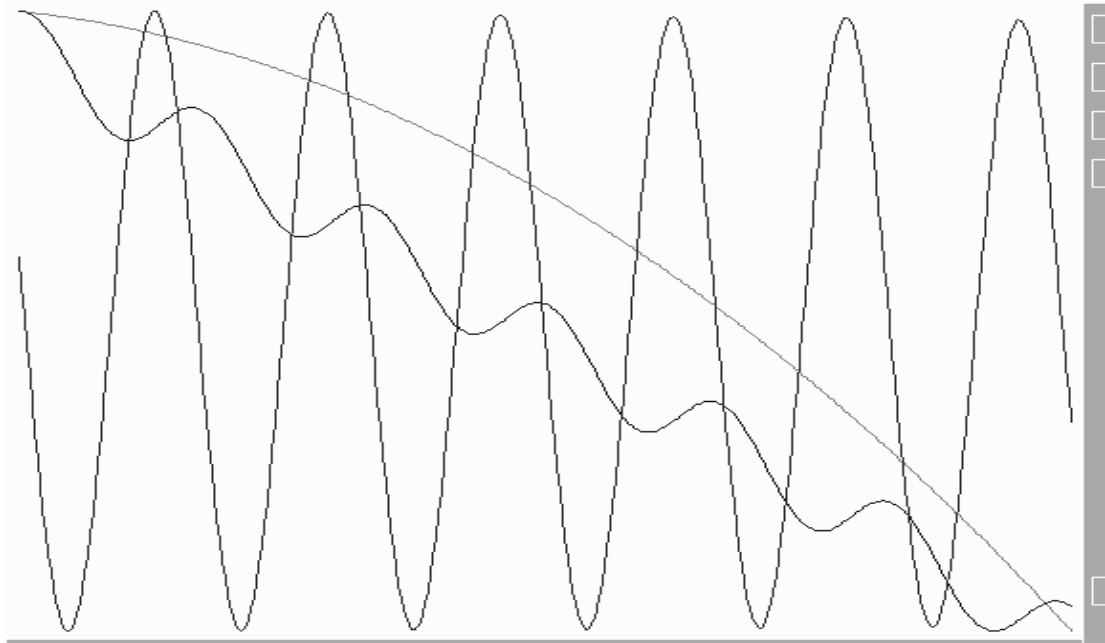
$$k_d = 0,015$$

Fig. A.13. Loading of elements of a toothed-belt gearing



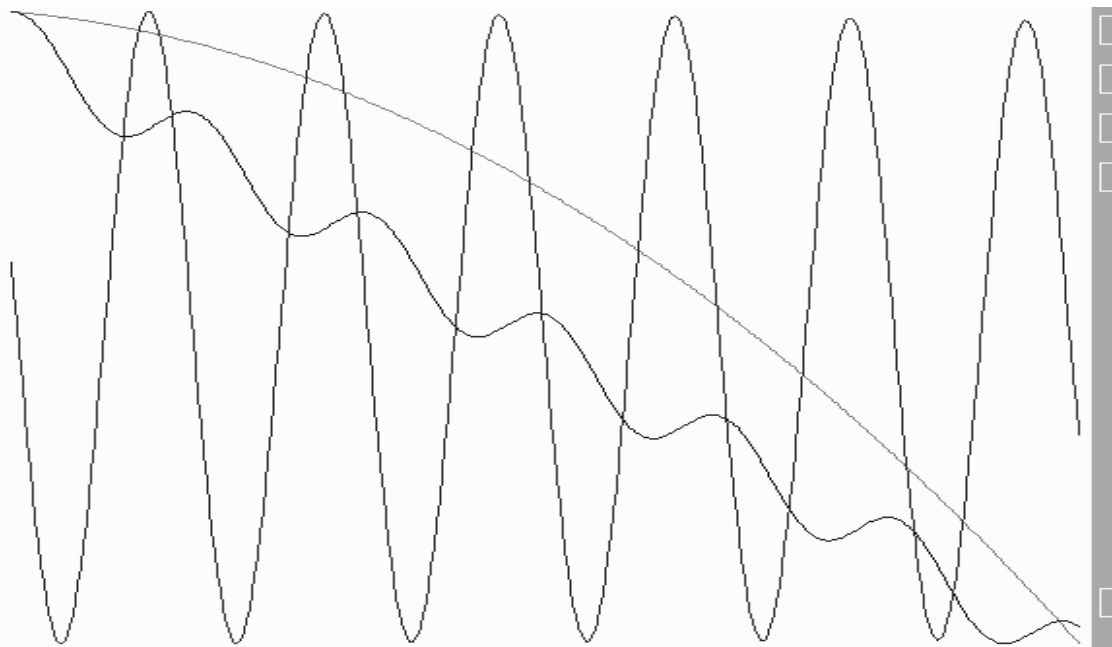
$$k_d = 0,055$$

Fig. A.14. Loading of elements of a toothed-belt gearing



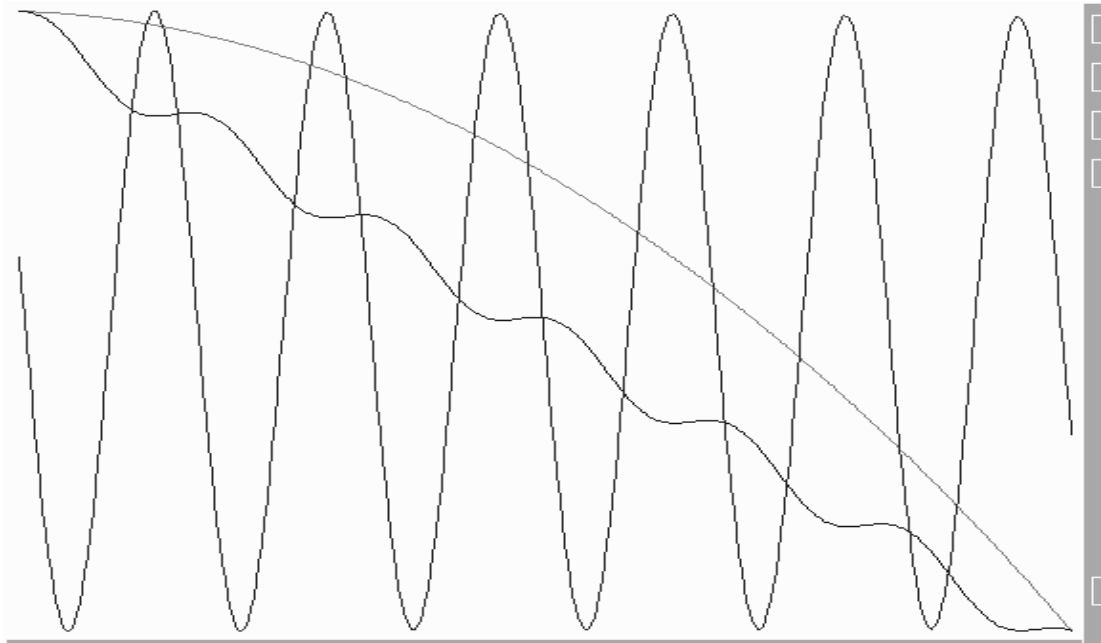
$$k_d = 0,075$$

Fig. A.15. Loading of elements of a toothed-belt gearing



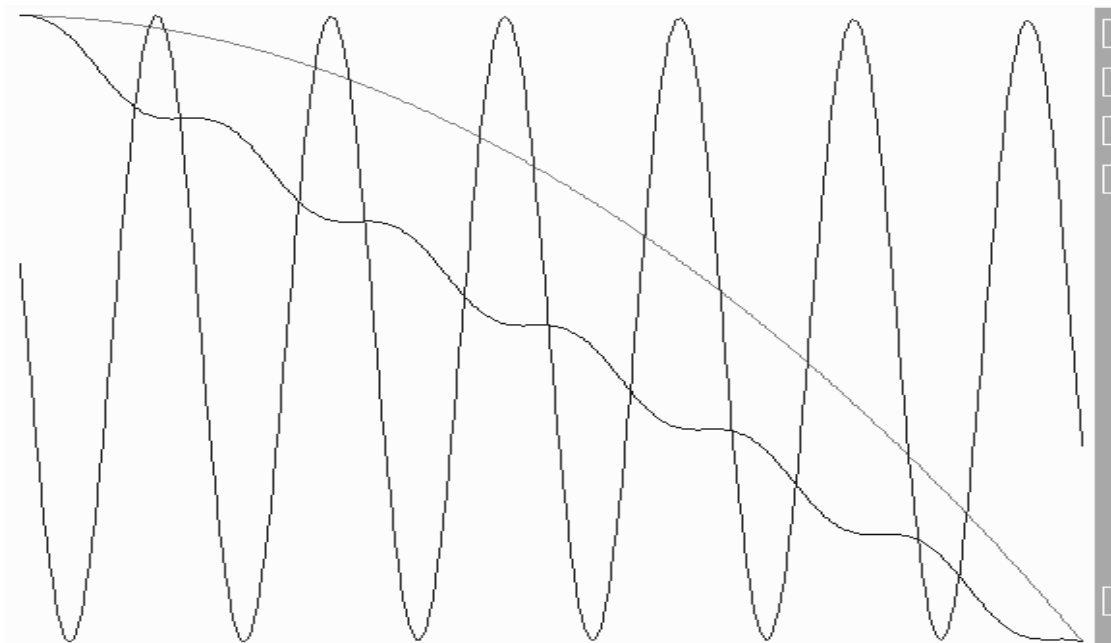
$$k_d = 0,1$$

Fig. A.16. Loading of elements of a toothed-belt gearing



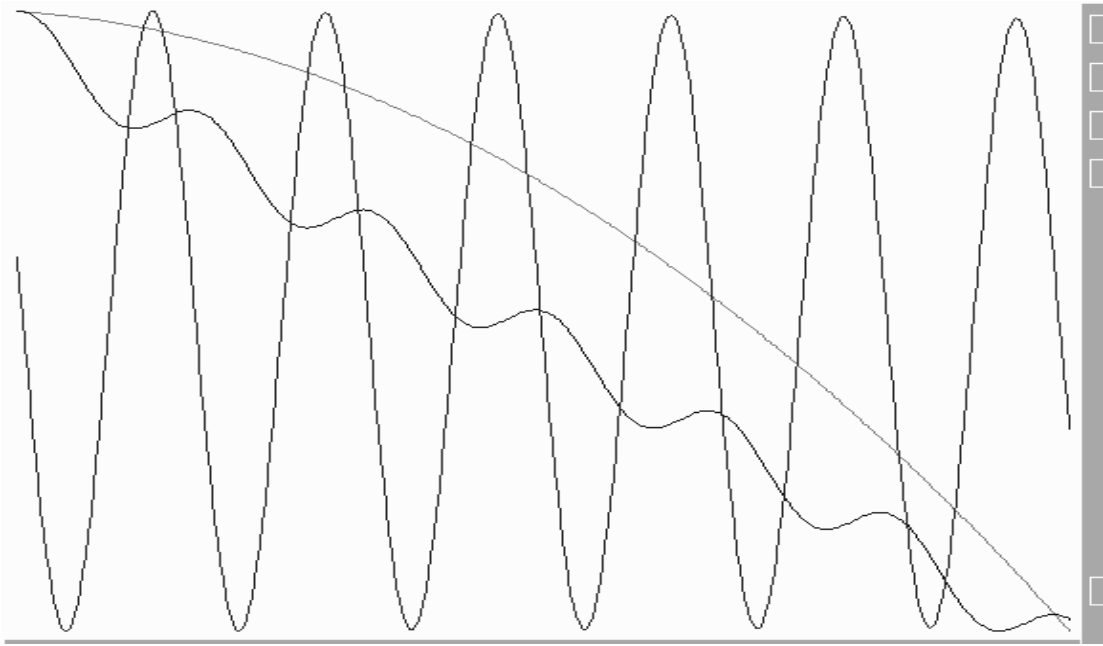
$$k_d = 0,3$$

Fig. A.17. Loading of elements of a toothed-belt gearing



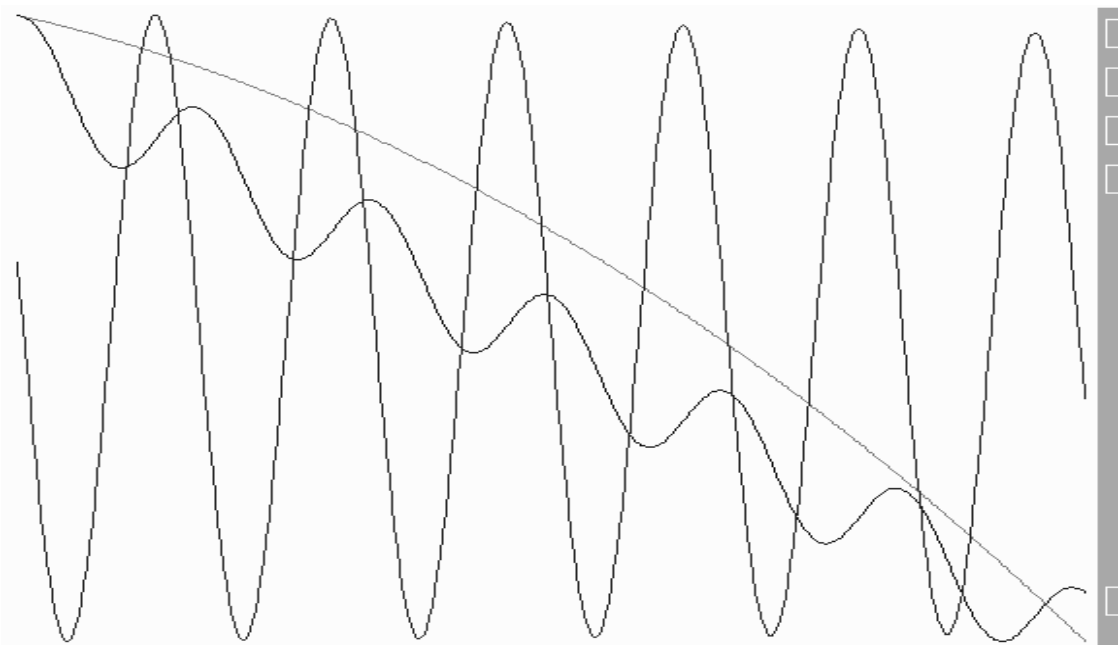
$$k_d = 0,5$$

Fig. A.18. Loading of elements of a toothed-belt gearing



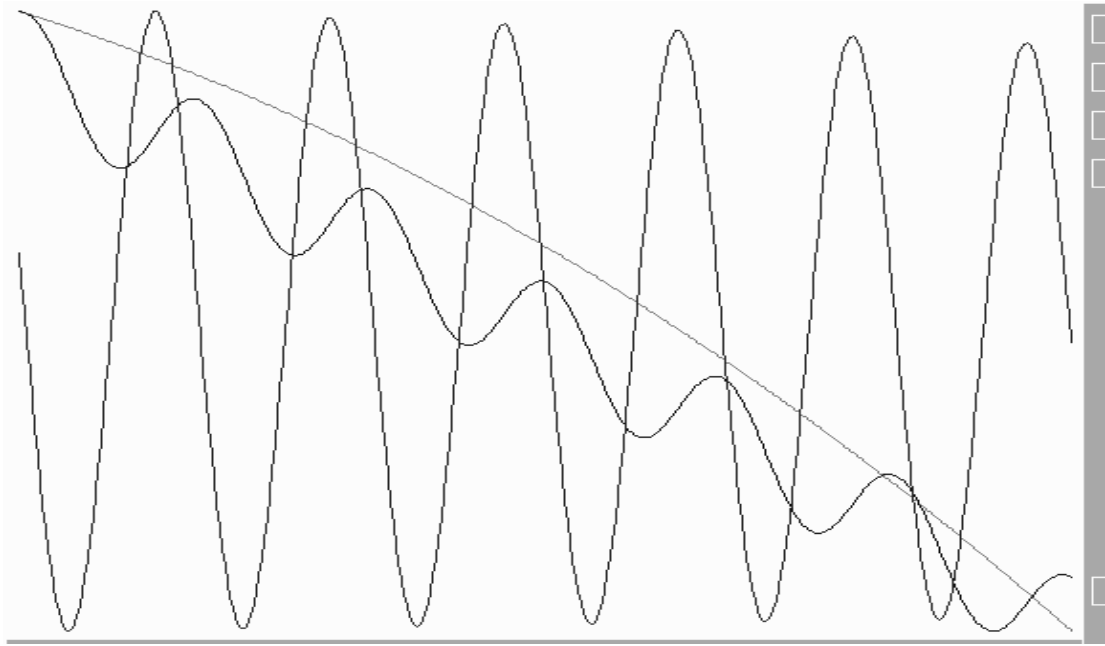
$c = 0,001$

Fig. A.19. Loading of elements of a toothed-belt gearing



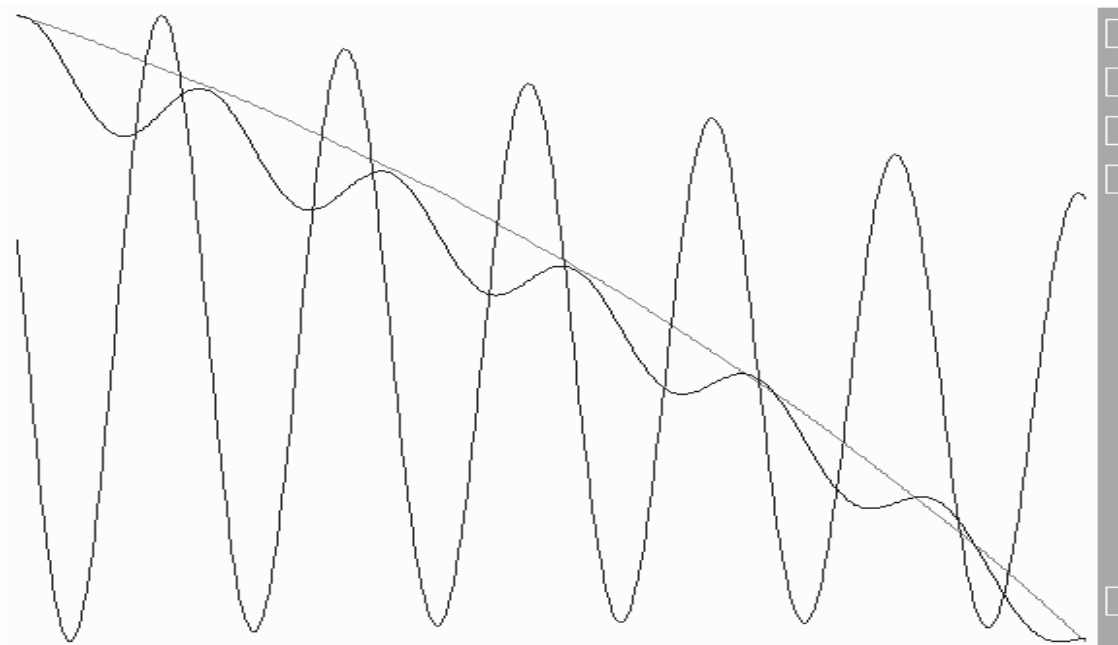
$c = 0,005$

Fig. A.20. Loading of elements of a toothed-belt gearing



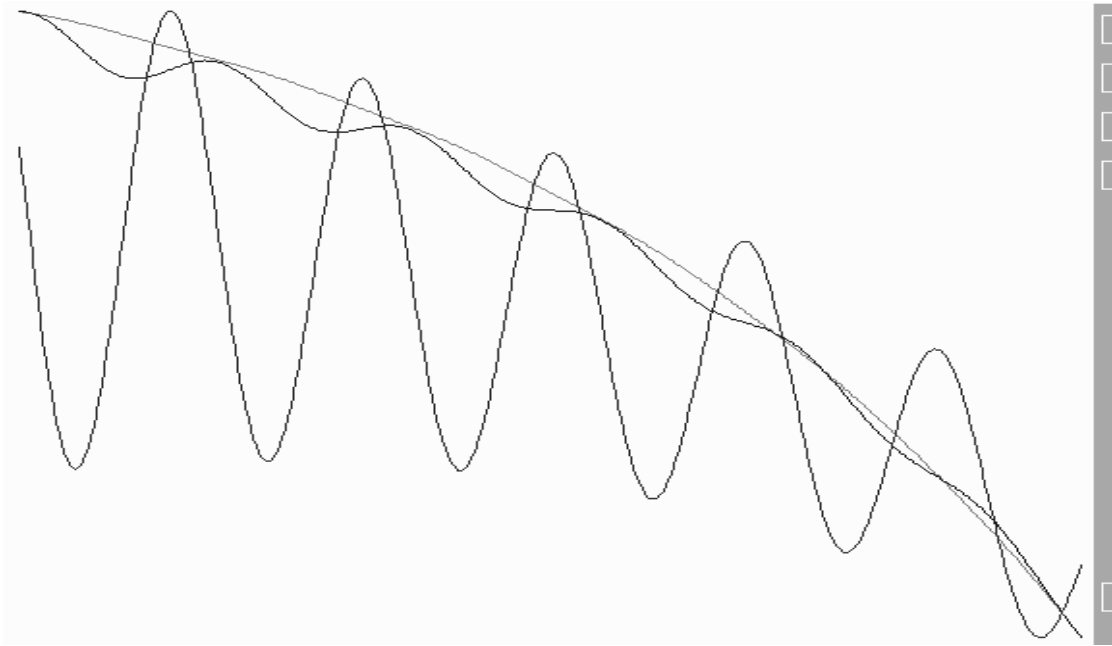
$c = 0,01$

Fig. A.21. Loading of elements of a toothed-belt gearing



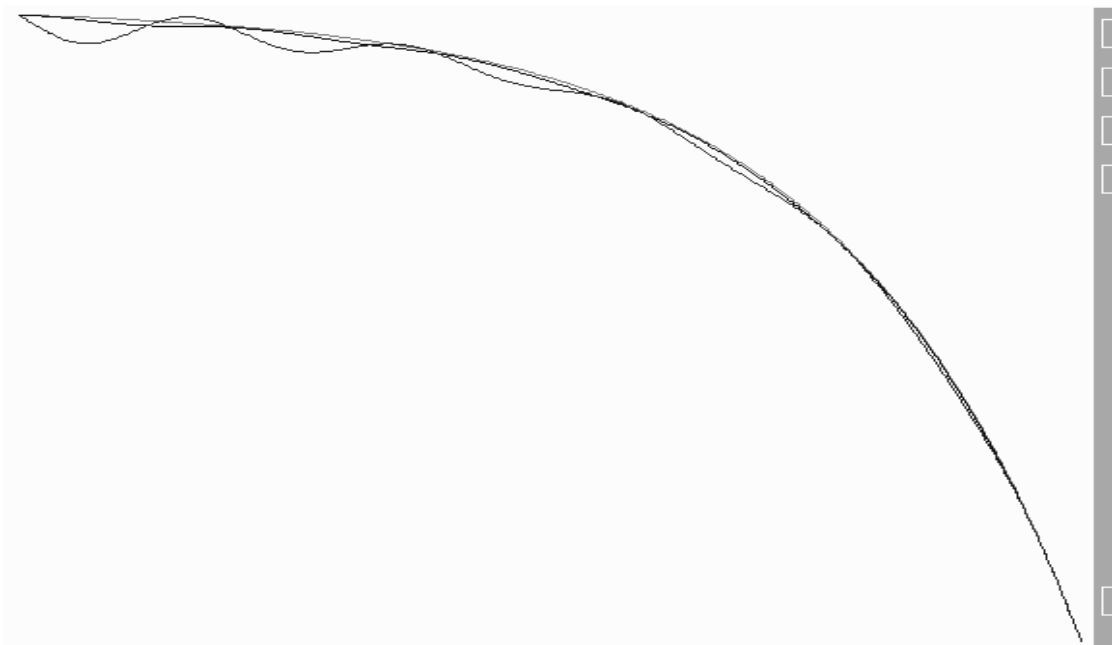
$c = 0,05$

Fig. A.22. Loading of elements of a toothed-belt gearing



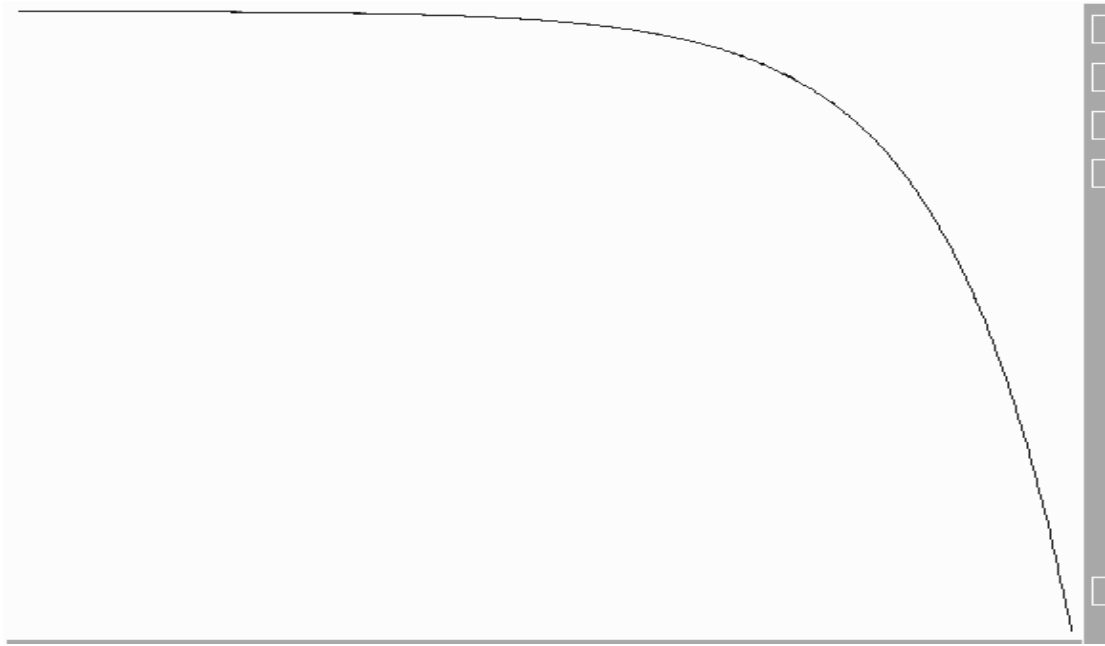
$$c = 0,1$$

Fig. A.23. Loading of elements of a toothed-belt gearing



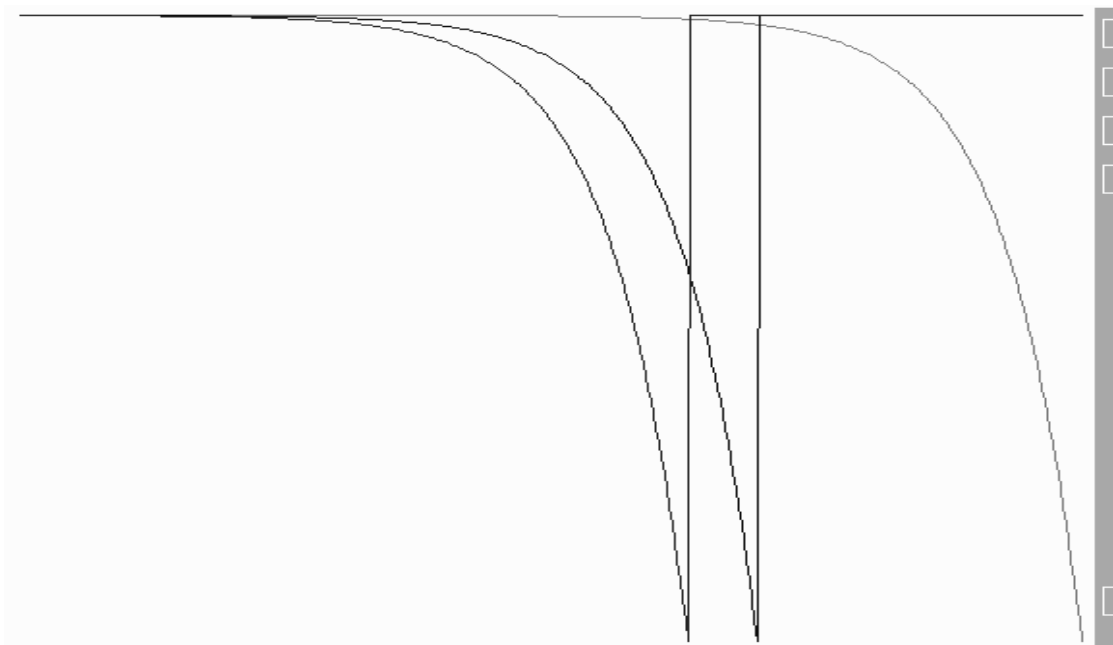
$$c = 0,2$$

Fig. A.24. Loading of elements of a toothed-belt gearing



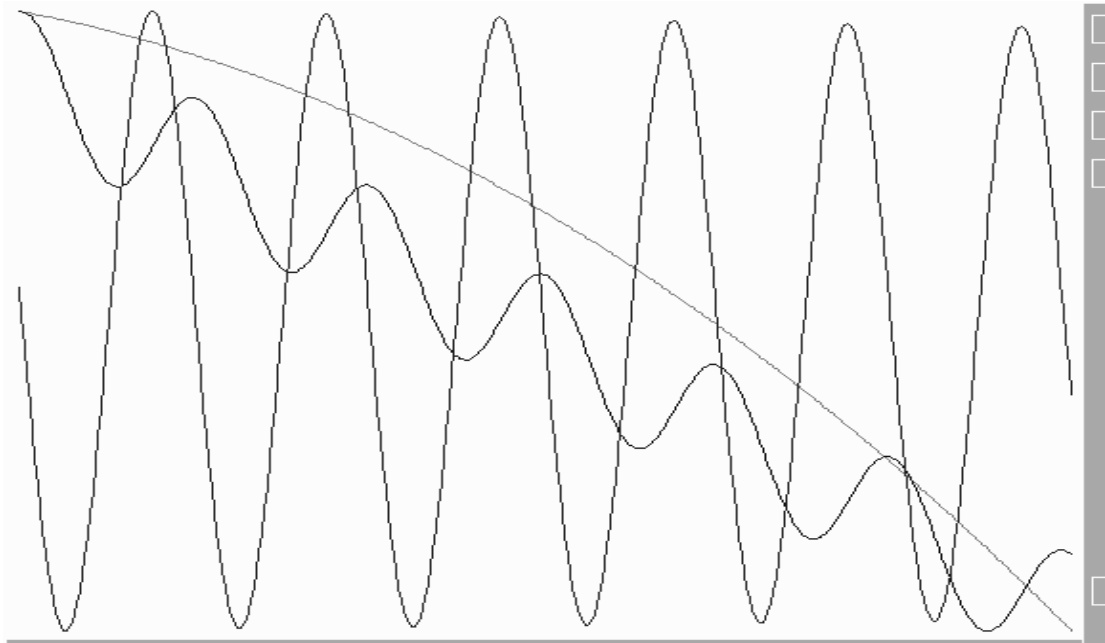
$$c = 0,3$$

Fig. A.25. Loading of elements of a toothed-belt gearing



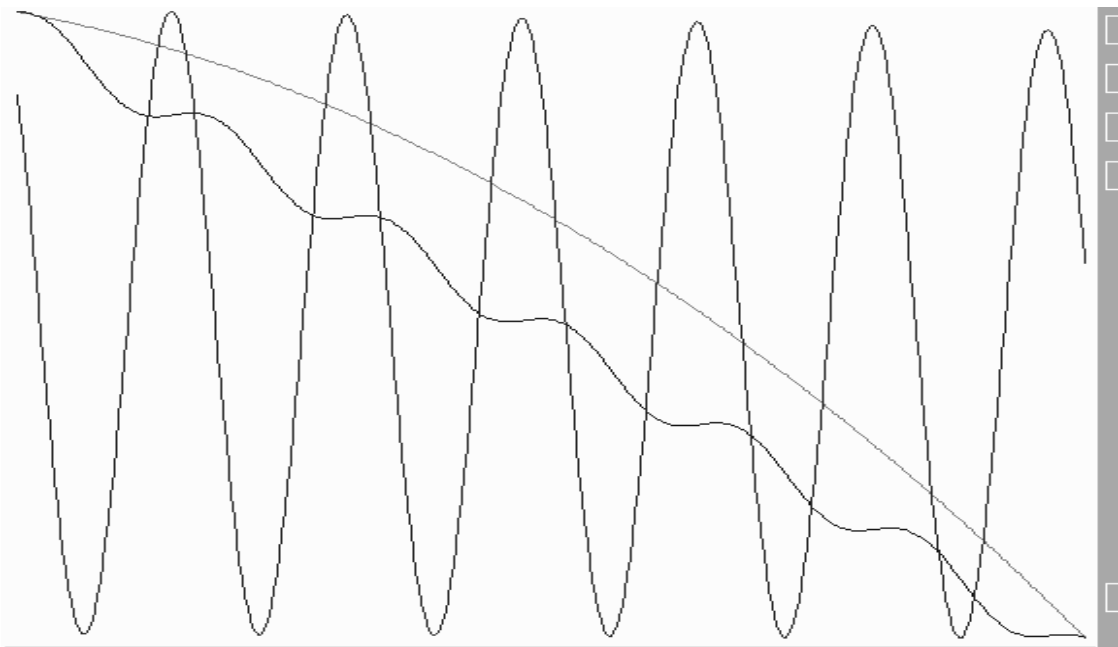
$$c = 0,4$$

Fig. A.26. Loading of elements of a toothed-belt gearing



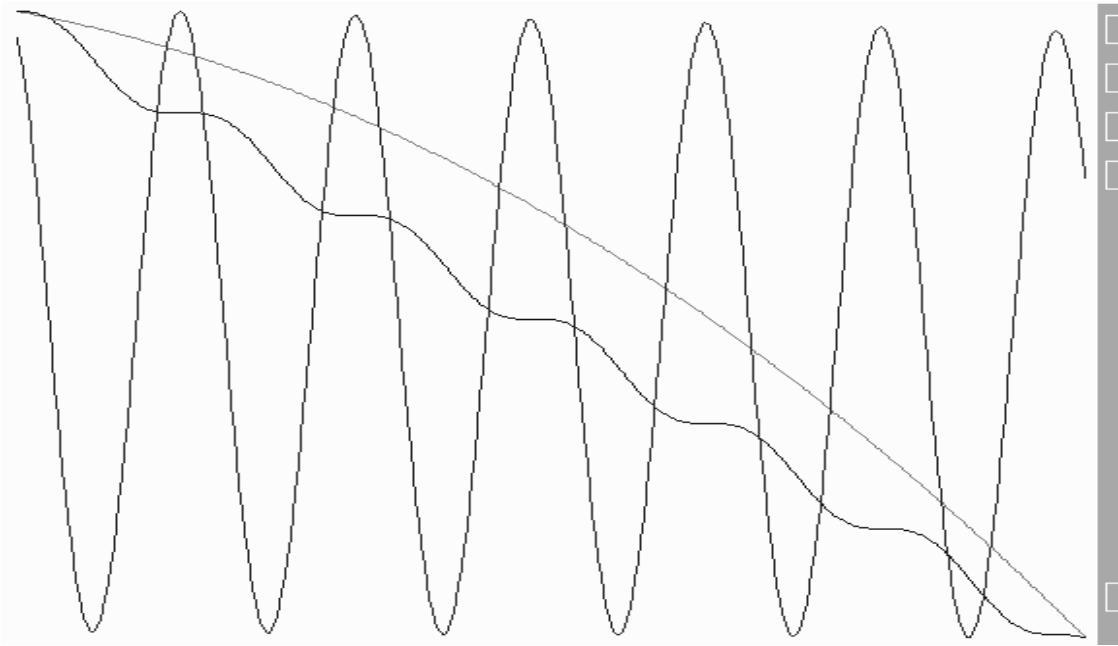
$$k_{vd} = 5$$

Fig. A.27. Loading of elements of a toothed-belt gearing



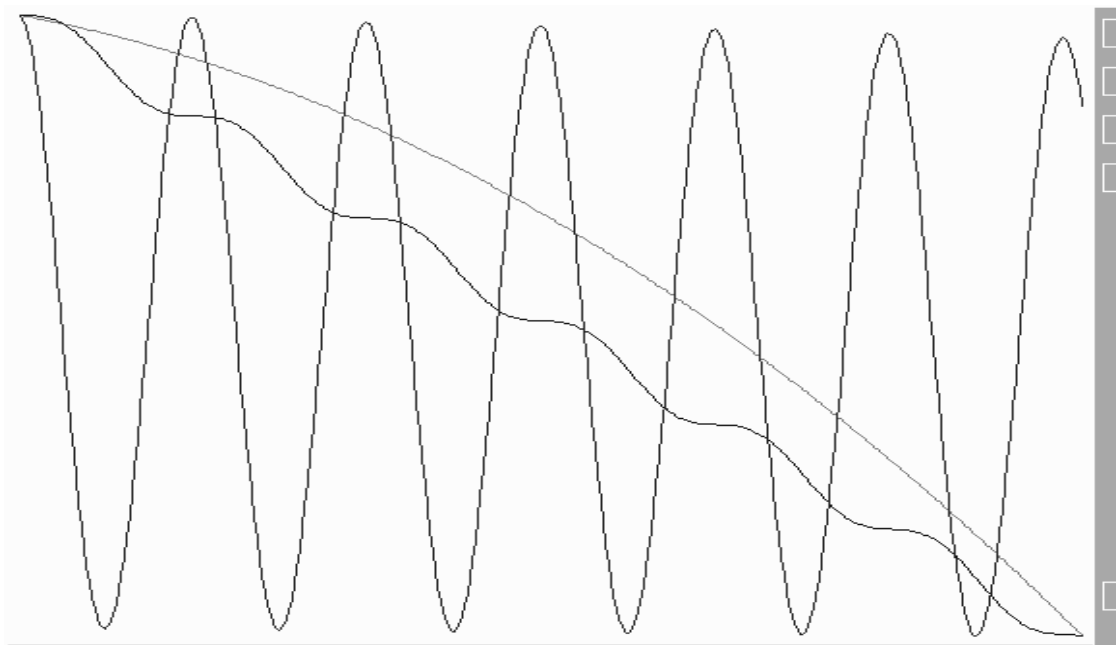
$$k_{vd} = 50$$

Fig. A.28. Loading of elements of a toothed-belt gearing



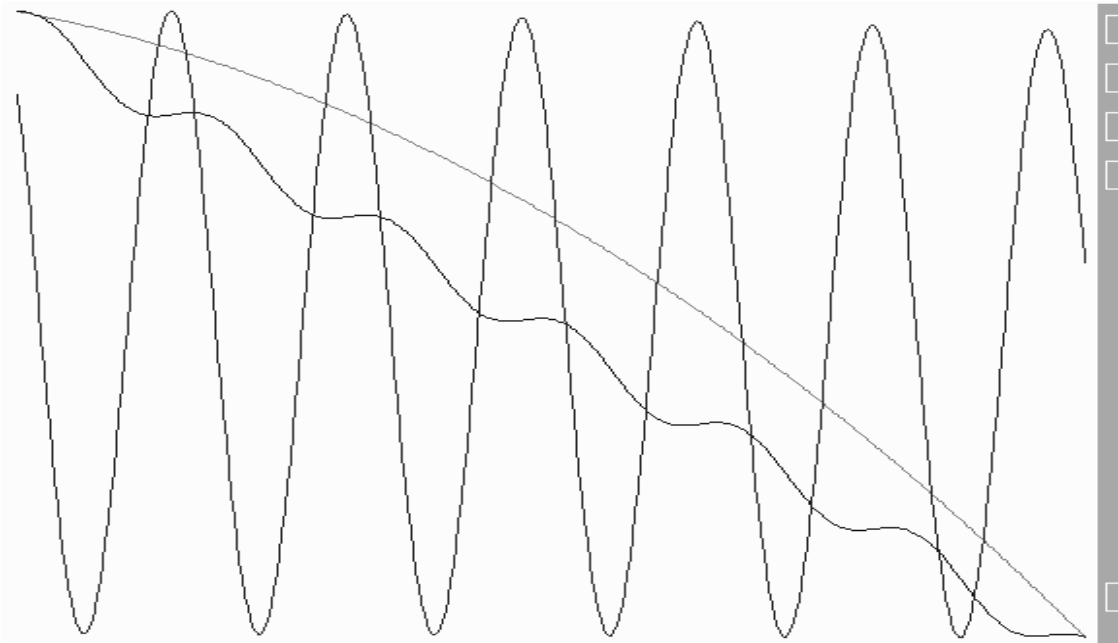
$$k_{vd} = 100$$

Fig. A.29. Loading of elements of a toothed-belt gearing



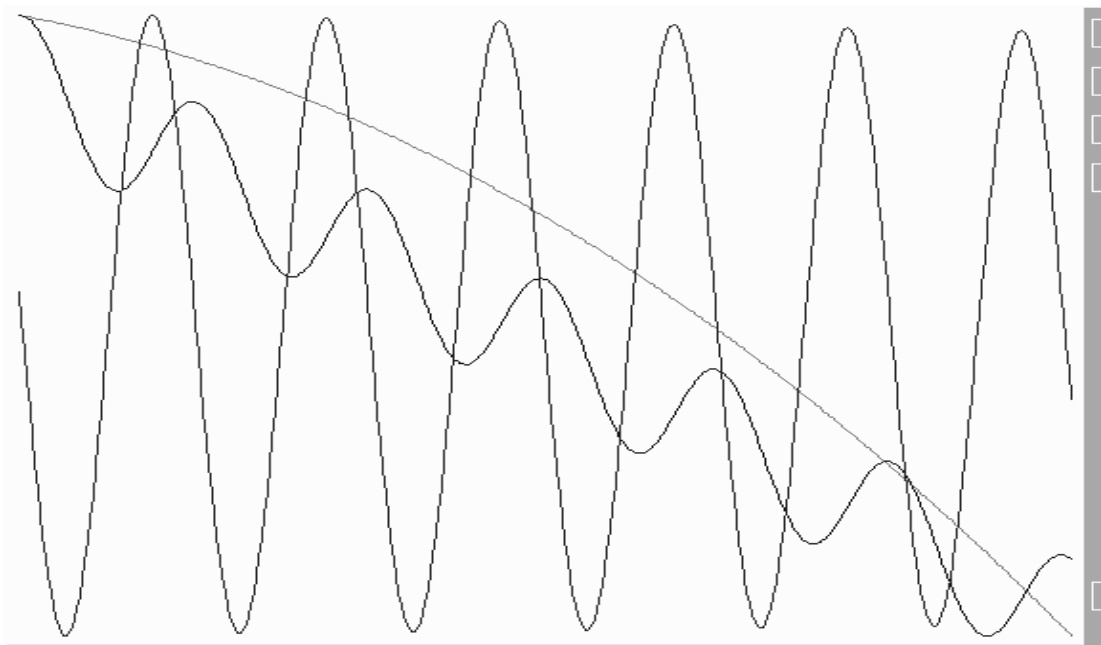
$$k_{vd} = 500$$

Fig. A.30. Loading of elements of a toothed-belt gearing



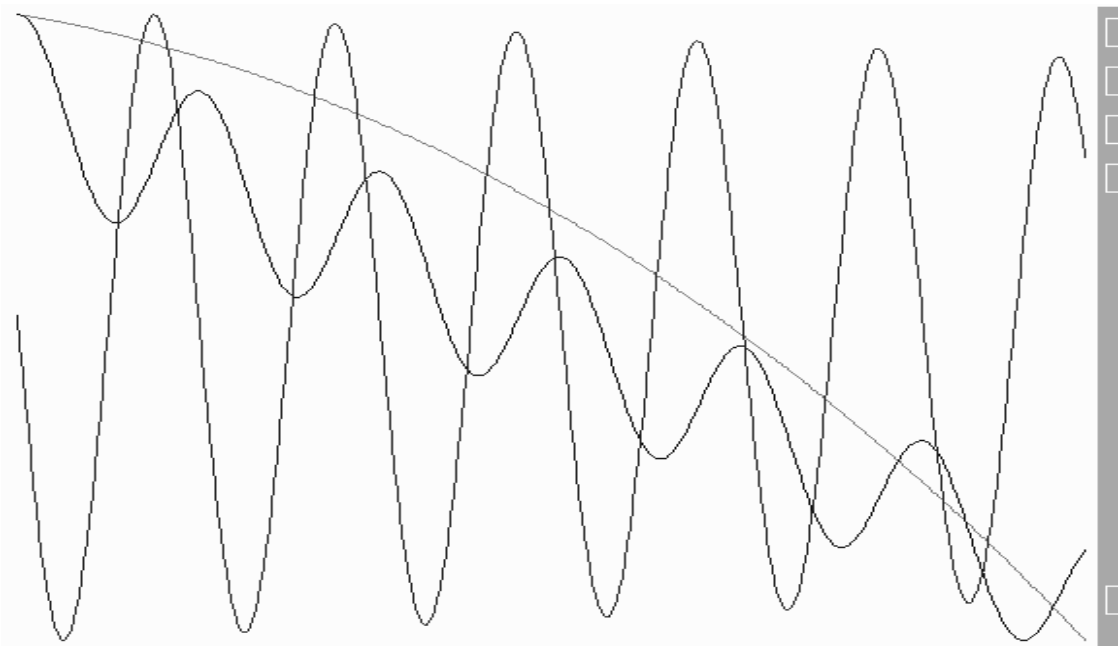
$$c_v = 0,1$$

Fig. A.31. Loading of elements of a toothed-belt gearing



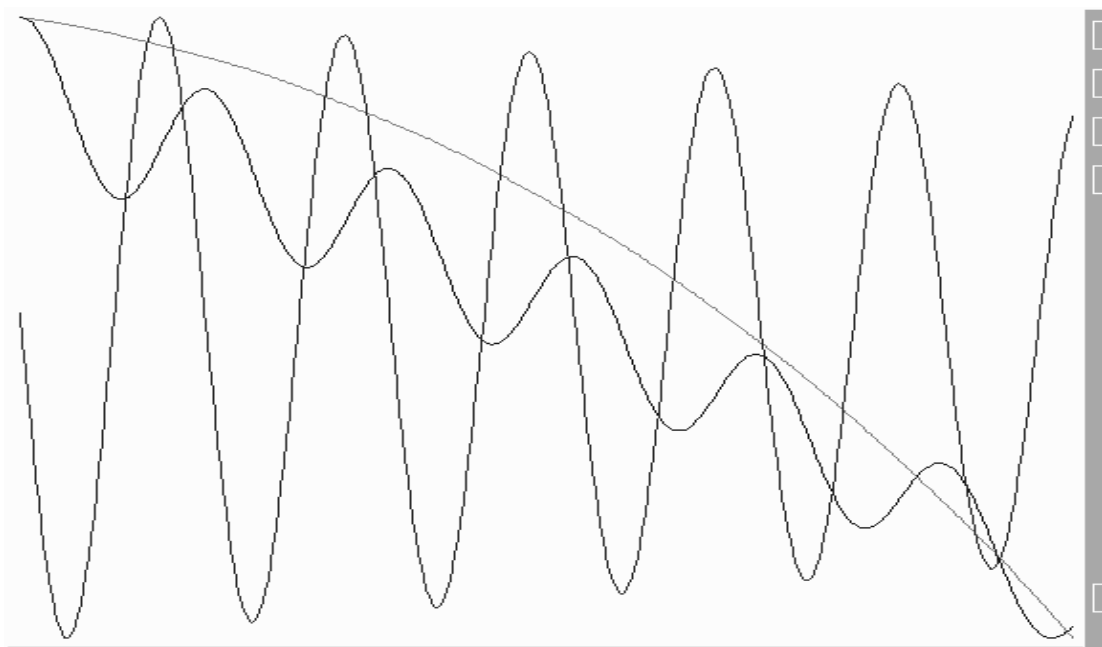
$$c_v = 1,0$$

Fig. A.32. Loading of elements of a toothed-belt gearing



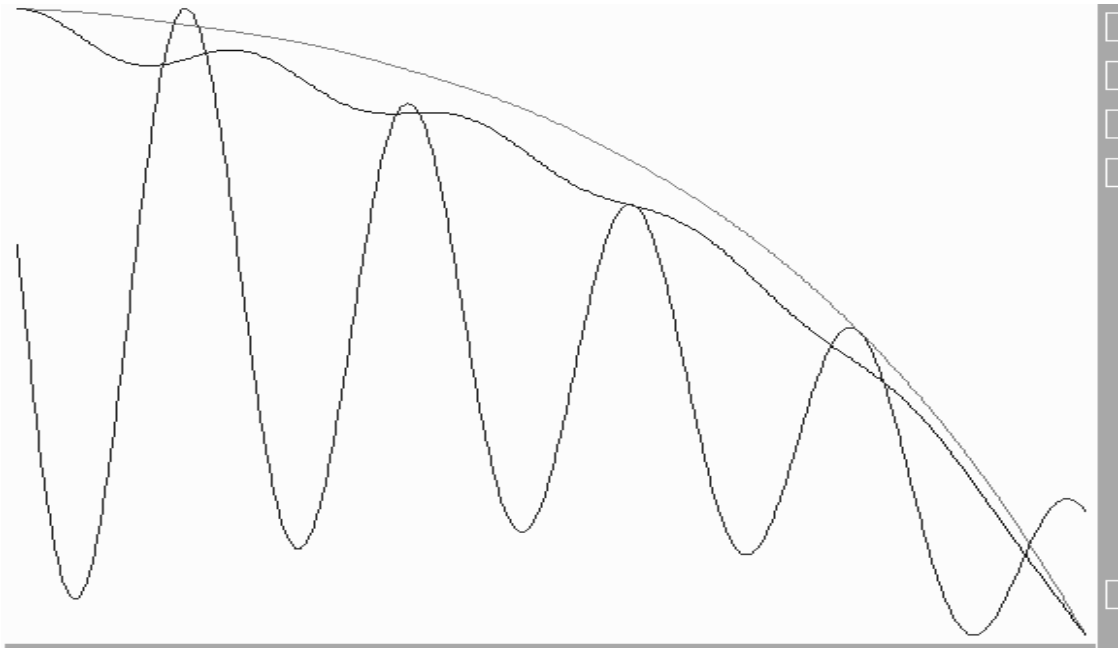
$$c_v = 5,0$$

Fig. A.33. Loading of elements of a toothed-belt gearing



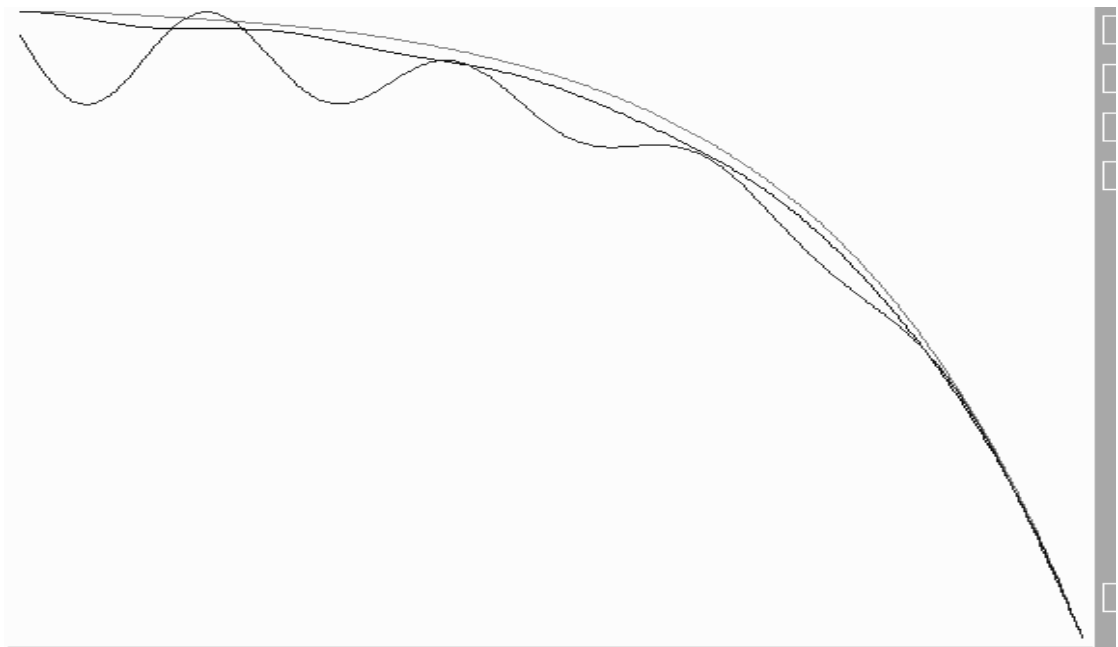
$$c_v = 10,0$$

Fig. A.34. Loading of elements of a toothed-belt gearing



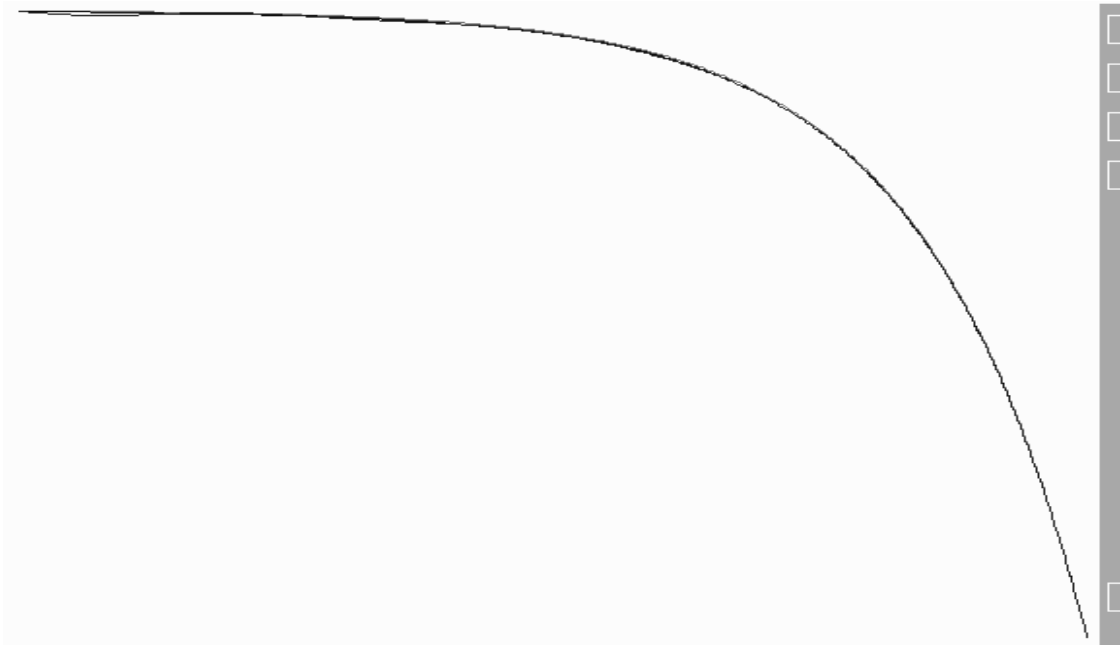
$$c_v = 30,0$$

Fig. A.35. Loading of elements of a toothed-belt gearing



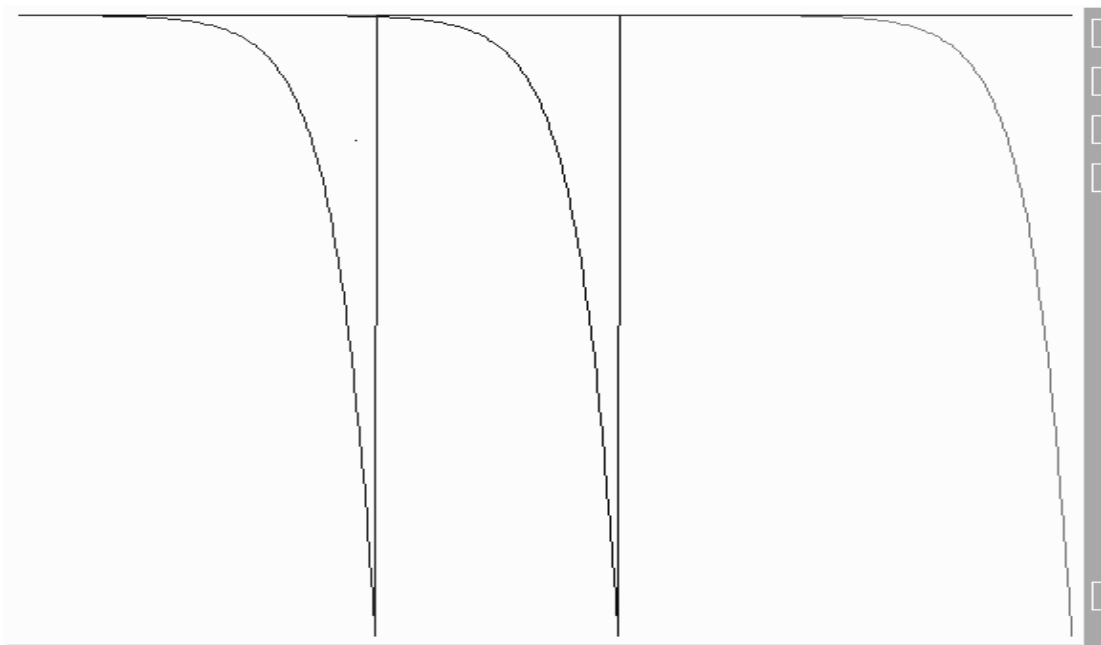
$$c_v = 40,0$$

Fig. A.36. Loading of elements of a toothed-belt gearing



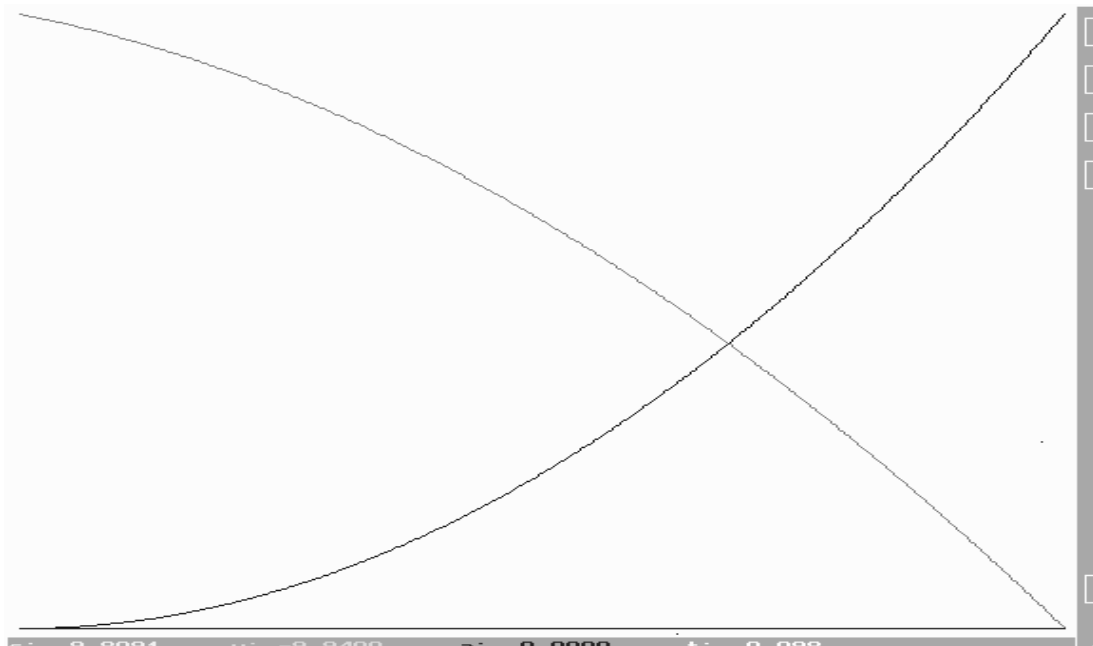
$$c_v = 50,0$$

Fig. A.37. Loading of elements of a toothed-belt gearing



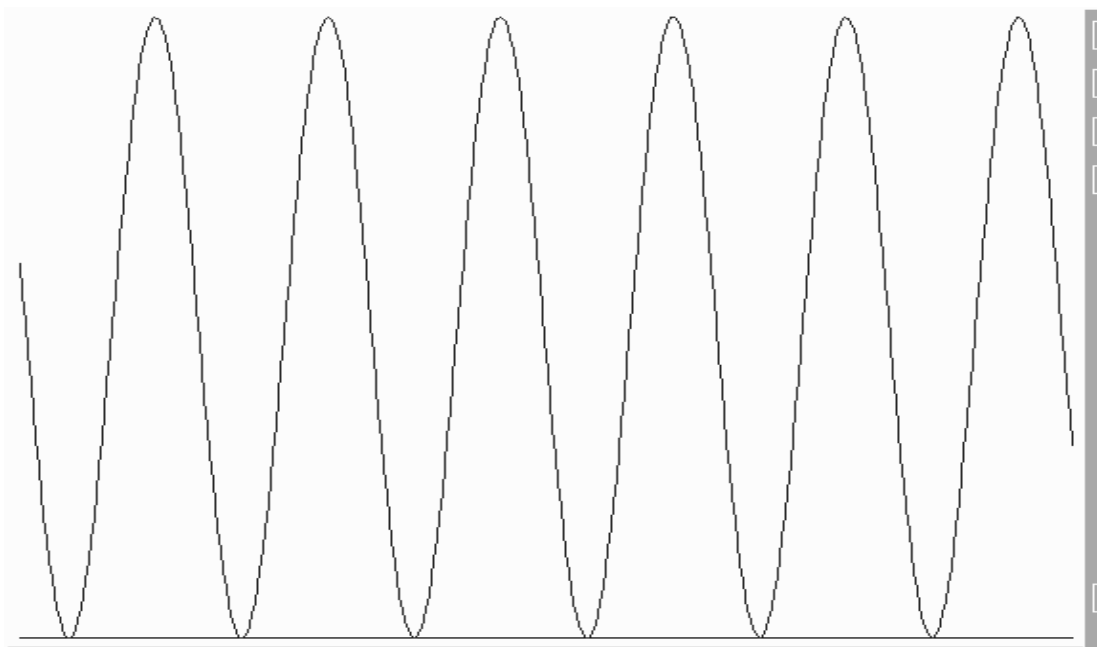
$$c_v = 100,0$$

Fig. A.38. Loading of elements of a toothed-belt gearing



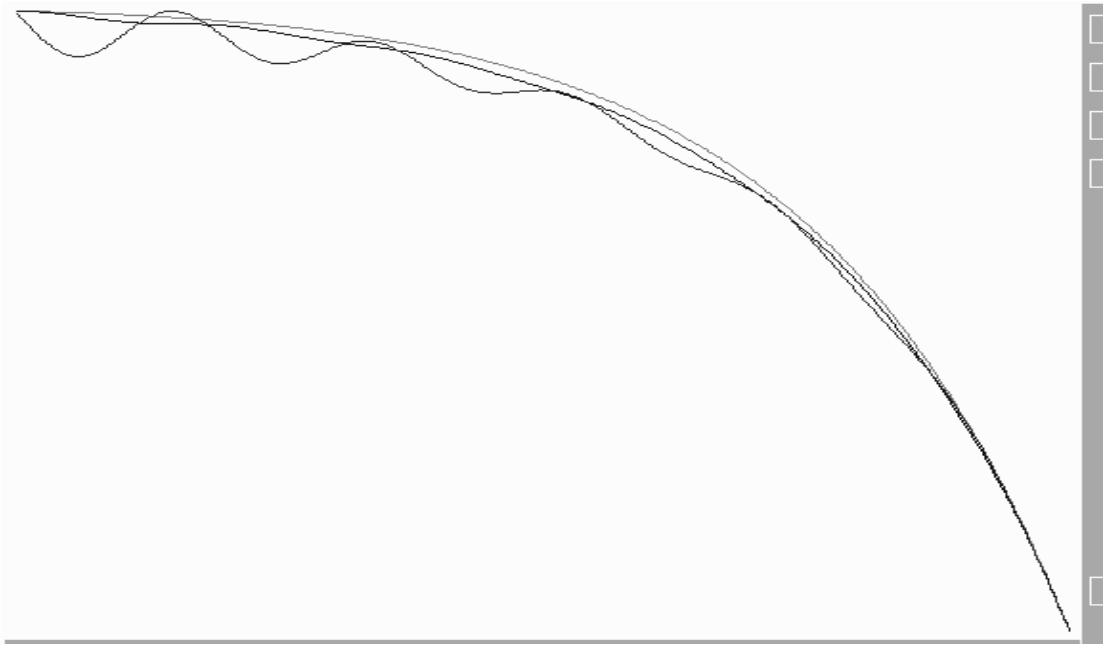
$$k_{vc} = 0$$

Fig. A.39. Loading of elements of a toothed-belt gearing



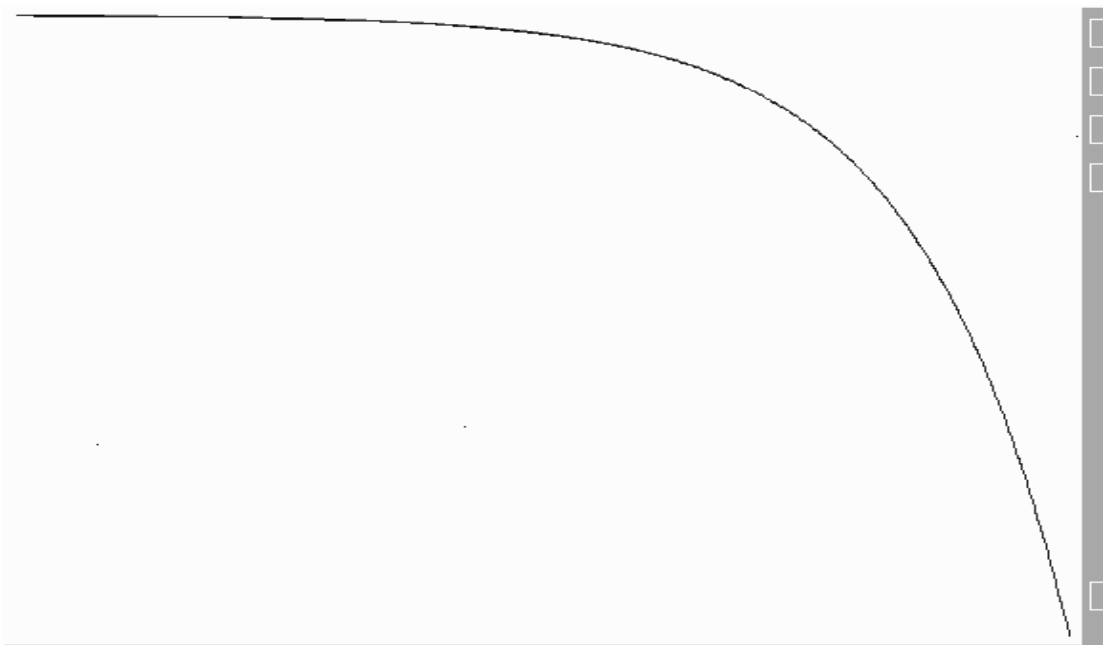
$$k_c = 0$$

Fig. A.40. Loading of elements of a toothed-belt gearing



$$k_c = 200$$

Fig. A.41. Loading of elements of a toothed-belt gearing



$$k_c = 300$$

Fig. A.42. Loading of elements of a toothed-belt gearing

GLOSSARY

А

Абразивный износ	Abrasive wear
Автоклав	Autoclave
Адгезия	Adhesion
Адгезионный слой	Adhesional layer
Аппроксимация	Approximation
Армирование	Reinforcement
Амплитуда крутильных колебаний	Amplitude of torsional vibrations
Амплитудно-частотная характеристика	Amplitude frequency characteristic
Анизотропия	Anisotropy

Б

Балка	Beam
Биение	Beat
Боковая грань зуба	Lateral side of the tooth
Буксование	Slipping

В

Вал	Shaft
Вариационный принцип (метод)	Variational principle (method)
Ведомый шкив	Driven pulley
Ведущий шкив	Drive pulley
Ведущая (ведомая) ветвь ремня	Driving (following) side of belt
Вероятность безотказной работы	Life probability
Вероятностный метод	Probability method
Вершина зуба	Tooth point
Вибрация	Vibration
Вид разрушения	Kind of destruction
Викель	Rolled-up stock
Возбуждение колебаний	Excitation of vibrations
Внутреннее трение	Internal friction
Впадина зуба	Tooth space
Втулочно-петлевое армирование	Sleeve-loopback reinforcement
Вулканизат	Vulcanizate
Выносливость	Endurance
Вынужденные колебания	Forced vibration
Высокоэластичность	High elasticity
Вязкость	Viscosity
Вязкоэластическая жесткость	Viscous-elastic rigidity
Вязкоупругая модель	Viscoelastic model
Вязкость пластического течения	Viscosity of plastic flow
Вязкость упругого последействия	Viscosity of elastic aftereffect

Г

Гармонический профиль	Harmonious profile
Гармоническое усилие	Harmonious effort
Геометрическое подобие	Geometrical similarity
Гибкая связь	Flexible link
Гибкость	Flexibility
Голономная система	Holonomic system
Гребенка	Comb

Д

Давление	Pressure
Давление прессования	Pressure of pressing
Датчик	Sensor
Делительный диаметр	Pitch diameter
Демпфирование	Damping
Деструкция	Destruction
Деформация	Deformation, strain
Деформированное состояние	Strained state
Диаграмма	Diagram
Диаграмма усталости	Diagram of fatigue
Диафрагма	Diaphragm
Диафрагменная вулканизация	Diaphragm vulcanization
Динамическая модель	Dynamic model
Дискретная схема	Discrete scheme
Долговечность	Durability
Допускаемое напряжение	Allowable stress
Дорн	Core
Дуга обхвата	Arc of strap
Дуга сцепления	Arc of mesh

Ж

Жесткость	Stiffness, rigidity
-----------	---------------------

З

Зазор	Clearance
Закон Гука	Hooke's law
Зацепление	Gearing
Зубчатый барабан	Sprocket
Зубчатый ремень	Toothed belt
Зуб ремня	Tooth of belt
Зубчато-ременная передача	Toothed-belt transmission (drive)
Зубчатый сердечник	Gear core

И

Изгиб	Bending
Изнашиваемость	Wearability
Износ	Wear
Износостойкость	Wear resistance
Индентор	Penetrator
Индикатор	Indicator
Интегрирование	Integration
Интенсивность	Intensity
Интенсивность изнашивания	Wear intensity
Интерференция	Interference
Испытание на усталость	Fatigue test
Итерационный метод	Iterative method

К

Канонические уравнения	Canonical equations
Касательная сила	Tangential force
Качение	Rolling
Каучук	Rubber
Квантиль нормального распределения	Quantile of normal distribution
Квадратичное отклонение	Quadric deviation
Клиноременная передача	V-belt transmission
Когезия	Cohesion
Колодочный тормоз	Block brake
Конечный элемент	Finite element
Контактная задача	Contact problem
Контакт зубьев	Contact of teeth
Контактное давление	Contact pressure
Контртело	Counterbody
Консоль	Cantilever beam
Консольно	In cantilever
Концентратор напряжений	Stress concentrator
Концентрация напряжений	Stress concentration
Конформное преобразование	Conformal transformation
Контактная задача	Contact problem
Контактное давление	Contact pressure
Корд, кордшнур	Cord
Корень характеристического уравнения	Root of the characteristic equation
Коррекция шага зубьев	Correction of a step of teeth
Коэффициент армирования	Reinforcement coefficient
Коэффициент асимметрии	Asymmetry coefficient
Коэффициент демпфирования	Damping factor

Коэффициент полезного действия	Efficiency
Коэффициент Пуассона	Poisson's ratio
Коэффициент трения	Coefficient of friction
Кривая усталости	Curve of fatigue, S-N curve
Крутильная жесткость	Torsional rigidity
Крутящий момент	Torque
Кручение	Torsion

Л

Литье	Moulding
Литьевой ремень	Mould belt
Локальный экстремум	Local extremum

М

Математическое ожидание	Mathematical expectation
Матричная запись	Matrix notation
Маховик	Flywheel
Матрица перехода	Transition matrix
Межзубная впадина	Interdental space
Межосевое расстояние	Spacing on centres
Металлокорд	Metal cord
Метод итерации	Iteration method
Метод конечных разностей	Finite difference method
Метод конечных элементов	Finite element method
Метод Рунге	Rit's method
Модуль	Modulus
Момент инерции	Moment of inertia
Момент трения	Moment of friction
Многопарное зацепление	Multipair gearing
Многоцикловая усталость	High-cycle fatigue
Модуль сдвига	Shear modulus
Модуль упругости	Modulus of elasticity
Мощность	Power

Н

Навивка	Coiling
Нагруженность зацепления	Loading of gearing
Нагрузка	Load
Надежность	Reliability
Намотка	Winding
Наполнитель	Filler
Напряжение	Stress
Напряженное состояние	State of stress, stressed state

Напряженно-деформированное состояние	Stress-strained state
Напряжение цикла	Cyclic stress
Натяжение	Tension
Начальная фаза	Initial phase
Неполнопрофильное зацепление	Incomplete profile gearing
Неравномерность нагружения	Irregularity of loading
Неравномерность распределения	Irregularity of distribution
Нерастяжимость	Non-extensibility
Несжимаемый материал	Incompressible material
Несущий слой	Load carrying layer
Несущая способность	Load carrying capacity
Нитеводитель	Thread carrier
Номограмма	Nomograph
Нормальное распределение	Normal distribution

О

Облой	Flash
Образец для испытаний	Test piece
Объектно-ориентиров. программирование	Object-oriented programming
Окружное усилие	Pull
Опора	Support
Орт нормали	Unit vector of normal
Осесимметричная задача	Axisymmetric problem
Оснастка	Equipment
Оциллограмма	Oscillogram
Ось симметрии	Axis of symmetry
Относительное удлинение	Unit elongation

П

Парабола	Parabola
Параллельность	Parallelism
Параметрический вид	Parametrical kind
Передаваемая нагрузка	Transferred loading
Передача	Transmission
Передаточное отношение	Reduction ratio
Периодическое нагружение	Cyclic loading
Переменная нагрузка	Changing load
Перемещение	Displacement
Пересопряжение зубьев	Reinterface of teeth
Пластическая деформация	Plastic deformation
Пластичность	Plasticity
Планшайба	Faceplate
Плоскость	Plane

Плоскоременная передача	Flat-belt transmission
Площадь контакта	Contact area
Площадь поперечного сечения	Cross-sectional area
Поверхность	Surface
Поверхностный слой	Surface layer
Повреждение	Damage
Погрешность	Error
Податливость	Compliance
Покрытие	Surface coat
Полезная нагрузка	Useful load
Поликлиноременная передача	PolyV-belt transmission
Полимер	Polymer
Ползучесть	Creep
Полная потенциальная энергия	Total potential energy
Полукруглый профиль	Semicircular profile
Полупарабола	Semiparabola
Полуполоса	Semistrip
Полуплоскость	Half-plane
Полубесконечная плоскость	Semi-infinite plane
Полуформа	Half-mould
Предварительное натяжение	Prestressing
Предел выносливости	Fatigue limit
Предел прочности	Breaking stress (strength)
Предел усталости	Fatigue strength
Прессование	Moulding
Пресс-форма	Mould
Приведенная масса	Reduced mass
Привод	Drive
Приводной ремень	Drive belt
Прогиб	Deflection
Программно-аппаратное моделирование	Hardware-software modelling
Прогнозирование	Prediction
Продолжительность испытаний	Test time
Проскальзывание	Slippage
Прочность	Strength
Профиль	Profile
Профилограф	Roughometer
Профилометр	Profilometer
Процесс изнашивания	Wear process
Пружина	Spring
Прямолинейный (криволинейный) участок	Rectilinear (curvilinear) site
Псевдозвольевентный профиль	Pseudoinvolute profile

Р

Работа внешних сил	External work
Работоспособность	Serviceability
Равновесие	Equilibrium
Радиус-вектор	Radius vector
Радиус качения	Rolling radius
Радиус кривизны	Radius of curvature
Радиус скругления	Radius of rounding-off
Разделённая разность	Divided difference
Разложение силы	Decomposition of force
Разность шагов	Difference of steps
Разрушение, разрыв	Fracture failure, rupture
Распределение нагрузок	Load distribution function
Распределение напряжений	Stress distribution function
Растяжение	Tension
Реакция связей	Reaction of constraints
Резонансная частота	Resonance frequency
Резина	Rubber
Резиновая смесь	Rubber mixture
Резинотехническое изделие	Rubber engineering article
Результирующая нагрузка	Resultant loading
Релаксация	Relaxation
Ременная передача	Belt drive
Ремонтопригодность	Maintainability
Ресурс	Resource
Ресурсное проектирование	Resource designing

С

Сборочный ремень	Assembly belt
Свободные колебания	Free vibration
Сдвиг	Shear
Сдвиг фаз	Phase difference
Сетка	Mesh
Сжатие	Compression
Сила трения	Friction force
Силовой контур	Power contour
Синусоида	Sinusoid
Система дифференциальных уравнений	System of the differential equations
Скольжение	Sliding
Скорость скольжения	Sliding velocity
Сложное напряженное состояние	Complex stress state
Слой	Layer

Смятие	Bearing stress
Собственная частота	Natural frequency
Сопротивление разрушению	Breaking strength
Среднее квадратичное отклонение	Standard deviation of a random
Среднее напряжение цикла	Mean stress of cycle
Станина	Frame
Статическая неопределимость	Static indefinability
Стеклокорд	Glass-fiber cord
Стержень	Rod, bar
Стойкость	Durability
Стрела прогиба	Maximum deflection
Суппорт	Support
Сцепление	Stick, adhesion

Т

Тангенциальная нагрузка	Tangential loading
Твердость зубьев	Hardness of teeth
Твердость по Шору	Shore hardness
Тензометрический шкив	Strain gauge pulley
Теория прочности	Theory of strength
Теория упругости	Theory of elasticity
Технологический процесс	Technological process
Тканевая обкладка	Fabric facing
Тождество	Identity
Торец	End face
Торцовое перекрытие	Face overlap
Тормозной момент	Braking torque
Торсионный вал	Torsion shaft
Трапецидальный профиль	Trapezoidal profile
Трение скольжения	Sliding friction
Трибометр	Tribometer
Трудоемкость	Labour content
Тяговая способность	Traction ability

У

Угол входа (выхода)	Entrance angle (outlet)
Угол наклона	Slope
Угол поворота	Arc of traverse
Угол сцепления	Angle of coupling
Угловая скорость	Angular velocity
Удар	Impact
Ударный вход зубьев в зацепление	Shock input of teeth in gearing
Упрочнение	Strain hardening

Упругость	Elasticity
Упругая балка	Elastic beam
Упругое последствие	Elastic after-effect
Упругое скольжение	Elastic sliding
Уравнение профиля	Equation of profile
Уравнение Эйлера	Euler equation
Усадка	Contraction
Усилие	Effort
Ускоренное испытание	Accelerated testing
Условие прочности	Strength condition
Условие совместности деформаций	Condition of compatibility
Усталость	Fatigue
Усталостная долговечность	Fatigue life
Усталостный износ	Fatigue wear
Усталостное разрушение	Fatigue failure
Усталостная прочность	Fatigue strength
Усталостная трещина	Fatigue crack
Устойчивость	Stability

Ф

Фаза зацепления	Phase of gearing
Физико-математическое моделирование	Physicomathematical modelling
Физико-механические свойства	Physicomechanical properties
Функционал	Functional
Футеровка	Lining

Ц

Цикл нагружения	Cycle of loading
-----------------	------------------

Ч

Частота вращения	Rotational speed
Частота нагружения	Frequency of loading
Численное моделирование	Numerical modelling
Число зубьев в зацеплении	Number of teeth in gearing
Число циклов	Number of cycles

Ш

Шаг зубьев	Step of teeth
Шевронный зубчатый ремень	Chevron toothed belt
Шероховатость	Roughness
Штамп	Press tool
Штифт	Pin
Шум	Noise

Э

Эвольвента	Involute
Эксплуатационный режим нагружения	Service loading
Эксплуатационный ресурс	Service resource
Эксцентриситет	Eccentricity
Эластичность	Elasticity
Эластомер	Elastomer
Электроимпульсное полирование	Electropulse polishing
Эмпирическая зависимость	Empirical dependence
Эпюра напряжений	Diagram of stress

LITERATURE

1. Бойков, В.П. Зубчатые ремни / В.П. Бойков, Ю.Н. Городничев, Г.Г. Козачевский. – М.: Химия, 1989. – 192 с.
2. Кожевников, С.Н. Конструирование и расчет механизмов с зубчатыми ременными передачами / С.Н. Кожевников, А.П. Погребняк. – Киев: Наукова думка, 1984. – 111 с.
3. Krause, W. Zahnriemengetrieben / W. Krause, D. Metzner. – Berlin: VEB Verlag Technik, 1988. – 120 s.
4. Metzner, D. Reibund und vesschleiss bei Zahnriemengetrieb / D. Metzner // Maschinenbautechnik. – 1984. – Vol. 33, No 9. – P. 415–418.
5. Никончук, А.Н. Усталостная прочность зубьев зубчатых ремней / А.Н. Никончук, В.И. Шпилевский; Белорус. политех. ин-т. – Минск, 1989. – 16 с. – Деп. во ВНИИТЭМР 19.10.89, № 296-МШ89 // РЖ: 48. Машиностр. мат-лы, констр. и расчет дет. машин. Гидропривод. – 1990. – № 2. – 2.48.439ДЕП. – С. 52.
6. Belt construction having enhanced tooth strength: пат. 4583963 США, МПК3 F 16 G 1/28 / L. March; заявитель Dayco Corp. – № 691240; заявл. 09.06.83; опубл. 14.01.85 // НКИ 474/205. – 16 с.
7. Зубчатый ремень: пат. 56-48021 Япония, МПК3 F 16 G 1/28 / Т. Koyama; заявитель Unikka Co. – № 53-131281; заявл. 24.10.76; опубл. 13.11.81. – 5 с.
8. Cicognani, M. Zur Anvengung von Zahnriemen fur den Antrieb / M. Cicognani // Motortechnische Zeitschrift. – 1978. – Vol. 39, No 12. – P. 551–556.
9. Cog-belt and method for its production: пат. 3772929 США, МПК3 F 16 G 5/00 / J. Redmond. – заявл. 14.10.71; опубл. 20.11.73.
10. Зубчатый ремень: пат. 63-24179 Япония, МПК4 F 16 G 5/06, B 29 D 29/10 / заявитель Мицубоси бэруто К. К. – № 54-154676; заявл. 28.11.79; опубл. 19.05.88. – 5 с.
11. Perfectionnements aux courroies de transmission de puissance: пат. 2624238 Франция, МПК3 F 16 G 5/10 / J. Simon; заявитель Hutchinson Co. – № 8717039; заявл. 08.12.87; опубл. 09.06.89. – 3 с.
12. Зубчатый ремень: а. с. 1709783 СССР, МПК5 F 16 G 5/00 / А.Т. Скойбеда [и др.]; Белорус. политех. ин-т. – № 4059035/27; заявл. 18.04.86; ДСП.

13. Зубчатый ремень: а. с. 1449745 СССР, МПК4 F 16 G 5/00 / А.Т. Скойбеда, А.Н. Зуб, А.Н. Наталевич; Белорус. политех. ин-т; заявл. 06.11.86; опубл. 07.01.89 // Открытия. Изобрет. – 1989. – № 1. – С. 42.
14. Приводной ремень для передачи высоких нагрузок: пат. 62-7416 Япония, МПК4 F 16 G 5/06 / заявитель Мицубоси бэруто К. К. – № 57-186631; заявл. 23.10.82; опубл. 17.02.87. – 4 с.
15. Power transmission belt: пат. 60-84439 Япония, МПК4 F 16 G 1/28 / W. Jirov, Y. Hatsudoki; – заявл. 15.10.83, опубл. 14.09.85. – 8 с.
16. Прогрессивные конструкции зубчатых ремней и технология их производства: тематический обзор / Н.В. Лапшина [и др.]. – М.: ЦНИИТЭнефтехим, 1987. – 55 с.
17. Courroi dentee: междунар. заявка РСТ 87/01779, МПК4 F 16 G 1/28 / V.V. Guskov [et al.]; Belorus. polytech. in-t. – заявл. 19.09.85; опубл. 26.03.87.
18. Козачевский, Г.Г. Повышение долговечности зубчато-ременных передач: дис. ... канд. техн. наук: 05.02.02 / Г.Г. Козачевский. – Минск, 1985. – 181 л.
19. McCormick, D. Getting step ruth hybrid belts / D. McCormick // Design Engineering. – 1981. – Vol. 52, No 4. – P. 19–26.
20. Дамаскин, Б.И. Передачи зубчатым ремнем в приводе швейных машин / Б.И. Дамаскин, В.А. Лобанов // Передаточные механизмы. – 1966. – № 4. – С. 217–232.
21. Гуревич, Ю.Е. Исследование зубчато-ременной передачи: дис. ... канд. техн. наук: 05.02.02 / Ю.Е. Гуревич. – М., 1972. – 202 л.
22. Арбузов, М.О. Выбор параметров и вопросы расчета передач зубчатым ремнем: дис. ... канд. техн. наук: 05.02.02 / М.О. Арбузов. – М., 1973. – 184 л.
23. Погребняк, А.П. Определение параметров зубчатых ременных передач, обеспечивающих повышение их надежности: дис. ... канд. техн. наук: 05.02.02 / А.П. Погребняк. – Киев, 1977. – 126 л.
24. Наталевич, А.Н. Исследование условий повышения работоспособности зубчато-ременных передач: дис. ... канд. техн. наук: 05.02.02 / А.Н. Наталевич. – Минск, 1982. – 196 л.
25. Polyurethane toothed belt structure: пат. 4614510 США, МПК3 F 16 G 1/28 / N. Yoji; заявитель Mitsubishi Belting Ltd. – № 709541; заявл. 08.03.85; опубл. 30.09.86 // НКИ 474-205. – 19 с.

26. Toothed belts: пат. 4614509 США, МПК3 F 16 G 1/28 / G. Tangorra; заявитель Industrie Pirelli S.p.A. – № 467794; заявл. 18.02.83; опубл. 30.09.86 // НКИ 474-205. – 10 с.
27. Zahnriemenaufbau aus polyurethan: пат. 3510740 ФРГ, МПК3 F 16 H 7/02 / N. Yoji, K. Aichi; заявитель Mitsuboshi Belting Ltd. – заявл. 25.03.85; опубл. 25.09.86. – 10 с.
28. Зубчато-ременная передача: а. с. 1665769 СССР, МПК5 F 16 H 7/00 / А.Т. Скойбеда [и др.]; Белорус. политех. ин-т; заявл. 29.05.86; ДСП.
29. Дамаскин, Б.И. Исследование геометрии зубчатого ремня привода швейных машин 97-го класса / Б.И. Дамаскин, В.А. Лобанов // Научн. тр. Моск. техн. ин-та легк. пром-сти. – 1965. – № 31. – С. 211–215.
30. Кузьмин, А.В. К вопросу о деформации зуба ремня в плоскозубчатой передаче / А.В. Кузьмин, А.Н. Наталевич // Машины и технология торфяного производства. – 1975. – № 5. – С. 136–142.
31. Кожевников, С.Н. Конструирование и расчет механизмов с зубчатыми ремнями передачами / С.Н. Кожевников, А.П. Погребняк. – Киев: Наукова думка, 1984. – 111 с.
32. Formschlussiges Antrieb mit Zahnriemen // Machine. – 1981. – Vol. 35, No 3. – P. 23–28.
33. Murukami, Y. Study of belt toughness through an examination of the strain on belt cords / Y. Murukami // SAE tech. rap. ser. – 1988. – № 880415.
34. Кравцов, Э.Д. Влияние конструктивных параметров передачи зубчатым ремнем на расчетную нагрузку: дис. ... канд. техн. наук: 05.02.02 / Э.Д. Кравцов. – Одесса, 1987. – 154 л.
35. Positive power transmission system: пат. 3756091 США, МПК3 F 16 G 1/28 / H. Miller; заявитель Uniroyal Inc.; заявл. 19.02.70; опубл. 4.09.73.
36. Воробьев, И.И. Зубчато-ременная передача с зубьями полукруглого профиля. Рекомендации по применению в станкостроении / И.И. Воробьев, А.А. Овчинников. – М.: ЭНИМС, 1986. – 14 с.
37. Massimo, R. Transmissioni dentate super torque / R. Massimo // Rap. conv. compon. mec. preciss. – Torino, 1987. – P. 1–20.
38. Bessere Leistungsüberertragung mit neuen Zahnriemen // Techn. Rept. – 1988. – Vol. 15, No 9A. – P. 36.

39. Toothed belt and toothed pulley transmission: пат. 4553952 США, МПК4 F 16 G 1/28 / G. Tangorra [et al.]; заявитель Industrie Pirelli. – № 467793; заявл. 26.02.82; опубл. 18.02.83 // НКИ 474/153 – 8 с.
40. Зубчато-ременная передача: а. с. 1820095 СССР, МПК5 F 16 H 7/02 / А.Н. Никончук; Белорус. политех. ин-т; заявл. 16.05.91; опубл. 07.06.93 // Открытия. Изобрет. – 1993. – № 21. – С. 91.
41. Шишкин, Б.В. Исследование работоспособности зубчато-ременной передачи: дис. ... канд. техн. наук: 05.02.02 / Б.В. Шишкин. – М., 1980. – 177 л.
42. Чехомов, Ю.К. Контрольные стендовые испытания плоскозубчатых ремней / Ю.К. Чехомов, Ю.А. Бовин, А.Г. Чиварзин // Производство шин, резинотехнических и асбестотехнических изделий. – 1983. – № 12. – С. 29–32.
43. Бартнев, Г.М. Прочность и разрушение высокоэластических материалов / Г.М. Бартнев, Ю.С. Зуев. – М.: Химия, 1964. – 387 с.
44. Бартнев, Г.М. Трение и износ полимеров / Г.М. Бартнев, В.В. Лаврентьев. – Л.: Химия, 1972. – 195 с.
45. Потураев, В.Н. Резиновые детали машин / В.Н. Потураев, В.И. Дырда. – М.: Машиностроение, 1977. – 216 с.
46. Лукомская, А.И. Основы прогнозирования механического поведения каучуков и резин / А.И. Лукомская, В.Ф. Евстратов. – М.: Химия, 1975. – 360 с.
47. Никончук, А.Н. Совершенствование методов исследований и выбора эксплуатационных параметров зубчатых ремней повышенной долговечности: дис. ... канд. техн. наук: 05.02.02 / А.Н. Никончук. – Минск, 1988. – 193 л.
48. Koyama, T. Study on strength of toothed belt / T. Koyama [et al.] // Report. effect of pitch difference on fatigue strength of toothed belt: bul. of the JSME. – Vol. 23, No 181. – P. 1240–1244.
49. Kunio, K. Зубчатые ремни / K. Kunio // Пуранто эндзин (Plant. engin.). – 1985. – Vol. 17, No 9. – P. 19–25.
50. Спицын, Н.А. Ременной привод без скольжения / Н.А. Спицын // Вес. машиностр. – 1963. – № 2. – С. 40–43.
51. Гуревич, Ю.Е. Распределение нагрузки в зубчато-ременной передаче / Ю.Е. Гуревич // Изв. вузов, Сер. машиностр. – 1987. – № 12. – С. 29–34.
52. Koyama, T. Study on strength of toothed belt / T. Koyama, M. Kagotani // Report. influence of pitch difference on load distribution: bul. of the JSME. – 1979. – Vol. 22, No 169. – P. 982–987.

53. Воробьев, И.И. Передачи с гибкой связью в приводах станков / И.И. Воробьев. – М.: Машиностроение, 1971. – 144 с.
54. Гуревич, Ю.Е. Особенности конструирования элементов зубчато-ременной передачи / Ю.Е. Гуревич // Вес. машиностр. – 1977. – № 4. – С. 27–29.
55. Бичкаускас, Л.К. Исследование ременных передач: дис. ... канд. техн. наук: 05.02.02 / Л.К. Бичкаускас. – Каунас, 1985. – 208 с.
56. Load distribution in timing belt / G. Gerbert [et al.] // Mech. des. – 1978. – Vol. 100, No 4. – P. 208–215.
57. Гуревич, Ю.Е. Распределение нагрузки между зубьями ремня и шкива с учетом случайной ошибки / Ю.Е. Гуревич // Изв. вузов, Сер. машиностр. – 1976. – № 8. – С. 56–59.
58. Арбузов, М.О. Влияние шага зубьев шкива на распределение нагрузки между зубьями ремня / М.О. Арбузов // Станки и инструмент. – 1972. – № 5. – С. 33–34.
59. Наталевич, А.Н. Коррекция шкивов как средство повышения долговечности передач зубчатым ремнем / А.Н. Наталевич, А.Т. Скойбеда, В.В. Никитин // Машиностроение. – 1987. – № 12. – С. 105–108.
60. Karolev, N. Zugkraftverlauf und Belastngsverteilung in Zahnriemenantrieben / N. Karolev // Konstruktion. – 1990. – Vol. 42, No 7-8. – P. 247–253.
61. Köster, L. Der Zugkraftverlauf in Zahnriemenantrieben / L. Köster // Konstruktion. – 1982. – Vol. 34, No 3. – P. 99–104.
62. Funk, W. Measurement of force variation in fast running toothed belts / W. Funk, L. Köster // World Congress Theory Mach. and Mech.: abstracts, New-Delhi, 15-20 dec. 1983 y. / New-York, 1984. – Vol. 2. – P. 1174–1177.
63. Заблонский, К.И. Изменение нагрузки на зуб зубчатого ремня в пределах дуги обхвата шкива / К.И. Заблонский, Э.Д. Кравцов // Детали машин. – 1980. – № 30. – С. 13–16.
64. Бондаренко, А.Г. Исследование продольной жесткости зубчатых ремней / А.Г. Бондаренко, А.Н. Никончук // Совершенствование технологических процессов и организации производства технического обслуживания и ремонта автомобилей: сб. науч. тр. / Бел. НИТИАТ; под ред. Н.Г. Интякова. – Минск, 1986. – С. 35–44.
65. Кравцов, Э.Д. Определение податливости несущего слоя зубчатых ремней / Э.Д. Кравцов // Детали машин. – 1989. – № 49. – С. 65–67.

66. Сабанчиев, Х.Х. Теория, расчёт и проектирование зубчато-ременных передач: дис. ... д-ра техн. наук: 05.02.02 / Х.Х. Сабанчиев. – СПб., 1991. – 396 л.
67. Никончук, А.Н. Нелинейная модель силового взаимодействия зубчато-го ремня со шкивом / А.Н. Никончук, А.Т. Скойбеда, В.И. Шпилевский // Вес. акад. наук БССР, Сер. фіз.-тэхн. навук. – 1990. – № 3. – С. 101–105.
68. Kim, H. Belt forces and surface model for a cloth-backed and rubber backed flat belt / H. Kim, K. Marchek // Transac. ASME. – 1988. – Vol. 110, No 2. – P. 93–99.
69. Воробьев, И.И. Ременные передачи / И.И. Воробьев. – М.: Машиностроение, 1979. – 168 с.
70. Передачи зубчатым ремнем. Метод расчета: ОСТ 38 05227-81. – Введ. 01.01.82. – М.: НИИРП Миннефтехимпрома СССР, 1981. – 22 с.
71. Пронин, Б.А. Бесступенчатые клиноременные и фрикционные передачи / Б.А. Пронин, Г.А. Ревков. – М.: Машиностроение, 1967. – 404 с.
72. Овчинников, А.А. Кинематика зацепления зубчато-ременной передачи / А.А. Овчинников, Н.В. Лапшина // Промышленность синтетического каучука, шин и резинотехнических изделий. – 1986. – № 5. – С. 30–33.
73. Research of pressure in toothed belts. Behavior of a belt in a zone of incomplete gearing / Т. Koyama [et al.] // Bul. of the JSME. – 1981. – Vol. 24, No 94. – P. 1500–1506.
74. Литвин, Ф.Л. Теория зубчатых зацеплений / Ф.Л. Литвин. – М.: Наука, 1968. – 584 с.
75. Рывкин, А.А. Справочник по математике / А.А. Рывкин, А.З. Рывкин, Л.С. Хренов. – М.: Высшая школа, 1987. – 479 с.
76. Аналитическая геометрия на плоскости / Н.В. Попова [и др.]; под общ. ред. Н.В. Поповой. – Минск: Вышэйшая школа, 1971. – 230 с.
77. Корн, Г. Справочник по математике для научных работников и инженеров. Определения, теоремы, формулы / Г. Корн, Т. Корн; пер. И.Г. Арамановича; под общ. ред. И.Г. Арамановича. – М.: Наука, 1984. – 831 с.
78. Скойбеда, А.Т. Расчет коэффициента перекрытия в зубчато-ременных передачах / А.Т. Скойбеда, М.А. Родионов, А.Н. Никончук // Вес. акад. навук Беларусі, Сер. фіз.-тэхн. навук. – 1991. – № 4. – С. 104–109.
79. Баханович, А.Г. Повышение несущей способности и долговечности зубчато-ременных передач путем выбора их рациональных параметров: дис. ... канд. техн. наук: 05.02.02 / А.Г. Баханович. – Минск, 1998. – 208 л.

80. Скольжение профилей зубьев в зубчато-ременной передаче / А.Г. Баханович [и др.] // Теория и практика машиностроения. – 2005. – № 2. – С. 59–61.
81. Андреев, А.В. Передачи трением / А.В. Андреев. – М.: Машиностроение, 1978. – 175 с.
82. Вирабов, Р.В. Скольжение в плоскоремненной передаче / Р.В. Вирабов // Машиноведение. – 1967. – № 4. – С. 43–51.
83. Белостоцкий, Б.Х. Передача окружного усилия растяжимой нитью / Б.Х. Белостоцкий, М.Ю. Очан // Машиноведение. – 1977. – № 1. – С. 46–50.
84. Firbank, T.C. Mechanics of the belt drive / T.C. Firbank // Int. J. Mech. Sci. – 1970. – No 12. – P. 1053–1063.
85. Иосилевич, Г.Б. Концентрация напряжений и деформаций в деталях машин / Г.Б. Иосилевич. – М.: Машиностроение, 1981. – 223 с.
86. Гуревич, Ю.Е. О силовом взаимодействии между зубьями ремня и шкива / Ю.Е. Гуревич // Изв. вузов, Сер. машиностр. – 1972. – № 9. – С. 17–22.
87. Гуревич, Ю.Е. Нагруженность ременной передачи, работающей без проскальзывания / Ю.Е. Гуревич // Изв. вузов, Сер. машиностр. – 1989. – № 4. – С. 139–144.
88. Кравцов, Э.Д. Исследование напряженно-деформированного состояния зубчатых ремней методом конечных элементов / Э.Д. Кравцов, А.А. Клименко // Детали машин. – 1983. – № 37. – С. 19–22.
89. HTD – Zahnriemen laufen geräseharm mit hohen Zestungvermögen // KE Konstruktion, Entwich. und Design. – 1984. – № 3. – P. 46–47.
90. Шпилевский, В.И. Повышение несущей способности и долговечности зубчатых ремней на основе применения рациональных методов их предварительного натяжения: дис. ... канд. техн. наук: 05.02.02 / В.И. Шпилевский. – Минск, 1993. – 185 л.
91. Кане, М.М. Основы научного исследования в технологии машиностроения / М.М. Кане. – Минск: Вышэйшая школа, 1987. – 231 с.
92. Арбузов, М.О. Приближенный метод решения задачи о распределении полезной нагрузки между зубьями на дуге обхвата шкива в зубчато-ременной передаче / М.О. Арбузов // Передачи и опоры. – М.: Мосстанкин, 1974. – С. 131–141.
93. Сулейманов, И.И. К методике определения усилий, передаваемых зубьями в зубчато-ременной передаче / И.И. Сулейманов, И.Х. Минц // Изв. АН УзССР, Сер. техн. наук. – 1987. – № 5. – С. 81–82.

94. Вирабов, Р.В. К расчету нагруженности зубьев в зубчато-ременной передаче / Р.В. Вирабов, Х.Х. Сабанчиев // Вес. машиностр. – 1989. – № 8. – С. 11–15.
95. Гуревич, Ю.Е. Выбор пределов допусков на шаг зубьев в зубчато-ременной передаче / Ю.Е. Гуревич // Изв. вузов, Сер. машиностр. – 1976. – № 12. – С. 49–54.
96. Расчет усилий в ветвях зубчато-ременных передач / А.Н. Никончук [и др.] // Весці АН Беларусі, Сер. фіз.-тэхн. навук. – Минск, 1992. – № 3. – С. 54–60.
97. Пронин, Б.А. Влияние изгибной жесткости на параметры ременной передачи / Б.А. Пронин, В.В. Верницкий // Вес. машиностр. – 1977. – № 12. – С. 39–43.
98. Дамаскин, Б.И. Анализ нагружения зубчатого ремня в приводе швейных машин / Б.И. Дамаскин, В.А. Лобанов // Научн. труды Моск. технолог. ин-та легк. пром-сти. – 1967. – Вып. 33. – С. 179–185.
99. Баханович, А.Г. Научные основы повышения технических и эксплуатационных характеристик зубчато-ременных передач путем комплексного развития методов проектирования и технологии изготовления: дис. ... докт. техн. наук: 05.02.02, 05.02.08 / А.Г. Баханович. – Минск, 2006. – 390 л.
100. Жуковский, Н.Е. Аналитическая механика / Н.Е. Жуковский; под ред. В.П. Ветчинкина. – М.-Л.: Оборонгиз, 1939. – 461 с.
101. Maduscka, L. Beanspruchung von Seilrabenverbindungen und Zweckmässige Gestaltung der Lewindeträger / L. Maduscka. – Berlin: Forsch. Geb. Ingenieurwesens, 1976. – 300 p.
102. Weber, P. Beanspruchung von Seilrabenverbindungen / P. Weber // Deutsche Luftfahrtforschung (DVL). – 1942. – P. 51–69.
103. Баханович, А.Г. Исследование нагруженности зубчато-ременных передач методом конечных разностей / А.Г. Баханович, Ю.Е. Гуревич // Механика машин, механизмов и материалов. – 2008. – № 5(4). – С. 40–44.
104. Ривин, Е.И. О модуле упругости клиновых ремней / Е.И. Ривин, В.В. Аугустайтис // Вес. машиностр. – 1963. – № 9. – С. 21–24.
105. Пронин, Б.А. Экспериментальное исследование упругих характеристик клинового ремня вариатора / Б.А. Пронин, В.П. Пурдик // Изв. вузов, Сер. машиностр. – 1986. – № 2. – С. 59–61.
106. Синякова, Э.Н. Исследование тяговой способности ременных передач сложных схем с закрепленными валами: дис. ... канд. техн. наук: 05.02.02 / Э.Н. Синякова. – М., 1982. – 139 л.

107. Бокерия, Р.А. Исследование колебательных процессов в приводе с плоскозубчатым ремнем (применительно к металлорежущим станкам): автореф. дис. ... канд. техн. наук: 05.02.02 / Р.А. Бокерия. – Тбилиси, 1974. – 19 с.
108. Скойбеда, А.Т. Методика и результаты исследований динамической жесткости зубьев зубчатых ремней / А.Т. Скойбеда, А.Н. Никончук, А.Г. Бондаренко // Детали машин: сб. науч.-метод. ст. – М.: МПИ, 1989. – С. 83–89.
109. Баханович, А.Г. Динамические процессы в зубчато-ременных передачах с упрочненными зубьями / А.Г. Баханович; Бел. гос. политехн. акад. – Минск, 1998. – 20 с. – Деп. в ВИНТИ 15.04.98, № 1128-В98 // РЖ: 48. Машиностр. мат-лы, констр. и расчет дет. машин. – 1998. – № 12. – 12.48.317ДЕП. – С. 37.
110. Бендат, Д. Прикладной анализ случайных данных / Д. Бендат, А. Пирсол. – М.: Мир, 1989. – 540 с.
111. Релаксационные явления в зубчато-ременных передачах / А.Н. Никончук [и др.] // Весці акад. навук Беларусі, Сер. фіз.-тэхн. навук. – 1992. – № 2. – С. 96–101.
112. Баханович, А.Г. Динамическое моделирование физических процессов передачи мощности гибкой связью / А.Г. Баханович, А.Т. Скойбеда // Теор. и прак. машиностр. – 2005. – № 1. – С. 57–62.
113. Herrmann, L.R. A reformulation of the elastic field equation, in terms of displacements, valid for all admissible values of Poisson's ratio / L.R. Herrmann, R.M. Toms // J. Appl. Mech. – 1964. – Vol. 31. – P. 148–149.
114. Herrmann, L.R. Elasticity equations for incompressible and nearly incompressible materials by a variational theorem / L.R. Herrmann // AIAA Journal. – 1965. – Vol. 3, No 10. – P. 1896–1900.
115. Каплун, А.Б. ANSYS в руках инженера: практическое руководство / А.Б. Каплун, Е.М. Морозов, М.А. Олферьева. – М.: Едиториал УРСС, 2003. – 272 с.
116. Eringen, A. Nonlinear theory of continuous media / А. Eringen. – New York: McGrawHill Book Co., 1962. – 448 p.
117. Седов, Л.И. Механика сплошной среды / Л.И. Седов. – М.: Наука, 1970. – 486 с.
118. Алфрей, Т. Механические свойства высокополимеров / Т. Алфрей; под ред. М.В. Волькенштейна. – М.: Издатинлит, 1952. – 619 с.
119. Гуль, В.Е. Структура и механические свойства полимеров / В.Е. Гуль, В.Н. Кулезнев. – М.: Высшая школа, 1972. – 320 с.

120. Аскадский, А.А. Деформация полимеров / А.А. Аскадский. – М.: Химия, 1973. – 448 с.
121. Резниковский, М.М. Механические испытания каучука и резины / М.М. Резниковский, А.И. Лукомская. – М.: Химия, 1968. – 500 с.
122. Вязкоупругая релаксация в полимерах / А.Я. Малкин [и др.]; под ред. А.Я. Малкина. – М.: Мир, 1974. – 270 с.
123. Лавендел, Э.Э. Расчет резинотехнических изделий / Э.Э. Лавендел. – М.: Машиностроение, 1976. – 232 с.
124. Рак, Я. Зубчато-ременная передача как средство создания энергоэффективных эластичных приводов: дис. ... д-ра техн. наук: 05.02.02 / Я. Рак. – Харьков, 1991. – 379 л.
125. Баханович, А.Г. Конечно-элементное моделирование напряженно-деформированного состояния зубчато-ременных передач / А.Г. Баханович, А.Т. Скойбеда // Вес. Полоц. гос. ун-та. Сер. С, Фундамент. науки. – 2005. – № 10. – С. 154–157.
126. Баханович, А.Г. Влияние несущего слоя на напряженно-деформированное состояние приводных зубчатых ремней / А.Г. Баханович // Вес. Могилев. гос. техн. ун-та. – 2004. – № 2 (7). – С. 17–20.
127. Гуревич, Ю.Е. Упругие характеристики зубчатых ремней / Ю.Е. Гуревич, К.П. Жуков // Передачи и опоры. – М.: Мосстанкин, 1974. – С. 101–113.
128. Сабанчиев, Х.Х. Исследование колебаний в плоскозубчатых передачах / Х.Х. Сабанчиев // Механические передачи. – М.: НИИмаш, 1971. – С. 184–189.
129. Пановко, Я.Г. Введение в теорию механических колебаний / Я.Г. Пановко. – М.: Наука, 1971. – 239 с.
130. Гуревич, Ю.Е. Определение динамической жесткости и коэффициента демпфирования колебаний зубчато-ременной передачи / Ю.Е. Гуревич, Б.В. Шишкин // Станки и инструмент. – 1980. – № 6. – С. 17–18.
131. Тамулевич, Г.Д. Приводные ремни / Г.Д. Тамулевич, Г.Г. Бобылев. – М.: Химия, 1990. – 23 с.
132. Соколовская, Ф.М. Клиновые ремни / Ф.М. Соколовская, Г.Д. Тамулевич. – М.: Химия, 1973. – 160 с.
133. Баханович, А.Г. Теория и практика зубчато-ременных передач: моногр. / А.Г. Баханович. – Минск, 2008. – 209 с.

134. Устройство для сборки конечных резиновых лент: а. с. 1761541 СССР, МПК5 В 29 D 29/08 / А.Н. Никончук [и др.]; Белорус. политех. ин-т. – № 4646028/05; заявл. 03.02.89; опубл. 15.09.92 // Открытия. Изобрет. – 1992. – № 34. – С. 77.
135. Устройство для сборки резиновых лент: а. с. 1431956 СССР, МПК5 В 29 D 29/07 / А.Т. Скойбеда [и др.]; Белорус. политех. ин-т. – № 4168917/05; заявл. 25.12.86; опубл. 23.10.88 // Открытия. Изобрет. – 1988. – № 39. – С. 58.
136. Баханович, А.Г. Зубчато-ременные передачи: моногр. / А.Г. Баханович, А.Т. Скойбеда. – Минск: БНТУ, 2005. – 364 с.
137. Скойбеда, А.Т. Прогрессивная импортозамещающая технология производства приводных зубчатых ремней из отечественных материалов / А.Т. Скойбеда, А.Г. Баханович, И.Г. Баханович // Вес. Бел. нац. техн. ун-та. – 2003. – № 3. – С. 38–42.
138. Пресс-форма для изготовления кольцевых полимерных изделий: а. с. 1407815 СССР, МПК5 В 29 С 33/10 / А.Т. Скойбеда [и др.]. – № 3901307/23-05; заявл. 06.06.85; опубл. 07.07.88 // Открытия. Изобрет. – 1988. – № 25. – С. 89.
139. Устройство для изготовления кольцевых изделий: а. с. 1683265 СССР, МПК5 В 29 С 35/02 / С.А. Беяев [и др.]; Белорус. политех. ин-т. – № 4784415/05; заявл. 19.01.90; ДСП.
140. Пресс-форма для изготовления двухсторонних зубчатых ремней: пат. 4789 Респ. Беларусь, МПК7 В 29 С 35/02, В 29 С 33/02, В 29 D 29/08, В 29 L 29/00 / А.Н. Никончук, А.Г. Баханович, А.Т. Скойбеда, И.Н. Никончук, И.А. Косырев; заявитель Бел. нац. техн. ун-т. – № а 19980100; заявл. 04.02.98; опубл. 30.12.2002 // Афіцыйны бюл. / Нац. цэнтр інтэлектуал. уласнасці. – 2002. – № 4. – С. 107.
141. Кошелев, Ф.Ф. Общая технология резины / Ф.Ф. Кошелев, А.Е. Корнев, А.М. Буканов. – М.: Химия, 1978. – 528 с.
142. Белозеров, Н.В. Технология резины / Н.В. Белозеров. – М.: Химия, 1979. – 472 с.
143. Баханович, А.Г. Повышение долговечности приводных зубчатых ремней методом оптимизации параметров технологического процесса производства / А.Г. Баханович // Вес. Бел. нац. техн. ун-та. – 2006. – № 1. – С. 38–42.

144. Баханович, А.Г. Исследование напряженно-деформированного состояния приводных зубчатых ремней армированных конструкций / А.Г. Баханович // Вес. Полоц. гос. ун-та. Сер. С, Фундамент. науки. – 2005. – № 10. – С. 121–124.
145. Харуо, Х. Шум в передачах зацеплением / Х. Харуо // Нихон кикай гаккай ромбунсю. – 1991. – Vol. 32, No 9. – P. 62–68.
146. Synchronriemen: пат. 3040157 ФРГ, МПК5 F 16 G 1/28 / Н. Eickhorn. – заявл. 09.10.81; опубл. 28.04.83. – 16 с.
147. Synchronous drive pulley and its combinations with a belt having oblique and offset teeth: пат. 5421789 США, МПК5 F 16 H 65/00 / М. Gregg. – № 43687; заявл. 08.08.93; опубл. 06.06.95 // НКИ 474-153. – 7 с.
148. Geräuschlose Zahnriemen // Technika (Suisse) – 1998. – Vol. 46, No 25-26. – P. 46–48.
149. Schrägverzahnung elimiert löstige Pfeifgeräusche // Ingenieur Anzeiger – 1999. – Vol. 12, No 15. – P. 58–59.
150. Зубчато-ременная передача: пат. 4790 Респ. Беларусь, МПК7 F 16 H 7/02 / А.Н. Никончук, А.Г. Баханович, И.А. Косырев, И.Н. Никончук; заявитель Бел. нац. техн. ун-т. – № а 19981199; заявл. 30.12.98; опубл. 30.12.2002 // Афіцыйны бюл. / Нац. цэнтр інтэлектуал. уласнасці. – 2002. – № 4. – С. 152.
151. Болотин, В.В. Механика многослойных конструкций / В.В. Болотин, Ю.Н. Новичков. – М.: Машиностроение, 1980. – 376 с.
152. Жемочкин, Б.Н. Теория упругости / Б.Н. Жемочкин. – М.: Госстройиздат, 1957. – 256 с.
153. Малков, В.П. Оптимизация упругих систем / В.П. Малков, А.Г. Угодчиков. – М.: Наука, 1981. – 288 с.
154. Третьяченко, Г.Н. Моделирование при изучении прочности конструкций / Г.Н. Третьяченко. – Киев: Наукова думка, 1979. – 230 с.
155. Напряжение и деформации в деталях и узлах машин / Н.И. Пригоровский [и др.]; под ред. Н.И. Пригоровского. – М.: Машгиз, 1961. – 564 с.
156. Галин, Л.А. Контактные задачи теории упругости / Л.А. Галин. – М.: Машиностроение, 1973. – 339 с.
157. Мусхелишвили, Н.И. Некоторые основные задачи математической теории упругости / Н.И. Мусхелишвили. – М.: Изд-во АН СССР, 1969. – 431 с.
158. Тимошенко, С.П. Теория упругости / С.П. Тимошенко, Д. Гудьер; пер. С.П. Тимошенко – М.: Наука, 1975. – 575 с.

159. Биргер, И.А. Расчет на прочность деталей машин / И.А. Биргер, Б.Ф. Шорр, Г.Б. Иосилевич. – М.: Машиностроение, 1979. – 702 с.
160. Баханович, А.Г. Минимизация контактного давления в зубчато-ременном зацеплении методом оптимизации геометрии зубьев / А.Г. Баханович, Ю.Е. Гуревич, И.Г. Баханович // Механика машин, механизмов и материалов. – 2009. – № 6(1). – С. 44–47.
161. Гуревич, Ю.Е. К применению зубчато-ременной передачи в приводе механизма газораспределения двигателя / Ю.Е. Гуревич, К.П. Жуков // Автомоб. промыш. – 1976. – № 5. – С. 7–8.
162. Скойбеда, А.Т. Продольная жесткость приводных ремней в условиях динамического нагружения / А.Т. Скойбеда, А.Н. Никончук, А.Г. Баханович // Вес. Нац. акад. наук Беларусі. Сер. фіз.-тэхн. навук. – 1999. – № 3. – С. 42–46.
163. Баханович, А.Г. Трибологический критерий ресурсного проектирования зубчато-ременных передач / А.Г. Баханович // Материалы, технологии, инструменты. – 2005. – Т. 10, № 1. – С. 46–50.
164. Sadao, A. Study on the fatigue behavior of the toothed belts / A. Sadao, F. Toru, K. Masayuki // Нихон кикай гаккай ромбунсю. – 1989. – Vol. 55, No 514. – P. 1477–1487.
165. Кравцов, Э.Д. Расчет зубьев зубчатых ремней на прочность / Э.Д. Кравцов // Детали машин. – 1990. – № 5. – С. 11–14.
166. Скойбеда, А.Т. Усталостная прочность зубчатых ремней и ее расчет / А.Т. Скойбеда, А.Н. Никончук, А.Г. Баханович // Вес. акад. навук Рэспублікі Беларусі. Сер. фіз.-тэхн. навук. – 1997. – № 4. – С. 38–45.
167. Решетов, Д.Н. Детали машин / Д.Н. Решетов. – М.: Машиностроение, 1989. – 496 с.
168. Гуревич, Ю.Е. К методике расчета передач зубчатым ремнем / Ю.Е. Гуревич, К.П. Жуков // Изв. вузов, Сер. машиностр. – 1980. – № 11. – С. 25–30.
169. Синькевич, Ю.В. Обеспечение геометрических параметров качества поверхности электроимпульсным полированием / Ю.В. Синькевич, И.Н. Янковский // Прогрессивные технологии и системы машиностроения. – Донецк: ДонНТУ, 2006. – Вып. 32. – С. 200–206.
170. Триботехнические характеристики и долговечность зубчато-ременных передач / А.Г. Баханович [и др.] // Механика машин, механизмов и материалов. – 2008. – № 4 (3). – С. 27–30.

171. Почтенный, Е.К. Прогнозирование долговечности и диагностика усталости деталей машин / Е.К. Почтенный. – Минск: Навука і тэхніка, 1983. – 246 с.
172. Большев, Л.Н. Таблицы математической статистики / Л.Н. Большев, Н.В. Смирнов. – М.: Наука, 1983. – 416 с.
173. Баханович, А.Г. Ресурсное проектирование зубчато-ременных передач / А.Г. Баханович, А.Т. Скойбеда // Вес. Полоц. гос. ун-та. Сер. В, Прикладн. науки. – 2005. – № 12. – С. 178–183.
174. Гусейнов, В.М. Отечественные приводные зубчатые ремни / В.М. Гусейнов // Машиностроитель. – 1986. – № 10. – С. 40–41.
175. Ленты конвейерные, ремни приводные из резины: ТУ РБ 00149438-073-95. – Введ. 01.01.95. – Минск: ИУТУ: Беларусьрезинотехника, 1995. – 24 с.
176. Metzner, D. Konstruktive Gestaltung von Zahnriemenscheiben / D. Metzner // Maschinenbautechnik. – 1983. – Vol. 32, No 3. – P. 122–125.
177. Кравцов, Э.Д. Разность шагов ремня и шкива, обеспечивающая уменьшение неравномерности распределения нагрузки в зацеплении передачи зубчатым ремнем / Э.Д. Кравцов, В.С. Похилук // Детали машин. – 1988. – № 46. – С. 26–28.
178. Гуревич, Ю.Е. Влияние деформаций ремня на зацепление в зубчато-ременной передаче / Ю.Е. Гуревич // Изв. вузов, Сер. машиностр. – 1977. – № 12. – С. 59–64.
179. Баханович, А.Г. Совершенствование методики проектного расчета зубчато-ременных передач повышенной несущей способности и долговечности путем рационального корригирования шкивов / А.Г. Баханович, И.Г. Баханович; Бел. гос. политехн. акад. – Минск, 2002. – 16 с. – Деп. в ВИНТИ 26.02. 2002, № 360-В2002 // РЖ: 48. Машиностр. мат-лы, констр. и расчет дет. машин. – 2003. – № 3. – 03.03-48.304ДЕП. – С. 34.
180. Протодьяконов, М.М. Методика рационального планирования эксперимента / М.М. Протодьяконов, Р.И. Тедер. – М.: Наука, 1970. – 76 с.
181. Баханович, А.Г. Методические аспекты повышения технических характеристик зубчато-ременных передач / А.Г. Баханович // Материалы, технологии, инструменты. – 2005. – Т. 10, № 1. – С. 41–45.
182. Баханович, А.Г. Методика проектного инженерного расчета зубчато-ременной передачи / А.Г. Баханович, А.Т. Скойбеда // Вес. Полоц. гос. ун-та. Сер. С, Фундамент. науки. – 2006. – № 4. – С. 135–145.

CONTENTS

INTRODUCTION.....	5
Chapter 1. COMMON DATA.....	7
1.1. Review and analysis of designs of transmissions of power by flexible link	7
1.1.1. Flat- belt transmissions	7
1.1.2. V-belt transmissions.....	10
1.1.3. Poly-V- belt transmissions	11
1.1.4. Toothed-belt transmissions.....	14
1.2. Geometry and kinematics of toothed-belt gearing.....	26
1.3. Load carrying capacity and durability of toothed- belt transmissions	31
1.4. Force interaction of teeth in gearing	37
1.5. Perspectives of the development of scientific principles of increasing of the engineering level of power transmissions by flexible link	39
Chapter 2. GEOMETRY AND KINEMATICS OF TRANSMISSIONS OF POWER BY FLEXIBLE LINK	42
2.1. Characteristics of geometry and kinematics of belt transmissions.....	42
2.2. Zones of an incomplete profile gearing of teeth of toothed-belt transmissions...	47
2.3. Sliding of teeth in the zones of the incomplete profile gearing of toothed-belt transmissions.....	66
2.4. Sliding of flexible link in the belt transmissions of a frictional type	68
2.5. Factor of a face overlap of teeth in toothed-belt transmissions.....	85
2.6. Experimental research of the sliding velocity of teeth.....	89
2.7. Phases of gearing and the rigidity of belt teeth.....	91
2.8. Conclusions.....	95
Chapter 3. DYNAMICS AND LOADING OF TRANSMISSIONS OF POWER BY FLEXIBLE LINK.....	97
3.1. Bases of the calculation of loading of a toothed-belt gearing.....	97
3.2. Loading of the arc of contact in view of the zones of the incomplete profile gearing of teeth.....	104
3.3. Research of loading of toothed-belt transmissions by the method of finite differences.....	109
3.4. Mathematical and physical modeling of the transmission of power.....	128

3.5. Variation principles of the research of the stress-strained state.....	139
3.6. Hardware-software modeling of the stress-strained state.....	142
3.7. Experimental research of the dynamic rigidity and the factor of damping of vibrations of a toothed-belt transmission.....	149
3.8. Conclusions.....	153
Chapter 4. DESIGN-ENGINEERING METHODS OF THE IMPROVEMENT OF THE TECHNICAL LEVEL OF TRANSMISSIONS OF POWER BY FLEXIBLE LINK.....	155
4.1. Energy and resource saving ecologically-safe technology of drive toothed belts	155
4.2. Parameters of the technological process of the manufacture of drive toothed belts..	163
4.2.1. Pressing pressure.....	163
4.2.2. Temperature of vulcanization.....	165
4.2.3. Duration of vulcanization.....	166
4.3. Progressive designs of the reinforced toothed belts.....	168
4.4. Toothed -belt transmissions with the improved technical and ecological parameters.....	172
4.5. Lowering of the contact pressure in a toothed -belt gearing by the method of optimization of geometry of teeth.....	177
4.6. Conclusions.....	201
Chapter 5. LOAD CARRYING CAPACITY AND OPERATIONAL RESOURCE OF TRANSMISSIONS OF POWER BY FLEXIBLE LINK.....	202
5.1. Wear resistance of toothed belts.....	202
5.2. Fatigue strength of toothed belts.....	209
5.3. Lowering of the sliding friction of teeth in gearing.....	225
5.4. Probabilistic methods of prediction of the durability of toothed belts.....	229
5.5. Design method of the improvement of technical characteristics of toothed -belt transmissions.....	238
5.6. Conclusions.....	244
CONCLUSION.....	246
APPENDICES.....	249
GLOSSARY.....	280
LITERATURE.....	290

Science edition

Alexander Gennadevich BAKHANOVICH
Jury Efimovich GUREVICH

MECHANICS OF TRANSMISSIONS
OF POWER BY FLEXIBLE LINK

Monography

Number of copies 103.
Printed in the United States of America.